UNIVERSITY OF SOUTHAMPTON

FACULTY OF ENGINEERING AND APPLIED SCIENCE

DEPARTMENT OF CIVIL ENGINEERING

PROJECT SUPERVISOR:PROFESSOR P.B.MORICE,PhD,DSc,CEng,FICE,FIStructE

A THEORETICAL STUDY OF THE FATIGUE CUMULATIVE DAMAGE ANALYSIS OF REINFORCED CONCRETE BEAMS AS A CONTRIBUTION TO THE DESIGN OF SHORT SPAN HIGHWAY BRIDGES IN REGIONS WHERE TRAFFIC IS NOT INTENSE

by

SADIQ A. H. A. MUSCATI, BSc, MSc, AMICE

A thesis submitted for the Degree of Doctor of Philosophy

October 1986

UNIVERSITY OF SOUTHAMPTON

ABSTRACT

FACULTY OF ENGINEERING AND APPLIED SCIENCE

DEPARTMENT OF CIVIL ENGINEERING

Doctor of Philosophy

A THEORETICAL STUDY OF THE FATIGUE CUMULATIVE DAMAGE ANALYSIS OF REINFORCED CONCRETE BEAMS AS A CONTRIBUTION TO THE DESIGN OF SHORT SPAN HIGHWAY BRIDGES IN REGIONS WHERE TRAFFIC IS NOT INTENSE

by Sadiq Abdul Husein Ali MUSCATI

Concern about fatigue of concrete structures has recently increased because of new uses of concrete. The aim of this study is to investigate fatigue life of reinforced concrete bridges, in rural areas, with simply supported short spans, subjected to simulated single lane truck loading.

The relationship between fatigue life, in years, and the section modulus of the bridge beams has been investigated. In the study five different span lengths have been used and the loading has been based upon three different intensities of traffic flow, across the bridge, expressed in terms of Trucks per hour. The section modulus is defined here as the ratio of the applied moment to the induced stress in the reinforcement of the beam section.

Making use of available statistical data, the truck models have been simulated by the Monte Carlo method, assuming that trucks' gross weights and their arrival times on the bridge are normally and exponentially distributed respectively. The time sequence of maximum and minimum moments (moment spectrum) has been obtained by passing the truck model across the bridge. By designing the bridge section to resist the maximum moment with a specified design stress in the reinforcement, the section modulus has been defined and used to convert the moment spectrum into a stress spectrum.

The 'rainflow' method has been used to perform the stress cycle counting. From the counted cycles, the fatigue life has been estimated using the Palmgren - Miner's linear rule.

For each combination of beam span and frequency of loading, a single curve has been obtained to represent the relationship between the section modulus and Log (life in years). This curve has been established by a new method, developed to ensure a 'safe' result, as it gives an interpolated life value which does not exceed the corresponding real one. The curve may be used to estimate the section modulus required to give a specified design fatigue life to the bridge.

ACKNOWLEDGEMENTS

It has been my privilege to perform this investigation under the friendly guidance of Professor P. B. Morice. I shall always remain grateful for his constant help and advice and for his kind efforts in securing the scholarship which enabled me to complete this study.

I am deeply indebted to Dr. A. Jefferson for his kind advice and constructive criticism.

Also, I wish to express my sincere thanks to the British Council for their financial support.

Finally, I wish to thank Mrs. J. Pelham for typing this thesis.

To Sada, Zahra and Haura

CONTENTS

		Page No.
	LIST OF SYMBOLS	iv
1.	INTRODUCTION	1
2.	FATIGUE OF MATERIALS UNDER REPEATED LOADING	5
2.1	Fatigue in General	5
2.1.1	Palmgren-Miner's Method	6
2.1.2	Inoue-Nakagawa's Method	7
2.1.3	The Double Linear Damage Method	10
2.1.4	Henry's Method	11
2.1.5	Gatt's Method	12
2.2	Fatigue of Concrete	13
2.2.1	Fatigue of Plain Concrete	13
2.2.2	Fatigue of Reinforced Concrete	14
2.2.2.1	Low Cycle Fatigue of Reinforced Concrete	17
2.2.3	Fatigue of Prestressed Concrete	18
3.	SIMULATION	19
3.1	Probability and Probability Functions	19
3.2	The Monte Carlo Simulation	20
3.3	Generation of Random Numbers	20
3.4	Generation of Random Variates	23
3.4.1	The Inverse Transformation Method	23
3.4.2	The Rejection Method	24
3.5	Traffic Simulation	24
3.5.1	Truck Classification	25
3.5.2	Multiple Presence of Trucks	29
3.5.3	Truck Gross Weight (GW)	33
3.5.4	Dynamic Factor	35
3.5.5	Truck Type Selection	38
3.6	Simulation of The Moment Spectrum	38
3.6.1	Time Interval (Dt)	39
3.7	Maximum Probable Moment	53
4.	DESIGN OF THE BRIDGE BEAMS	57
4.1	The Modular - Ratio Theory	57
4.2	The Limit - State Theory	60
4.2.1	Characteristic Strengths and Loads	61
4.2.2	Partial Safety Factors	61

		Page No.
4.3	Beam Section Design for Moment	62
	4.3.1 Design Assumptions	62
	4.3.2 Dimensions of The Beam Section	65
	4.3.3 Reinforcement Area	73
	4.3.4 Determination of The Actual Stresses in The Reinforcing Bars	76
4.4	Design Moments and Shears	81
4.5	Computer Program for The Design of The Bridge Beams	83
4.6	Discussion of The Design Results	85
4.7	Section Modulus	87
	4.7.1 Choosing a Section Modulus Suitable for All Loading Stages	99
	4.7.2 Sections of The 15.0 m Bridge	107
4.8	Sections with Highly Stressed Reinforcement	110
4.9	Design Tables	113
5.	ANALYSIS OF THE FATIGUE CUMULATIVE DAMAGE	200
5.1	Simulation of The Stress Spectrum	203
5.2	Cycle Counting Methods	204
	5.2.1 Range - Mean Method	205
	5.2.2 Rainflow Method	207
	5.2.2.1 First Procedure - Rainflow	207
	5.2.2.2 Second Procedure, Maximum - Minimum	212
	5.2.2.3 Third Procedure - Pattern Classification	215
5.3	Computer Program	219
5.4	Tables of The Stress Simulation Parameters	221
6.	RESULTS AND DISCUSSION	228
6.1	The Variation of The Bridge Fatigue Life with The Section Modulus	228
6.2	Sections with Low Stresses in The Reinforcement	238
6.3	Curve Fitting	241
	6.3.1. Safe Curve Method	242
6.4	Log (life) - F_L Safe Curves	245
6.5	The Centroidal Stress Range Giving a (100 yrs) Fatigue Life	255
6.6	The Effect of The Section Modulus Definition on The Predicted Fatigue Life	258
6.7	Recommendation for Future Work	264
6.8	Fatigue Life Tables and Curves	265

	Page No.
REFERENCES	312
BIBILIOGRAPHY	316
APPENDICES	321
A. Derivation of Inoue - Nakagawa's Equation	322
B. The Rainflow Computer Program	326
C. The Least Squares Method and Its Computer Program	330
D. The Safe Curve Computer Program	336
E. The Effect of an Increased Value of The Section Modulus on The Fatigue Life	342
F. Computer Program for The Fatigue Life Prediction	345
G. Computer Program for The Design of Beam Sections	360

LIST OF SYMBOLS

Fatigue and Bridge Loading Parameters:

L	: bridge span in m.
U	: loading frequency in trucks per hour.
$(life)_m$	: bridge fatigue life, estimated by the Palmgren-Miner's theory, in years.
$(life)_n$	: bridge fatigue life, estimated by the Inoue-Nakagawa's theory, in years.
G_m	: partial safety factor for material strength.
G_f	: partial safety factor for load.
S	: the applied stress.
N	: number of cycles to failure at stress S.
S_e	: the fatigue endurance limit.
S_{eo}	: the fatigue endurance limit for the virgin material.

Moment and Shear Values:

M and V	: the maximum live load moment in KN.M, and shear in KN, including impact, to be shared between the bridge two beams.
M_L	: the maximum live load moment (including impact), in KN.M.
M_D	: the dead load moment in KN.M.
M_T	: the maximum total moment = $M_D + M_L$, in KN.M.
M_H	: the average total moment = $M_D + \frac{1}{2} M_L$, in KN.M.

M_e : the limiting value of the live load moment (including impact), which causes a stress range equivalent to the endurance limit, in KN.M.

M_p : the maximum probable live load moment (including impact), in KN.M.

M_A : the applied moment.

V_T : the maximum total shear in KN.

V_L : the maximum live load shear (including impact), in KN.

Moment and Stress Spectra:

N_p : number of the peak points of the moment spectrum, simulated for one week.

N_c : number of the stress cycles in one week.

N_{ec} : number of the effective stress cycles, which exceed the endurance limit, in one week.

Characteristics of The Beam Section:

b : section width in mm.

h : section height in mm.

d : the actual effective depth of the section in mm.

d_{req} : the required effective depth of the section in mm.

d' : the lever arm of the section in mm.

d_p : the distance, from the tension face to the centre of the total tensile force = h - d, in mm.

d_{pt} , d_{ph} , d_{pd} , d_{pp} : d_p values, resulting from the maximum total moment (M_T) , the average total moment (M_H), the dead load moment (M_D) and the total probable moment ($M_p + M_D$), respectively, in mm.

x : neutral axis depth in mm.

R : neutral axis depth ratio = x/d.

R_T , R_H , R_D , R_p : R values resulting from the moments, M_T , M_H , M_D and, $M_p + M_D$, respectively.

C : the total compressive force in the section, in N.

Characteristics of The Steel Reinforcement:

n_b : number of the reinforcing bars in one layer.

N_b : the total number of the reinforcing bars in the section.

A_s : the total reinforcement area in mm^2.

R_R : the reinforcement ratio = $A_s/bd \times 100$.

c : the distance from the centre of the outer layer to the tension face of the beam, in mm.

s : vertical spacing between reinforcement layers, in mm. (s = 25 + bar diameter)

s' : clear horizontal spacing between bars = 25 mm or bar diameter, whichever is more.

ϕ : bar diameter for the shear reinforcement, in mm.

T : the total tensile force in the reinforcing steel, in N.

Actual Stresses and Strains:

f_{cu} : concrete compressive strength in N/mm^2.

f_c : maximum compressive stress in concrete, in N/mm^2.

μ : the ratio of the average concrete compressive stress to f_{cu} , (see Figure I, page xiv).

f_y : yield stress of the reinforcement, in N/mm^2.

f_u : ultimate strength of the reinforcement, in N/mm^2.

f_s : the centroidal stress in the reinforcement, which corresponds to the strain at the centroid of the reinforcement, in N/mm^2.

f_{sc} : the stress in the reinforcement which corresponds to a strain equivalent to the maximum allowable concrete strain (0.0035).

f_{si} : the initial design value of f_s , in N/mm^2.

f_{sa} , f_{sh} , f_{sd} , f_{sp} : the stress f_s values, caused by the maximum total moment (M_T), the average total moment (M_H), the dead load moment (M_D) and the total probable moment ($M_p + M_D$), respectively, in N/mm^2.

f_{se} : the stress in the outer layer of the reinforcing bars, in Nmm^2.

f_{sae} , f_{she} , f_{sde} , f_{spe} : the stress f_{se} values, caused by the moments M_T , M_H , M_D and, $M_p + M_D$, respectively, in N/mm^2.

e_s : the strain at the centroid of the reinforcement.

e_{sa} , e_{sh} , e_{sd} , e_{sp} : the strains at the reinforcement centroid, which correspond to the stresses f_{sa} , f_{sh} , f_{sd} , f_{sp} respectively.

e_{se} : the strain at the outer layer of the reinforcing bars.

e_{sae} , e_{she} , e_{sde} , e_{spe} : the strains at the outer layer of the reinforcing bars, which correspond to the stresses f_{sae} , f_{she} , f_{sde} , f_{spe} respectively.

S_e : the fatigue endurance limit of the outer layer of bars = $161.5 - 0.33\ f_{sde}$, in N/mm^2.

f_{sr} , f_{sre} : the centroidal and outer bar stress ranges, caused by the maximum total moment (M_T), in N/mm^2. ($f_{sr} = f_{sa} - f_{sd}$, $f_{sre} = f_{sae} - f_{sde}$)

f_{srh} , f_{srhe} : the centroidal and outer bar stress ranges, caused by the average total moment (M_H), in N/mm^2 . ($f_{srh} = f_{sh} - f_{sd}$, $f_{srhe} = f_{she} - f_{sde}$)

f_{sr100} : the predicted centroidal stress range which is needed to produce a design fatigue life of (100) years, in N/mm^2.

v : the maximum shear stress = $1000\ V_T/bd$, in N/mm^2.

e_c : the maximum concrete strain.

e_{ca} , e_{ch} , e_{cd} , e_{cp} : the maximum concrete strains caused by the moments M_T , M_H , M_D and, $M_p + M_D$, respectively.

e_o : the initial plastic strain in the concrete.

Strain Factors and Their Relative Difference:

S_f : the ratio of the outer bar strain to the centroidal strain of the reinforcement. [from Figure I, page (xiv): $S_f = (d - R.d + d_p - c) / (d - R.d)$]

S_{FT} , S_{FH} , S_{FD} , S_{Fp} : the strain factor values, corresponding to the maximum total moment (M_T), the average total moment (M_H), the dead load moment (M_D) and the total probable moment ($M_p + M_D$), respectively.

S_F : the strain factor which is taken to represent the section through all loading stages. [S_F = the maximum of S_{FH} and $0.5\ (S_{FT} + S_{FD})$]

$$D_{Sf} = \left[\frac{\text{the maximum of } (S_{FT} , S_{FH} , S_{FD})}{\text{the minimum of } (S_{FT} , S_{FH} , S_{FD})} - 1\right] \times 100$$

Section Moduli [all in KN.M/(N/mm^2)]:

Z : The ratio of the applied moment to the induced centroidal stress in the reinforcement.

Z_T , Z_{TH} , Z_D , Z_p : the section modulus Z values, based on the centroidal stress, which correspond to the maximum total moment (M_T), the average total moment (M_H), the dead load moment (M_D) and the total probable moment ($M_p + M_D$), respectively. [$Z_T = M_T/f_{sa}$, $Z_{TH} = M_H/f_{sh}$, $Z_D = M_D/f_{sd}$, $Z_p = (M_p + M_D)/f_{sp}$]

Z_L , Z_{LH} , Z_{Lp} : the live load section modulus values, based on the centroidal stresses, which correspond to the moments M_L , $\frac{1}{2} M_L$ and M_p respectively. [$Z_L = M_L/(f_{sa} - f_{sd})$, $Z_{LH} = 0.5\ M_L/(f_{sh} - f_{sd})$, $Z_{Lp} = M_p/(f_{sp} - f_{sd})$]

Z' : the ratio of the applied moment to the induced outer bar stress in the reinforcement.

Z'_T , Z'_{TH} , Z'_D : the section modulus Z' values, based on the outer bar stresses, which correspond to the moments M_T , M_H and M_D respectively. [$Z'_T = M_T/f_{sae}$, $Z'_{TH} = M_H/f_{she}$, $Z'_D = M_D/f_{sde}$]

Z'_L , Z'_{LH} : the live load section modulus values, based on the outer bar stresses, which correspond to the moments M_L and $\frac{1}{2} M_L$ respectively. [$Z'_L = M_L/(f_{sae} - f_{sde})$, $Z'_{LH} = 0.5\ M_L/(f_{she} - f_{sde})$]

F : the combined load section modulus, which is examined to see whether it could be taken to represent the section through all loading stages. [F = the minimum of Z_{TH} and $0.5\ (Z_T + Z_D)$]

F_L : the live load section modulus, which is taken to represent the section through all loading stages. [F_L = the minimum of Z_L and Z_{LH}]

Relative Differences of The Section Moduli:

$$D_{Z1} = \left[\frac{\text{the maximum of } (Z_T , Z_{TH} , Z_D)}{\text{the minimum of } (Z_T , Z_{TH} , Z_D)} - 1 \right] \times 100$$

$$D_{Z2} = \frac{| Z_T - Z_{TH} |}{\text{the minimum of } (Z_T , Z_{TH})} \times 100$$

$$D_{Z3} = \frac{| Z_L - Z_{LH} |}{\text{the minimum of } (Z_L , Z_{LH})} \times 100$$

$$D'_{Z1} = \left[\frac{\text{the maximum of } (Z'_T , Z'_{TH} , Z'_D)}{\text{the minimum of } (Z'_T , Z'_{TH} , Z'_D)} - 1 \right] \times 100$$

$$D'_{Z2} = \frac{| Z'_T - Z'_{TH} |}{\text{the minimum of } (Z'_T , Z'_{TH})} \times 100$$

$$D'_{Z3} = \frac{| Z'_L - Z'_{LH} |}{\text{the minimum of } (Z'_L , Z'_{LH})} \times 100$$

$$D_p = \left[\frac{\text{the maximum of } (Z_p , F)}{\text{the minimum of } (Z_p , F)} - 1 \right] \times 100$$

$$D_{Lp} = \left[\frac{\text{the maximum of } (Z_{Lp} , F_L)}{\text{the minimum of } (Z_{Lp} , F_L)} - 1 \right] \times 100$$

Lever Arm Effective Depth Ratios:

j : the ratio of the lever arm (the distance between the centre of the total compressive force and the centre of the total tensile force) to the effective depth (d).

j_T , j_H , j_D , j_p : j values resulting from the moments M_T , M_H , M_D and, $M_p + M_D$, respectively.

j_L : $Z_L/A_s(h-d_{pt})$

j_{LH} : $Z_{LH}/A_s(h-d_{ph})$

j' : the ratio of the depth of the centre of the total compressive force to the effective depth of the section. [$j' = 1 - j$]

Simulated Stresses and Strains, and Their Relative Differences:

S_{RT} : the centroidal stress range, based on the combined load modulus (F), which is caused by the maximum total moment (M_T), in N/mm^2.
[$S_{RT} = M_T/F - f_{sd}$]

S_r , S_{RL} : the centroidal stress range, based on the live load modulus (F_L), which is caused by the maximum live load moment (M_L), in N/mm^2.
[$S_r = S_{RL} = M_L/F_L$]

$$D_S = \left[\frac{| S_{RT} - S_{RL} |}{\text{the minimum of } (S_{RT} , S_{RL})} \right] \times 100$$

f_{ss} : the total centroidal stress, caused by the moment M_T , in N/mm^2.
[$f_{ss} = S_r + f_{sd}$]

e_{ss} : the centroidal reinforcement strain which corresponds to the total centroidal stress f_{ss} .

e_{sse} : the strain in the outer layer of bars.
$[e_{sse} = S_F \times e_{ss}]$

f_{sse} : the total outer bar stress which corresponds to the outer bar strain e_{sse} , in N/mm^2.

S_{re} : the outer bar stress range, caused by the moment M_T , in N/mm^2.
$[S_{re} = f_{sse} - f_{sde}]$

S_{RHT} : the centroidal stress range, based on the combined load modulus (F), which is caused by the average total moment (M_H), in N/mm^2.
$[S_{RHT} = M_H/F - f_{sd}]$

S_{rh} , S_{RHL} : the centroidal stress range, based on the live load modulus (F_L), which is caused by the average live load moment ($0.5\ M_L$), in N/mm^2.
$[S_{rh} = S_{RHL} = 0.5\ M_L/F_L]$

$$D_{SH} = \left[\frac{|S_{RHT} - S_{RHL}|}{\text{the minimum of } (S_{RHT} , S_{RHL})} \right] \times 100$$

S_{rhe} : the outer bar stress range, caused by the moment M_H , in N/mm^2.

f_{sel} : the limiting outer bar stress which gives a stress range equivalent to the endurance limit of the outer layer of bars, in N/mm^2.
$[f_{sel} = S_e + f_{sde}]$

f_{sl} : the limiting centroidal stress which corresponds to the stress f_{sel} , in N/mm^2.

e_{sl} : the centroidal strain which corresponds to the stress f_{sl} .

Relative Differences between The Actual and The Simulated Stress Ranges

D_f : the relative difference between the actual and the simulated centroidal stress ranges, caused by the maximum total moment (M_T), is N/mm^2 .

$$[D_f = \left(\frac{S_r - f_{sr}}{\text{the minimum of } (S_r , f_{sr})}\right) \times 100]$$

D_{fe} : as above, but for the outer bar stress ranges.

$$[D_{fe} = \left(\frac{S_{re} - f_{sre}}{\text{the minimum of } (S_{re} , f_{sre})}\right) \times 100]$$

D_{fh} : the relative difference between the actual and the simulated centroidal stress ranges, caused by the average total moment (M_H), in N/mm^2.

$$[D_{fh} = \left(\frac{S_{rh} - f_{srh}}{\text{the minimum of } (S_{rh} , f_{srh})}\right) \times 100]$$

D_{fhe} : as above, but for the outer bar stress ranges.

$$[D_{fhe} = \left(\frac{S_{rhe} - f_{srhe}}{\text{the minimum of } (S_{rhe} , f_{srhe})}\right) \times 100]$$

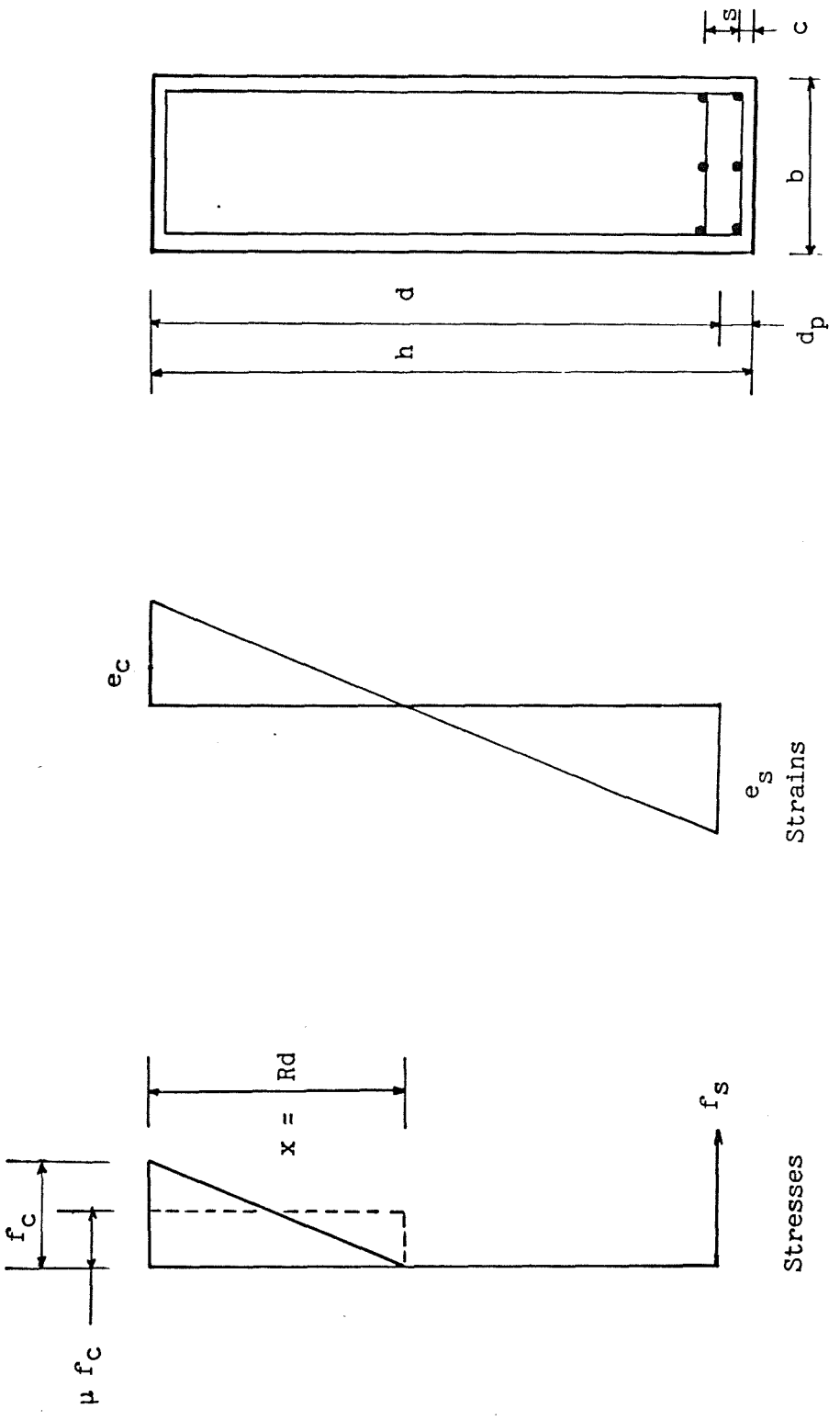

Figure (I) - The strain and stress diagrams for singly reinforced concrete section

CHAPTER 1

INTRODUCTION

Current methods for designing reinforced concrete structures to resist fatigue damage are less advanced than those for steel structures. Fatigue damage control in reinforced concrete structures is achieved mainly by keeping reinforcement stress ranges below a limiting value (1, 14, 23). On the other hand, concern about fatigue of concrete structures has recently increased because of new uses of concrete. In some types of structures, occasional overloadings are to be expected, whilst the full design loading may be repeated for a large number of cycles (14).

The aim of this study is to investigate life deterioration of reinforced concrete bridges, in rural areas, with simply supported short spans, subjected to simulated single lane truck loading. The relationship between the fatigue life in years and the section modulus has been investigated, for a set of specified bridge beams, of different span lengths (L), subjected to different rates of repeated loading (U), resulting from traffic passing across the bridge, defined in terms of Trucks per hour.

The section modulus which is defined here as the ratio of the applied moment to the induced stress in the reinforcement, has been calculated by designing the bridge beams using the limit state theory and varying the design stress in the reinforcement. The section modulus is believed to have a direct relationship with the fatigue life (40), as it incorporates the effect of the stress in the reinforcement and the applied moment associated with a certain truck model and span length.

By making use of the available statistical data based on previous traffic surveys (35), the truck models have been simulated by the Monte Carlo method assuming the trucks' gross weights and their arrival times on the bridge are normally and exponentially distributed respectively, as established by previous researchers (37, 38, 39, 40, 42).

The time sequence of maximum and minimum moment values (moment spectrum) has been obtained by passing the truck model across the bridge. By designing the bridge section to resist the absolute maximum moment of the spectrum, with a specified design stress in the reinforcement, the section modulus has been defined and is used to convert the moment spectrum into a reinforcement stress spectrum.

Fatigue parameters have been established experimentally (7,50) using samples tested under constant amplitude stress cycles. In order to use a predicted stress spectrum as a basis for the design, the spectrum must be reduced to a series of equivalent cycles and half cycles; a process which is known as cycle counting.

In this study, the rainflow method (7,52) has been used to perform the stress cycle counting. From the counted cycles, the fatigue life has been estimated using Palmgren - Miner's linear rule, applied to the characteristics of the outer layer of the particular steel reinforcement used. It is well established that, in most cases, compressive stress changes in concrete do not lead to a significant chance of fatigue failure and it is the steel which governs the fatigue life of reinforced concrete structures.

Bridges with 15 - 20 m spans are very common in highway systems. In this study, the fatigue lives of bridges with 15.0, 17.5 and 20.0 m spans have been investigated. Also the fatigue lives of two longer spans of 25.0 and 27.5 m have been investigated to examine the effect, on the fatigue life, of the higher dead load stresses, which then arise.

BS5400 specifies that the number of trucks, that are assumed to travel along a single carriageway lane of a bridge, may be taken to be (1.5×10^6) per year ($\sim$ 170 Trucks per hour). In this study three rates of truck frequency (U) have been used for the analysis (90, 180 and 360 T/hr.)

The calculations, which have been carried out, result in a relationship which can be expressed graphically in the form shown in Figure (1.1). Here we plot Log(life in years) against the section modulus of the beam as a single line for each combination of values of beam span (L) and frequency of loading (U).

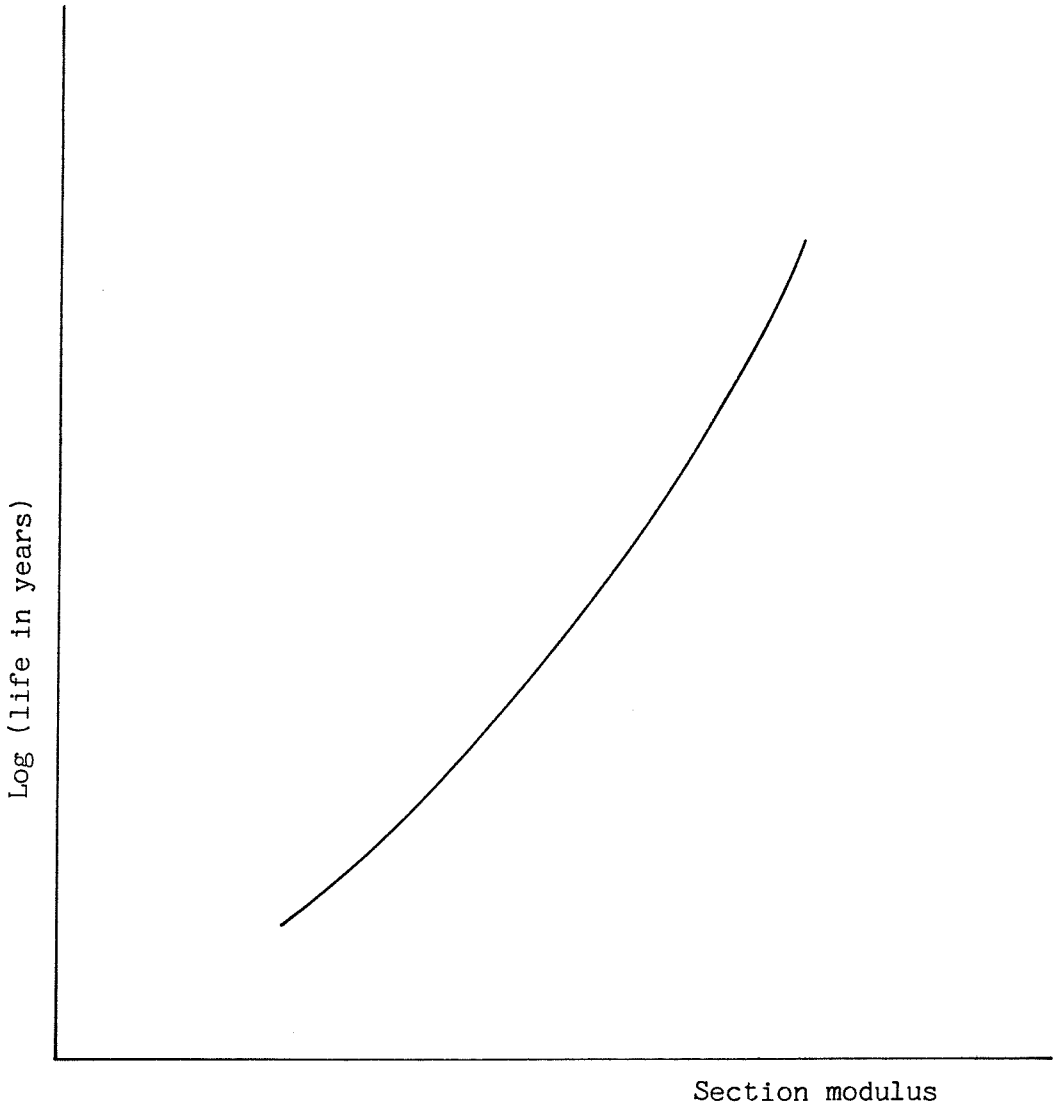

Figure (1.1) : Log(life) - Section modulus curve for a specific value of span (L) and rate of loading (U)

The Log (life) - Section modulus curves may be used to estimate the section modulus required to give a specified design fatigue life to a bridge beam. Knowing the required section modulus and the design moment, the resulting design stress in the reinforcement can be determined. The beam can therefore be dimensioned so that the actual maximum stress in the reinforcement does not exceed that needed to achieve the required fatigue life.

CHAPTER 2

FATIGUE OF MATERIALS UNDER REPEATED LOADING

2.1 Fatigue in General

Fatigue is the damage caused to structural elements by the repeated applications of a load which is insufficient to induce failure by a single application (1, 2).

The fatigue phenomenon is a very complex one, and fatigue studies have shown that its damage depends on many parameters. The effect, of the stress spectrum parameters such as the mean stress, the stress peaks and the low stress amplitudes, on the fatigue life of a specimen has been observed by many investigators (3).

Fatigue in metals is usually caused by stress cycles whose values are higher than a limiting value described as the 'fatigue endurance limit'. Below this stress limit, the material can sustain a very large, or even a nominally infinite number of loading cycles, without failure.

Apparently, the material behaviour, when subjected to a large number of low amplitude stress cycles, is different from that under a small number of high amplitude stress cycles. The latter case, known as low cycle fatigue, is distinguished by macroscopic cyclic plastic straining of the material, which does not occur under low loading (5,6). Plasticity is non linear and history (path) dependent and it is this property which appears to carry over to low cycle fatigue, in which the stress-strain relations are cyclic dependent.

For low cycle fatigue (which might be considered for metals to occur in less than 10^5 cycles), a straight line relationship (5) between the strain and the number of cycles to failure on a log-log scale has been noted (Coffin - Manson law). It takes the form:-

$$\Delta e \, N^m = C$$

where:

Δe = strain range (presumably maximum principal direct strain range)

N = number of cycles to failure

m,C = material constants

For the case of small loads, and therefore a large number of cycles to failure, known as high cycle fatigue, the relationship between the number of cycles to failure (N) and the stress range (S) (Wohler or S-N curve) can be approximated in metals (7) by the equation:

$$NS^q = K$$

where K and q are constants which depend upon the material concerned and the design detail (stress concentrations, weld joint, etc.).

Many theories have been proposed to represent fatigue cumulative damage in quantitative terms, but each theory has its own shortcomings. These result from the assumptions introduced to simplify the many complications associated with the fatigue process.

Interest was shown in the fatigue of metals (4) as early as 1829 when Albert subjected mine hoist chains to repeated proof loadings. Even so, after 150 years we are still far from reaching the stage of having a full understanding of the process and a technique to evaluate the fatigue cumulative damage in an accurate and reliable way. In the following sections, some of the methods developed to estimate fatigue damage are described.

2.1.1 Palmgren - Miner's Method (8)

This method is the most well known and widely used in current engineering practice. The method is based on the assumption that the phenomenon of cumulative damage to a specimen under repeated loading is related to the net hysteresis work absorbed by the specimen. The number of loading cycles applied, expressed as a percentage of the number to failure at a given stress level, would be the proportion of useful life expended. When the total damage, as

defined by this concept, reaches 100 percent, the specimen should fail by fatigue. The method is expressed mathematically as :

$$\sum \frac{n_i}{N_i} = 1$$

where, n_i is the number of cycles applied at stress S_i and N_i is the average value of the number of stress cycles to cause failure at stress S_i (the stress level S_i is, of course, greater than the fatigue endurance limit S_e) .

It is known that this method does not give an accurate prediction of fatigue life. Numerous tests have shown that the average damage sum $[D = \sum (n_i/N_i)]$ at failure may be sometimes considerably higher or lower than unity. Use of the minimum value of the number of stress cycles to failure, instead of the average value N_i , improves considerably the safety of using this method (3).

2.1.2 Inoue - Nakagawa's Method (9)

Inoue and Nakagawa have assumed that the hysteresis loop of an element subjected to fully reversed straining (zero mean strain) is as shown in Figure (2.1). Also they have assumed that when an element is subjected to n cycles of constant strain amplitude e_a , the form of the hysteresis loop is constant during the life of the element. Consequently the total strain energy of the element (which is represented by the area enclosed by the hysteresis loop) is a function of the yield strain e_i .

It has been assumed that fatigue failure takes place when the strain energy accumulated in the most defective element, having the maximum hysteresis loop, reaches a certain value. This value has been found experimentally to be constant with respect to the variation in the strain amplitude.

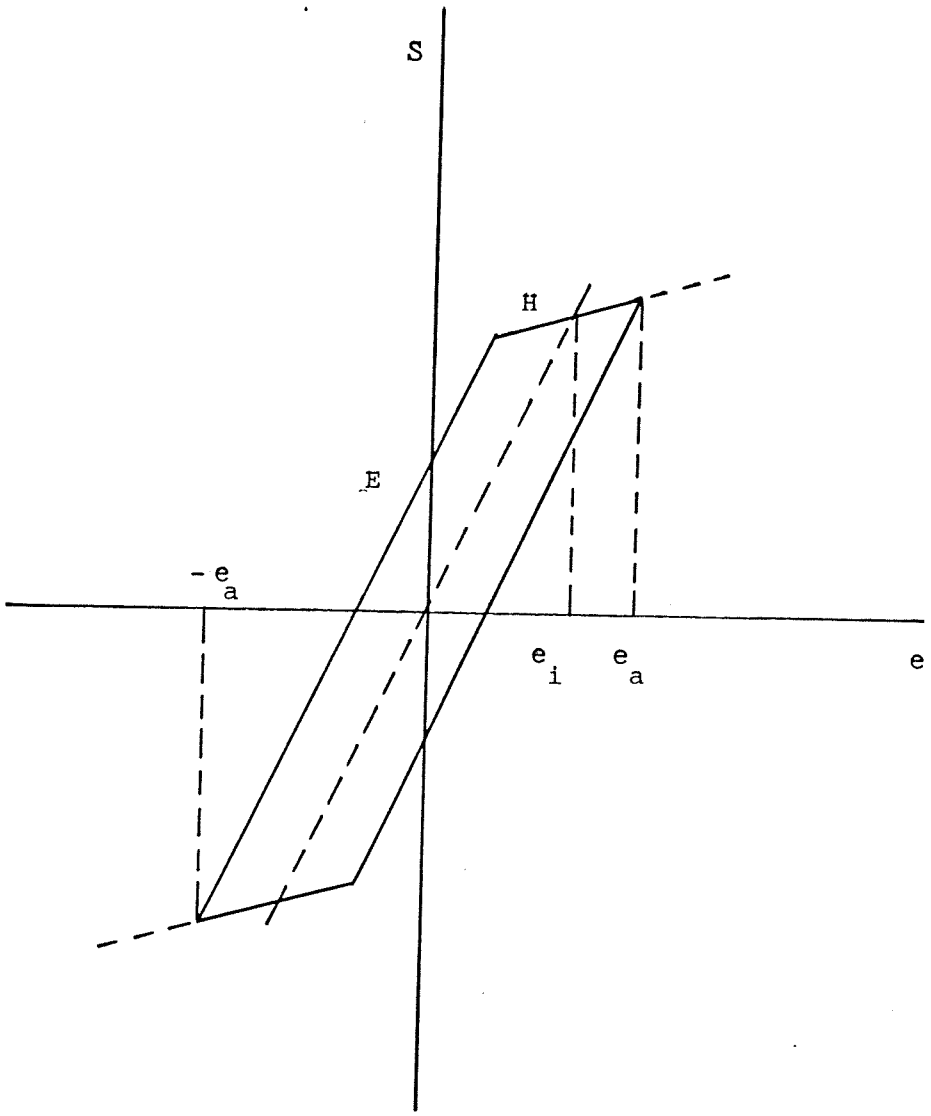

Figure (2.1)

Stress-strain hysteresis loop of an element with yield strain e_i

The method is expressed mathematically as :

$$\sum \frac{n_i}{\sqrt{N_{SC} N_i}} = 1$$

where n_i , N_i have been defined previously and $N_{SC} = \sum n_i$. Derivation of the aforementioned equation is given in Appendix A.

The aforementioned two methods neglect many factors, amongst which are possible changes in the value of the fatigue endurance limit, the stress amplitudes below the initial fatigue endurance limit and the loading sequence, all of which appear to have an effect (3, 10).

The fatigue endurance limit for a virgin specimen is normally higher than that for a similar specimen with a prior loading history. However, in some strain-aging materials, an appropriate sequence of loading may raise the fatigue endurance limit. Stress amplitudes below the initial fatigue endurance limit, in most cases, add to the damage and should be accounted for (10).

Change of the loading sequence (without changing other loading parameters) affects the damage sums. These are mostly larger than unity in the tests performed by applying low stress amplitudes followed by high stress amplitudes. They are usually smaller than unity in the tests performed by applying high stress amplitudes followed by low stress amplitudes. However there are some cases where a reversed sequence of effects has been observed (3).

Palmgren - Miner's method is the only cumulative damage method presently used in the design of structures. Numerous attempts have been made to develop more comprehensive methods which account for other effects, but these methods have had little real success in practical component design (3). However, for completeness, some of these methods are described briefly here.

2.1.3 The Double Linear Damage Method (10)

In this method, originally developed by Manson et al (10), the damage sum $[D = \sum (n_i/N_i)]$ is applied separately for the crack initiation and crack propagation stages. Failure is assumed to occur when the sum is equal to unity for both stages.

The number of cycles, required for the crack propagation stage, N_g is expressed, in terms of the number of cycles to failure N, by the relation:

$$N_g = g\, N^a$$

where g and a are constants. Consequently, the number of cycles, required for the crack initiation stage, N_o is given by :

$$N_o = N - N_g = N - g\, N^a$$

Failure occurs when,

$$\sum \frac{n_o}{N_o} = 1 \text{ for the initiation stage}$$

and

$$\sum \frac{n_g}{N_g} = 1 \text{ for the propagation stage}$$

where n_o and n_g are the number of cycles applied under the initiation and propagation stages respectively.

Manson et al (10) have suggested that, at a certain high stress level corresponding to a value of N smaller than a specified value N_s , the effective crack is assumed to exist from the first cycle,
(i.e. for $N < N_s$, $N_o \approx 0$).

In the light of some experimental results,the constants a and g for metals have been assumed to be equal to (0.6) and (14) respectively. Consequently :

$$N_s = (14)^{\frac{1}{1-0.6}} \simeq 730 \text{ cycles}$$

It follows that for any high stress for which the number of cycles to failure (N) is less than (730) cycles, the effective crack is assumed to exist from the first cycle.

An extension of this method has been made by Bui - Quoc and Biron (11), to predict the cumulative damage effect under strain controlled fatigue at high temperatures.

2.1.4 Henry's Method (12)

In order to evaluate the decrease in the fatigue endurance limit resulting from repeated loading, Henry (12) has assumed that the S - N curve for a steel specimen can be represented for moderate stress values by :

$$N = \frac{K_o}{S - S_{eo}}$$

where K is a material constant, K_o is its value for the virgin material and S_{eo} is the endurance limit for the virgin material.

He has assumed also that, when fatigue damage accumulates, the new K value is proportional to the new endurance limit value, S_e . Also, at failure the endurance limit is assumed to be zero. Consequently the damage ratio D (a dimensionless parameter whose value is (0) for the virgin material and (1) at failure) may be defined by :

$$D = \frac{S_{eo} - S_e}{S_{eo}}$$

Making use of the aforementioned assumptions, D can be expressed as :

$$D = \frac{n/N}{1 + \frac{S_{eo}\,(1-n/N)}{S - S_{eo}}}$$

2.1.5 Gatt's Methods (13)

Gatt's method (13) is similar to Henry's method. Instead of assuming that the endurance limit (S_e) is zero at failure, Gatt's has assumed that its value at any stage is a constant fraction of the material strength. At failure, the material strength is equivalent to the stress S which causes the failure. Hence, the endurance limit at failure can be given by :

$$S_e = C.S$$

where C is a material constant, whose value can be found by assuming that the stress causing failure in the first cycle is equivalent to the ultimate tensile strength S_u (i.e.; $C = S_{eo}/S_u$).

Also, he has assumed that the energy associated with a stress above the endurance limit, and with a strain in excess of the strain corresponding to the endurance limit, is proportional to the damage caused by the nth cycle. This energy has been assumed to represent the decrease rate of the strength with respect to time. By representing the stress-strain curve, from the endurance limit to the maximum stress of the cycle, by a straight line, it has been found that the endurance limit S_e is given by :

$$S_e = S\left[1 - \frac{1}{\frac{n/N}{1-C} + \frac{S\,(1 - n/N)}{S - S_{eo}}}\right]$$

In this method, a damage ratio D (whose value is (0) for the virgin material and (1) at failure) may be defined by :

$$D = \frac{S_{eo} - S_e}{S_{eo} - CS}$$

2.2 Fatigue of Concrete

2.2.1 Fatigue of Plain Concrete

Investigations have shown that the fatigue life of concrete, tested in compression under a constant amplitude loading, with the stress f varying from the same minimum to different maxima, may be considered to vary linearly with the maximum stress of the cycle (14). Apparently there is no endurance limit below which, the plain concrete will sustain an infinite number of load cycles (4, 14, 15, 16, 17,18).

For concrete in compression, the relation between the maximum and minimum stress, f_{max} and f_{min} respectively, and the corresponding number of cycles to failure N, is given (14) for design purposes as :

$$\log N = \frac{1 - f_{max}/f'_c}{q(1 - f_{min}/f_{max})} - 1.9$$

where f'_c is the compressive strength, and the constant q is approximately equal to (0.0685).

Another design equation for the fatigue of concrete in compression is recommended by the Japan Society of Civil Engineers (14) as follows:

$$f_{max} - f_{min} = (0.9\ k\ f'_c - f_{min})\ (1 - \frac{\log N}{15})$$

where k is a coefficient taken equal to (0.85) to cover the differences in strength between standard cylinders and in-place concrete.

For cyclic tension, it has been shown (14) that the fatigue strength under loadings producing tension is about the same as for compression. Cyclic loading from compression to tension has been reported to be more damaging than zero - to - tension loadings (14).

Material parameters such as cement content, water/cement ratio, curing conditions, and age at loading, have been found (14) to affect fatigue strength in a proportionate manner to the static strength of the concrete.

For concrete submerged in salt water, it has been reported that the fatigue strength of concrete is reduced (14).

2.2.2 Fatigue of Reinforced Concrete

Fatigue of reinforcing bars occurs as a result of the initiation and propagation of a crack under cyclic loading. It has been found that the reinforcing elements will be more likely to limit the life of the member than the concrete itself (4, 14, 19, 20, 22). This is particularly true in the case of members subjected to predominantly flexural high-cycle, low-amplitude loadings between (10^3) and (10^7) cycles (14). Laboratory data, from tests on bars in air and on bars embedded in concrete beams, have shown that most test results on bars in air are generally a little lower than on bars from the same lot embedded in a concrete beam (14).

It has been found, from numerous tests which incorporated variations of the effects of the stress range, minimum stress, bar diameter, size of beam and grade of bar, that the stress range is the predominant factor in determining the fatigue life of the reinforcing bars (14, 16, 20, 21). The minimum stress level is also significant (14, 21).

For design purposes, it has been concluded that there is a limiting stress range which may be taken as a fatigue endurance limit. At stress ranges above this limit, a reinforcing bar will have a finite life, while below this limit the bar will have a very long life and may be able to resist an unlimited number of cycles. The transition from the finite life to the long life region occurs in the range of one to two million cycles (14, 21).

Other variables that are important, from a design viewpoint, are the geometry of deformations on the bar, radius of bends, welding and corrosion. Other factors such as bar size, type and orientation, yield strength and chemical composition, have been reported to have only minor effects (14, 19, 21).

Also the fatigue strength, of the main reinforcement in straight reinforced concrete beams of sound normal weight concrete, has been found not to be affected by the beam dimensions or the concrete strength and modulus, except as they affect the reinforcement stresses (20, 21).

Because of its effect in reducing the fatigue strength of bars, it is advisable to avoid welding in construction that will be subjected to repetitive loads (14). Where welding cannot be avoided, reference should be made to fatigue design criteria for comparable welded details in structural steel (1, 14).

Based on a study of deformed bars, made by four different U.S. manufacturers, which has included tests on (353) concrete beams, each containing a single straight test bar as the main reinforcement, the following equation has been developed to determine the limiting service load stress range in the long life region, below which fatigue damage is unlikely to occur in straight hot rolled bars with no welds:

$$f_f = [145 - 0.33 f_{min} + 55 (r/h)] \quad \text{in N/mm}^2 \quad ....(2.1)$$

In this equation, f_f is the limiting stress range, f_{min} is the minimum stress level (positive when tensile). (r/h) is the ratio of base radius to height of rolled on transverse deformations (0.3 to be used when the actual value is not known). This equation includes an adjustment to represent approximatley a 95 percent probability that 95 out of a hundred test results will exceed.

Although the above mentioned equation is a lower limit for bars, made by U.S. manufacturers, conforming to ASTM designation A615, it is believed to be reasonably applicable to other reinforcing bars, whose surface geometry has not been controlled in a manner that assures higher fatigue strength (14). This equation has been adopted, in U.S. design specifications, to define the maximum allowable range between a maximum tension stress and a minimum stress, in straight reinforcement bars, caused by live service load plus impact (14).

It is recommended that no bends in primary reinforcement shall be allowed at locations where the stress range is near the above limit f_f .

An equation has been also developed for a safe fatigue life (14, 21), for all stress ranges above the endurance limit represented by Equation (2.1). This equation is given as :

$$\log N = 6.1044 - 591\ (10)^{-5} f_r - 200\ (10)^{-5} f_{min} + 103\ (10)^{-5} f_u - 8.77\ (10)^{-5} A_s + 0.0127\ d(r/h) \quad \ldots\ (2.2)$$

where f_r is the stress range in N/mm^2 , f_u is the ultimate strength of the steel bar in N/mm^2 , A_s is the area of the bar in mm^2 and d is the nominal diameter of the bar in mm. Other terms have been defined previously.

Equation (2.2) may be used to design a reinforcing bar for a safe fatigue life resulting from stress ranges above the endurance limit. However, such design must be cautious because of the potential for brittle fracture due to a sudden overload, after a fatigue crack has been initiated (21). Moreover, Eq.(2.2) has been developed, as a result of an extensive testing programme (14, 21), to give a safe

fatigue life. Even though, because of the wide scatter associated usually with fatigue tests, it is unrealistic to assume that it will necessarily give absolute safe results for other testing programmes carried out under different or even similar conditions.

Equations (2.1) and (2.2) should be used cautiously in circumstances where time-dependent effects (like severe salt water corrosion and extreme temperature conditions) may change the reinforcing bars properties.

Equations (2.1) and (2.2) are adopted in this study and have been used, with Palmgren - Miner's rule, to predict the fatigue lives of 32 and 25 mm straight hot rolled reinforcing bars whose yield stress is, fy = 425 N/mm^2. For such bars, an average value of 730 N/mm^2 has been used (20, 21) for the ultimate strength (f_u).

This study deals with simply supported bridges, and if we neglect the beneficial negative stresses (compressive) caused by the trucks' dynamic effects, then the value of f_{min} used becomes the positive stress (tensile) caused by the bridge dead load. Assigning the above values for the parameters in Equations (2.1) and (2.2), with (r/h = 0.3), gives the following two equations :

$$f_f = 161.5 - 0.33\, f_{min} \quad \ldots\ (2.3)$$

$$\log N = A_N - 200\,(10^{-5})\, f_{min} - 591\,(10^{-5})\, f_r \quad \ldots\ (2.4)$$

where, A_N = 6.9077 for 32 mm bars and 6.9085 for 25 mm bars.

2.2.2.1 Low Cycle Fatigue of Reinforced Concrete

Most of the previous research has been directed toward high cycle-low amplitude fatigue loading in the range of (1000 - 10^7) cycles (14). Low cycle - high amplitude fatigue loading of less than (1000) cycles may occur as a result of earthquakes or other events that cause a loading of the structure beyond its normal service load.

Under a low cycle - high amplitude loading, the influence of the time dependent conditions should be expected to remain inelastic with increasing residual deformations.

A recent study has been carried out at the University of Southampton (24). This involved testing seven beams, reinforced with one straight unwelded hot-rolled 16 mm deformed bar. From these tests, which have been performed under about (85 - 95) percent of the collapse load; whose value has been determined experimentally by testing a proto-type beam, the following has been concluded:

1- The applied repeated load has to be higher than the yield load, if the beam is to fail in about (100) cycles. This means that beams are reasonably safe for up to (100) cycles,provided that the repeated loads cause steel stress which are lower than the yield stress.

2- Reinforced concrete beams can withstand safely a (100) cycles of about 92 percent of the collapse load.

3- Cracks are formed in the concrete when the load is about 25 percent of the collapse load. Once they are formed, the cracks widen very slowly until the beam is about to collapse. Also, cracks are formed initially with a considerable length, but their propogation is very slow. Significant inclined cracks are also formed in both shear spans.

4- All beams have exhibited an under-reinforced form of failure.

2.2.3 Fatigue of Prestressed Concrete

Fatigue of prestressing tendons is similar to that of bars in that it occurs as a result of the initiation and propagation of a crack under cyclic loading. But it is generally accepted that a sufficient level of prestressing prevents or limits the extent of flexural cracking, and adherence to static limitations is believed to preclude the possibility of fatigue failure (14). This is mainly because, in prestressed concrete, the steel stress fluctuations under load are proportionally very much less than those experienced by reinforcing steel in reinforced concrete structures.

CHAPTER 3

SIMULATION

Simulation is the imitation of a real situation by some form of model. The principal advantage of the simulation is to determine the effects of the changes in the system variables on a specific parameter, where analytical formulation is not available and experimental procedure is not possible or expensive and time consuming (27). To investigate the fatigue life of bridges under truck loading, the Monte Carlo method can be used to simulate trucks' weights and arrival times. This can be achieved by defining probability distributions which represent adequately these system random variables, as demonstrated in the following sections.

3.1 Probability and Probability Functions

If we suppose that in a sequence of n trials of a certain experiment, the event E occurs n_E times, then the probability of occurrence of E is given (25) by:

$$p(E) = \lim_{n \to \infty} (n_E/n)$$

For a random variable X, $(X_L \leq X \leq X_U)$, we define:

$$P(a \leq X \leq b) = \int_a^b f(x)\, dx$$

where the function (f), denoted as the probability density function (p.d.f.), satisfies the following conditions (26):

(a) $f(x) \geq 0$ for all $X_L \leq x \leq X_U$ and

(b) $$\int_{X_L}^{X_U} f(x)\, dx = 1$$

The distribution function or cumulative distribution function (as it is sometimes called) of the random variable X, (which is the probability of getting a value of X smaller than or equal to a certain value), is denoted as F and defined by:

$$F(x) = P(X \leq x) \text{ for all } X_L \leq x \leq X_U \text{ , then (26) :}$$

$$F(x) = \int_{X_L}^{x} f(x)\,dx \qquad 0 \leq F(x) \leq 1$$

3.2 The Monte Carlo Simulation

The Monte Carlo method is a new numerical procedure which takes advantage of the high speed of the digital computer in solving complex science and engineering problems. The Monte Carlo method predicts the final outcome by substituting for a random variable a set of actual values having the statistical properties of the random variable. The substituted values are called random numbers, on the grounds that they could have been produced by chance by a suitable random process (28).

3.3 Generation of Random Numbers

In practice, a sequence of uniformly distributed random numbers is usually required. The cumulative distribution function for the uniform distribution is defined as:

$$F(x) = \begin{cases} 0, & x \leq 0 \\ x, & 0 < x < 1 \\ 1, & x \geq 1 \end{cases}$$

The following methods have been used by practitioners to generate sequences of random numbers

1. Manual methods
2. Library tables
3. Computer methods

Manual methods are the simplest but the least practicable of the methods because they are too slow for general use. They include mechanical and electronic devices, coin flipping, dice rolling, card shuffling and roulette wheels. These methods have the disadvantage that it is impossible to reproduce a sequence of random numbers generated by such devices.

A number of library tables of random numbers have been published. These numbers must first be generated by one of the aforementioned methods. This method is slow and has the disadvantage that some problems require more random numbers than have been published. Also, using the same random data for every problem might sometimes be unacceptable.

Computers are capable of generating random numbers with repeatable or unrepeatable sequences. Congruential methods are widely used to generate random numbers. They are based on a fundamental congruence relationship which may be expressed as the recursive formula given by Equation (3.1), [Two integers a and b are congruent modulo m if their difference is an integral multiple of m. The congruence relation is expressed by the notation, $a \equiv b \pmod{m}$].

$$n_{i+1} \equiv a\, n_i + c \pmod{m} \qquad \ldots (3.1)$$

where n_i, a, c and m are all non-negative integers. Three basic methods have been developed by using different versions of Equ.(3.1). These methods are the additive congruential method, the multiplicative congruential method, and the mixed congruential method.

The additive congruential method assumes k starting values, where k is a positive integer and computes a sequence of numbers using the following relation:

$$n_{i+1} \equiv n_i + n_{i-k} \pmod{m}$$

This is the only method that gives periods larger than m.

The multiplicative congruential method computes a sequence $[n_i]$ of non-negative integers, each less than m, using the relation:

$$n_{i+1} \equiv a\, n_i \pmod{m}$$

The multiplicative method has been found to behave quite well statistically. That is, frequency tests and serial tests, as well as other tests for randomness, when applied to sequences generated by this method indicate that the random numbers are uncorrelated and uniformly distributed. It is possible to impose conditions on the multiplier (a) and the starting value (n_o) to insure a maximum period for sequences generated by this method. From the integers in the sequence $[n_i]$, rational numbers in the unit interval (0,1) can be obtained by forming the sequence $[r_i] = [n_i/m]$

Numbers obtained using Equation (3.1) with a and c both greater than zero are said to be generated by the mixed congruential method. This method has some small advantages over the multiplicative method in terms of increased computational speeds (29, 30, 31, 32, 33).

In this study the built-in routine G05CBF of the ICL 2976 computer at the University of Southampton has been used. This routine generates numbers between (0) and (1) with repeatable sequence by the multiplicative congruential method. Procedures with repeatable sequence have the advantage of allowing checking process to be performed, if desired.

G0CBF sets the internal variable N used by another routine G05CAF to a value calculated from any integer I:

$$N = 2\,I + 1$$

It then calls G05CAF to shuffle N.

G05CAF computes random real numbers taken from a uniform distribution between (0) and (1). The routine uses a multiplicative congruential method:

$$N = 13^{13} \; N \pmod{2^{59}}$$

C05CBF will give different subsequent sequences of random numbers if called with different values of I, but the sequences will be repeatable in different runs of the calling program (34). The standard cycle length of this routine (31) is (2^{57}).

3.4 Generation of Random Variates

Two methods have been used in this study to generate random variates.

3.4.1 The Inverse Transformation Method

If we wish to generate random variates (x_i's) from some particular statistical population whose density function is given by f(x) and distribution function is given by F(x), since:

$$0 \leq F(x) \leq 1$$

then, we can generate uniformly distributed random numbers ($0 \leq r \leq 1$) and put:

$$F(x) = r$$

which gives: $x = F^{-1}(r)$

where $F^{-1}(r)$ is the inverse transformation (31).

For many probability distributions, it is impossible to express x in terms of $F^{-1}(r)$. In such case, we may use the rejection method.

3.4.2 The Rejection Method

If f(x) is a (p.d.f.) and if x is bounded and has a finite range say: $a \leq x \leq b$. The rejection method requires the following steps:

(a) Normalize the range of f(x) by a scale factor m such that:

$$m.f(x) \leq 1 \qquad a \leq x \leq b$$

(b) Define x as a linear function of r, where $0 \leq r \leq 1$:

$$x = a + (b-a)\, r \qquad \ldots (3.2)$$

(c) Generate pairs of random numbers (r_1, r_2).

If $r_2 \leq m.\ f(a+ (b-a)\ r_1)$, then the pairs are accepted and $(x = a + (b-a)r_1)$ is the required random variate. This is because the probability of r_2 being less than or equal to m. f(x) is:

$$P(r_2 \leq m.f(x)) = m.f(x)$$

Consequently if x is chosen at random from the range (a,b) according to Equation (3.2) and then rejected if $r_2 > (m.f(x))$, the (p.d.f.) of the accepted (x's) is exactly f(x) (31, 32).

3.5 Traffic Simulation

Bridges are generally designed to carry a static vertical load caused by a design truck plus a given increase to include the dynamic effects (1, 35, 36). Even when passenger cars are constituting the major part (42, 45) of traffic (in number), they are usually disregarded because of their insignificant contribution to the induced stresses (1, 37).

To simulate the traffic, the variation of the following factors should be investigated (37, 38, 39):

1. Multiple presence of trucks
2. Truck gross weight
3. Truck type with the axle spacings and axle load fractions

It has been found (37, 38, 40) that a wide variety of truck types could be combined into a limited number of truck types with specified axle load fractions and axle spacings.

3.5.1 Truck Classification

Heins (35) has concluded that trucks in the U.S.A. could be classified as shown in Figure (3.1). His work has been based on numerous field surveys. For each truck type, the following parameters have been specified:

1. Average gross weight
2. Standard deviation of the gross weight
3. Range of the gross weight

The average frequency of these truck types relative to the location of the road system (Metropolitan, Urban, Rural) is shown in Table (3.1).

Heins' study (35) has been based on data collected in the U.S.A. in and before 1972. An extensive literature survey has been undertaken by the author to get some more updated related data. For the same purpose, the specialised authorities in the U.K. have been approached. Unfortunately, it seems that such data are unavailable.

Comparing Figure (3.1) and Table (3.1) with vehicles of 5, 4, 3 and 2 axles given by Table (11) of BS5400: Part 10: 1980, given here at Fig. (3.2), reveals that there is a reasonable agreement between the data given by BS5400 and those given by Figure (3.1) and classified in Table (3.1) as the metropolitan traffic. Vehicles with more than five axles are given by BS5400 : Part 10 : 1980

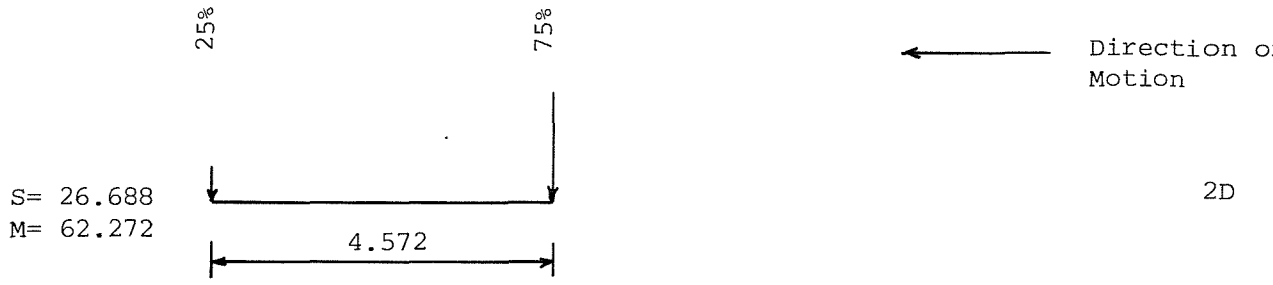

22.24 ≤ G.W. ≤ 222.40

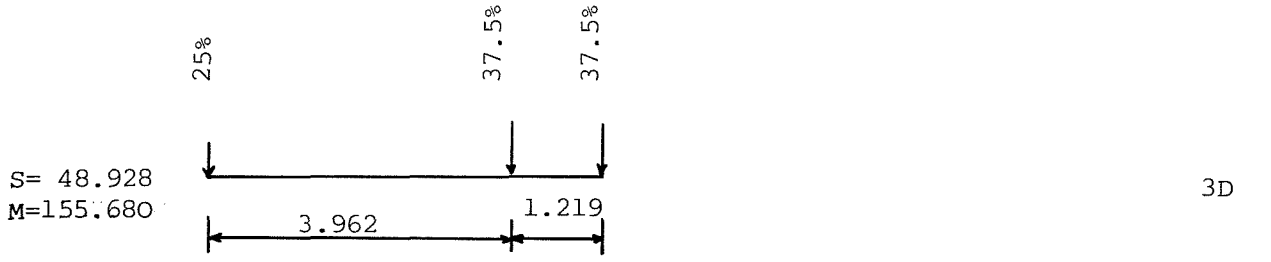

44.48 ≤ G.W. ≤ 355.84

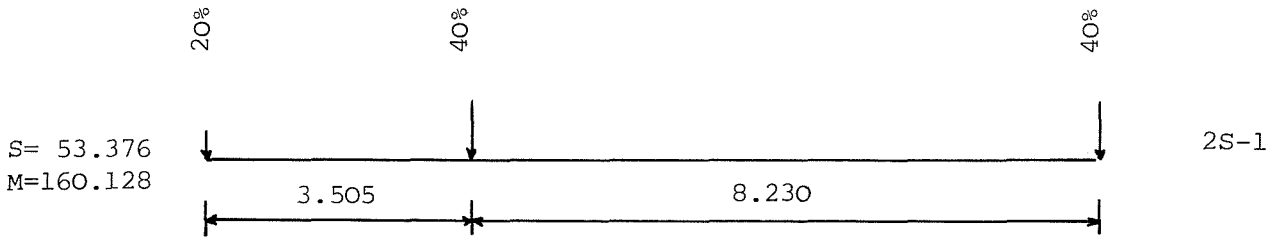

44.48 ≤ G.W. ≤ 400.32

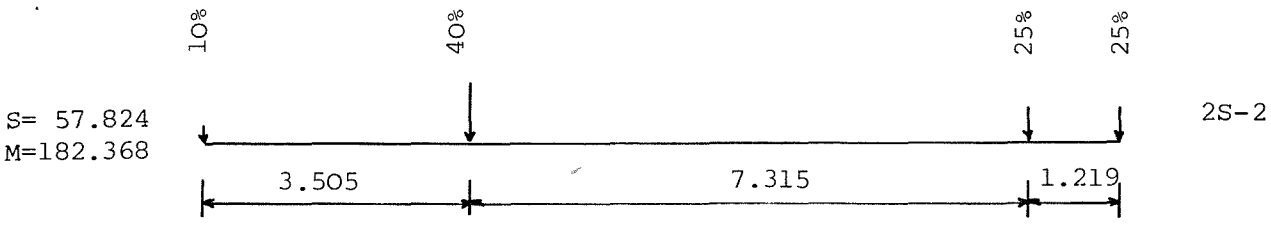

44.48 ≤ G.W. ≤ 444.80

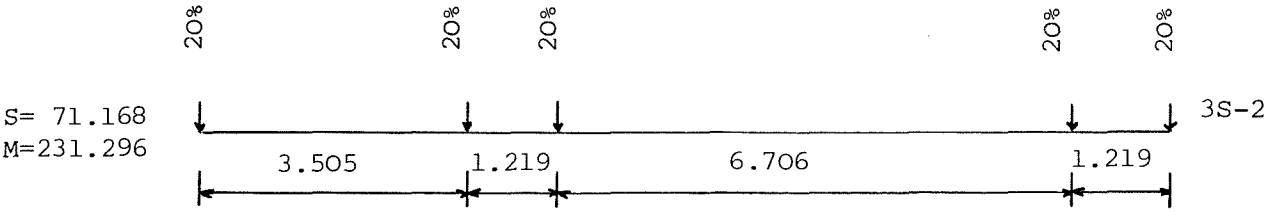

88.96 ≤ G.W. ≤ 533.76

Figure (3.1)
Typical truck types
(all dimensions in metres)

G.W. = The gross weight (KN)
S = The standard deviation of G.W. (KN)
M = The mean G.W. (KN)

Truck Type	Metropolitan	Urban	Rural
2D	35.0	13.0	21.0
3D	23.0	3.0	6.0
2S-1	6.0	10.0	7.0
2S-2	11.0	30.0	25.0
3S-2	25.0	44.0	41.0

Table 3.1 Average Distribution of Trucks by Type

Table 11. Typical commercial vehicle groups

Total axles	Chassis type	Average axle spacings, m	Loading Group	Total weight, kN	Axle loads, kN	No. in each group per million commercial vehicles	Vehicle designation
18	Girder Trailer and 2 tractors	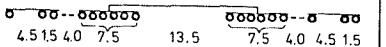	H	3 680	80 160 160 240 (6 no.) 240 (6 no.) 80 160 160	10	18GT-H
			M	1 520	80 160 160 60 (6 no.) 60 (6 no.) 80 160 160	30	18GT-M
9	Tray Trailer and tractor	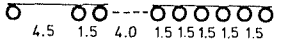	H	1 610	70 140 140 210 210 210 210 210 210	20	9TT-H
			M	750	50 110 110 80 80 80 80 80 80	40	9TT-M
7	Girder Trailer and tractor	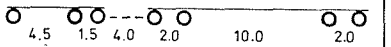	H	1 310	70 140 140 240 240 240 240	30	7GT-H
			M	680	60 130 130 90 90 90 90	70	7GT-M
	Articulated	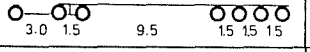	H	790	70 100 100 130 130 130 130	20	7A-H
5		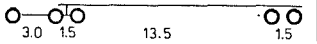	H	630	70 130 130 150 150	280	5A-H
	Articulated	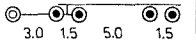	M	360	60 70 70 80 80	14 500	5A-M
			L	250	40 45 45 60 60	15 000	5A-L
4	Articulated	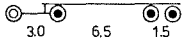	H	335	55 100 90 90	90 000	4A-H
			M	260	45 85 65 65	90 000	4A-M
			L	145	35 50 30 30	90 000	4A-L
	Rigid	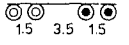	H	280	50 50 90 90	15 000	4R-H
			M	240	40 40 80 80	15 000	4R-M
			L	120	20 20 40 40	15 000	4R-L
3	Articulated	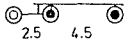	H	215	45 85 85	30 000	3A-H
			M	140	30 55 55	30 000	3A-M
			L	90	20 35 35	30 000	3A-L
	Rigid	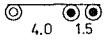	H	240	60 90 90	15 000	3R-H
			M	195	55 70 70	15 000	3R-M
			L	120	40 40 40	15 000	3R-L
2	Rigid		H	135	50 85	170 000	2R-H
			M	65	30 35	170 000	2R-M
			L	30	15 15	180 000	2R-L

Key. ◉ Standard axle, 4 tyre, 1.8 m track ◎ Steering axle, 2 tyre, 2.0 m track O Special axle, 2 to 8 tyres, up to 3.4 m outer track

Figure (3.2) - Typical truck groups (BS 5400)

to constitute 0.022 percent of the total truck traffic. Consequently, truck data for rural traffic given by Figure (3.1) and Table (3.1) have been adopted. In this study, only bridges in rural areas have been considered, because it is possible to assume that rural traffic is reasonably smooth and without jams. Traffic smoothness makes it reasonable to assume that the probability density of headway time (time lapse between trucks passing a point) may be represented by a negative distribution as demonstrated in the following section.

3.5.2 Multiple Presence of Trucks

Multiple presence is controlled by headway distances between trucks, and it is primarily dependent upon the length of the bridge and truck traffic volume (38, 39). It is almost independent of other parameters, like truck speed and time of day. Based on observations of truck traffic moving on several highways, it is assumed (39,40) that the probability density of headway time may be represented by a negative distribution which is shown in Figure (3.3):

$$f(t) = Ue^{-Ut} \qquad 0 \leq t < \infty$$

where $f(t)$ is the probability distribution function and U is the average number of trucks per unit of time.

Obviously, due to the physical nature of the situation, t cannot be less than a certain minimum value. Harman and Davenport (39) have assumed a distance of 7.30 m to account for a minimum clearance between the trucks and to account for the projections of the trucks beyond their rear and front axles. Since truck speed is not a significant factor in determining the probability of multiple presence (38), a constant speed of 50 km/hr has been assumed in this study. This means that the minimum headway time, for the front axle of a certain truck, is dependent on the length of the truck preceding it, as shown in Table (3.2).

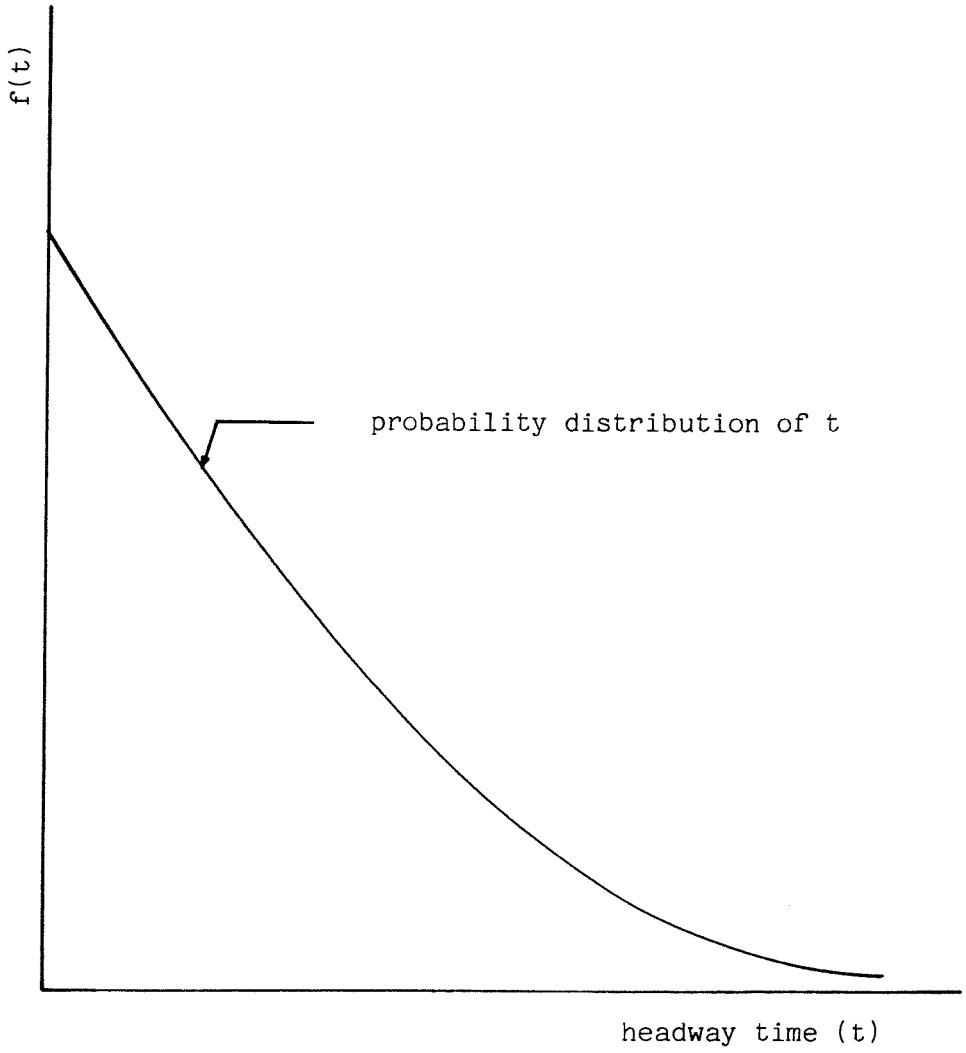

Figure (3.3)

The form of the probability distribution function of the headway time (t)

Truck Type	t_{min} for the following truck (sec)
2D	0.855
3D	0.899
2S-1	1.371
2S-2	1.392
3S-2	1.436

Table 3.2 Minimum Headway Time (Front Axle)

A truncation factor, T_f , should be introduced to account for the minimum headway time, and to make the total area under the truncated curve = 1.0, making the probability distribution function as below:

$$f(t) = T_f \; U \; e^{-Ut} \qquad t_{min} \leq t$$

where $$\int_{t_{min}}^{+\infty} T_f \; U \; e^{-Ut} \, dt = 1.0$$

then $$T_f \left[-e^{-Ut} \right]_{t_{min}}^{+\infty} = 1.0$$

$$T_f \; e^{-U \, t_{min}} = 1.0$$

so $$T_f = e^{U \, t_{min}}$$

therefore $$f(t) = Ue^{U(t_{min} - t)} \qquad t_{min} \leq t$$

The cumulative distribution function F(t) is obtained as below (F(t) is the probability that the time between successive trucks is less than or equal to t)

$$F(t) = \int_{t_{min}}^{t} U \; e^{U(t_{min} - t)} \, dt$$

$$F(t) = \left[- e^{U(t_{min} - t)} \right]_{t_{min}}^{t}$$

$$F(t) = 1 - e^{U(t_{min} - t)} \qquad t_{min} \leq t$$

Since F(t) exists in explicit form, the inverse transformation technique provides a straight forward method to generate the random variate t. Because of the symmetry of the uniform distribution, F(t) and [1- F(t)] are interchangeable (31). Therefore :

$$r = 1 - F(t) = e^{U(t_{min} - t)} \qquad t_{min} \leq t$$

Consequently

$$t = t_{min} - \frac{\ln(r)}{U} \qquad 0 \leq r \leq 1$$

To avoid the situation of getting infinite time resulting from (r = 0), the computer has been instructed to consider all values of r less than (1.2×10^{-77}) to be equal to (1.2×10^{-77}) rather than zero (in the ICL 2900 series, all values in the range, $- 1.2 \times 10^{-77}$ to $+ 1.2 \times 10^{-77}$ approximately, are held as zero (41)). This involves an error in the order of (1.2×10^{-77}) which is negligible by all practical measures. By doing so, the maximum time simulated by the computer is :

$$t_{max} = \frac{177}{U} + t_{min}$$

(for U = 360 Trucks/hr., $t_{max} \approx \frac{1}{2}$ hr)

3.5.3 Truck Gross Weight (GW)

Truncated bimodal composite normal and normal distributions have been suggested by researchers to represent the gross weight (37, 38, 39, 42). In this study a normal distribution with the truncation of the upper and lower tails has been adopted. The following distribution (shown in Figure 3.4) represents the probability density function of the gross weight for each truck type:

$$f(w) = \frac{T_w}{S\sqrt{2\pi}} e^{-\frac{(w - M)^2}{2S^2}} \qquad W_L \leq w \leq W_U \qquad \ldots\ (3.3)$$

Figure (3.4) - The truncated normal probability distribution curve of trucks' gross weights (w), compared to the histogram values generated by the rejection method

o represents histogram generated values

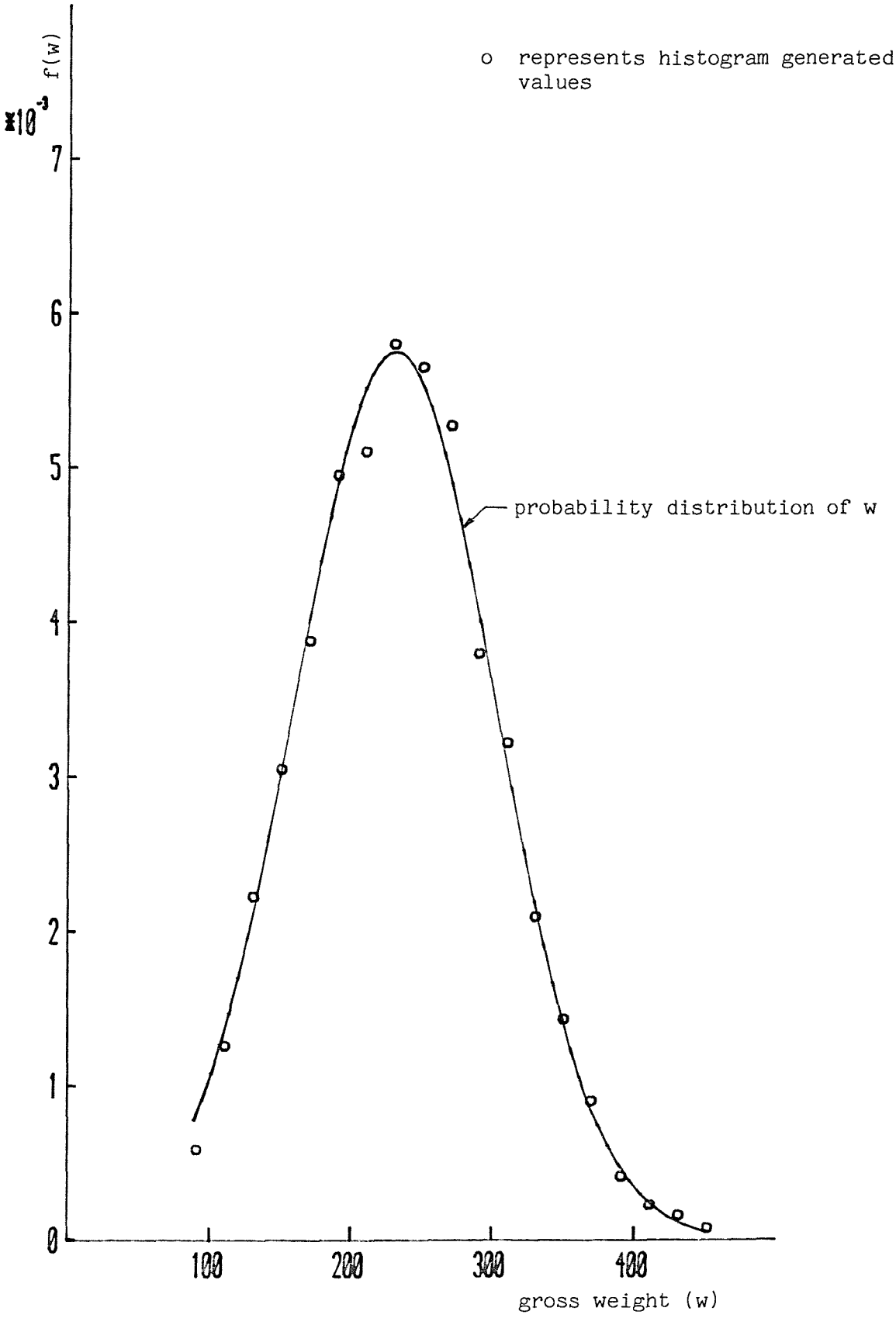

where T_W is a truncation factor introduced to make the total area under the truncated curve = 1.0 .

Because F(w) cannot be expressed explicitly as a function of w and since w varies within a finite range, then the rejection method has been used to generate the random variate w. If m is the scale factor required to normalize the range of f(w) (Section 3.4.2), then:

$$m\, f(w) \leq 1 \qquad W_L \leq w \leq W_U$$

but $$f(w)_{max} = \frac{T_W}{S\sqrt{2\pi}}$$

then $$m = \frac{S\sqrt{2\pi}}{T_W}$$

and $$m\, f(w) = e^{-(w - M)^2/2\, S^2}$$

In Figure (3.4), the curve is for the truncated normal equation representing the gross weight of Truck type (3S-2), while the plotted circles represent a histogram obtained by analysing truck weights (5970 values) generated by the rejection method. As can be seen, the agreement seems to be very good. Values of the truncation factors for the truck types are not needed in the simulation, even so, their values are given here in Table (3.3). These values have been calculated from Eq. (3.3), using the statistics tables for the normal curve (43).

3.5.4 Dynamic Factor

When a truck crosses a simply supported bridge, the maximum deflection is increased by about 12 percent above the static value, due to the dynamic effects. When two closely spaced similar trucks cross the bridge, the maximum response is 70 percent larger than the static response due to one of the vehicles alone (40). The dynamic factors depend on vehicle speed and the dynamic characteristics of both bridge and vehicle (40). For design purposes, an impact factor

is used to allow for the dynamic effects of the traffic loading. In Japan, the impact fraction I of the live load is given by:

$$I = \frac{20}{50 + L}$$

where L is the span length (42).

In this study, impact factor is determined by the following equation used in the U.S.A.:

$$I = \frac{50}{L + 125}$$

where I is the impact fraction and L is the length in feet. The impact value is limited (44) to a maximum value of 30 percent.

Truck Type	T_f (for the gross weight distribution)
2D	1.0716
3D	1.0116
2S-1	1.0153
2S-2	1.0087
3S-2	1.0233

Table 3.3 Truncation Factors for The Gross Weight Distribution

3.5.5 Truck Type Selection

From Table (3.1), trucks type (2D) represent 21 percent of the total truck rural traffic. This means that :

the probability of getting trucks longer than 2D = 0.79

similarly :

the probability of getting trucks longer than 3D = 0.73
the probability of getting trucks longer than 2S-1 = 0.66
the probability of getting trucks longer than 2S-2 = 0.41
the probability of getting trucks longer than 3S-2 = 0.00

If uniformly distributed random numbers are generated such that $(0 \leq r \leq 1)$, then the probability of getting $r_1 < r \leq r_2$ is simply equal to $(r_2 - r_1)$.

By this, it is possible to make the following assumption (for rural traffic):

if $0.00 \leq r \leq 0.41$ then truck type is 3S-2
if $0.41 < r \leq 0.66$ then truck type is 2S-2
if $0.66 < r \leq 0.73$ then truck type is 2S-1
if $0.73 < r \leq 0.79$ then truck type is 3D
if $0.79 < r \leq 1.00$ then truck type is 2D

3.6 Simulation of The Moment Spectrum

As mentioned in Chapter (1), the simulated bridge has been assumed to be a single lane simply supported bridge. The span has been varied to investigate its effect on the fatigue life of the bridge (7). Fatigue life has been investigated for bridges with five different span lengths (L), subjected to three different rates of repeated loading (U) resulting from traffic passing across the bridge and defined in terms of Trucks per hour. The simulated truck models generated by the Monte Carlo method have been assumed repeating itself every week (40).

As shown in the preceding sections, the types of trucks, their weights and arrival times have been simulated by the Monte Carlo simulation method. This method requires the generation of random numbers and in this case, these have been obtained using a routine, GØ5CBF (I), which exists in the University ICL computer. When running this routine, the set of random numbers produced by it depends upon specifying a positive integer I. The set produced lies between (0.0) and (1.0) and each set is repeatable by specifying the same integer I, when the program is run.

For our purposes four different sets of random numbers have been required. The first specifies the types of trucks. The second specifies the arrival times, whilst the third and fourth are used to provide random values of the gross weights of the trucks. The need for two sets of numbers is explained in Section (3.4.2).

In order to produce entirely unrelated sets of random numbers, the routine itself has been used to generate the specifying integers I. This has been done by starting with (I = 0) and taking the first four random numbers produced, as the integers for the four working sets (infact multiplied by 1000 and rounded). These four I values have been kept constant regardless of the U value. This makes each single set of the four working sets for a specific value of the loading frequency (U), a part of a larger set for the U value exceeding it. This similarity is believed to be acceptable because it does not affect the randomness of the trucks data for a specific value of U, while on the other hand, it helps to reduce the number of maximum design moments for a specific value of the span (L), as will be shown later.

3.6.1 Time Interval (Dt)

A computer program has been written, which generates a truck model for one week and passes it across the bridge to simulate the moment spectrum for one week. The program examines the bridge at a time interval Dt. If the bridge is loaded, then it calculates the mid span moment and the maximum shears. If the bridge is found unloaded, the program moves the trucks stream and places the front axle of the

next truck on the bridge support. Now, the program starts again to examine the bridge every Dt and so on. A flow chart is given in Figure (3.5).

In order to include as many events as possible, Dt should be taken as small as possible. On the other hand, a very small value of Dt would result in very long computer runs. It is important to find a suitable value of Dt which gives a reasonably accurate moment spectrum without wasting computer time. To choose such value, several trial runs have been made using different values of Dt. Some of the results are given in Tables (3.4), (3.5) and (3.6). In these tables, the moment (M) and shear (V) values represent the total maximum live load moment and shear (including impact), on the bridge.

Dt_1 values in Table (3.6) represent the time required for each single axle to move a distance of L/48. Since trucks' speed has been assumed previously to be 50 km/hr (13.889 m/sec), then Dt_1 in seconds is:

$$Dt_1 = \frac{L}{48} \times \frac{1}{13.889} = 0.0015 \times L$$

where L is the span of the bridge in metres. With such a value of Dt, the duration of the longest computer run is just under the maximum available to the author in the University computer centre. If we establish that this value of Dt gives a reasonably accurate moment spectrum, then we may adopt it as the required Dt value.

Separate runs have been made using a decreased value of (Dt = 0.001 x L) to examine the effect of such decrease on the values of the maximum live load moment and shear, and the number of peaks, N_p, for a simulation period of one week (Tables 3.6 and 3.7).

From Table (3.6), it seems that the shear values are more sensitive to such decrease than the moment values. This is because of the nature of their influence lines (Figure 3.6). For example if two equal loads pass across the bridge, there is an infinite number of positions (from X = L/2 - S to X = L/2), which give the same value of the maximum moment, while maximum shears can be obtained by two

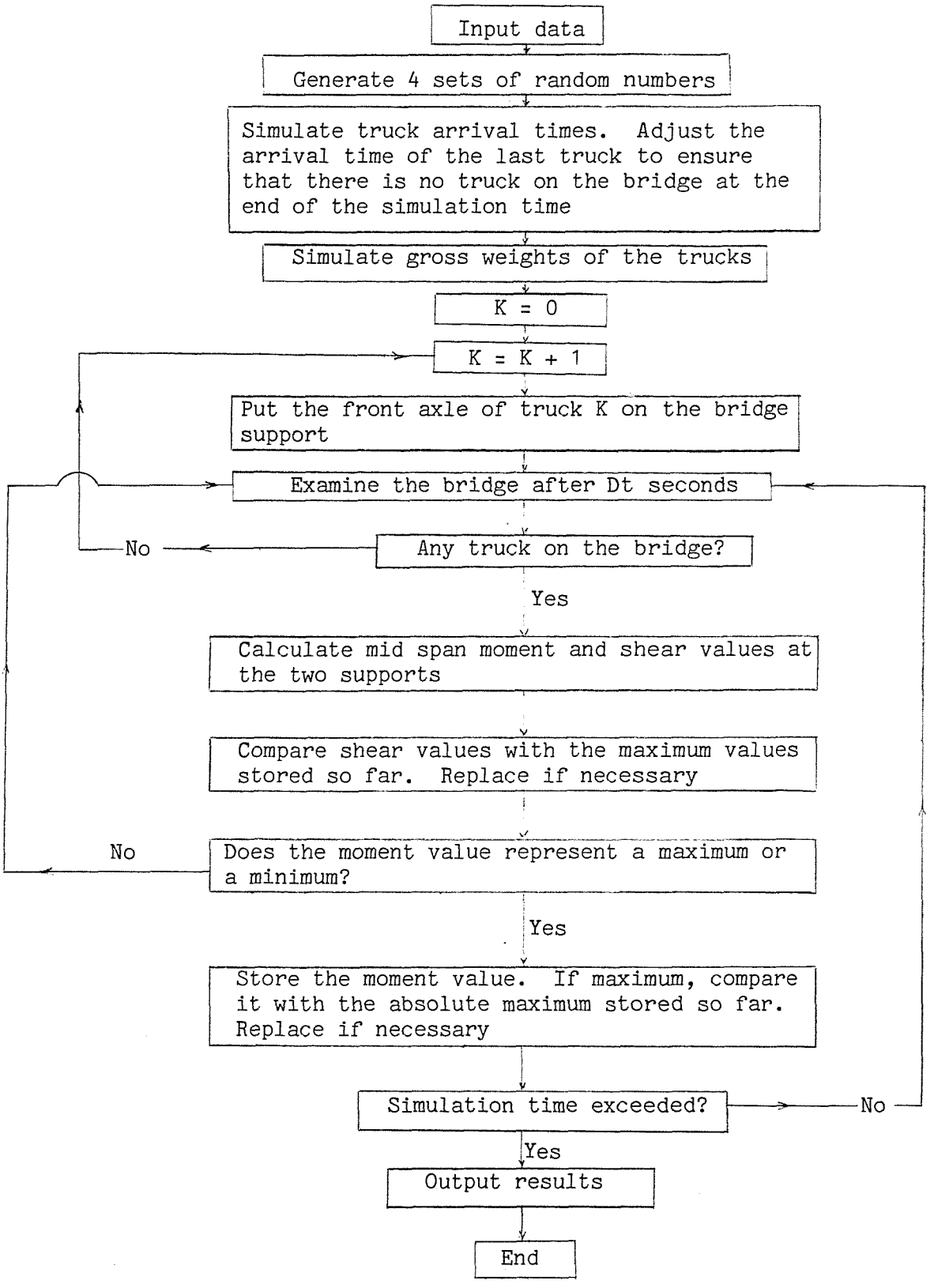

Figure 3.5 - Flow chart of the computer program for the moment spectrum simulation

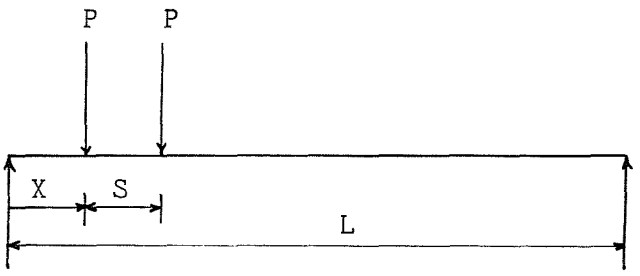

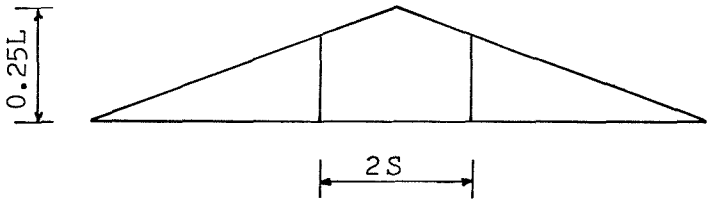

Influence line - mid span moment

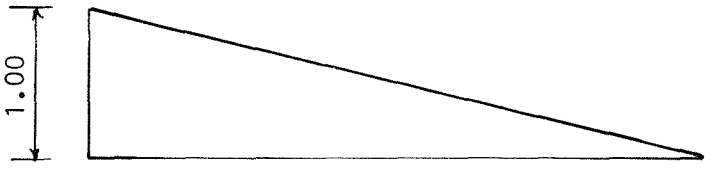

Influence line - shear at L.H. support

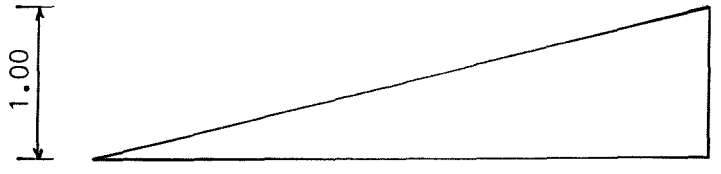

Influence line - shear at R.H. support

Figure (3.6) - Moment and shear influence lines

positions only. Bearing in mind that the moment values and the spectrum are the governing factors in this study and since there are no appreciable differences between the values resulting from Dt = 0.001 x L, and those resulting from Dt = 0.0015 x L, as can be seen from Tables (3.6) and (3.7), then it is believed that the last Dt value is proper and adequate for the purpose of this study.

Moreover, other separate runs have been made to define the type, weight, location and sequence of the truck(s) causing the maximum live load moment (M) and shear (V), for each combination of L and U. This has been done by storing, at every Dt, those particulars related to the truck(s) causing the maximum live load moment. From this information, given in Figures (3.7), (3.8) and (3.9), the real maximum live load moment and shear in one week, can be calculated from their influence lines. In Table (3.9) the real values of M are compared with the values obtained by specifying Dt = 0.0015 x L. The fact that the deviations between these two values are very small, gives more justification for adopting Dt = 0.0015 x L.

Span (m)	Loading frequency (T/hr.)	Dt_1 (sec.)	M_1 (KN.M)	Dt_2 (sec.)	M_2 (KN.M)	M_2/M_1
15.0	360	0.800	1170.378	0.100	1170.378	1.0000
15.0	90	0.105	1122.506	0.100	1135.472	1.0116
15.0	90	0.100	1135.472	0.095	1114.985	0.9820
15.0	90	0.095	1114.985	0.090	1126.547	1.0104
15.0	90	0.090	1126.547	0.085	1117.883	0.9923
15.0	90	0.085	1117.883	0.080	1135.472	1.0157
15.0	90	0.080	1135.472	0.070	1122.506	0.9886
27.5	90	0.150	2947.274	0.100	2938.528	0.9970

Table (3.4)

The effect of the time interval (Dt)
on the maximum live load moment (M)

- M_1 and M_2 are the moment values corresponding to Dt_1 and Dt_2 respectively

Span (m)	Loading frequency (T/hr.)	Dt_1 (sec.)	M_1 (KN.M)	Dt_2 (sec.)	M_2 (KN.M)	M_2/M_1
15.0	$\frac{90}{180}$ +	0.105	1122.506	0.02250	1137.964	1.0138
15.0	360	0.105	1195.116	0.02250	1200.302	1.0043
17.5	all values	0.125	1447.969	0.02625	1473.371	1.0175
20.0	all values	0.140	1802.223	0.03000	1845.783	1.0042
25.0	all values	0.175	2585.956	0.03750	2596.718	1.0042
27.5	all values	0.190	2964.165	0.04125	2955.619	0.9971

Table (3.5)

The effect of the time interval (Dt)
on the maximum live load moment (M)

- M_1 and M_2 are the moment values
corresponding to Dt_1 and Dt_2 respectively

Span (m)	Loading frequency (T/hr.)	Dt_1 (sec.)	M_1 (KN.M)	V_1 (KN)	Dt_2 (sec.)	M_2 (KN.M)	V_2 (KN)	M_2/M_1	V_2/V_1
15.0	90 180+	0.02250	1137.964	370.526	0.01500	1139.934	374.989	1.0017	1.0120
15.0	360	0.02250	1200.302	370.526	0.01500	1204.955	374.989	1.0039	1.0120
17.5	all values	0.02625	1473.371	407.183	0.01750	1467.637	402.765	0.9961	0.9891
20.0	all values	0.03000	1845.783	426.847	0.02000	1854.537	431.224	1.0047	1.0103
25.0	all values	0.03750	2596.718	457.251	0.02500	2590.464	461.556	0.9976	1.0094
27.5	all values	0.04125	2955.619	465.041	0.02750	2955.619	469.314	1.0000	1.0092

Table (3.6) The effect of the time interval (Dt) on the maximum live load moment (M) and shear (V)

- (M_1, V_1) and (M_2, V_2) are the moment and shear values corresponding to Dt_1 and Dt_2 respectively

Span (m)	Loading frequency (T/hr.)	Dt_1 (sec.)	N_{p1}	Dt_2 (sec.)	N_{p2}	N_{p1}/N_{p2}
15.0	360	0.02250	92338	0.01500	92356	1.00019
15.0	180	0.02250	48778	0.01500	48786	1.00016
15.0	90	0.02250	25227	0.01500	25229	1.00008
17.5	360	0.02625	53581	0.01750	53664	1.00155
17.5	180	0.02625	28258	0.01750	28287	1.00103
17.5	90	0.02625	14583	0.01750	14589	1.00041
20.0	360	0.03000	54018	0.02000	54074	1.00104
20.0	180	0.03000	28360	0.02000	28372	1.00042
20.0	90	0.03000	14610	0.02000	14613	1.00021
25.0	360	0.03750	53611	0.02500	53718	1.00200
25.0	180	0.03750	28275	0.02500	28298	1.00081
25.0	90	0.03750	14584	0.02500	14588	1.00027
27.5	360	0.04125	53636	0.02750	53744	1.00201
27.5	180	0.04125	28279	0.02750	28302	1.00081
27.5	90	0.04125	14597	0.02750	14600	1.00021

Table (3.7) The effect of the time interval (Dt) on the number of peak points (Np) of the moment spectrum in one week

- N_{p1} and N_{p2} correspond to Dt_1 and Dt_2

Loading frequency (T/hr.)	Total number of simulated trucks
360	53398
180	28209
90	14578

Table (3.8) The total number of trucks in one week
Simulation time = 1 week

Span (m)	Loading frequency (T/hr.)	M_1 (KN.M)	V_1 (KN)	M_2 (KN.M)	V_2 (KN)	M_2/M_1	V_2/V_1
15.0	90 + 180	1137.964	370.526	1142.286	377.532	1.0038	1.0189
15.0	360	1200.302	370.526	1205.373	377.532	1.0042	1.0189
17.5	all values	1473.371	407.183	1474.356	411.233	1.0007	1.0099
20.0	all values	1845.783	426.847	1854.625	435.282	1.0048	1.0198
25.0	all values	2596.718	457.251	2598.948	466.469	1.0009	1.0202
27.5	all values	2955.619	465.041	2964.238	476.855	1.0029	1.0254

Table (3.9) Real maximum moment and shear values in one week compared to the values associated with Dt = 0.0015 x L

- M_1 and V_1 are the maximum live load moment and shear, including impact, associated with Dt = 0.0015 x L

- M_2 and V_2 are the real maximum live load moment and shear in one week, including impact

Notes Regarding The Following Figures (3.7, 3.8 and 3.9)

1. Direction of motion is from the left to the right.

2. K represents the sequence of each truck in the truck stream generated for one week.

3. X is the distance between the front wheel and the left hand support. X_1 defines the position which gives the maximum simulated live load moment M_1 or shear V_1, with Dt = 0.0015 x L. X_2 defines the position which gives the real maximum moment (M_2) or shear (V_2), in one week.

4. G.W. is the gross weight of the truck.

5. I.F. represents the impact factor = $\frac{50}{125 + 3.281 \times L}$

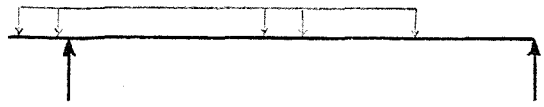

L	=	15.0 m
U	=	90+180 T/hr.
Truck type	=	3S-2
G.W.	=	499.30 KN
K	=	10113
I.F.	=	0.287
Dt	=	0.02250 sec.
X_1	=	10.938 m
M_1	=	1137.964 KN.M
X_2	=	11.005 m
M_2	=	1142.286 KN.M

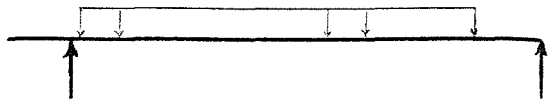

L	=	15.0 m
U	=	90+180 T/hr.
Truck type	=	3S-2
G.W.	=	499.30 KN
K	=	10113
I.F.	=	0.287
Dt	=	0.02250 sec.
X_1	=	12.813 m
V_1	=	370.526 KN
X_2	=	12.649 m
V_2	=	377.532 KN

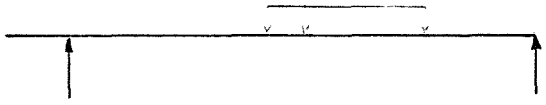

L	=	15.0 m
U	=	360 T/hr.
Truck type	=	3D
G.W.	=	309.49 KN
K	=	28281
I.F.	=	0.287
Dt	=	0.02250 sec.
X_1	=	11.563 m
M_1	=	1200.302 KN.M
X_2	=	11.462 m
M_2	=	1205.373 KN.M

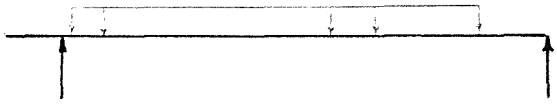

L	=	15.0 m
U	=	360 T/hr.
Truck type	=	3S-2
G.W.	=	499.30 KN
K	=	10113
I.F.	=	0.287
Dt	=	0.02250 sec.
X_1	=	12.813 m
V_1	=	370.526 KN
X_2	=	12.649 m
V_2	=	377.532 KN

Figure (3.7) Details of the maximum moment and shear for L = 15.0 m

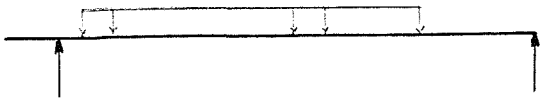

L	=	17.5 m
U	=	all values
Truck type	=	3S-2
G.W.	=	499.30 KN
K	=	10113
I.F.	=	0.274
Dt	=	0.02625 sec.
X_1	=	13.490 m
M_1	=	1473.371 KN.M
X_2	=	13.474 m
M_2	=	1474.356 KN.M

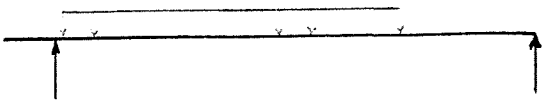

L	=	17.5 m
U	=	all values
Truck type	=	3S-2
G.W.	=	499.30 KN
K	=	10113
I.F.	=	0.274
Dt	=	0.02625 sec.
X_1	=	12.761 m
V_1	=	407.183 KN
X_2	=	12.649 m
V_2	=	411.233 KN

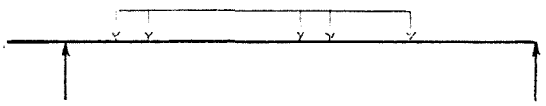

L	=	20.0 m
U	=	all values
Truck type	=	3S-2
G.W.	=	499.30 KN
K	=	10113
I.F.	=	0.262
Dt	=	0.03000 sec.
X_1	=	14.583 m
M_1	=	1845.783 KN.M
X_2	=	14.724 m
M_2	=	1854.625 KN.M

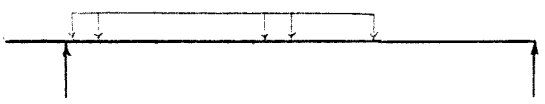

L	=	20.0 m
U	=	all values
Truck type	=	3S-2
G.W.	=	499.30 KN
K	=	10113
I.F.	=	0.262
Dt	=	0.03000 sec.
X_1	=	12.917 m
V_1	=	426.847 KN
X_2	=	12.649 m
V_2	=	435.282 KN

Figure (3.8) Details of the maximum moment and shear for L = 17.5 and 20.0 m

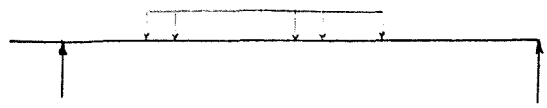

L	=	25.0 m
U	=	all values
Truck type	=	3S-2
G.W.	=	499.30 KN
K	=	10113
I.F.	=	0.242
Dt	=	0.03750 sec.
X_1	=	17.188 m
M_1	=	2596.718 KN.M
X_2	=	17.224 m
M_2	=	2598.948 KN.M

L	=	25.0 m
U	=	all values
Truck type	=	3S-2
G.W.	=	499.30 KN
K	=	10113
I.F.	=	0.242
Dt	=	0.03750 sec.
X_1	=	13.021 m
V_1	=	457.251 KN
X_2	=	12.649 m
V_2	=	466.469 KN

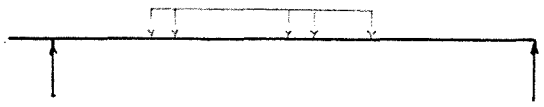

L	=	27.5 m
U	=	all values
Truck type	=	3S-2
G.W.	=	499.30 KN
K	=	10113
I.F.	=	0.232
Dt	=	0.04125 sec.
X_1	=	18.333 m
M_1	=	2955.619 KN.M
X_2	=	18.474 m
M_2	=	2964.238 KN.M

L	=	27.5 m
U	=	all values
Truck type	=	3S-2
G.W.	=	499.30 KN
K	=	10113
I.F.	=	0.232
Dt	=	0.04125 sec.
X_1	=	13.177 m
V1	=	465.041 KN
X_2	=	12.649 m
V_2	=	476.855 KN

Figure (3.9) Details of the maximum moment and shear for L = 25.0 and 27.5 m

3.7 Maximum Probable Moment

As mentioned earlier, the truck model has been assumed repeating itself every week. This assumption is necessary to cope with the available computer resources. Consequently each design moment is the maximum moment, taken from a moment spectrum simulated for one week. This means that the design moment is not necessarily equal to the maximum probable moment which might occur during the bridge life. For sections with highly stressed reinforcement, there is not enough margin to cater for moments larger than the design moment. This implies that we have to check the behaviour of these sections, if subjected to moments higher than the design moment. To do so, we have to estimate for each span length, the amount of the maximum moment which might result from the worst combination of the heaviest trucks shown in Figure (3.1). Table (3.10) shows the details of these combinations.

It should be made clear that checking the effect of the maximum probable moments on some sections, does not reflect the belief in their occurance during the fatigue life of the bridge. On the contrary, it is believed, in fact, that the probability of getting such high moment values is quite low for the shorter spans and very low for the longer spans. This is because for the longer spans, this high moment is caused by the presence of several trucks, each one of which has the maximum gross weight of its type, and all are spaced by the minimum amount of 7.30 m. The joint probability of all these events happening at the same time is very low, indeed.

Notes Regarding Table (3.10)

C_N = the serial number of each truck combination.

N_T = the sequence number of each truck on the bridge. $N_T = 1$, represents the nearest truck to the downstream support.

X = the distance between the front axle and the downstream support.

G.W. = the gross weight of the truck.

M = the mid span live load moment caused by the truck, including impact.

- Truck details are given in Figure (3.1).

- Impact factor $= \frac{50}{125 + 3.281 \times L}$

- The minimum distance from the rear axle of a truck to the front axle of the truck following it, has been assumed to be 7.30 m, as mentioned in Section (3.5.2).

Span (m)	C_N	N_T	Truck type	X (m)	G.W. (KN)	M (KN.M)
15.0	1	1	3D	11.462	355.84	1385.893
17.5	1	1	3S-2	13.474	533.76	1576.111
	2	1	3S-2	0.231	533.76	15.708
		2	3D	12.712	355.84	1655.230
20.0	1	1	3S-2	14.724	533.76	1982.625
	2	1	3S-2	1.481	533.76	99.761
		2	3D	13.962	355.84	1920.308
25.0	1	1	3S-2	17.224	533.76	2778.319
		2	2D	29.096	222.40	49.305
	2	1	3S-2	3.981	533.76	295.468
		2	3D	16.462	355.84	2442.317
		3	3D	28.943	355.84	104.163
	3	1	3S-2	3.981	533.76	295.468
		2	3D	16.462	355.84	2442.317
		3	2D	28.334	222.40	128.236
	4	1	2S-1	3.981	400.32	245.268
		2	3D	16.462	355.84	2442.317
		3	3D	28.943	355.84	104.163
	5	1	2S-1	3.981	400.32	245.268
		2	3D	16.462	355.84	2442.317
		3	2D	28.334	222.40	128.236

Table (3.10a)

The worst loading combinations for 15.0, 17.5, 20.0 and 25.0 m spans

Span (m)	C_N	N_T	Truck type	X (m)	G.W. (KN)	M (KN.M)
27.5	1	1	3S-2	18.474	533.76	3168.820
		2	2D	30.346	222.40	177.344
	2	1	3S-2	18.474	533.76	3168.820
		2	3D	30.955	355.84	183.550
	3	1	3S-2	5.231	533.76	490.827
		2	3D	17.712	355.84	2696.649
		3	3D	30.193	355.84	308.822
	4	1	2S-1	5.231	400.32	428.241
		2	3D	17.712	355.84	2696.649
		3	3D	30.193	355.84	308.822
	5	1	3D	5.231	355.84	395.076
		2	3D	17.712	355.84	2696.649
		3	3D	30.193	355.84	308.822
	6	1	3S-2	5.231	533.76	490.827
		2	3D	17.712	355.84	2696.649
		3	2D	29.584	222.40	255.639
	7	1	2S-1	5.231	400.32	428.241
		2	3D	17.712	355.84	2696.649
		3	2D	29.584	222.40	255.639
	8	1	3D	5.231	355.84	395.076
		2	3D	17.712	355.84	2696.649
		3	2D	29.584	222.40	255.639

Table (3.10 b)

The worst loading combinations for 27.5 m span

CHAPTER 4

DESIGN OF THE BRIDGE BEAMS

As mentioned in Chapter (1), the aim of this study is to find a relationship, between the fatigue life in years and the section modulus, for a set of specified bridge beams under loads due to rural traffic. The section modulus Z is defined as:

$$Z = \frac{M_A}{f_s}$$

where M_A is the total applied moment and f_s is the stress in the reinforcement resulting from M_A . For design purposes, the stress f_s can be estimated using the equations relevant to the adopted design method, for the reinforced concrete beams, as is shown in the following sections.

4.1 The Modular-Ratio Theory

In the modular-ratio (i.e. elastic-stress) theory, the forces on a structure are calculated from the real values of the loads, but the allowable stresses in the reinforcement and the concrete are limited to chosen fractions of their actual strengths, in order to give an adequate factor of safety. To ensure that failure (if it occurs) would be due to the reinforcement yielding, which gives advance warning of failure rather than the explosive concrete crushing, a greater safety factor is used to calculate the allowable concrete stress than that used for the allowable stress in the reinforcement. In this method the strain distribution across the beam section is assumed to be linear and the concrete strength in tension is usually neglected. Also, steel and concrete are assumed to behave perfectly elastically (46).

From the strain diagram in Figure (4.1), it is clear that:

$$\frac{e_c}{x} = \frac{e_s}{d-x} \qquad \ldots\ (4.1)$$

Since steel and concrete are both assumed to behave elastically then:

$$e_c = f_c/E_c$$

$$e_s = f_s/E_s$$

$$M_A = f_s A_s (d - \tfrac{x}{3})$$

$$C = \tfrac{1}{2} f_c bx$$

where E_c and E_s are the moduli of elasticity for concrete and steel respectively, M_A is the moment and C is the total compressive force. Substituting e_c and e_s into Equation (4.1) gives:

$$f_c = R_E f_s \frac{x}{d-x}$$

where $$R_E = \frac{E_c}{E_s}$$

From the equality between the tensile and the compressive forces, we get:

$$C = \tfrac{1}{2} f_c bx = A_s f_s$$

then $$f_c = \frac{2A_s f_s}{bx} = R_E f_s \frac{x}{d-x}$$

and $$R_E bx^2 + 2A_s x - 2A_s d = 0 \qquad \ldots\ (4.2)$$

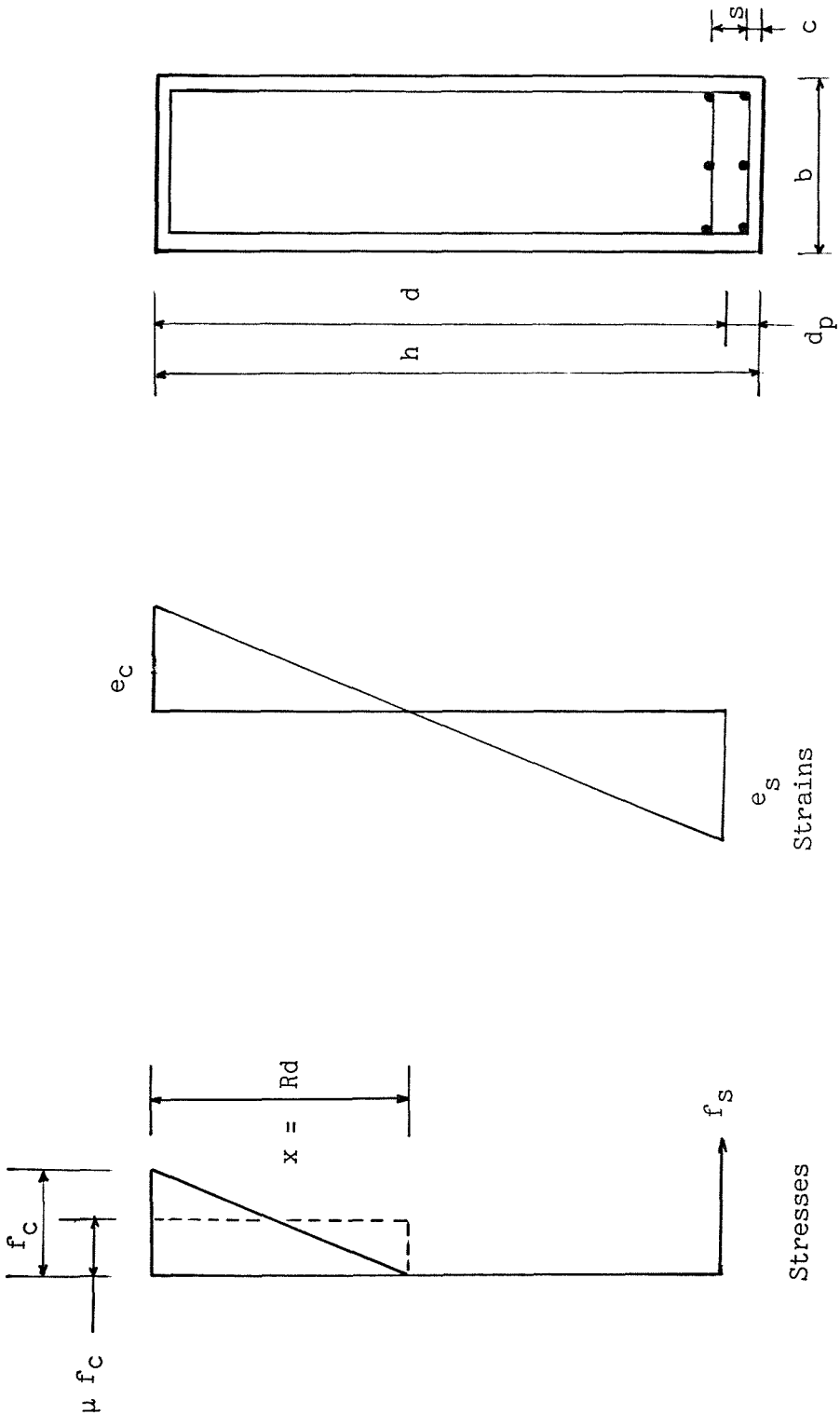

Figure (4.1) - The strain and stress diagrams for singly reinforced concrete section

Equation (4.2) implies that the depth of the neutral axis (x) does not depend on the loading stage (i.e. the amount of the external applied moment). Since:

$$Z = \frac{M_A}{f_s} = A_s \left(d - \frac{x}{3}\right) \qquad \ldots\ldots (4.3)$$

then Z also does not depend on the loading stage. This results directly from the assumption that both the steel and the concrete behave perfectly elastically. This assumption is not acceptable for high stresses (46) and by using this method, it is impossible to estimate accurately the real safety factor (i.e. the ratio between collapse load and service load). To overcome this and other shortcomings, the limit state theory can be used instead.

4.2 The Limit-State Theory

Structures must be designed to sustain safely the loads and deformations which may occur during construction and in use. A structure as a whole or as a part is unfit for use when it reaches a limit state. There are two categories of limit states:

1. The ultimate limit state, which is reached when the structure as a whole or as a part collapses.

2. The serviceability limit states resulting from excessive deflection, cracking, vibration, etc.

In design, the ultimate limit state and the serviceability limit states of excessive deflection and cracking under service loads are normally considered. The structure is usually designed for the ultimate limit state and checked for the serviceability limit states.

Under normal loading, the probability of reaching the ultimate limit state is made very low, say 10^{-6}, while a much higher probability of reaching a serviceability limit state is acceptable (47).

Limit state design is based on the application of statistics to the variations in the loads and the material strengths (47).

4.2.1 Characteristic Strengths and Loads

The compressive strength of concrete specimens, made as identically as possible, may have (47) a coefficient of variation of as high as $\pm$ 10 percent. Therefore, it is not practicable to specify that the concrete or the steel should have a particular precise strength. The characteristic strength (f_k) is that value of the compressive strength of concrete or the yield stress of reinforcement, below which not more than a specified percentage (usually 5 percent) of the test results should fall. Since the strengths of concrete and steel are currently assumed to be normally distributed, then:

$$f_k = f_m - 1.64\ S$$

where f_m is the mean strength, and S is the standard deviation (47).

The characteristic load is that value which has an accepted probability of not being exceeded during the life of the structure. Because of a lack of statistical data, it is not possible at present to define loads in truly statistical terms, and currently the characteristic loads are simply loads accepted by widespread agreement (47).

4.2.2 Partial Safety Factors

The load used for each limit state is called the design load for that limit state. The design load is given as:

$$\text{design load} = G_f \times \text{characteristic load}$$

Where G_f is the partial safety factor for loads. This factor is introduced to cover the probable loading variations in design and construction. It depends on the nature of the limit state under consideration.

Similarly design strength is given as:

$$\text{design strength} = \frac{1}{G_m} \times \text{characteristic strength}$$

where G_m is the partial safety factor for strength appropriate to the material and the limit state (47).

4.3 Beam Section Design for Moment

In this study, the analysis is somewhat different from the classical beam design problem in that the design stress in the reinforcing steel is a parameter which can be varied to affect the fatigue life of the beam. The actual design procedure suggested and used, is based on the limit state theory and the requirements, of BS 5400 : Part 4 : 1984 and CP 110 : Part 1 : 1972, and is as follows.

We start by choosing an initial design steel stress (f_{si}) with a chosen diameter of the reinforcing bars, and a chosen combination of beam span (L) and loading frequency (U). The maximum live load moment, including impact, leads to the basic section design. We note, in passing, that in order to obtain a low dead weight beam, the narrowest and deepest rectangular beam cross section is chosen.

The basic section has to be modified to produce a realistic actual section in which acceptable dimensions (rounded to say 50 mm) are used and the appropriate number of reinforcing bars is chosen.

The dead weight and live load stresses are then computed for the actual beam section, and it is these values which are used for the analytical study.

4.3.1 Design Assumptions

1 - Each bridge is assumed to be a single lane carriageway, the slab of which is supported by two beams. The dead load of the slab, finishes, etc., is estimated to be (25 KN/M) per beam.

The live load moment caused by the traffic has been calculated from a stream of truck axles passing centrally on the slab across the bridge and hence multiplied by ($\frac{1}{2}$) to give the moment supported by each beam.

2 - Material's strength: The following values have been chosen in accordance with common practice:

$$f_y = 425 \text{ N/mm}^2 \quad (23)$$

$$f_{cu} = 50 \text{ N/mm}^2 \quad (23)$$

3 - Partial safety factors have been chosen as follows:

G_m (material factor) = 1.3 for concrete (49)
= 1.0 for steel (49)

G_f (load factor) = 1.0 for dead load (49)
= 1.0 for live load (49)

4 - The beam is rectangular and reinforced in tension only. For such a beam, the depth of the concrete in compression is limited by a reasonable percentage of reinforcement to not more than half the effective depth of the beam (48).

5 - The distribution of the strain across any section is assumed to be linear, i.e. plain sections before bending remain plane after bending, and the strain at any point is proportional to its distance from the neutral axis (46).

6 - The stress - strain relationships of the reinforcing steel and of the concrete are as shown in Figures (4.2) and (4.3) (BS 5400).

7 - The maximum strain in the concrete is (0.0035) and the tensile strength of the concrete is ignored (46).

8 - The reinforcement cover has been chosen to be 20 mm which corresponds to conditions of moderate exposure (46).

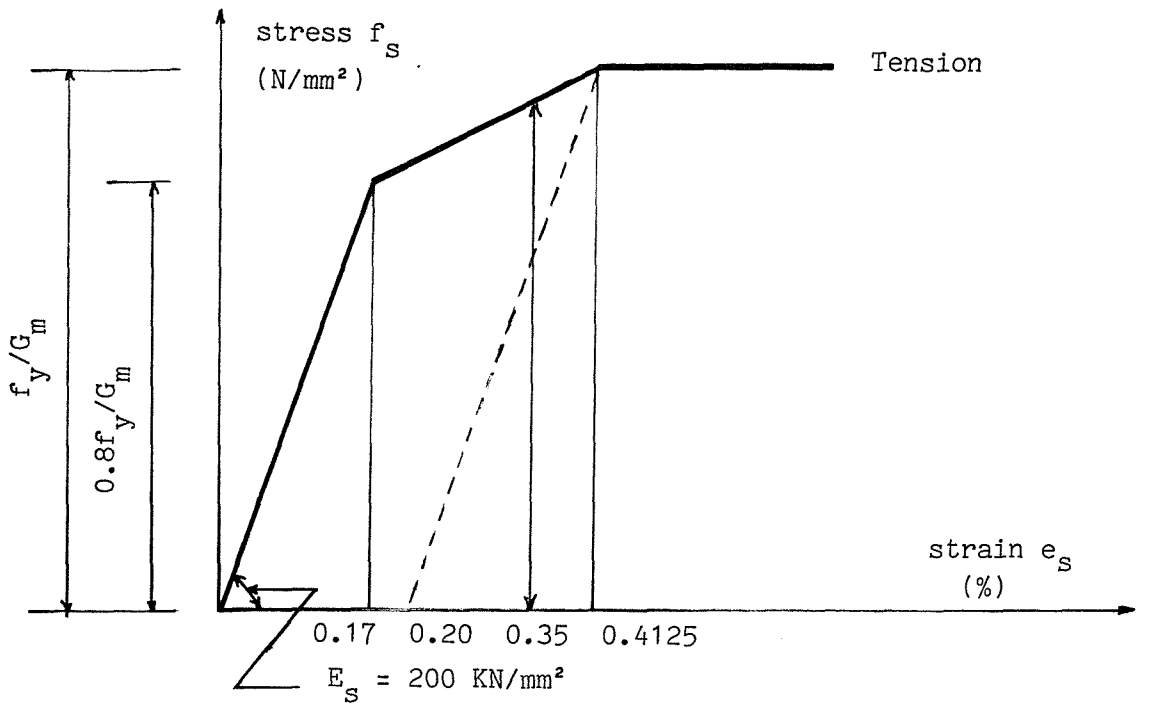

Figure (4.2) : Stress - strain curve of the reinforcement

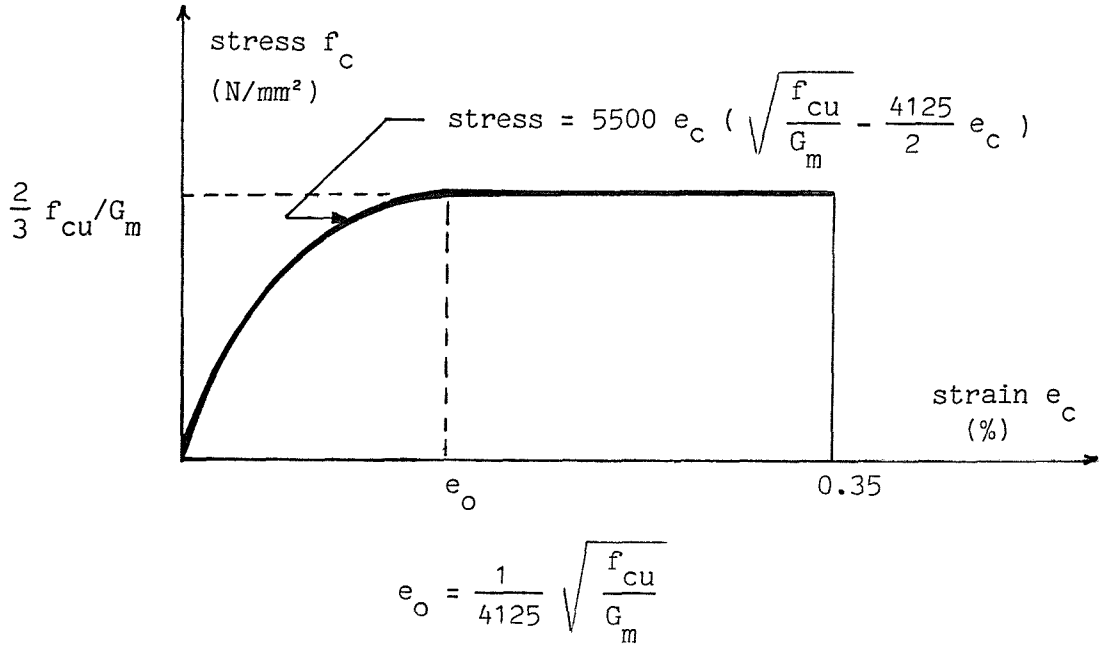

Figure (4.3) : Stress - strain curve of the concrete

4.3.2 Dimensions of The Beam Section

In order to calculate the dimensions of the beam, we shall use the following parameters:

w = unit weight of the concrete = 24 KN/M^3 .

M_L = the maximum mid span moment caused by the live load, including impact.

M_{ds} = mid span moment caused by the bridge dead load other than the beam self weight.

b = the width of the beam.

d = the effective depth of the beam.

h = the height of the beam.

d' = the lever arm of the beam.

x = the depth of the neutral axis.

C = the resultant compressive force in the concrete.

j' = $(d - d')/x$

h' = the distance from the tension face to the centroid of the reinforcement = $h - d$

Then:

$$M_L + M_{ds} + \frac{wb(d + h')\,L^2}{8} = C.d' \qquad \ldots. (4.4)$$

To solve Equation (4.4) for d, both C and d' have to be represented in terms of b and d only. To minimize the beam weight, b, the width, should be taken as small as possible, which leads to d, the depth, being as large as possible. Since BS 5400 : part 4 - clause 5.3.1.3 specifies that the width to span ratio is limited, to avoid lateral instability, so that :

$$b \geq \frac{L}{60}$$

Thus, the initial value chosen for b is defined by the above requirement. h' is assumed to be 100 mm as an initial value, which has to be checked after calculating reinforcement area and finding the required number of bars.

After calculating d from Equation (4.4), the following two criteria have to be checked and if necessary, d or / and b values have to be revised accordingly :

1 - $L \leq 60b$ or $\frac{250\ b^2}{d}$ whichever is the lesser.

(BS 5400 : Part 4 - clause 5.3.1.3)

2 - For a reasonably proportional beam, we will restrict the beam depth to the range:

$$L/10 \geq h \geq L/17$$

The variation of the compressive force (C) and the lever arm (d'), with the beam width (b) and the effective depth (d), depends on the amount of the concrete strain (e_c) and the corresponding strain in the steel (e_s). e_c and e_s are related (as can be seen from Figure 4.4) :

$$e_s = e_c \left(\frac{d}{x} - 1\right) = e_c \left(\frac{1}{R} - 1\right)$$

where the neutral axis depth ratio; $R = x/d \leq \frac{1}{2}$

Hence :

$$\frac{e_s}{e_c} = \frac{1}{R} - 1 \geq 1 \qquad \ldots\ (4.5)$$

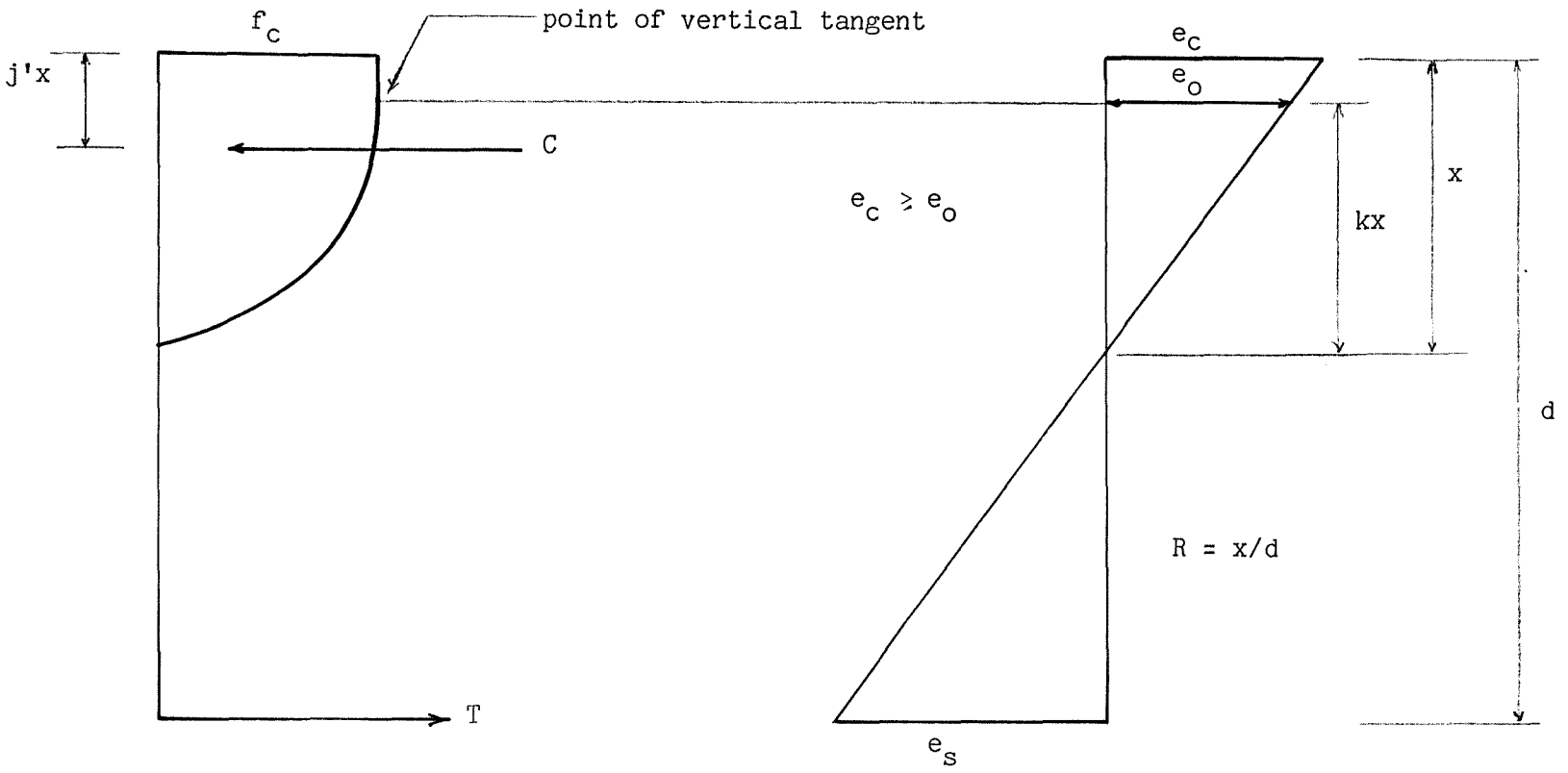

Figure (4.4) - Stress and strain diagrams for beam section with maximum concrete strain not less than the initial plastic strain (e_o)

Case (1); steel strain larger than allowable maximum concrete strain.

Equation (4.5) indicates that if the steel stress value (f_s) is not less than a value f_{sc} which corresponds to a strain e_s = 0.0035, then the outer fibre concrete strain (e_c) can be assumed to attain its maximum value of (0.0035) and the neutral axis depth ratio (R) is defined by Equation (4.5).

Consequently for case (1) the following relations are valid :

$$e_s \geq 0.0035$$

$$e_c = 0.0035$$

$$x = Rd = \frac{e_c}{e_s + e_c} d$$

$$f_c = \frac{2}{3} \frac{f_{cu}}{G_m}$$

$$k = \frac{e_o}{e_c} = \frac{e_o}{0.0035}$$

where e_o is the initial plastic strain in the concrete.

The compressive force (C) and the lever arm (d') can be calculated by making use of the geometric properties (46) of the parabola (as shown in Figure 4.5):

$$C = f_c (x - kx)b + \frac{2}{3} f_c kbx$$

Hence :

$$C = f_c \frac{3-k}{3} bx \qquad \ldots\ (4.6)$$

and :

$$C\, j'x = f_c \frac{(x-kx)^2}{2} b + \frac{2}{3} f_c \left(x - \frac{5}{8} kx\right) kbx$$

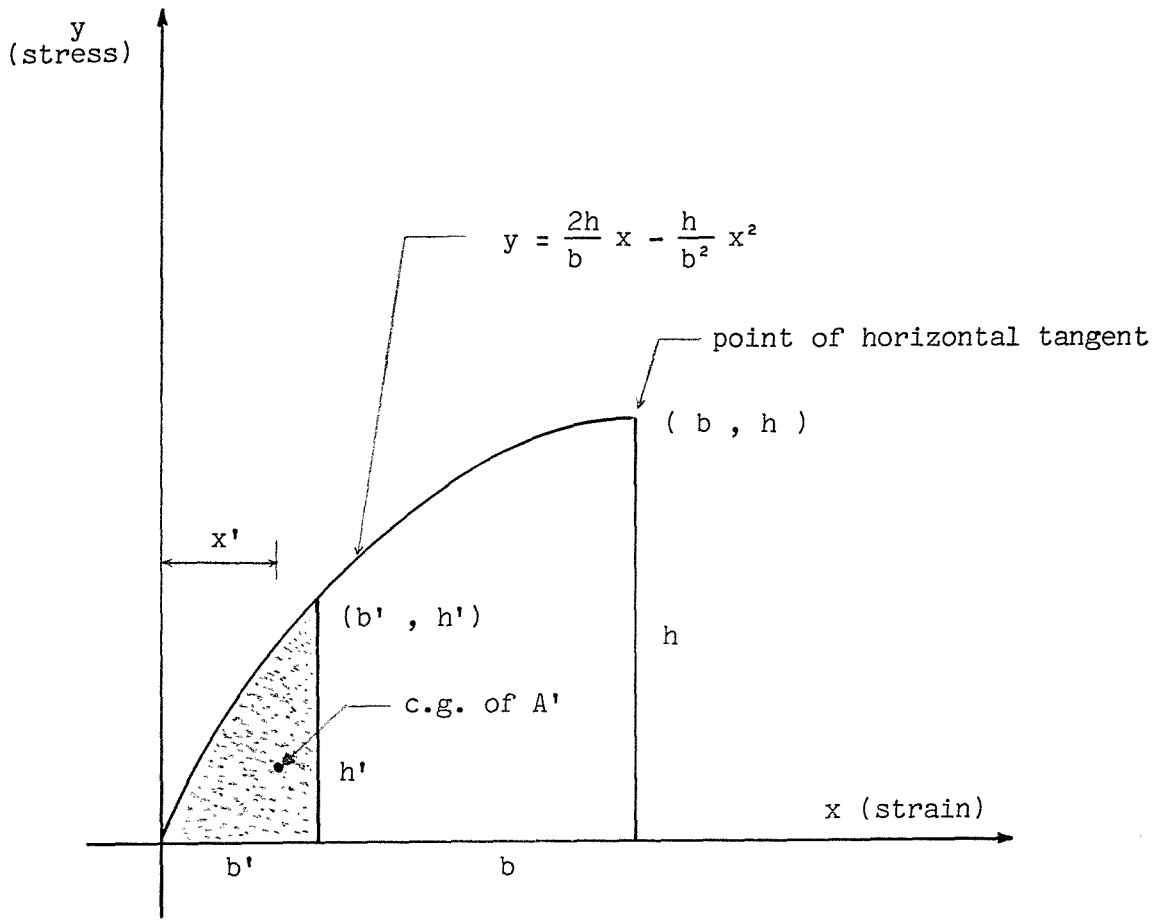

A' = the area of the shaded part

r = b'/b

$$A' = \frac{3 - r}{3(2 - r)} b' h' \qquad \text{(for } r = 1, \quad A = \frac{2}{3} bh\text{)}$$

$$x' = \frac{8 - 3r}{4(3 - r)} b' \qquad \text{(for } r = 1, \quad x' = \frac{5}{8} b\text{)}$$

Figure (4.5) - Geometric properties of the parabola

Substituting C and simplifying leads to the factor, for the depth of the centre of force on the concrete:

$$j' = \frac{k^2 - 4k + 6}{4(3 - k)} \qquad \ldots\ (4.7)$$

Since j' is defined to be :

$$j' = \frac{d - d'}{x}$$

then the lever arm is:

$$d' = d - j'x \qquad \ldots\ (4.8)$$

For case (1), if the design value of the stress f_{si} is known, then the steel strain (e_s) can be found. Since e_s is determined, then x, C and d' can be represented in terms of b and d only, and Equation (4.4) can be solved for d.

Cases (2) and (3); steel strain less than the maximum allowable concrete strain.

If f_{si} is less than f_{sc} , where f_{sc} is the stress corresponding to e_s = 0.0035, then Equation (4.5) :

$$\frac{e_s}{e_c} = \frac{1}{R} - 1 \geq 1 \qquad \ldots\ (4.5)$$

indicates that e_c cannot be assumed to attain its maximum value of (0.0035), because such an assumption leads to a value of R more than ($\frac{1}{2}$). Accordingly, R is assumed to have its limiting value of a half, R = $\frac{1}{2}$, and hence, $e_s = e_c$.

From Figure (4.3), it is clear that the concrete stress (f_c) is constant if the strain e_c is greater than the initial minimum plastic strain (e_o). Case (2) deals with e_c values greater than e_o , while case (3) deals with e_c values less than e_o .

Case (2)

For case (2) the following relations are valid :

$$e_c = e_s \qquad \text{where} \qquad e_o \leq e_c < 0.0035$$

$$f_c = \frac{2}{3} \frac{f_{cu}}{G_m}$$

$$k = \frac{e_o}{e_c}$$

$$x = \frac{1}{2} d$$

since C and d' are defined by Equations (4.6) and (4.8), then d, the effective depth, can be calculated as in case (1).

Case (3)

For this case, e_c is less than e_o . This means that the concrete stress value (f_c) is not constant, and f_c has to be defined by the parabolic relationship :

$$f_c = 5500 \; e_c \left(\sqrt{\frac{f_{cu}}{G_m}} - \frac{4125}{2} e_c \right)$$

If we imagine that the beam strain diagram (Figure 4.6) is extended, above the beam top surface, to the point where the concrete strain reaches the initial plastic value, then from the properties of a parabola (Figure 4.5), we conclude that the compressive force is :

$$C = \frac{3-r}{3(2-r)} f_c \, Rbd \qquad \ldots\ (4.9)$$

where $r = \frac{e_c}{e_o} < 1.0$ and the lever arm is:

$$d' = (1-R)d + Rd \frac{8-3r}{4(3-r)}$$

hence: $$d' = \left(1 - \frac{R(4-r)}{4(3-r)}\right) d \qquad \ldots\ (4.10)$$

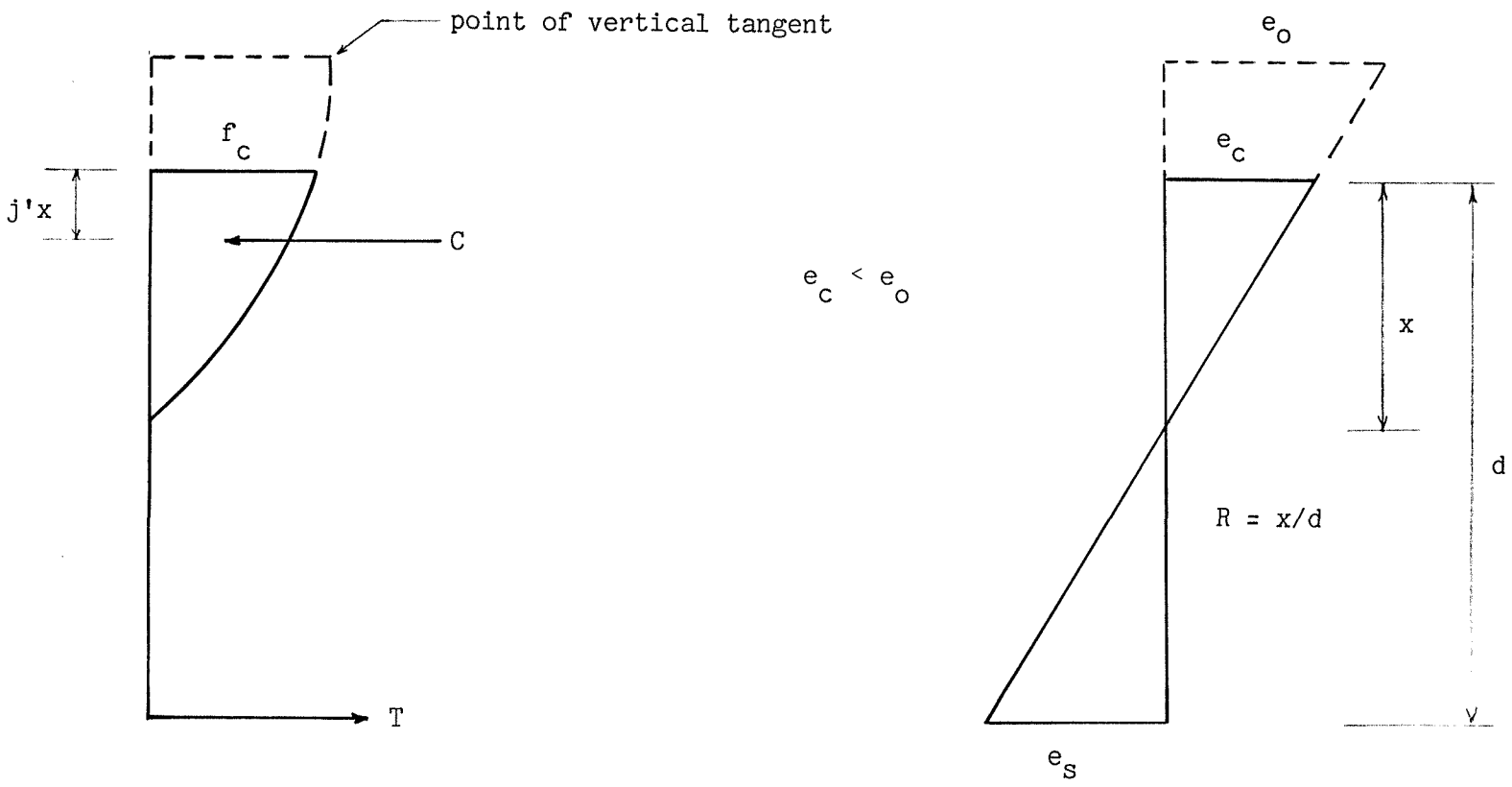

Figure (4.6) - Stress and strain diagrams for beam section with maximum concrete strain less than the initial plastic strain (e_o)

Knowing, for this case, that R = 1/2, Equations (4.9) and (4.10) can be substituted into Equation (4.4), which then can be solved to determine the value of the depth d.

4.3.3 Reinforcement Area

After determining b and h, their values are revised (if necessary) and rounded to 50 mm. The next step is to determine the actual value of R which results from the real rounded dimensions of the section. If R is known, A_s can be calculated as follows:

Case (R1)

First we assume that, $e_c \geq e_o$, then as shown earlier:

$$C = f_c \, Rd \, \frac{3-k}{3} \, b \quad , \qquad k = \frac{e_o}{e_c}$$

$$f_c = \frac{2}{3} \, \frac{f_{cu}}{G_m}$$

$$e_s = e_c \left(\frac{1}{R} - 1\right)$$

$$d' = d - j'x = d \left(1 - R \, \frac{k^2 - 4k + 6}{4(3 - k)}\right)$$

since:

$$M_T = M_L + M_D = Cd'$$

then:

$$M_T = \frac{2}{3} \, \frac{f_{cu}}{G_m} \, Rd \, \frac{3-k}{3} \, b \, d \left(1 - R \, \frac{k^2 - 4k + 6}{4(3 - k)}\right) \qquad ....(4.11)$$

However, since : $k = \frac{e_o}{e_c}$ and $ec = \frac{e_s}{\frac{1}{R} - 1}$

then: $$k = \frac{e_o}{e_s} \left(\frac{1}{R} - 1\right) \qquad .... (4.12)$$

Now let us introduce the parameters :

$$q = \frac{e_o}{e_s} \qquad \text{and} \qquad g = 18M_T G_m / f_{cu} bd^2$$

Combining Equations (4.11) and (4.12) gives :

$$g + 4q + q^2 = R(12 + 8q + 2q^2) - R^2 (6 + 4q + q^2) \quad .... \quad (4.13)$$

For a specific value of the initial design steel stress (f_{si}), q is readily calculated and Equation (4.13) can be solved directly for R. Thus it will be expected to be not more than (1/2). Knowing R and e_s , the concrete strain (e_c) can be determined and compared with the initial plastic value (e_o).

Case (R2)

If we find from the above that, $e_c < e_o$, that is we are on the parabolic part of the stress - strain curve of the concrete, then as shown earlier the stress is given by :

$$f_c = 5500 \; e_c \left(\sqrt{\frac{f_{cu}}{G_m}} - \frac{4125}{2} e_c\right)$$

so that the compressive force will be :

$$C = \frac{3-r}{3(2-r)} f_c \, Rbd \qquad \text{where} \qquad r = \frac{e_c}{e_o} < 1.0$$

Also, lever arm is given by :

$$d' = \left(1 - \frac{R(4-r)}{4(3-r)}\right)d$$

Since the concrete strain is less than the initial plastic value by the factor r :

$$e_c = r\, e_o$$

then we can express the steel strain as :

$$e_s = e_c \left(\frac{1}{R} - 1\right) = re_o \left(\frac{1}{R} - 1\right)$$

It follows therefore that the neutral axis depth ratio is given by :

$$R = \frac{r}{\frac{e_s}{e_o} + r} \qquad \ldots\ (4.14)$$

and the maximum stress in the concrete is given by :

$$f_c = 5500\, re_o \left(\sqrt{\frac{f_{cu}}{G_m}} - \frac{4125}{2} re_o\right)$$

and the moment is : $M_T = Cd'$

Substituting the compressive force (C) and the lever arm (d'), gives the following equation for the moment M_T :

$$M_T = 5500\, r\, e_o \left(\sqrt{\frac{f_{cu}}{G_m}} - \frac{4125}{2} r\, e_o\right) \frac{3-r}{3(2-r)} Rbd \left(1 - \frac{R(4-r)}{4(3-r)}\right)d \qquad .. (4.15)$$

Now let us introduce the parameters :

$$q_1 = \frac{e_s}{e_o} \quad \text{and} \quad g_1 = \frac{12\, M_T}{5500\, e_o\, bd^2}$$

$$a = \sqrt{\frac{f_{cu}}{G_m}} \quad \text{and} \quad p = \frac{4125}{2} e_o$$

Combining Equations (4.14) and (4.15) gives :

$$g_1(2q_1^2 + 4q_1r + 2r^2 - q_1^2r - 2q_1r^2 - r^3) =$$

$$12aq_1r^2 + 8ar^3 - 4aq_1r^3 - 12pq_1r^3$$

$$-3ar^4 - 8pr^4 + 4pq_1r^4 + 3pr^5 \qquad \ldots\ (4.16)$$

Equation (4.16) can be solved now for r, which is the ratio of the concrete strain (e_c) to the initial plastic value ($r = e_c/e_o$), by the Newton-Raphson Method (starting with r = 1/2). Knowing r, the neutral axis depth ratio (R) can be determined from Equation (4.14).

All the parameters required to calculate the compressive force (C) can now be calculated using the appropriate equations for case R1 or case R2. The required reinforcement area, A_{sr} , can be obtained simply from the compressive force (C) and the initial design stress in the reinforcement (f_{si}) : $A_{sr} = C/f_{si}$. From the required reinforcement area (A_{sr}) the correct number of bars can be calculated and the actual reinforcement area, A_{sp} , can be found.

4.3.4 Determination of The Actual Stresses in The Reinforcing Bars

The actual stresses which correspond to the real dimensions and reinforcement area are calculated as follows.

Case (S1), corresponding to case (R1)

First, we assume that the maximum concrete strain (e_c) is not less than the initial plastic value (e_o) :

$$e_c \geq e_o$$

In this case Equation (4.13) is applicable :

$$g + 4q + q^2 = R(12 + 8q + 2q^2) - R^2\,(6 + 4q + q^2) \quad \ldots.(4.13)$$

where the parameters q and g have been defined previously by:

$$q = \frac{e_o}{e_s} \qquad \text{and} \qquad g = \frac{18\ M_T G_m}{f_{cu}\ bd^2}$$

By replacing e_o/e_s by q in Equation (4.12), we get :

$$k = \frac{e_o}{e_s} \left(\frac{1}{R} - 1 \right) = q\left(\frac{1}{R} - 1\right)$$

By equating the compressive force (C) with the tensile force (T) we get :

$$C = f_c \, Rbd \, \frac{3-k}{3} = T = A_s f_s \qquad \ldots\ldots (4.17)$$

where, the maximum concrete stress (f_c) is constant since the strain is in the plastic range ;

$$f_c = \frac{2}{3} \frac{f_{cu}}{G_m}$$

If we represent the reinforcement strain (e_s) in terms of its stress (f_s): $e_s = a_o f_s + b_o$ (see Figure 4.3), where a_o and b_o are material constants, then the stress f_s is given by:

$$f_s = \frac{e_s - b_o}{a_o}$$

Since q has been defined by : $q = \frac{e_o}{e_s}$, then:

$$e_s = \frac{e_o}{q} \quad \text{and} \quad f_s = \frac{e_o/q - b_o}{a_o} = \frac{a_1}{q} - b_1$$

where:

$$a_1 = \frac{e_o}{a_o} \qquad \text{and} \qquad b_1 = \frac{b_o}{a_o}$$

Substituting k and f_s in Equation (4.17) gives :

$$\frac{2}{3} \frac{f_{cu}}{G_m} \, Rbd \, \frac{3 - q(1/R - 1)}{3} = A_s\left(\frac{a_1}{q} - b_1\right)$$

and by simplifying, we get :

$$3R - q + qR = (\frac{a_1}{q} - b_1)g_2$$

where g_2 is a parameter :

$$g_2 = \frac{9\ A_s\ G_m}{2\ f_{cu} bd}$$

Solving for R gives :

$$R = \frac{(a_1 - b_1 q)g_2 + q^2}{3q + q^2} = \frac{C_1 - C_2 q + q^2}{3q + q^2} \qquad \ldots\ (4.18)$$

where:

$$C_1 = a_1\ g_2 \qquad \text{and} \qquad C_2 = b_1\ g_2$$

Substituting Equation (4.18) in Equation (4.13) gives :

$$A_0 + A_1 q + A_2 q^2 + A_3 q^3 + A_4\ q^4 = 0 \qquad \ldots\ (4.19)$$

where :

$$A_0 = -6\ C_1^{\,2}$$

$$A_1 = -4\ C_1^{\,2} + 12\ C_1\ C_2 + 36\ C_1$$

$$A_2 = -9g - C_1^{\,2} + 24C_1 - 36C_2 + 8C_1\ C_2 - 6C_2^{\,2}$$

$$A_3 = -6g + 6C_1 - 24C_2 + 2C_1\ C_2 - 4C_2^{\,2}$$

$$A_4 = -g - 3 - 6C_2 - C_2^{\,2}$$

Equation (4.19) can now be solved for the parameter $q = e_o/e_s$ by the Newton-Raphson Method. The initial value of q is determined as follows:

1 - For the maximum design moment ($M_T = M_L + M_D$), we take,

$$f_{s1} = f_{si}\ A_{sr} / A_{sp} \qquad \text{where :}$$

f_{s1} = the first estimate of the actual maximum stress f_{sa} .

f_{si} = the design value of the stress.

A_{sr} = the required reinforcement area.

A_{sp} = the provided reinforcement area.

2 - For any lesser value of the moment, M'_T , we take the first estimate of the reinforcement stress as : $f_{s1} = f_{sa}\ M'_T/M_T$

From f_{s1}, the corresponding strain e_s and the initial value of $q = e_o/e_s$ can be obtained.

Solving Equation (4.19) gives the actual value of q, from which the actual reinforcement strain $e_s = e_o/q$, and hence stress, can be found. The neutral axis depth ratio (R) is determined from Equation (4.18). Finally, the maximum concrete strain (e_c) is to be found and compared with the initial plastic value (e_o) :

$$e_c = \frac{e_o}{k} = \frac{e_o}{q(\frac{1}{R} - 1)}$$

Case (S2), corresponding to case (R2)

If we find from the above analysis that the actual concrete strain is less than the initial plastic value, i.e. $e_c < e_o$, then Equation (4.16) is applicable, whence:

$$g_1\ (2q_1^2 + 4q_1 r + 2r^2 - q_1^2 r - 2q_1\ r^2 - r^3) =$$

$$12\ a\ q_1 r^2 + 8a\ r^3 - 4aq_1 r^3 - 12pq_1 r^3 - 3ar^4$$

$$- 8pr^4 + 4pq_1 r^4 + 3pr^5 \qquad \ldots\ (4.16)$$

where the following parameters have been defined previously by :

$$r = \frac{e_c}{e_o} \quad , \quad q_1 = \frac{e_s}{e_o} \quad , \quad g_1 = \frac{12\ M_T}{5500 e_o b d^2}$$

$$a = \sqrt{\frac{f_{cu}}{G_m}} \quad , \quad p = \frac{4125}{2}\ e_o$$

Since the neutral axis depth ratio (R) is given by:

$$R = \frac{r}{q_1 + r} \qquad \text{and the maximum concrete stress is:}$$

$$f_c = 5500\ r e_o\ (a - pr)$$

then by equating the compressive force (C) and the tensile force (T) and substituting for f_c and R, we get:

$$C = \frac{3 - r}{3(2 - r)}\ f_c\ Rbd = T = A_s\ f_s$$

and

$$\frac{3 - r}{3(2-r)}\ 5500\ r e_o\ (a - pr)\ \frac{r}{q_1 + r}\ bd = A_s\ f_s \qquad \ldots\ (4.20)$$

If we assume the reinforcement strain (e_s) to be :

$e_s = a_o f_s + b_o$, then the stress f_s is given by:

$$f_s = \frac{e_s - b_o}{a_o} = \frac{q_1 e_o - b_o}{a_o}$$

Substituting f_s in Equation (4.20) gives :

$$\frac{3-r}{3(2-r)} \; 5500 \; re_o \; (a - pr) \; \frac{r}{q_1 + r} \; bd = A_s \; \frac{q_1 e_o - b_o}{a_o}$$

The above equation cannot be simplified to give r, which is the ratio of the concrete strain (e_c) to the initial plastic value (e_o), as an explicit function of q_1. Instead, the following procedure has to be applied to determine the stress in the reinforcement, f_s:

1 - Take an initial value, $r_i = 1.0$, when Equation (4.16) can be solved for q_1. From this, the reinforcement strain ($e_s = q_1 \; e_o$) and stress f_s can be found.

2 - Calculate the left and right hand sides of Equation (4.20) and compare them. If the difference is not within a specified limit (say 1 percent), then:

3 - Take a new value for r ($r_{i+1} = r_i - 0.001$) and repeat the procedure until it converges to give an acceptable value for the approximate actual stress.

As a final step in the design, the maximum reinforcement ratio and shear stress are to be calculated and compared with their allowable values (CP110 and BS5400).

4.4 - Design Moments and Shears

Design live load moments (M_L) and shears (V_L), including impact, for each of the two bridge beams are given in Table (4.1). These are based on a computational time interval, Dt = 0.0015 x L, as mentioned in Chapter (3).

Span (m)	Loading frequency (T/hr.)	M_L (KN.M)	V_L (KN)
15.0	360	600.151	185.26
15.0	90 + 180	568.982	185.263
17.5	all values	736.686	203.592
20.0	all values	922.892	213.424
25.0	all values	1298.359	228.626
27.5	all values	1477.810	232.521

Table (4.1) - Design values for the maximum live load moment (M_L) and shear (V_L), based on a computational time interval, Dt(in sec.) = 0.0015 x Span

4.5 Computer Program for The Design of The Bridge Beams

The proposed design procedure has been programmed to design the bridge beams. Two sets of bridge sections have been obtained from these calculations. For the first set, the reinforcing bar diameter is 32 mm, while for the second set it is 25 mm.

The program starts by assuming an initial design value of the stress in the reinforcement (f_{si}) as below:

$$f_{si} = 450 - Df_s \times I \qquad \text{in } N/mm^2$$

where I is an increasing integer with a starting value, I = 0, and:

$Df_s = 17.5\ N/mm^2$ for 32 mm bars
$Df_s = 10.0\ N/mm^2$ for 25 mm bars

The procedure is repeated by reducing f_{si} value until the stress range, in the outer layer of bars, is slightly higher or lower than the endurance limit (S_e), given in Chapter (2) by:

$S_e = 161.5 - 0.33\ f_{min}$ here f_{min} is the dead load stress.

A flow chart for the program is given in Figure (4.7). The details of the beams designed by the aforementioned procedure are given at the end of this chapter.

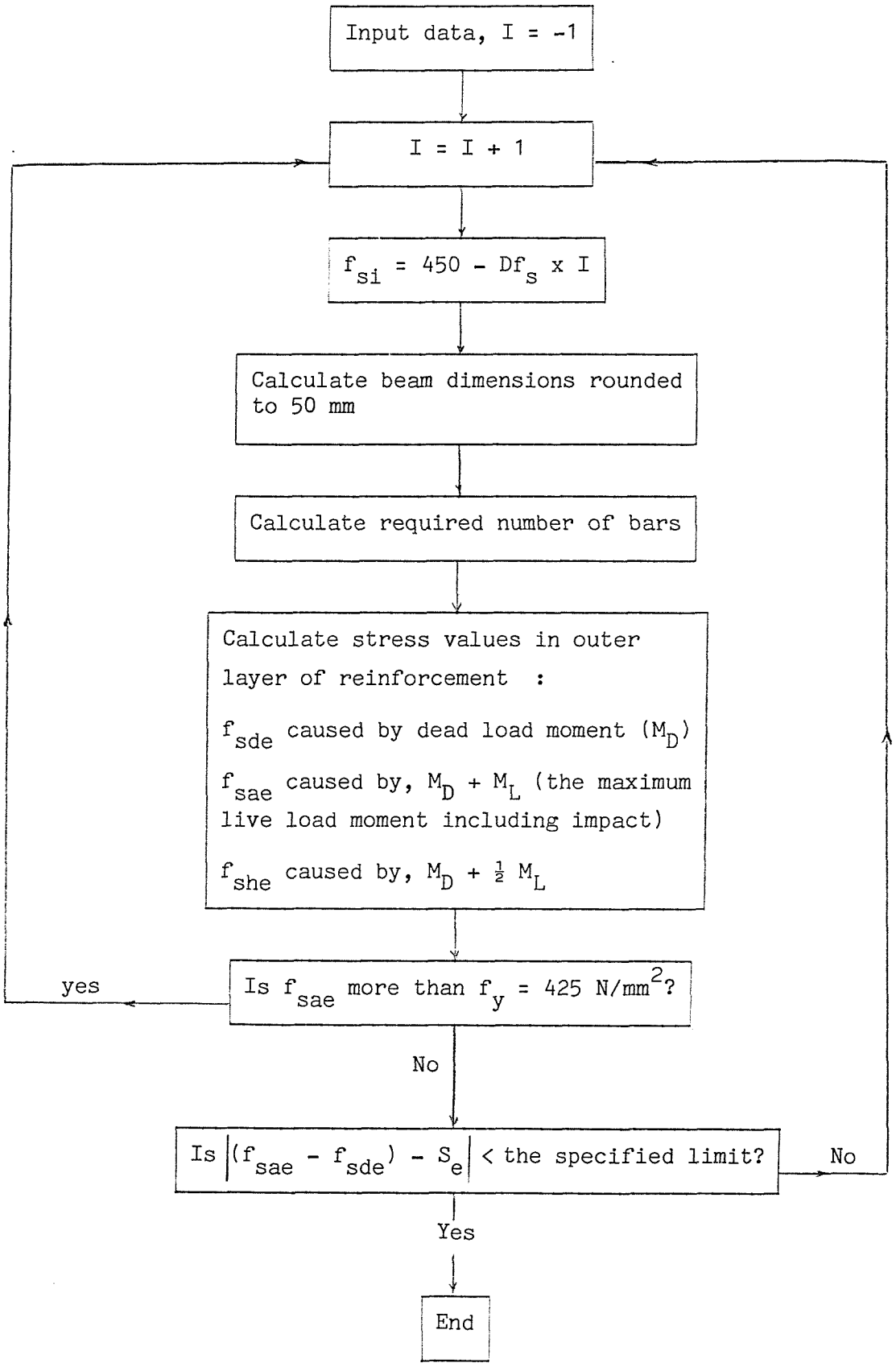

Figure (4.7)
Flow chart of the computer program for the beam design

4.6 Discussion of The Design Results

In the design tables (p 113) at the end of this chapter, it is interesting to note that the required effective depth (d_{req}),for high values of the initial steel stress (f_{si}), decreases with decreasing steel stress. For lower values of f_{si} , the reverse is found to be the case. As shown in Section (4.3.2), design case (1) deals with initial steel stress values (f_{si}), which are not less than that producing a strain of (0.0035). This steel stress value is, $f_{sc} \simeq 403.1$ N/mm^2, for a yield stress f_y = 425 N/mm^2 as can be seen in Figure (4.3). The following is an explanation of this effect .

The design equation which has to be solved for the effective depth (d) is given as :

$$A_1 + A_2 d = A_3 d^2 y \qquad \ldots\ (a)$$

where A_1, A_2 and A_3 are positive constants.

For design case (1), the parameter y can be defined by : $y = R - 0.435\ R^2$, where R is the neutral axis depth ratio. This means that y increases with increasing R, for all R values less than (1.15). This is true for all design cases, since the neutral axis must lie within the beam.

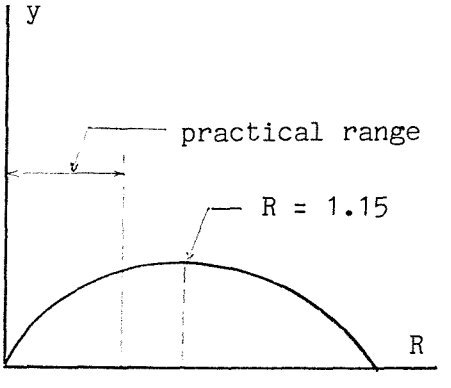

For design case (1), R is related to the reinforcement strain (e_s) by :

$$R = \frac{0.0035}{0.0035 + e_s} \qquad \ldots\ (b)$$

Equation (b) implies that R, and hence y, increase with decreasing values of e_s and thus the initial design stress (f_{si}). This requires the effective depth (d) to decrease to keep the two sides of Equation (a) equal.

Another explanation is that, decreasing f_{si} within the range, $f_{sc} \leq f_{si} \leq 425$, increases the neutral axis depth ratio (R). Since for case (1) the maximum concrete strain is constant ($e_c = 0.0035$), then the compressive force increases. In order to produce the same moment, the lever arm and the required depth will correspondingly decrease.

For design cases (2) and (3), where the initial design steel stress (f_{si}) is less than the limiting value, f_{sc}, the neutral axis depth ratio (R) is fixed, R = 1/2. Consequently the maximum concrete strain (e_c) and the steel strain (e_s) are equal. Decreasing f_{si} would therefore result in a decrease in e_c. This means that the effective depth (d) has to increase to cause an increase in the compressive force and the lever arm. Both are necessary to maintain the resulting moment. Alternatively, for design case (2), the parameter y can be defined by :

$$y = (1 - 0.5\ j')\ (3 - k)$$

where, $k = e_o/e_c$

(e_o is the initial plastic strain = 0.0015 in this study)

$$j' = \frac{k^2 - 4k + 6}{4(3-k)}$$

From Table (a), it is clear that the parameter y decreases with decreasing f_{si}, which confirms that the effective depth (d) has to increase to keep the equality between the two sides of Equation (a).

f_{si} (N/mm^2)	$(e_s = e_c) \times 10^3$	k	j'	$y = (1 - 0.5j')(3-k)$
397.5	3.34	0.449	0.432	2.000
380.0	2.84	0.528	0.421	1.952
362.5	2.34	0.641	0.408	1.878
345.0	1.84	0.815	0.389	1.760

Table (a) - y values for design case (2)

A similar mathematical proof can be established for design case (3).

The maximum reinforcement ratio obtained is 3.24 percent which is less than the specified limiting 4 percent value (48). The maximum shear stress value is 1.94 N/mm^2 which is also less than the allowable value of 4.75 N/mm^2 (48).

4.7 Section Modulus

The section modulus, Z, is defined as :

$$Z = \frac{M_A}{f_s}$$

where M_A is the moment and f_s is the resulting stress in the reinforcement.

If the modulus Z has a fixed value which does not depend on the moment M_A , then the simulated stress spectrum could be established easily from the moment spectrum. However, this is not the case because the modulus Z varies with the moment, due to non linear behaviour of the section.

Perhaps, it would be ideal to use the aforementioned design procedure to calculate the stress value which corresponds to every single maximum or minimum point in the moment spectrum and use it as a point in the stress spectrum. Unfortunately, such operation is very expensive and time consuming (for the computer). By ruling out such a possibility, we are left with two options:

1 - The first is to calculate the modulus value using Equations (4.2) and (4.3). These two equations define the modulus regardless of the moment value. They are based on the modular - ratio theory. As mentioned in Section (4.1), some of the assumptions underlying this theory are not acceptable for high stresses (46).

2 - The second option, is to use the proposed procedure (Sec. 4.3) to calculate the modulus values resulting from the two extreme moments (the dead load moment and the total live plus dead load moment) and from some intermediate value (say the half live plus dead load moment, which we may call the "average" total moment). If the relative differences between the resulting three values of the modulus are small enough, then we may adopt some chosen value of the modulus and consider it representing each section regardless of the loading stage.

The second option has been adopted, because it is believed to be more reasonable. Two sets of section moduli have been calculated. The first set consists of three values of what we may call the "combined" load modulus:

$$Z_T = M_T/f_{sa}$$

$$Z_D = M_D/f_{sd}$$

$$Z_{TH} = M_H/f_{sh}$$

where:

M_T : is the moment caused by the total dead load and the maximum live load (including impact).

M_D : is the total dead load moment.

M_H : is the average total moment = $0.5\ (M_D + M_T)$.

f_{sa} , f_{sd} , f_{sh} : are the stresses in the reinforcement caused by the moments M_T , M_D and M_H respectively.

The second set consists of two values of what we may call the "live" load modulus:

$$Z_L = \frac{M_L}{f_{sa} - f_{sd}}$$

$$Z_{LH} = \frac{0.5\ M_L}{f_{sh} - f_{sd}}$$

where :

M_L : is the maximum live load moment, including impact, and

f_{sa} , f_{sd} , f_{sh} : have been defined previously.

First, all moduli values were calculated taking the centre of gravity of the steel area as the centre of the resultant tensile force (T).

Since this is not precisely the centre of action of the effective steel tensile force (T), due to the strain gradient from the top to the bottom of the group of bars, a second run has been made using the actual centre of T. This has been located by trial and error to an adequate accuracy. This has helped in decreasing the relative differences, in the modulus values, by about 20 percent.

Two groups of the modulus values have been calculated. The first one is based on the steel stress in the outer bar. This group is denoted by Z' in the design tables, at the end of this chapter. The second group is based on the steel stress, corresponding to the strain at the centre of the tensile force, (which we may call the centroidal stress). The second group is denoted in the tables by Z.

Let us, now consider the live load moduli based on the outer bar stress (i.e. Z'_L and Z'_{LH}) and their relative difference D'_{Z3} . We can see from the design tables (part c), that the value of D'_{Z3} , the relative difference, is quite high for any section whose outer bar stresses caused by the total live load moment and the half live load moment are on different lines of the stress - strain curve. The relative differences D'_{Z3} are as high as 13.7 percent for 32 mm bars and 19.2 percent for 25 mm bars. On the other hand it appears that the live load moduli based on the centroidal stress (i.e. Z_L and Z_{LH}) are appreciably less sensitive to the double linearity of the stress - strain curve. In this case the maximum relative difference is only 5.5 percent.

The combined load modulus based on the centroidal stress can be seen as:

$$Z = \frac{M_A}{f_s} = \frac{A_s f_s d'}{f_s} = A_s d'$$

where M_A is the moment, f_s is the resulting centroidal stress, A_s is the reinforcement area and d' is the lever arm. Similarly the combined load modulus based on the outer bar stress f_{se} can be seen as :

$$Z' = \frac{M_A}{f_{se}} = \frac{A_s f_s d'}{f_{se}} = Z \frac{f_s}{f_{se}}$$

Apparently, the ratio (f_s/f_{se}) has a significant effect in getting high values for the relative difference in the live load moduli, based on the outer bar stress.

Based on the aforementioned behaviour, it is believed more convenient to investigate the use of the modulus based on the centroidal stress, as the required modulus for design to represent the section through all loading stages.

Then, to simulate the stress in the outer bar, the variation of the strain factor, S_f , with the applied moment at different loading stages, has been examined (S_f is the ratio of the outer bar strain to the strain at the centre of the tensile force, which we may call the centroidal strain).

The maximum relative difference of the strain factor, D_{Sf} , has been found to be about 1.0 percent for 32 mm bars and 1.4 percent for 25 mm bars, which seem to be adequately small, especially if we notice that for some sections, the stress values are calculated by trial and error, to a chosen degree of accuracy. As a result of the strain factor (S_f) being almost constant, it is interesting to note that if the centroidal stresses are higher than (340 N/mm^2=0.8 f_y),

i.e. they fall on the second line of the stress - strain curve, then the stress range in the outer bar, f_{sre} , is smaller than the centroidal stress range f_{sr} . This results from the strain factor being almost constant, and from the double linearity of the stress - strain curve, as is shown below.

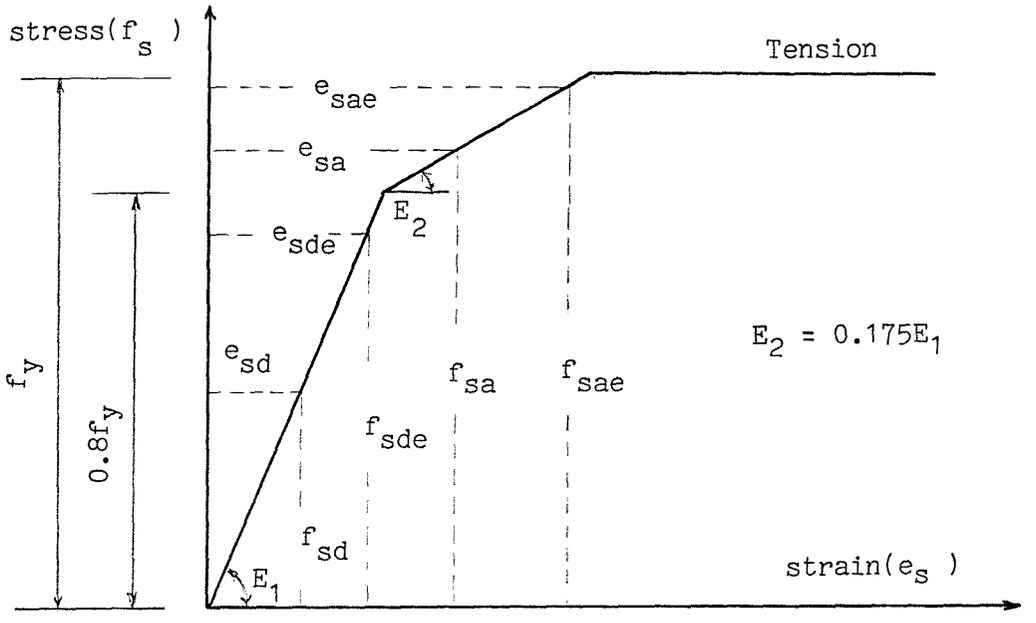

The stress - strain curve of the reinforcement

Since the dead load stresses, in this study, are in all cases less than (340.0 N/mm^2 = 0.8 f_y), then the centroidal stress f_{sd} and the outer bar stress f_{sde} , caused by the dead load moment, are given by:

$$f_{sd} = E_1 e_{sd} \qquad f_{sde} = E_1 e_{sde}$$

where e_{sd} and e_{sde} are the corresponding strains. By definition, the strain factor corresponding to the dead load, S_{FD} , is given by:

$$S_{FD} = \frac{e_{sde}}{e_{sd}} \quad \text{and} \quad e_{sde} = S_{FD}\, e_{sd}$$

Consequently, the dead load outer bar stress can be found by:

$$f_{sde} = E_1 e_{sde} = E_1 S_{FD} e_{sd} = f_{sd} S_{FD}$$

The slope of the second part of the stress - strain curve, E_2 , can be defined by :

$$\frac{f_{sae} - f_{sa}}{e_{sae} - e_{sa}} = E_2 = 0.175\ E_1$$

where; f_{sae} , f_{sa} are the outer bar stress and the centroidal stress, caused by the total moment; e_{sae} , e_{sa} are the corresponding strains.

By definition, the strain factor corresponding to the total load, S_{FT} , is given by :

$$S_{FT} = \frac{e_{sae}}{e_{sa}} \qquad \text{and} \qquad e_{sae} = S_{FT}\ e_{sa}$$

Substituting for e_{sae} gives the following equation for the slope E_2 :

$$\frac{f_{sae} - f_{sa}}{S_{FT}\ e_{sa} - e_{sa}} = E_2 = 0.175\ E_1$$

Simplifying the last equation gives :

$$f_{sae} - f_{sa} = 0.175\ E_1\ (S_{FT} - 1)\ e_{sa}$$

Hence the outer bar stress is :

$$f_{sae} = f_{sa} + 0.175\ E_1\ (S_{FT} - 1)\ e_{sa}$$

But the outer bar stress range is the stress due to the total moment less that due to the dead load moment, i.e.

$$f_{sre} = f_{sae} - f_{sde} = f_{sa} + 0.175\ E_1\ (S_{FT} - 1)\ e_{sa} - f_{sde}$$

Now, since : $f_{sde} = f_{sd}\ S_{FD}$ then this stress range is :

$$f_{sre} = f_{sa} + 0.175\ E_1\ (S_{FT} - 1)\ e_{sa} - f_{sd}\ S_{FD}$$

which can also be written:

$$f_{sre} = f_{sa} - f_{sd} + 0.175\ E_1\ e_{sa}\ (S_{FT} - 1) - f_{sd}\ (S_{FD} - 1)$$

Since the strain factor is almost constant, both S_{FT} and S_{FD} can be replaced by an average value which we will denote by S_F. Consequently in the above equation, we can substitute S_F for S_{FT} and S_{FD} when we obtain the following expression for the outer bar stress range :

$$f_{sre} = f_{sa} - f_{sd} + (0.175\ E_1\ e_{sa} - f_{sd})\ (S_F - 1)$$

In fact, the expression $(f_{sa} - f_{sd})$ in this equation represents the centroidal stress range (f_{sr}), and we can therefore write it as :

$$f_{sre} = f_{sr} - (S_F - 1)\ (f_{sd} - 0.175\ E_1\ e_{sa})$$

If we let : $r = e_{sa}/e_{sd}$, the ratio of the total strain to dead load strain, then, $e_{sa} = r\ e_{sd}$, and:

$$f_{sre} = f_{sr} - (S_F - 1)\ (f_{sd} - 0.175\ E_1\ r\ e_{sd})$$

Since the dead load stress is given by: $f_{sd} = E_1\ e_{sd}$, then, the outer bar stress range is:

$$f_{sre} = f_{sr} - (S_F - 1)\ f_{sd}\ (1 - 0.175\ r)$$

The definition of the strain factor (S_f) implies that its value is always greater than unity, i.e. $S_f > 1.0$. From the last equation, it is clear that for all r values smaller than $(1/0.175 = 5.714)$, the outer bar stress range (f_{sre}) is less than the corresponding centroidal stress range (f_{sr}). In reality the r value will be well below (5.714).

Table (4.2) shows, the maximum values of the relative differences of the strain factor (D_{Sf}), the live load modulus based on the centroidal stress (D_{Z3}) and the live load modulus based on the outer bar stress (D'_{Z3}), for the various combinations of the span (L) and loading frequency (U).

Span (m)	Loading frequency (T/hr.)	Maximum D_{Sf} (%)	Maximum D_{Z3} (%)	Maximum D'_{Z3} (%)
15.0	360	1.01	4.30	12.53
15.0	180 +90	1.03	3.80	11.59
17.5	all values	0.70	2.93	12.35
20.0	all values	0.34	3.10	11.63
25.0	all values	0.15	3.61	12.76
27.5	all values	0.15	4.21	13.71

Table (4.2 a)

The maximum relative differences of strain factor and moduli, for the various span and loading frequency combinations. Bar dia = 32 mm

- Strain factor relative difference :

$$D_{Sf} = \frac{\text{the maximum of } (S_{FT} , S_{FH} , S_{FD})}{\text{the minimum of } (S_{FT} , S_{FH} , S_{FD})} - 1$$

- Relative difference of live load section modulus based on centroidal stresses :

$$D_{Z3} = \frac{|Z_L - Z_{LH}|}{\text{the minimum of } (Z_L , Z_{LH})}$$

- Relative difference of live load section modulus based on outer bar stresses :

$$D'_{Z3} = \frac{|Z'_L - Z'_{LH}|}{\text{the minimum of } (Z'_L , Z'_{LH})}$$

Span (m)	Loading frequency (T/hr.)	Maximum D_{Sf} (%)	Maximum D_{Z3} (%)	Maximum D'_{Z3} (%)
15.0	360	1.37	4.95	16.56
15.0	180 +90	1.43	4.63	15.65
17.5	all values	1.03	4.24	16.05
20.0	all values	0.50	2.60	16.00
25.0	all values	0.18	5.48	16.88
27.5	all values	0.18	5.17	19.15

Table (4.2 b)

The maximum relative differences of strain factor and moduli for the various span and loading frequency combinations. Bar dia = 25 mm

- For the definitions of the terms, see Table (4.2 a)

Based on the aforementioned observations, it is suggested that we may simulate the stress range spectrum in the outer bar, from the moment spectrum, using the modulus values based on the centroidal stress, Z. This can be done by simulating the centroidal stress in the steel (f_s), and calculating the corresponding strain (e_s). The strain in the outer bar is given by : $e_{se} = e_s S_F$ where S_F is the strain factor, and thus the corresponding stress, f_{se} , can be calculated. Hence, the stress range is :

$$f_{sre} = f_{se} - f_{sde} \qquad \text{where } f_{sde} \text{ is the dead load stress.}$$

This means that we have to define some proper values for the modulus (Z) and the strain factor (S_F), which could be considered as representing each section adequately through all stages of loading. But before doing so, let us examine the way by which the modulus (Z) varies from one loading stage to another. To help us in that, values of the neutral axis depth ratio (R) and the lever arm effective depth ratio (j) have been calculated, and given in part (d) of each design table (p 113).

The lever arm effective depth ratio (j) value, for spans L = 15.0 and 17.5 m, increases consistently as the moment, we consider, decreases below the design moment. This behaviour is expected and may be explained by examining Figure (4.7) which represents the stress block for the concrete.

In this figure, the position of the centre of the area, x' , of the stress block is given by:

$$x' = \frac{6a^2 + 8ba + 3b^2}{4(3a + 2b)}$$

Whence the rate of change of x' with respect to a is :

$$\frac{\partial x'}{\partial a} = \frac{1}{4} \quad \frac{18a^2 + 24ab + 7b^2}{(3a + 2b)^2} > 0$$

Hence, it will be seen from above, that x' increases as the portion of concrete which has become plastic, a, gets deeper in the section, i.e. the bending strains increase.

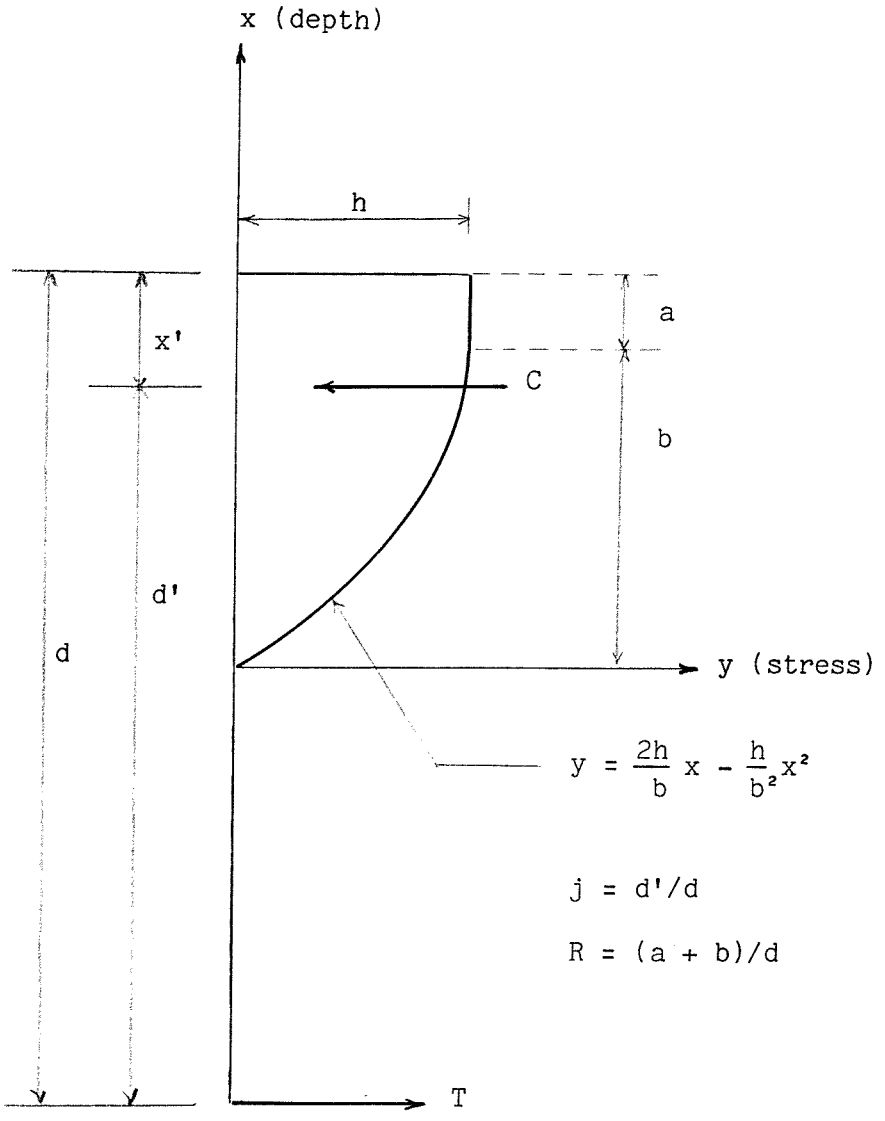

Figure (4.7) - The concrete stress block in a highly stressed section

As the moment decreases, the plastic region, a, decreases and consequently x' also decreases. Hence, the lever arm effective depth ratio (j) increases.

For all beams of 25.0 m span and over and for some of 20.0 m span, deflection will control the design, and hence the section depth will have to be increased beyond the minimum based upon stress conditions. In these cases, the lever arm effective depth ratio (j) seems to have two patterns of behaviour. The first behaviour is associated with sections for which, the steel and concrete stresses are low. This behaviour of increasing the lever arm effective depth ratio (j) with decreasing moment, is exactly similar to the aforementioned.

In the second kind of behaviour, which is associated with sections for which the steel and concrete stresses are high, the lever arm effective depth ratio (j) seems to fluctuate with the moment values. This may be explained by examining the following relation which is based on the strain diagram (Fig 4.4 and 4.6):

$$e_c = \frac{e_s}{\frac{1}{R} - 1} \qquad \text{.... Equation (c)}$$

In Eq. (c), e_c is the maximum concrete strain, e_s is the steel centroidal strain and R is the neutral axis depth ratio.

If the effective depth (d), used to satisfy the deflection limitation, is considerably larger than the value required to satisfy the stress limits. Then the lever arm (d') is large, and the compression area (and hence R) for the sections, with high stresses in the concrete, tends to be small. If the moment decreases below the design moment, then the stresses will decrease, and both e_c and e_s will be less.

However from Equation (c), we see that since R is small, the rate of change of e_c with respect to e_s is also small. Hence the change in the compressive force (C) will itself be small. Thus in order to balance the reduced moment, the lever arm will have to reduce. Whence

the neutral axis will drop in the section, and the R value will increase. Consequently the rate of change of e_c with respect to e_s starts to increase, and the corresponding rate of change of the compressive force (C) is larger.

If the moment decreases further, it seems that the resulting decrease in the compressive force (C) is large enough to cause the lever arm to increase to balance the new moment.

Since the modulus Z can be seen as :

$$Z = \frac{M_A}{f_s} = \frac{A_s f_s jd}{f_s} = A_s jd$$

then the modulus behaviour could be considered similar to the behaviour of the lever arm effective depth ratio (j).

4.7.1 Choosing a Section Modulus Suitable for All Loading Stages

Let us now consider the combined load section moduli Z_T , Z_{TH} , Z_D . The section modulus based on the dead load moment (Z_D) could not be used as the required modulus, because for about 85 percent of the cases the simulated values, for the stresses caused by the maximum total moment (M_T) and the average total moment ($M_H = 0.5\ M_L + M_D$), would be lower than the corresponding actual values.

If the section modulus based on the maximum total moment (Z_T) is used as the required modulus, then the simulated values of the stresses, caused by the maximum total moment (M_T), would be exactly equal to the corresponding actual values, but the simulated values of the stress ranges S_{rh} , caused by the average total moment (M_H), would deviate appreciably from the corresponding actual values f_{srh} , as can be seen from Table (4.3).

This means that an intermediate value of the section modulus, between the value based on the maximum total moment (Z_T) and that caused by the dead load moment (Z_D) is more appropriate.

	$F = Z_T$ KN.M/(N/mm^2)	S_{rh} (a) (N/mm^2)	f_{srh} (b) (N/mm^2)	$\frac{\lvert a - b \rvert}{\text{Minimum of (a,b)}}$ (%)
L = 15.0 m U = 360 T/hr.	3.719	85.54	82.80	3.31
	3.903	85.60	77.89	9.90
	4.395	75.83	69.24	9.52
	4.735	68.62	64.34	6.65
	5.038	64.10	60.45	6.04
	5.596	56.74	53.44	6.18
	5.956	52.40	50.50	3.76
L = 25.0 m all values of U	11.106	55.77	59.15	6.06
	11.951	53.55	55.32	3.31
	12.745	51.68	51.81	0.25
	13.539	50.19	48.70	3.06
	14.398	47.84	46.61	2.64
	15.248	45.77	43.48	5.27

Table (4.3a)

Comparison of the actual stress ranges f_{srh} caused by the average total moment (M_H), to their simulated values (S_{rh}) using a combined section modulus equivalent to that caused by the maximum total moment, (Z_T). Bar dia = 32 mm

	$F = Z_T$ (KN.M/(N/mm^2))	S_{rh} (a) (N/mm^2)	f_{srh} (b) (N/mm^2)	$\frac{\lvert a - b \rvert}{\text{Minimum of (a,b)}}$ (%)
L = 17.5 m all values of U	5.420	73.93	69.64	6.17
	5.734	70.92	64.82	9.41
	6.081	66.45	62.39	6.50
	6.467	61.13	57.25	6.78
	6.808	58.32	54.86	6.30
	7.148	56.14	52.62	6.69
	7.584	51.65	49.41	4.53
	7.958	49.17	47.15	4.29
L = 20.0 m all values of U	6.991	67.69	67.73	0.06
	7.380	65.19	64.09	1.72
	7.725	64.28	60.45	6.34
	8.129	60.93	57.77	5.47
	8.527	58.01	55.45	4.62
	8.902	56.37	53.25	5.86
	9.285	54.00	51.06	5.76
	9.683	51.69	48.98	5.53
	10.068	49.14	46.89	4.80

Table (4.3b)

Comparison of the actual stress ranges f_{srh} caused by the average total moment (M_H), to their simulated values (S_{rh}) using a combined section modulus equivalent to that caused by the maximum total moment, (Z_T). Bar dia = 25 mm

Consequently, let us assume that the combined load section modulus, F, which we will choose to use, is to be defined as the minimum of that corresponding to the average total moment (Z_{TH}) and the average of that corresponding to the maximum total moment (Z_T) plus that corresponding to the dead load (Z_D). We can express this as :

$$F = \text{the minimum of } Z_{TH} \text{ and } 0.5\ (Z_T + Z_D)$$

If we consider the section moduli based on live load moment alone, then it is believed proper to define the section modulus, F_L , as the minimum of that corresponding to the maximum live load moment (Z_L) and that corresponding to the average live load moment (Z_{LH}). We can express this as :

$$F_L = \text{the minimum of } Z_L \text{ and } Z_{LH}$$

The section modulus as defined above (F_L) is equal to Z_L in about 80 percent of the cases. In the same cases, defining the section modulus F_L as above would make the simulated centroidal stress ranges S_{rh} , due to the average total moment, larger than the corresponding actual values f_{srh} .

In about 80 percent of the cases, the maximum value of the strain factor S_f is equal to the value caused by the maximum total moment, S_{FT} . Remembering that in most cases, the section modulus F_L as defined above, would make the simulated centroidal stress ranges caused by the average total moment (M_H) higher than the corresponding actual values. Consequently, if we select the strain factor caused by the maximum total moment to represent the section through all loading stages (i.e. $S_F = S_{FT}$), this for most cases would increase further the deviation between the simulated outer bar stress ranges caused by the average total moment and the corresponding actual values.

For this reason, an intermediate value of the strain factor (S_F) is chosen, which is defined as the maximum of that corresponding to the average total moment (S_{FH}) and the average of that corresponding to the maximum total moment (S_{FT}) plus that corresponding to the dead load (S_{FD}). We can express this as :

$$S_F = \text{the maximum of } S_{FH} \text{ and } 0.5\ (S_{FT} + S_{FD})$$

Noting that S_F as defined above, is in most cases smaller than S_{FT}, and in most cases, the section modulus F_L is equal to the value based on the maximum live load moment (Z_L). Consequently for most cases, the simulated outer bar stress range values S_{re}, based on the live load modulus (F_L), are slightly lower than the actual values f_{sre}. The largest negative deviation is 0.65 percent for 32 mm bars and 0.7 percent for 25 mm bars, which is considered to be quite small.

As mentioned earlier, the combined load modulus (F), the live load modulus (F_L) and the strain factor (S_F) are defined as below:

F = the minimum of Z_{TH} and $0.5\ (Z_T + Z_D)$

F_L = the minimum of Z_L and Z_{LH}

S_F = the maximum of S_{FH} and $0.5\ (S_{FT} + S_{FD})$

Where (Z_T , S_{FT}), (Z_{TH} , S_{FH}) and (Z_D , S_{FD}) are the combined load modulus and the strain factor corresponding to the maximum total moment (M_T), the average total moment (M_H) and the dead load moment (M_D) respectively. Z_L and Z_{LH} are the live load moduli based on the total and average live load moments respectively.

We have to investigate now whether F or F_L is more appropriate. For the maximum stress ranges caused by the maximum total moment ($M_T = M_D + M_L$), the stress range values based on the live load modulus (F_L) are larger than those based on the combined load modulus (F), in more than 95 percent of the cases.

Also, for the maximum total moment (M_T), in 85 percent of the cases, the simulated stress range values based on the live load modulus (F_L) are nearer to the actual values, than those based on the combined load modulus (F).

However, for the average total moment ($M_H = M_D + 0.5\ M_L$), in all cases, the stress range values based on the live load modulus (F_L) are not less than those based on the combined load modulus (F).

Also, for the average total moment (M_H), in all cases, the stress range values based on the combined load modulus (F) are nearer to the actual values, than those based on the live load modulus (F_L).

Consequently it is believed that the live load modulus (F_L) should be used to represent the section modulus, since it simulates the stress ranges caused by the maximum total moment (M_T) in a more proper way. Also, using the modulus F would make the simulated centroidal stress ranges, caused by the maximum total moment, lower than the actual values.

Since, in most cases, the live load modulus (F_L) is equal to the modulus Z_L which corresponds to the maximum live load moment, then the simulated stress ranges, caused by the average total moment ($M_H = M_D + 0.5\ M_L$), are larger than the actual values. The maximum relative difference between the simulated and the actual values is 5.24 percent for 32 mm bars and 6.31 percent for 25 mm bars. Table (4.4) shows the maximum relative differences. Since they are generally less than 5.0 percent, except in few cases where they are around 6.0 percent, then it is believed reasonable to define the section modulus as the minimum of that corresponding to the maximum live load moment (Z_L), and that corresponding to the average live load moment (Z_{LH}).

To give more justification to this, two sets of fatigue lives have been calculated for the combination of loading frequency U = 90 T/hr. and span L = 15.0 m. The first set is based on section modulus values defined as above, while the second set is based on section modulus values defined as the maximum of that corresponding to the maximum live load moment (Z_L), and that corresponding to the average live load moment (Z_{LH}).

From these two sets of points, two section modulus values, which give a specified design life (25, 50, 100 and 200 years), have been interpolated and their relative difference has been found to be quite small (around 1.0 percent), as will be shown later in Chapter (6).

	Span (m)	Loading frequency (T/hr.)	Maximum D_S (%)	Maximum D_f (%)	Maximum + D_{fe} (%)	Maximum - D_{fe} (%)
Maximum total moment	15.0	360	4.87	0.00	0.01	0.60
	15.0	180 +90	4.52	0.00	0.00	0.65
	17.5	all values	4.11	0.00	0.00	0.53
	20.0	all values	3.16	+ 3.10	3.43	0.47
	25.0	all values	2.60	+ 3.61	4.03	0.23
	27.5	all values	1.44	+ 4.21	4.71	0.17
Average total moment	15.0	360	2.05	+ 4.30	5.24	0.00
	15.0	180 +90	1.85	+ 3.80	4.89	0.00
	17.5	all values	1.57	+ 2.93	3.29	0.00
	20.0	all values	1.11	+ 2.92	2.99	0.00
	25.0	all values	0.76	+ 1.56	1.59	0.00
	27.5	all values	0.38	+ 2.55	2.54	0.00

Table (4.4a)
Maximum relative differences for the various loading frequency and span combinations
Bar dia = 32 mm

D_S = the relative difference of the simulated centroidal stress ranges based on the live load modulus (F_L) and the combined load modulus (F).

D_f , D_{fe} = the relative differences of the simulated and actual centroidal and outer bar stress ranges respectively.

	Span (m)	Loading frequency (T/hr.)	Maximum D_S (%)	Maximum D_f (%)	Maximum $+D_{fe}$ (%)	Maximum $-D_{fe}$ (%)
Maximum total moment	15.0	360	5.58	0.00	0.00	0.64
	15.0	180 +90	5.33	0.00	0.00	0.66
	17.5	all values	4.15	0.00	0.00	0.70
	20.0	all values	3.38	1.88	2.10	0.64
	25.0	all values	2.16	5.48	6.20	0.31
	27.5	all values	2.03	5.17	5.97	0.24
Average total moment	15.0	360	2.36	4.95	6.31	0.00
	15.0	180 +90	2.18	4.63	6.23	0.00
	17.5	all values	1.58	4.24	5.43	0.00
	20.0	all values	1.19	2.60	3.16	0.00
	25.0	all values	0.60	1.80	1.80	0.00
	27.5	all values	0.41	2.24	2.24	0.00

Table (4.4b)
Maximum relative differences for the various loading frequency and span combinations
Bar dia = 25 mm

- For the definitions of the terms, see Table (4.4a).

4.7.2. Sections of The 15.0 m Bridge

As can be seen from Figure (3.7) and Table (4.1), for a span of 15.0 m, the maximum moments, for the loading frequency U = 90 T/hr. and 180 T/hr., are equal and they are slightly smaller than the corresponding value for U = 360 T/hr. This makes it necessary to design two sets of sections, one for U = 90 T/hr. and U = 180 T/hr. and the other for U = 360 T/hr.

However, the two sets have some common sections which have the same dimensions and reinforcement, but have slightly different values of the section modulus (F_L) and the strain factor (S_F).

For such sections, F_L and S_F for both are taken to be:

$$F_L = 0.5\ (F_{L1} + F_{L2}) \quad , \quad S_F = 0.5\ (S_{F1} + S_{F2})$$

where F_{L1} and S_{F1} correspond to the first set of sections, while F_{L2} and S_{F2} correspond to the second set of sections, as given in Table (4.5).

For a few sections, the final rounded value of the strain factor (S_F) is very slightly lower than the ratio of the outer bar dead load stress to the centroidal dead load stress (i.e. f_{sde}/f_{sd}). For very small values of the live load moment, such a value of the strain factor (S_F) would produce fictitious negative stress ranges with very small absolute values. To avoid this, the related strain factor values have been increased very slightly and taken to be (f_{sde}/f_{sd}), as shown in Table (4.6).

U = 360 T/hr.			U = 90 and 180 T/hr.				
section number	F_{L1}	S_{F1}	section number	F_{L2}	S_{F2}	$F_L = \frac{1}{2}(F_{L1}+F_{L2})$	$S_F = \frac{1}{2}(S_{F1}+S_{F2})$
12	3.694	1.085	110	3.718	1.085	3.71	1.085
13	4.164	1.104	111	4.188	1.104	4.18	1.104
14	4.546	1.097	112	4.564	1.097	4.56	1.097
15	4.855	1.091	113	4.871	1.090	4.86	1.090
16	5.438	1.108	114	5.468	1.107	5.45	1.107

Table (4.5a)

Section modulus (F_L) and strain factor (S_F) values for span = 15.0 m. Bar dia = 32 mm

- F_L values in KN.M/(N/mm²)

section number	S_F	f_{sde}/f_{sd}
41	1.028	1.028034
~~51~~	~~1.022~~	~~1.022778~~
53	1.028	1.028082
54	1.034	1.034135

Table (4.6a)

Modified strain factor (S_F) values

Bar dia = 32 mm

U = 360 T/hr.			U = 90 and 180 T/hr.				
section number	F_{L1}	S_{F1}	section number	F_{L2}	S_{F2}	$F_L = \frac{1}{2}(F_{L1}+F_{L2})$	$S_F = \frac{1}{2}(S_{F1}+S_{F2})$
117	3.786	1.108	127	3.804	1.108	3.80	1.108
118	4.207	1.096	128	4.225	1.096	4.22	1.096
119	4.500	1.112	129	4.518	1.112	4.51	1.112
120	4.807	1.105	130	4.835	1.105	4.82	1.105
121	5.131	1.119	131	5.150	1.119	5.14	1.119
123	5.849	1.123	133	5.860	1.123	5.85	1.123

Table (4.5b)

Section modulus (F_L) and strain factor (S_F) values for span = 15.0 m. Bar dia = 25 mm

- F_L values in KN.M/(N/mm²)

section number	S_F	f_{sde}/f_{sd}
411	1.040	1.040100
512	1.037	1.037644

Table (4.6b)

Modified strain factor (S_F) values

Bar dia = 25 mm

4.8 Sections with Highly Stressed Reinforcement

As demonstrated in Section (3.7), beam sections with highly stressed reinforcement might not be capable of sustaining moments higher than the design moment. Maximum probable moment values for the various spans are given in Table (3.10).

The computer program, used to design the bridge sections and calculate the stresses and moduli for the different loading stages, has been used to analyse bridge sections under the maximum probable moments. The results are given in Table (4.7), from which it appears that we have to neglect sections 11, 19, 41, 116, 126, 210, 310, 410 and 511 and disregard them, because of the probability that their reinforcement might yield before reaching the point of fatigue failure.

section number	stresses (N/mm^2)		section moduli [$KN.M/(N/mm^2)$]		relative differences (%)		strain factor	maximum concrete strain (1×10^{-3})	neutral axis - depth ratio	lever arm - effective depth ratio	
	f_{spe}	f_{sp}	Z_p	Z_{Lp}	D_p	D_{Lp}	S_{Fp}	e_{cp}	R_p	j_p	d_{pp} (mm)
19	470.98	460.34	3.381	3.175	3.85	3.91	1.059	4.190	0.449	0.800	74.50
11	433.23	425.57	3.677	3.536	2.01	2.15	1.053	2.957	0.417	0.823	74.50
12 and 110	416.26	404.95	3.843	3.600	3.75	2.94	1.091	3.339	0.485	0.791	86.45
21	409.70	403.42	5.161	4.959	1.61	1.59	1.051	2.620	0.427	0.822	74.50
22	372.40	366.09	5.687	5.407	2.00	0.48	1.074	2.132	0.466	0.813	84.00
31	402.15	397.92	6.946	6.873	0.06	3.20	1.036	2.031	0.377	0.850	71.34
32	366.16	362.61	7.623	7.442	0.41	1.11	1.043	1.655	0.414	0.842	74.50
41	423.19	419.51	11.089	11.285	0.83	2.82	1.026	1.801	0.312	0.879	73.91
42	391.01	387.77	11.996	12.175	0.92	3.76	1.030	1.551	0.336	0.873	76.50
52	414.24	411.10	14.554	14.940	1.17	4.48	1.024	1.643	0.306	0.883	74.31
53	388.75	385.91	15.504	15.649	0.88	4.68	1.027	1.460	0.327	0.875	76.50

Table (4.7a) - The effect of the maximum probable moment on sections with highly stressed reinforcement. Bar dia = 32 mm

section number	stresses (N/mm^2)		section moduli [$KN.M/(N/mm^2)$]		relative differences (%)		strain factor	maximum concrete strain (1×10^{-3})	neutral axis - depth ratio	lever arm - effective depth ratio	
	f_{spe}	f_{sp}	Z_p	Z_{Lp}	D_p	D_{Lp}	S_{Fp}	e_{cp}	R_p	j_p	d_{pp} (mm)
116 and 126	436.99	422.74	3.682	3.430	4.09	3.21	1.100	3.710	0.477	0.791	87.62
117 and 127	404.75	391.85	3.972	3.699	3.99	2.60	1.116	3.163	0.499	0.786	92.29
210	423.14	412.95	5.042	4.807	2.08	1.81	1.077	2.856	0.430	0.819	84.78
211	396.41	387.04	5.379	5.124	2.10	1.35	1.088	2.490	0.450	0.814	88.93
310	428.49	421.40	6.559	6.427	0.32	0.91	1.050	2.326	0.366	0.851	78.22
311	403.33	396.58	6.970	6.854	0.29	0.60	1.058	2.067	0.384	0.847	82.50
410	426.19	421.39	11.039	11.206	0.73	2.61	1.034	1.827	0.312	0.878	77.84
411	406.38	401.70	11.580	11.710	1.06	5.03	1.039	1.676	0.326	0.875	81.35
511	422.91	418.41	14.300	14.697	0.97	2.88	1.033	1.710	0.303	0.884	80.22
512	405.84	401.48	14.903	15.256	1.20	4.98	1.036	1.588	0.315	0.881	83.14

Table (4.7b) - The effect of the maximum probable moment on sections with highly stressed reinforcement. Bar dia = 25 mm

4.9 Design Tables

Stresses and stress ranges in N/mm^2

All dimensions in mm

Moment values in KN.M

Shear values in KN

Modulus values in $KN.M/(N/mm^2)$

Strain values in (1×10^{-3})

Relative differences in %

Span (m)	beam width (mm)	n_b	ϕ (mm)	s (mm)	c (mm)	μ_{max}
15.00	250	3	10	57	46	0.424
17.50	300	4	10	57	46	0.393
20.00	350	5	10	57	46	0.371
25.00	450	6	12	57	48	0.357
27.50	500	7	12	57	48	0.356

Table I - Some design details for the various spans
Bar dia = 32 mm

n_b : number of the reinforcing bars in one layer

ϕ : bar diameter for the shear reinforcement

s : vertical spacing between reinforcement layers

c : the distance between the centre of the outer layer to the tension face of the beam

μ_{max} : the maximum value for the ratio of the average concrete compressive stress to the concrete compressive strength (f_{cu})

Span (m)	beam width (mm)	n_b	ϕ (mm)	s (mm)	c (mm)	μ_{max}
15.0	250	4	10	50	42.5	0.420
17.5	300	5	10	50	42.5	0.402
20.0	350	6	10	50	42.5	0.389
25.0	450	8	12	50	44.5	0.359
27.5	500	9	12	50	44.5	0.354

Table II - Some design details for the various spans
Bar dia = 25 mm

- For the definitions of the terms, see Table I

Table (1) - Beam details for 15.0 m span and loading frequency, U = 360 T/hr. Bar dia = 32 mm

section number	initial steel stress	required beam depth	actual beam depth	beam width	beam height	total number of bars	reinf. ratio (%)	max. shear stress	various centroidal stresses			various outer bar stresses		
	f_{si}	d_{req}	d	b	h	N_b	R_R	v	f_{sa}	f_{sh}	f_{sd}	f_{sae}	f_{she}	f_{sde}
11	450.0	881.3	925.5	250	1000	6	2.09	1.81	395.8	312.4	229.6	401.8	328.8	241.3
12	415.0	838.2	863.3	250	950	7	2.61	1.93	375.0	290.4	212.5	383.5	314.2	229.3
13	362.5	853.6	861.3	250	950	8	2.99	1.93	333.0	258.1	188.9	344.9	285.0	207.9
14	345.0	883.5	908.8	250	1000	8	2.83	1.84	310.9	243.2	178.9	340.3	266.7	195.7
15	310.0	914.4	958.0	250	1050	8	2.69	1.75	293.8	230.7	170.2	321.1	251.5	185.2
16	292.5	927.6	951.6	250	1050	9	3.04	1.77	264.5	207.6	154.2	293.7	229.9	170.3
17	257.5	961.5	1001.1	250	1100	9	2.89	1.69	250.0	197.7	147.2	275.7	217.5	161.7
18	240.0	983.5	992.5	250	1100	10	3.24	1.70	229.3	180.6	134.4	257.8	202.7	150.5

Table (1a): L = 15.0 m, U = 360 T/hr., dia = 32 mm

section	various total moment values			max. shear	various max. concrete strains			various strain factors and their relative difference						
number	M_T	M_H	M_D	V_T	e_{ca}	e_{ch}	e_{cd}	S_{FT}	S_{FH}	S_{FD}	D_{Sf}	d_{pt}	d_{ph}	d_{pd}
11	1472.0	1172.0	871.9	417.8	2.30	1.19	0.82	1.052	1.052	1.051	0.13	74.50	73.54	73.60
12	1463.6	1163.5	863.4	415.5	2.47	1.31	0.88	1.090	1.082	1.079	1.01	86.68	83.41	83.60
13	1463.6	1163.5	863.4	415.5	1.87	1.27	0.86	1.105	1.104	1.101	0.41	88.70	91.13	91.41
14	1472.0	1172.0	871.9	417.8	1.57	1.12	0.77	1.100	1.097	1.094	0.53	91.16	91.75	91.94
15	1480.5	1180.4	880.3	420.0	1.37	1.00	0.70	1.093	1.090	1.088	0.42	92.03	92.24	92.38
16	1480.5	1180.4	880.3	420.0	1.33	0.97	0.68	1.110	1.107	1.105	0.51	98.39	98.63	98.81
17	1488.9	1188.8	888.8	422.3	1.18	0.88	0.63	1.103	1.100	1.098	0.40	98.95	99.12	99.25
18	1488.9	1188.8	888.8	422.3	1.16	0.87	0.61	1.125	1.122	1.120	0.44	107.50	107.80	108.01

Table (1b): L = 15.0 m, U = 360 T/hr., dia = 32 mm

sec.	section moduli based on centroidal stresses and their relative differences								section moduli based on outer bar stresses and their relative differences							
no.	Z_T	Z_{TH}	Z_D	Z_L	Z_{LH}	D_{Z1}	D_{Z2}	D_{Z3}	Z'_T	Z'_{TH}	Z'_D	Z'_L	Z'_{LH}	D'_{Z1}	D'_{Z2}	D'_{Z3}
11	3.719	3.751	3.797	3.612	3.624	2.09	0.85	0.33	3.664	3.564	3.613	3.740	3.431	2.78	2.78	9.01
12	3.903	4.007	4.064	3.694	3.853	4.10	2.65	4.30	3.817	3.703	3.765	3.893	3.537	3.06	3.06	10.08
13	4.395	4.508	4.571	4.164	4.334	4.01	2.56	4.07	4.243	4.082	4.152	4.381	3.893	3.94	3.94	12.53
14	4.735	4.819	4.875	4.546	4.664	2.95	1.77	2.59	4.325	4.394	4.455	4.149	4.226	3.01	1.60	1.86
15	5.038	5.117	5.172	4.855	4.964	2.64	1.56	2.24	4.610	4.694	4.752	4.417	4.531	3.07	1.81	2.58
16	5.596	5.685	5.710	5.438	5.615	2.02	1.59	3.26	5.040	5.135	5.168	4.863	5.040	2.54	1.88	3.63
17	5.956	6.013	6.038	5.839	5.942	1.37	0.96	1.76	5.401	5.465	5.497	5.265	5.373	1.77	1.18	2.05
18	6.495	6.582	6.612	6.328	6.493	1.81	1.34	2.62	5.775	5.866	5.905	5.592	5.754	2.26	1.58	2.90

Table (1c): L = 15.0 m, U = 360 T/hr., dia = 32 mm

section number	neutral axis depth ratios			lever arm effective depth ratios				
	R_T	R_H	R_D	j_T	j_H	j_D	j_L	j_{LH}
11	0.411	0.433	0.416	0.833	0.839	0.849	0.809	0.811
12	0.478	0.474	0.453	0.803	0.821	0.833	0.760	0.790
13	0.529	0.495	0.476	0.793	0.816	0.827	0.751	0.784
14	0.503	0.479	0.463	0.810	0.825	0.834	0.777	0.798
15	0.482	0.465	0.451	0.817	0.830	0.839	0.788	0.806
16	0.501	0.484	0.470	0.812	0.826	0.829	0.789	0.815
17	0.485	0.471	0.459	0.822	0.830	0.834	0.806	0.820
18	0.503	0.489	0.478	0.814	0.825	0.829	0.793	0.814

Table (1d): L = 15.0 m, U = 360 T/hr., dia = 32 mm

section	live load modulus	strain factor	combined load modulus	centroidal simulated stress ranges based on F and F_L			centroidal simulated and actual stress ranges			outer bar simulated and actual stress ranges			fatigue limit
number	F_L	S_F	F	S_{RT}	S_{RL}	D_S	S_r	f_{sr}	D_f	S_{re}	f_{sre}	D_{fe}	S_e
11	3.612	1.052	3.751	162.80	166.15	2.06	166.15	166.15	0.00	160.47	160.46	0.008	81.86
12	3.694	1.085	3.983	154.93	162.47	4.87	162.47	162.47	0.00	153.63	154.14	- 0.34	85.82
13	4.164	1.104	4.483	137.58	144.13	4.76	144.13	144.13	0.00	136.92	136.99	- 0.05	92.88
14	4.546	1.097	4.805	127.50	132.02	3.54	132.02	132.02	0.00	144.48	144.64	- 0.11	96.92
15	4.855	1.091	5.105	119.78	123.62	3.20	123.62	123.62	0.00	135.20	135.86	- 0.49	100.37
16	5.438	1.108	5.653	107.71	110.36	2.46	110.36	110.36	0.00	122.66	123.40	- 0.60	105.29
17	5.839	1.101	5.997	101.08	102.78	1.68	102.78	102.78	0.00	113.44	113.98	- 0.48	108.14
18	6.328	1.122	6.553	92.79	94.85	2.22	94.85	94.85	0.00	106.77	107.33	- 0.53	111.84

Table (1e) - Actual and simulated stress ranges caused by the maximum total moment (M_T)
L = 15.0 m, U = 360 T/hr., dia = 32 mm

section number	centroidal simulated stress ranges based on F and F_L			centroidal simulated and actual stress ranges			outer bar simulated and actual stress ranges		
	S_{RHT}	S_{RHL}	D_{SH}	S_{rh}	f_{srh}	D_{fh}	S_{rhe}	f_{srhe}	D_{fhe}
11	82.80	83.07	0.33	83.07	82.80	0.33	87.74	87.46	0.33
12	79.60	81.23	2.05	81.23	77.89	4.30	89.29	84.84	5.24
13	70.65	72.06	2.01	72.06	69.24	4.07	80.19	77.08	4.04
14	65.05	66.01	1.47	66.01	64.34	2.59	72.94	71.00	2.72
15	61.00	61.81	1.32	61.81	60.45	2.24	67.79	66.22	2.37
16	54.63	55.18	1.01	55.18	53.44	3.26	61.55	59.54	3.37
17	51.04	51.39	0.69	51.39	50.50	1.76	56.88	55.85	1.85
18	47.00	47.42	0.91	47.42	46.21	2.62	53.55	52.16	2.67

Table (1f) - Actual and simulated stress ranges caused by the average total moment, $M_H = 0.5\ (M_T + M_D)$
L = 15.0 m, U = 360 T/hr., dia = 32 mm

Table (2) - Beam details for 15.0 m span and loading frequency, U = 180 and 90 T/hr. Bar dia = 32 mm

section number	initial steel stress	required beam depth	actual beam depth	beam width	beam height	total number of bars	reinf. ratio (%)	max. shear stress	various centroidal stresses			various outer bar stresses		
	f_{si}	d_{req}	d	b	h	N_b	R_R	v	f_{sa}	f_{sh}	f_{sd}	f_{sae}	f_{she}	f_{sde}
19	432.5	849.8	875.5	250	950	6	2.20	1.90	414.5	326.1	242.1	422.2	340.8	255.3
110	397.5	816.4	863.3	250	950	7	2.61	1.93	365.5	286.2	212.5	373.2	309.6	229.3
111	362.5	844.0	860.7	250	950	8	2.99	1.93	324.7	254.6	188.9	343.4	281.1	207.9
112	327.5	893.3	908.5	250	1000	8	2.83	1.84	303.5	240.0	178.9	333.9	263.2	195.7
113	292.5	916.9	957.9	250	1050	8	2.69	1.75	287.0	227.7	170.2	313.6	248.2	185.2
114	275.0	932.6	951.6	250	1050	9	3.04	1.77	258.2	205.5	154.2	286.6	227.5	170.3
115	257.0	951.3	1001.0	250	1100	9	2.89	1.69	244.9	195.4	147.2	270.0	215.0	161.7

Table (2a) : L = 15.0 m, U = 180 and 90 T/hr., dia = 32 mm

section number	various total moment values			max. shear	various max. concrete strains			various strain factors and their relative difference						
	M_T	M_H	M_D	V_T	e_{ca}	e_{ch}	e_{cd}	S_{FT}	S_{FH}	S_{FD}	D_{Sf}	d_{pt}	d_{ph}	d_{pd}
19	1432.4	1147.9	863.4	415.5	2.90	1.32	0.91	1.057	1.056	1.055	0.23	74.50	73.01	73.44
110	1432.4	1147.9	863.4	415.5	2.23	1.28	0.88	1.091	1.082	1.079	1.03	86.70	83.42	83.60
111	1432.4	1147.9	863.4	415.5	1.79	1.24	0.86	1.106	1.104	1.101	0.46	89.29	91.16	91.41
112	1440.9	1156.4	871.9	417.8	1.52	1.10	0.77	1.100	1.096	1.094	0.54	91.47	91.76	91.94
113	1449.3	1164.8	880.3	420.0	1.33	0.98	0.70	1.093	1.090	1.088	0.39	92.06	92.24	92.38
114	1449.3	1164.8	880.3	420.0	1.29	0.96	0.68	1.110	1.107	1.105	0.47	98.42	98.65	98.81
115	1457.7	1173.2	888.8	422.3	1.15	0.87	0.63	1.102	1.100	1.098	0.36	98.97	99.13	99.25

Table (2b): L = 15.0 m, U = 180 and 90 T/hr., dia = 32 mm

sec.	section moduli based on centroidal stresses and their relative differences								section moduli based on outer bar stresses and their relative differences							
no.	Z_T	Z_{TH}	Z_D	Z_L	Z_{LH}	D_{Z1}	D_{Z2}	D_{Z3}	Z'_T	Z'_{TH}	Z'_D	Z'_L	Z'_{LH}	D'_{Z1}	D'_{Z2}	D'_{Z3}
19	3.455	3.520	3.567	3.299	3.386	3.22	1.88	2.64	3.393	3.369	3.382	3.410	3.331	0.71	0.71	2.37
110	3.919	4.011	4.064	3.718	3.859	3.69	2.35	3.80	3.838	3.708	3.765	3.955	3.544	3.52	3.52	11.59
111	4.411	4.508	4.571	4.188	4.327	3.63	2.20	3.32	4.172	4.084	4.153	4.202	3.888	2.16	2.16	8.05
112	4.747	4.818	4.875	4.564	4.651	2.69	1.49	1.90	4.315	4.394	4.455	4.117	4.216	3.24	1.82	2.41
113	5.049	5.115	5.172	4.871	4.947	2.42	1.30	1.56	4.622	4.693	4.752	4.434	4.518	2.82	1.53	1.89
114	5.612	5.668	5.710	5.468	5.541	1.74	0.99	1.34	5.056	5.120	5.168	4.892	4.976	2.22	1.26	1.72
115	5.952	6.004	6.038	5.823	5.899	1.44	0.86	1.30	5.399	5.457	5.497	5.254	5.336	1.81	1.07	1.57

Table (2c): L = 15.0 m, U = 180 and 90 T/hr., dia = 32 mm

section number	neutral axis depth ratios			lever arm effective depth ratios				
	R_T	R_H	R_D	j_T	j_H	j_D	j_L	j_{LH}
19	0.431	0.448	0.428	0.818	0.832	0.843	0.781	0.800
110	0.479	0.472	0.453	0.806	0.822	0.833	0.765	0.791
111	0.525	0.494	0.476	0.797	0.816	0.827	0.756	0.783
112	0.500	0.478	0.463	0.812	0.824	0.834	0.781	0.796
113	0.480	0.464	0.451	0.819	0.830	0.839	0.790	0.803
114	0.499	0.483	0.470	0.815	0.823	0.829	0.794	0.805
115	0.483	0.470	0.459	0.821	0.829	0.834	0.804	0.814

Table (2d): L = 15.0 m, U = 180 and 90 T/hr., dia = 32 mm

section	live load modulus	strain factor	combined load modulus	centroidal simulated stress ranges based on F and F_L			centroidal simulated and actual stress ranges			outer bar simulated and actual stress ranges			fatigue limit
number	F_L	S_F	F	S_{RT}	S_{RL}	D_S	S_r	f_{sr}	D_f	S_{re}	f_{sre}	D_{fe}	S_e
19	3.299	1.056	3.511	165.89	172.47	3.96	172.47	172.47	0.00	166.72	166.88	- 0.10	77.24
110	3.718	1.085	3.991	146.41	153.03	4.52	153.03	153.03	0.00	143.39	143.87	- 0.33	85.82
111	4.188	1.104	4.491	130.06	135.86	4.46	135.86	135.86	0.00	135.31	135.42	- 0.08	92.88
112	4.564	1.097	4.811	120.64	124.66	3.34	124.66	124.66	0.00	137.30	138.19	- 0.65	96.92
113	4.871	1.090	5.111	113.37	116.80	3.03	116.80	116.80	0.00	127.72	128.33	- 0.47	100.37
114	5.468	1.107	5.661	101.84	104.06	2.18	104.06	104.06	0.00	115.64	116.31	- 0.58	105.29
115	5.823	1.100	5.995	95.96	97.71	1.82	97.71	97.71	0.00	107.81	108.30	- 0.45	108.14

Table (2e) - Actual and simulated stress ranges caused by the maximum total moment (M_T)
L = 15.0 m, U = 180 and 90 T/hr., dia = 32 mm

section number	centroidal simulated stress ranges based on F and F_L			centroidal simulated and actual stress ranges			outer bar simulated and actual stress ranges		
	S_{RHT}	S_{RHL}	D_{SH}	S_{rh}	f_{srh}	D_{fh}	S_{rhe}	f_{srhe}	D_{fhe}
19	84.87	86.23	1.61	86.23	84.02	2.64	85.84	85.41	0.49
110	75.13	76.51	1.85	76.51	73.71	3.80	84.20	80.27	4.89
111	66.72	67.93	1.82	67.93	65.75	3.32	75.57	73.16	3.29
112	61.50	62.33	1.34	62.33	61.17	1.90	68.91	67.47	2.13
113	57.70	58.40	1.21	58.40	57.50	1.56	64.04	62.97	1.70
114	51.58	52.03	0.87	52.03	51.34	1.34	58.02	57.17	1.49
115	48.50	48.85	0.72	48.85	48.23	1.30	54.05	53.31	1.39

Table (2f) - Actual and simulated stress ranges caused by the average total moment, $M_H = 0.5\ (M_T + M_D)$
L = 15.0 m, U = 180 and 90 T/hr., dia = 32 mm

Table (3) - Beam details for 17.5 m span, with all values of the loading frequency
Bar dia = 32 mm

section number	initial steel stress	required beam depth	actual beam depth	beam width	beam height	total number of bars	reinf. ratio (%)	max. shear stress	various centroidal stresses			various outer bar stresses		
	f_{si}	d_{req}	d	b	h	N_b	R_R	v	f_{sa}	f_{sh}	f_{sd}	f_{sae}	f_{she}	f_{sde}
21	415.0	886.4	975.5	300	1050	8	2.20	1.67	381.2	307.9	234.9	386.3	323.5	246.5
22	380.0	885.4	966.0	300	1050	9	2.50	1.69	347.2	277.7	211.6	352.1	296.7	225.7
23	345.0	935.7	962.4	300	1050	10	2.79	1.69	316.3	253.2	193.6	340.6	274.5	209.4
24	310.0	969.0	1011.6	300	1100	10	2.65	1.62	299.8	240.9	185.0	324.1	259.9	199.3
25	292.5	983.3	1006.1	300	1100	11	2.93	1.63	275.8	221.7	169.6	301.9	242.1	185.0
26	265.0	1010.9	1055.6	300	1150	11	2.79	1.56	261.8	211.6	162.7	284.9	229.8	176.5
27	257.5	1020.1	1050.9	300	1150	12	3.06	1.57	242.6	196.3	150.4	266.9	215.5	164.9

Table (3a): L = 17.5 m, all values of U, dia = 32 mm

section	various total moment values			max. shear	various max. concrete strains			various strain factors and their relative difference						
number	M_T	M_H	M_D	V_T	e_{ca}	e_{ch}	e_{cd}	S_{FT}	S_{FH}	S_{FD}	D_{Sf}	d_{pt}	d_{ph}	d_{pd}
21	1983.1	1614.8	1246.4	488.5	2.14	1.22	0.87	1.051	1.051	1.049	0.15	74.50	73.61	73.66
22	1983.1	1614.8	1246.4	488.5	1.73	1.19	0.85	1.074	1.068	1.067	0.70	83.56	81.65	81.76
23	1983.1	1614.8	1246.4	488.5	1.59	1.16	0.83	1.087	1.084	1.082	0.43	87.62	88.22	88.37
24	1996.9	1628.6	1260.2	491.6	1.39	1.05	0.76	1.081	1.079	1.077	0.37	88.44	88.60	88.71
25	1996.9	1628.6	1260.2	491.6	1.36	1.02	0.75	1.095	1.092	1.090	0.41	93.95	94.15	94.29
26	2010.7	1642.3	1274.0	494.8	1.22	0.93	0.69	1.088	1.086	1.085	0.32	94.39	94.53	94.64
27	2010.7	1642.3	1274.0	494.8	1.19	0.91	0.67	1.100	1.098	1.096	0.36	99.13	99.29	99.40

Table (3b): L = 17.5 m, all values of U, dia = 32 mm

sec.	section moduli based on centroidal stresses and their relative differences								section moduli based on outer bar stresses and their relative differences							
no.	Z_T	Z_{TH}	Z_D	Z_L	Z_{LH}	D_{Z1}	D_{Z2}	D_{Z3}	Z'_T	Z'_{TH}	Z'_D	Z'_L	Z'_{LH}	D'_{Z1}	D'_{Z2}	D'_{Z3}
21	5.203	5.244	5.305	5.038	5.048	1.97	0.80	0.20	5.134	4.991	5.056	5.272	4.785	2.86	2.86	10.17
22	5.712	5.814	5.891	5.433	5.568	3.13	1.79	2.49	5.632	5.442	5.523	5.826	5.186	3.48	3.48	12.35
23	6.271	6.378	6.440	6.004	6.179	2.70	1.72	2.93	5.822	5.883	5.951	5.614	5.664	2.23	1.06	0.88
24	6.660	6.759	6.811	6.417	6.587	2.27	1.49	2.65	6.161	6.266	6.324	5.902	6.076	2.64	1.70	2.95
25	7.240	7.347	7.429	6.938	7.082	2.61	1.49	2.08	6.613	6.728	6.814	6.296	6.449	3.03	1.73	2.43
26	7.680	7.763	7.831	7.433	7.536	1.96	1.07	1.38	7.057	7.145	7.218	6.794	6.905	2.29	1.26	1.64
27	8.287	8.369	8.468	7.992	8.040	2.18	0.98	0.60	7.533	7.623	7.725	7.223	7.288	2.55	1.19	0.91

Table (3c): L = 17.5 m, all values of U, dia = 32 mm

section number	neutral axis depth ratios			lever arm effective depth ratios				
	R_T	R_H	R_D	j_T	j_H	j_D	j_L	j_{LH}
21	0.427	0.443	0.427	0.829	0.835	0.845	0.803	0.804
22	0.476	0.461	0.446	0.817	0.829	0.841	0.777	0.794
23	0.501	0.478	0.463	0.810	0.825	0.833	0.776	0.799
24	0.482	0.465	0.452	0.819	0.831	0.837	0.789	0.810
25	0.497	0.480	0.468	0.813	0.826	0.835	0.780	0.796
26	0.481	0.468	0.457	0.822	0.831	0.839	0.796	0.807
27	0.495	0.482	0.472	0.817	0.825	0.835	0.788	0.793

Table (3d): L = 17.5 m, all values of U, dia = 32 mm

section	live load modulus	strain factor	combined load modulus	centroidal simulated stress ranges based on F and F_L			centroidal simulated and actual stress ranges			outer bar simulated and actual stress ranges			fatigue limit
number	F_L	S_F	F	S_{RT}	S_{RL}	D_S	S_r	f_{sr}	D_f	S_{re}	f_{sre}	D_{fe}	S_e
21	5.038	1.051	5.244	143.20	146.22	2.11	146.22	146.22	0.00	139.72	139.74	- 0.016	80.14
22	5.433	1.070	5.801	130.25	135.60	4.11	135.60	135.60	0.00	126.20	126.45	- 0.20	87.02
23	6.004	1.084	6.355	118.50	122.71	3.55	122.71	122.71	0.00	131.08	131.21	- 0.099	92.39
24	6.417	1.079	6.736	111.44	114.80	3.01	114.80	114.80	0.00	124.23	124.82	- 0.47	95.74
25	6.938	1.092	7.334	102.63	106.19	3.46	106.19	106.19	0.00	116.38	117.00	- 0.53	100.47
26	7.433	1.087	7.756	96.56	99.11	2.63	99.11	99.11	0.00	107.98	108.43	- 0.42	103.25
27	7.992	1.098	8.369	89.83	92.18	2.62	92.18	92.18	0.00	101.52	101.99	- 0.47	107.08

Table (3e) - Actual and simulated stress ranges caused by the maximum total moment (M_T)
L = 17.5 m, all values of U, dia = 32 mm

section number	centroidal simulated stress ranges based on F and F_L			centroidal simulated and actual stress ranges			outer bar simulated and actual stress ranges		
	S_{RHT}	S_{RHL}	D_{SH}	S_{rh}	f_{srh}	D_{fh}	S_{rhe}	f_{srhe}	D_{fhe}
21	72.96	73.11	0.20	73.11	72.96	0.20	77.12	76.97	0.19
22	66.76	67.80	1.57	67.80	66.16	2.49	73.37	71.03	3.29
23	60.54	61.35	1.35	61.35	59.61	2.93	66.98	65.04	2.99
24	56.76	57.40	1.13	57.40	55.92	2.65	62.30	60.62	2.77
25	52.41	53.09	1.31	53.09	52.01	2.08	58.38	57.11	2.22
26	49.07	49.55	0.98	49.55	48.88	1.38	54.13	53.34	1.48
27	45.81	46.09	0.60	46.09	45.81	0.60	50.91	50.54	0.73

Table (3f) - Actual and simulated stress ranges caused by the average total moment, $M_H = 0.5\ (M_T + M_D)$
L = 17.5 m, all values of U, dia = 32 mm

Table (4) - Beam details for 20.0 m span, with all values of the loading frequency
Bar dia = 32 mm

section number	initial steel stress	required beam depth	actual beam depth	beam width	beam height	total number of bars	reinf. ratio (%)	max. shear stress	various centroidal stresses			various outer bar stresses		
	f_{si}	d_{req}	d	b	h	N_b	R_R	v	f_{sa}	f_{sh}	f_{sd}	f_{sae}	f_{she}	f_{sde}
31	415.0	945.5	1128.7	350	1200	9	1.83	1.43	384.3	319.1	249.9	388.0	331.0	259.0
32	380.0	944.0	1125.5	350	1200	10	2.04	1.43	352.3	289.5	226.9	355.4	301.9	236.5
33	345.0	998.8	1119.6	350	1200	11	2.26	1.44	325.7	266.3	208.8	340.7	281.0	220.1
34	310.0	1035.4	1113.6	350	1200	12	2.48	1.45	301.7	246.2	193.8	322.2	262.6	206.4
35	292.5	1050.9	1108.7	350	1200	13	2.69	1.45	280.5	229.4	180.9	302.6	247.0	194.5
36	275.0	1069.4	1104.4	350	1200	14	2.91	1.46	262.9	215.4	168.9	286.2	234.0	183.1
37	257.5	1091.2	1100.7	350	1200	15	3.13	1.46	247.1	202.3	158.5	271.2	221.5	173.3

Table (4a): L = 20.0 m, all values of U, dia = 32 mm

section number	various total moment values			max. shear	various max. concrete strains			various strain factors and their relative difference						
	M_T	M_H	M_D	V_T	e_{ca}	e_{ch}	e_{cd}	S_{FT}	S_{FH}	S_{FD}	D_{Sf}	d_{pt}	d_{ph}	d_{pd}
31	2676.9	2215.4	1754.0	564.2	1.81	1.11	0.82	1.036	1.037	1.036	0.098	71.30	70.77	70.79
32	2676.9	2215.4	1754.0	564.2	1.49	1.07	0.80	1.044	1.043	1.042	0.14	74.50	73.91	73.94
33	2676.9	2215.4	1754.0	564.2	1.35	1.04	0.78	1.056	1.055	1.054	0.18	80.36	80.73	80.78
34	2676.9	2215.4	1754.0	564.2	1.32	1.02	0.76	1.068	1.066	1.065	0.27	86.39	86.49	86.57
35	2676.9	2215.4	1754.0	564.2	1.29	1.00	0.75	1.079	1.077	1.075	0.31	91.32	91.44	91.53
36	2676.9	2215.4	1754.0	564.2	1.27	0.98	0.74	1.088	1.086	1.085	0.34	95.59	95.73	95.83
37	2676.9	2215.4	1754.0	564.2	1.25	0.97	0.73	1.097	1.095	1.093	0.36	99.32	99.49	99.60

Table (4b): L = 20.0 m, all values of U, dia = 32 mm

sec.	section moduli based on centroidal stresses and their relative differences								section moduli based on outer bar stresses and their relative differences							
no.	Z_T	Z_{TH}	Z_D	Z_L	Z_{LH}	D_{Z1}	D_{Z2}	D_{Z3}	Z'_T	Z'_{TH}	Z'_D	Z'_L	Z'_{LH}	D'_{Z1}	D'_{Z2}	D'_{Z3}
31	6.967	6.942	7.020	6.867	6.660	1.13	0.35	3.10	6.899	6.693	6.773	7.152	6.407	3.07	3.07	11.63
32	7.599	7.654	7.731	7.360	7.374	1.74	0.72	0.19	7.532	7.338	7.417	7.759	7.050	2.64	2.64	10.05
33	8.219	8.320	8.401	7.892	8.025	2.22	1.23	1.68	7.857	7.884	7.969	7.653	7.579	1.42	0.35	0.98
34	8.872	8.998	9.052	8.550	8.800	2.03	1.42	2.92	8.307	8.437	8.498	7.967	8.216	2.30	1.57	3.13
35	9.542	9.658	9.697	9.262	9.513	1.62	1.21	2.71	8.847	8.970	9.019	8.539	8.790	1.94	1.39	2.94
36	10.180	10.284	10.388	9.808	9.906	2.04	1.01	1.00	9.355	9.468	9.578	8.959	9.074	2.38	1.21	1.29
37	10.832	10.951	11.067	10.410	10.529	2.18	1.10	1.14	9.871	10.000	10.123	9.426	9.562	2.55	1.31	1.44

Table (4c): L = 20.0 m, all values of U, dia = 32 mm

section number	neutral axis depth ratios			lever arm effective depth ratios				
	R_T	R_H	R_D	j_T	j_H	j_D	j_L	j_{LH}
31	0.379	0.409	0.398	0.853	0.849	0.859	0.841	0.815
32	0.421	0.424	0.413	0.840	0.845	0.854	0.813	0.814
33	0.454	0.439	0.428	0.830	0.840	0.848	0.797	0.810
34	0.467	0.453	0.441	0.826	0.837	0.842	0.796	0.819
35	0.480	0.466	0.454	0.823	0.833	0.837	0.799	0.821
36	0.491	0.477	0.466	0.819	0.827	0.836	0.789	0.797
37	0.502	0.488	0.478	0.816	0.825	0.834	0.784	0.793

Table (4d): L = 20.0 m, all values of U, dia = 32 mm

section	live load modulus	strain factor	combined load modulus	centroidal simulated stress ranges based on F and F_L			centroidal simulated and actual stress ranges			outer bar simulated and actual stress ranges			fatigue limit
number	F_L	S_F	F	S_{RT}	S_{RL}	D_S	S_r	f_{sr}	D_f	S_{re}	f_{sre}	D_{fe}	S_e
31	6.660	1.037	6.942	135.76	138.57	2.07	138.57	134.40	3.10	133.47	129.04	3.43	76.04
32	7.360	1.043	7.654	122.87	125.40	2.06	125.40	125.40	0.00	118.90	118.95	- 0.04	83.46
33	7.892	1.055	8.310	113.35	116.93	3.16	116.93	116.93	0.00	120.54	120.59	- 0.04	88.86
34	8.550	1.067	8.962	104.92	107.95	2.88	107.95	107.95	0.00	115.41	115.84	- 0.37	93.38
35	9.262	1.077	9.620	97.39	99.64	2.31	99.64	99.64	0.00	107.61	108.08	- 0.44	97.32
36	9.808	1.086	10.284	91.46	94.10	2.89	94.10	94.10	0.00	102.54	103.02	- 0.47	101.07
37	10.410	1.095	10.949	85.99	88.65	3.09	88.65	88.65	0.00	97.42	97.91	- 0.50	104.32

Table (4e) - Actual and simulated stress ranges caused by the maximum total moment (M_T)
L = 20.0 m, all values of U, dia = 32 mm

section number	centroidal simulated stress ranges based on F and F_L			centroidal simulated and actual stress ranges			outer bar simulated and actual stress ranges		
	S_{RHT}	S_{RHL}	D_{SH}	S_{rh}	f_{srh}	D_{fh}	S_{rhe}	f_{srhe}	D_{fhe}
31	69.28	69.28	0.00	69.28	69.28	0.00	72.03	72.03	0.00
32	62.58	62.70	0.19	62.70	62.58	0.19	65.57	65.45	0.19
33	57.82	58.47	1.11	58.47	57.50	1.68	61.91	60.89	1.68
34	53.43	53.97	1.01	53.97	52.44	2.92	57.84	56.16	2.99
35	49.42	49.82	0.81	49.82	48.51	2.71	53.96	52.49	2.78
36	46.58	47.05	1.00	47.05	46.58	1.00	51.42	50.85	1.12
37	43.85	44.33	1.09	44.33	43.83	1.14	48.87	48.26	1.26

Table (4f) - Actual and simulated stress ranges caused by the average total moment, $M_H = 0.5\ (M_T + M_D)$
L = 20.0 m, all values of U, dia = 32 mm

Table (5) - Beam details for 25.0 m span, with all values of the loading frequency
Bar dia = 32 mm

section number	initial steel stress	required beam depth	actual beam depth	beam width	beam height	total number of bars	reinf. ratio (%)	max. shear stress	various centroidal stresses			various outer bar stresses		
	f_{si}	d_{req}	d	b	h	N_b	R_R	v	f_{sa}	f_{sh}	f_{sd}	f_{sae}	f_{she}	f_{sde}
41	415.0	1061.0	1426.1	450	1500	11	1.38	1.16	406.7	351.7	292.5	410.1	353.7	300.7
42	380.0	1059.2	1423.5	450	1500	12	1.51	1.16	378.0	325.4	270.1	380.9	335.8	278.6
43	362.5	1082.8	1416.9	450	1500	13	1.64	1.17	354.4	303.6	251.8	357.4	315.6	261.6
44	345.0	1123.5	1413.0	450	1500	14	1.77	1.17	333.6	284.2	235.5	341.6	297.4	246.3
45	327.5	1151.3	1407.9	450	1500	15	1.90	1.17	313.7	267.4	220.8	330.6	281.5	232.3
46	310.0	1166.7	1403.8	450	1500	16	2.04	1.18	296.3	251.4	207.9	313.9	266.2	220.0
47	292.5	1184.8	1400.3	450	1500	17	2.17	1.18	280.5	238.3	197.9	298.8	253.6	210.5

Table (5a): L = 25.0 m, all values of U, dia = 32 mm

section number	various total moment values			max. shear	various max. concrete strains			various strain factors and their relative difference						
	M_T	M_H	M_D	V_T	e_{ca}	e_{ch}	e_{cd}	S_{FT}	S_{FH}	S_{FD}	D_{Sf}	d_{pt}	d_{ph}	d_{pd}
41	4517.1	3867.9	3218.8	743.6	1.65	1.07	0.81	1.0265	1.0278	1.0280	0.15	73.90	73.90	73.75
42	4517.1	3867.9	3218.8	743.6	1.43	0.98	0.78	1.030	1.032	1.031	0.15	76.50	76.32	76.34
43	4517.1	3867.9	3218.8	743.6	1.26	0.96	0.77	1.0396	1.0395	1.0390	0.05	83.10	82.36	82.38
44	4517.1	3867.9	3218.8	743.6	1.14	0.93	0.75	1.0464	1.0465	1.0459	0.05	87.01	87.59	87.62
45	4517.1	3867.9	3218.8	743.6	1.12	0.92	0.73	1.054	1.053	1.052	0.13	92.13	92.17	92.20
46	4517.1	3867.9	3218.8	743.6	1.10	0.90	0.72	1.060	1.059	1.058	0.14	96.16	96.21	96.24
47	4517.1	3867.9	3218.8	743.6	1.08	0.88	0.71	1.0653	1.0644	1.0636	0.16	99.75	99.80	99.84

Table (5b): L = 25.0 m, all values of U, dia = 32 mm

sec.	section moduli based on centroidal stresses and their relative differences								section moduli based on outer bar stresses and their relative differences							
no.	Z_T	Z_{TH}	Z_D	Z_L	Z_{LH}	D_{Z1}	D_{Z2}	D_{Z3}	Z'_T	Z'_{TH}	Z'_D	Z'_L	Z'_{LH}	D'_{Z1}	D'_{Z2}	D'_{Z3}
41	11.106	10.998	11.003	11.371	10.975	0.98	0.98	3.61	11.016	10.937	10.703	11.876	12.264	2.92	0.72	3.27
42	11.951	11.887	11.918	12.035	11.734	0.54	0.54	2.56	11.858	11.520	11.554	12.686	11.351	2.94	2.94	11.75
43	12.745	12.740	12.783	12.651	12.531	0.34	0.04	0.96	12.640	12.256	12.303	13.562	12.028	3.14	3.14	12.76
44	13.539	13.611	13.669	13.226	13.331	0.96	0.54	0.79	13.223	13.007	13.069	13.622	12.707	1.66	1.66	7.20
45	14.398	14.466	14.580	13.966	13.927	1.26	0.47	0.28	13.665	13.740	13.856	13.215	13.193	1.39	0.55	0.16
46	15.248	15.385	15.480	14.700	14.930	1.52	0.90	1.56	14.389	14.529	14.628	13.828	14.057	1.66	0.98	1.66
47	16.104	16.234	16.263	15.722	16.092	0.99	0.81	2.35	15.117	15.252	15.290	14.703	15.062	1.15	0.89	2.44

Table (5c): L = 25.0 m, all values of U, dia = 32 mm

section number	neutral axis depth ratios			lever arm effective depth ratios				
	R_T	R_H	R_D	j_T	j_H	j_D	j_L	j_{LH}
41	0.314	0.346	0.356	0.880	0.872	0.872	0.901	0.870
42	0.340	0.375	0.367	0.870	0.865	0.867	0.876	0.854
43	0.374	0.386	0.378	0.860	0.860	0.862	0.854	0.845
44	0.406	0.397	0.389	0.851	0.856	0.860	0.831	0.838
45	0.416	0.407	0.400	0.848	0.852	0.858	0.822	0.820
46	0.425	0.417	0.410	0.844	0.852	0.857	0.814	0.827
47	0.434	0.426	0.418	0.841	0.848	0.850	0.821	0.841

Table (5d): L = 25.0 m, all values of U, dia = 32 mm

section	live load modulus	strain factor	combined load modulus	centroidal simulated stress ranges based on F and F_L			centroidal simulated and actual stress ranges			outer bar simulated and actual stress ranges			fatigue limit
number	F_L	S_F	F	S_{RT}	S_{RL}	D_S	S_r	f_{sr}	D_f	S_{re}	f_{sre}	D_{fe}	S_e
41	10.975	1.028	10.998	118.18	118.31	0.11	118.31	114.18	3.61	113.73	109.33	4.03	62.26
42	11.734	1.032	11.887	109.94	110.65	0.65	110.65	107.88	2.56	105.35	102.35	2.93	69.57
43	12.531	1.039	12.740	102.76	103.61	0.83	103.61	102.63	0.96	96.75	95.73	1.07	75.16
44	13.226	1.046	13.604	96.57	98.17	1.66	98.17	98.17	0.00	95.32	95.31	0.001	80.23
45	13.927	1.053	14.466	91.49	93.22	1.90	93.22	92.97	0.28	98.31	98.25	0.06	84.84
46	14.700	1.059	15.364	86.08	88.32	2.60	88.32	88.32	0.00	93.68	93.89	- 0.23	88.89
47	15.722	1.064	16.184	81.20	82.58	1.70	82.58	82.58	0.00	88.07	88.31	- 0.27	92.03

Table (5e) - Actual and simulated stress ranges caused by the maximum total moment (M_T)
L = 25.0 m, all values of U, dia = 32 mm

section number	centroidal simulated stress ranges based on F and F_L			centroidal simulated and actual stress ranges			outer bar simulated and actual stress ranges		
	S_{RHT}	S_{RHL}	D_{SH}	S_{rh}	f_{srh}	D_{fh}	S_{rhe}	f_{srhe}	D_{fhe}
41	59.15	59.15	0.00	59.15	59.15	0.00	52.94	52.94	0.00
42	55.32	55.32	0.00	55.32	55.32	0.00	57.19	57.19	0.00
43	51.81	51.81	0.00	51.81	51.81	0.00	53.97	53.97	0.00
44	48.85	49.08	0.48	49.08	48.70	0.79	51.49	51.09	0.79
45	46.61	46.61	0.00	46.61	46.61	0.00	49.23	49.21	0.05
46	43.83	44.16	0.76	44.16	43.48	1.56	46.91	46.18	1.59
47	41.09	41.29	0.49	41.29	40.34	2.35	44.12	43.10	2.36

Table (5f) - Actual and simulated stress ranges caused by the average total moment, $M_H = 0.5\ (M_T + M_D)$
L = 25.0 m, all values of U, dia = 32 mm

Table (6) - Beam details for 27.5 m span, with all values of the loading frequency
Bar dia = 32 mm

section number	initial steel stress	required beam depth	actual beam depth	beam width	beam height	total number of bars	reinf. ratio (%)	max. shear stress	various centroidal stresses			various outer bar stresses		
	f_{si}	d_{req}	d	b	h	N_b	R_R	v	f_{sa}	f_{sh}	f_{sd}	f_{sae}	f_{she}	f_{sde}
52	415.0	1118.1	1575.7	500	1650	13	1.33	1.08	393.3	345.8	294.1	396.0	347.4	301.6
53	380.0	1116.2	1573.5	500	1650	14	1.43	1.08	369.1	323.6	274.2	371.5	332.9	281.9
54	362.5	1141.4	1567.8	500	1650	15	1.54	1.08	349.5	303.7	257.8	351.9	314.1	266.6
55	345.0	1185.2	1563.9	500	1650	16	1.65	1.09	330.9	287.1	243.5	340.7	298.6	253.2
56	327.5	1215.1	1559.5	500	1650	17	1.75	1.09	313.3	270.9	230.6	327.6	283.1	240.8
57	310.0	1231.6	1555.8	500	1650	18	1.86	1.09	297.7	258.2	218.9	312.7	271.1	229.7

Table (6a): L = 27.5 m, all values of U, dia = 32 mm

section	various total moment values			max. shear	various max. concrete strains			various strain factors and their relative difference						
number	M_T	M_H	M_D	V_T	e_{ca}	e_{ch}	e_{cd}	S_{FT}	S_{FH}	S_{FD}	D_{Sf}	d_{pt}	d_{ph}	d_{pd}
52	5712.8	4973.9	4235.0	848.5	1.45	1.00	0.79	1.0242	1.02555	1.02561	0.14	74.30	74.30	74.25
53	5712.8	4973.9	4235.0	848.5	1.28	0.93	0.77	1.0273	1.0285	1.0282	0.12	76.50	76.43	76.44
54	5712.8	4973.9	4235.0	848.5	1.15	0.91	0.75	1.0345	1.0344	1.0341	0.04	82.20	81.73	81.74
55	5712.8	4973.9	4235.0	848.5	1.07	0.90	0.74	1.0401	1.0399	1.0395	0.05	86.12	86.40	86.42
56	5712.8	4973.9	4235.0	848.5	1.05	0.88	0.73	1.0455	1.0450	1.0445	0.09	90.52	90.55	90.57
57	5712.8	4973.9	4235.0	848.5	1.03	0.87	0.72	1.0502	1.0497	1.0492	0.10	94.24	94.27	94.29

Table (6b): L = 27.5 m, all values of U, dia = 32 mm

sec.	section moduli based on centroidal stresses and their relative differences								section moduli based on outer bar stresses and their relative differences							
no.	Z_T	Z_{TH}	Z_D	Z_L	Z_{LH}	D_{Z1}	D_{Z2}	D_{Z3}	Z'_T	Z'_{TH}	Z'_D	Z'_L	Z'_{LH}	D'_{Z1}	D'_{Z2}	D'_{Z3}
52	14.525	14.385	14.400	14.895	14.299	0.97	0.97	4.17	14.425	14.316	14.040	15.653	16.130	2.74	0.76	3.05
53	15.479	15.369	15.445	15.579	14.949	0.72	0.72	4.21	15.378	14.943	15.021	16.504	14.514	2.91	2.91	13.71
54	16.344	16.379	16.427	16.109	16.109	0.51	0.22	0.004	16.233	15.834	15.885	17.318	15.544	2.52	2.52	11.41
55	17.263	17.325	17.390	16.909	16.959	0.74	0.36	0.29	16.766	16.660	16.729	16.874	16.275	0.64	0.64	3.68
56	18.232	18.360	18.369	17.851	18.306	0.75	0.70	2.55	17.439	17.569	17.586	17.032	17.474	0.84	0.74	2.59
57	19.189	19.261	19.348	18.745	18.778	0.83	0.38	0.17	18.271	18.350	18.441	17.800	17.844	0.93	0.43	0.25

Table (6c): L = 27.5 m, all values of U, dia = 32 mm

section number	neutral axis depth ratios			lever arm effective depth ratios				
	R_T	R_H	R_D	j_T	j_H	j_D	j_L	j_{LH}
52	0.310	0.347	0.350	0.882	0.873	0.874	0.904	0.868
53	0.336	0.366	0.359	0.874	0.867	0.872	0.879	0.844
54	0.368	0.376	0.369	0.864	0.866	0.868	0.852	0.851
55	0.392	0.385	0.378	0.858	0.861	0.864	0.840	0.843
56	0.400	0.394	0.387	0.855	0.861	0.862	0.837	0.859
57	0.408	0.401	0.395	0.852	0.855	0.859	0.832	0.834

Table (6d): L = 27.5 , all values of U, dia = 32 mm

section	live load modulus	strain factor	combined load modulus	centroidal simulated stress ranges based on F and F_L			centroidal simulated and actual stress ranges			outer bar simulated and actual stress ranges			fatigue limit
number	F_L	S_F	F	S_{RT}	S_{RL}	D_S	S_r	f_{sr}	D_f	S_{re}	f_{sre}	D_{fe}	S_e
52	14.299	1.026	14.385	103.04	103.35	0.30	103.35	99.21	4.17	98.80	94.41	4.65	61.96
53	14.949	1.028	15.369	97.51	98.86	1.39	98.86	94.86	4.21	93.76	89.54	4.71	68.46
54	16.109	1.034	16.379	90.98	91.74	0.83	91.74	91.74	0.00	85.33	85.33	0.00	73.52
55	16.909	1.040	17.325	86.22	87.40	1.36	87.40	87.40	0.00	87.57	87.58	- 0.01	77.96
56	17.851	1.045	18.300	81.61	82.79	1.44	82.79	82.79	0.00	86.62	86.76	- 0.17	82.03
57	18.745	1.050	19.261	77.71	78.84	1.45	78.84	78.84	0.00	82.87	83.02	- 0.18	85.72

Table (6e) - Actual and simulated stress ranges caused by the maximum total moment (M_T)
L = 27.5 m, all values of U, dia = 32 mm

section number	centroidal simulated stress ranges based on F and F_L			centroidal simulated and actual stress ranges			outer bar simulated and actual stress ranges		
	S_{RHT}	S_{RHL}	D_{SH}	S_{rh}	f_{srh}	D_{fh}	S_{rhe}	f_{srhe}	D_{fhe}
52	51.67	51.67	0.00	51.67	51.67	0.00	45.81	45.81	0.00
53	49.43	49.43	0.00	49.43	49.43	0.00	50.91	50.91	0.00
54	45.87	45.87	0.00	45.87	45.87	0.00	47.54	47.54	0.00
55	43.57	43.70	0.29	43.70	43.57	0.29	45.53	45.40	0.29
56	41.24	41.39	0.38	41.39	40.36	2.55	43.36	42.29	2.54
57	39.35	39.42	0.17	39.42	39.35	0.17	41.49	41.41	0.20

Table (6f) - Actual and simulated stress ranges caused by the average total moment, $M_H = 0.5\ (M_T + M_D)$
L = 27.5 m, all values of U, dia = 32 mm

Table (7) - Beam details for 15.0 m span and loading frequency, U = 360 T/hr. Bar dia = 25 mm

section number	initial steel stress	required beam depth	actual beam depth	beam width	beam height	total number of bars	reinf. ratio (%)	max. shear stress	various centroidal stresses			various outer bar stresses		
	f_{si}	d_{req}	d	b	h	N_b	R_R	v	f_{sa}	f_{sh}	f_{sd}	f_{sae}	f_{she}	f_{sde}
116	410.0	831.9	862.0	250	950	11	2.51	1.93	390.9	302.4	220.7	401.8	330.1	240.3
117	380.0	836.9	857.5	250	950	12	2.75	1.94	363.0	280.0	204.5	372.6	309.2	225.1
118	350.0	872.7	912.3	250	1000	12	2.58	1.83	336.7	264.3	194.0	345.2	289.7	212.2
119	340.0	896.8	905.7	250	1000	13	2.82	1.84	314.8	246.9	181.4	341.9	274.6	201.2
120	310.0	914.6	954.4	250	1050	13	2.67	1.76	297.2	233.8	172.4	329.2	258.2	190.0
121	290.0	929.8	949.1	250	1050	14	2.90	1.77	279.0	218.9	162.0	313.0	244.7	180.8
122	265.0	953.4	998.4	250	1100	14	2.75	1.69	263.6	208.2	154.6	293.6	231.3	171.4
123	260.0	959.1	993.6	250	1100	15	2.96	1.70	248.7	196.2	146.1	280.1	220.3	163.8
124	245.0	977.2	989.4	250	1100	16	3.18	1.71	234.9	185.9	137.3	267.3	210.9	155.5
125	230.0	997.7	1038.6	250	1150	16	3.02	1.63	223.6	176.7	132.0	252.5	199.1	148.4

Table (7a): L = 15.0 m, U = 360 T/hr., dia = 25 mm

section number	various total moment values			max. shear	various max. concrete strains			various strain factors and their relative difference						
	M_T	M_H	M_D	V_T	e_{ca}	e_{ch}	e_{cd}	S_{FT}	S_{FH}	S_{FD}	D_{Sf}	d_{pt}	d_{ph}	d_{pd}
116	1463.6	1163.5	863.4	415.5	2.76	1.33	0.90	1.099	1.092	1.089	0.89	87.85	84.75	84.95
117	1463.6	1163.5	863.4	415.5	2.32	1.30	0.88	1.116	1.104	1.101	1.37	92.50	88.87	89.09
118	1472.0	1172.0	871.9	417.8	1.62	1.15	0.79	1.097	1.096	1.094	0.32	87.69	89.35	89.50
119	1472.0	1172.0	871.9	417.8	1.60	1.13	0.78	1.115	1.112	1.109	0.55	94.27	95.31	95.53
120	1480.5	1180.4	880.3	420.0	1.39	1.01	0.71	1.108	1.104	1.102	0.49	95.64	95.88	96.04
121	1480.5	1180.4	880.3	420.0	1.37	1.00	0.70	1.122	1.118	1.116	0.54	100.90	101.22	101.44
122	1488.9	1188.8	888.8	422.3	1.21	0.90	0.64	1.114	1.111	1.109	0.42	101.61	101.83	101.99
123	1488.9	1188.8	888.8	422.3	1.19	0.89	0.63	1.126	1.123	1.121	0.47	106.38	106.64	106.82
124	1488.9	1188.8	888.8	422.3	1.18	0.88	0.62	1.138	1.135	1.132	0.49	110.59	110.89	111.11
125	1497.3	1197.3	897.2	424.5	1.06	0.80	0.57	1.129	1.127	1.125	0.40	111.36	111.58	111.74

Table (7b): L = 15.0 m, U = 360 T/hr., dia = 25 mm

sec.	section moduli based on centroidal stresses and their relative differences								section moduli based on outer bar stresses and their relative differences							
no.	Z_T	Z_{TH}	Z_D	Z_L	Z_{LH}	D_{Z1}	D_{Z2}	D_{Z3}	Z'_T	Z'_{TH}	Z'_D	Z'_L	Z'_{LH}	D'_{Z1}	D'_{Z2}	D'_{Z3}
116	3.744	3.848	3.912	3.526	3.676	4.49	2.78	4.24	3.642	3.524	3.593	3.716	3.341	3.35	3.35	11.23
117	4.031	4.155	4.222	3.786	3.973	4.73	3.06	4.95	3.928	3.764	3.836	4.068	3.569	4.37	4.37	13.99
118	4.372	4.435	4.494	4.207	4.272	2.78	1.43	1.54	4.265	4.046	4.109	4.514	3.872	5.42	5.42	16.56
119	4.676	4.746	4.806	4.500	4.581	2.77	1.50	1.80	4.305	4.268	4.333	4.264	4.090	1.52	0.86	4.25
120	4.981	5.048	5.106	4.807	4.886	2.52	1.36	1.64	4.497	4.571	4.633	4.311	4.400	3.03	1.66	2.06
121	5.306	5.393	5.433	5.131	5.280	2.39	1.64	2.91	4.730	4.823	4.869	4.540	4.691	2.94	1.96	3.33
122	5.648	5.710	5.749	5.504	5.598	1.80	1.11	1.71	5.072	5.140	5.185	4.913	5.013	2.23	1.35	2.03
123	5.986	6.060	6.081	5.849	5.999	1.60	1.25	2.56	5.316	5.396	5.426	5.160	5.308	2.08	1.51	2.87
124	6.339	6.396	6.473	6.150	6.179	2.12	0.91	0.48	5.571	5.638	5.717	5.368	5.416	2.62	1.20	0.89
125	6.697	6.776	6.799	6.549	6.706	1.53	1.18	2.40	5.931	6.013	6.046	5.767	5.919	1.94	1.39	2.63

Table (7c): L = 15.0 m, U = 360 T/hr., dia = 25 mm

section number	neutral axis depth ratios			lever arm effective depth ratios				
	R_T	R_H	R_D	j_T	j_H	j_D	j_L	j_{LH}
116	0.467	0.469	0.448	0.804	0.824	0.838	0.757	0.787
117	0.496	0.482	0.462	0.798	0.819	0.833	0.750	0.783
118	0.490	0.465	0.449	0.814	0.827	0.838	0.783	0.796
119	0.504	0.478	0.462	0.809	0.822	0.833	0.779	0.794
120	0.483	0.464	0.451	0.818	0.829	0.839	0.789	0.802
121	0.495	0.477	0.463	0.813	0.827	0.833	0.787	0.810
122	0.479	0.464	0.453	0.823	0.832	0.838	0.802	0.816
123	0.490	0.476	0.464	0.818	0.829	0.832	0.799	0.820
124	0.501	0.486	0.476	0.816	0.823	0.833	0.791	0.795
125	0.486	0.475	0.465	0.821	0.831	0.834	0.803	0.822

Table (7d): L = 15.0 m, U = 360 T/hr., dia = 25 mm

section	live load modulus	strain factor	combined load modulus	centroidal simulated stress ranges based on F and F_L			centroidal simulated and actual stress ranges			outer bar simulated and actual stress ranges			fatigue limit
number	F_L	S_F	F	S_{RT}	S_{RL}	D_S	S_r	f_{sr}	D_f	S_{re}	f_{sre}	D_{fe}	S_e
116	3.526	1.094	3.828	161.63	170.21	5.31	170.21	170.21	0.00	160.95	161.48	- 0.33	82.19
117	3.786	1.108	4.127	150.15	158.54	5.58	158.54	158.54	0.00	146.91	147.53	- 0.43	87.23
118	4.207	1.096	4.433	138.04	142.66	3.35	142.66	142.66	0.00	132.90	132.96	- 0.05	91.48
119	4.500	1.112	4.741	129.07	133.38	3.34	133.38	133.38	0.00	140.57	140.74	- 0.12	95.10
120	4.807	1.105	5.043	121.14	124.84	3.06	124.84	124.84	0.00	138.41	139.22	- 0.58	98.79
121	5.131	1.119	5.370	113.68	116.97	2.90	116.97	116.97	0.00	131.35	132.20	- 0.64	101.84
122	5.504	1.111	5.698	106.70	109.05	2.20	109.05	109.05	0.00	121.54	122.16	- 0.51	104.93
123	5.849	1.123	6.033	100.63	102.60	1.96	102.60	102.60	0.00	115.64	116.30	- 0.57	107.45
124	6.150	1.135	6.396	95.48	97.59	2.21	97.59	97.59	0.00	111.15	111.80	- 0.58	110.20
125	6.549	1.127	6.748	89.94	91.64	1.89	91.64	91.64	0.00	103.56	104.07	- 0.49	112.53

Table (7e) - Actual and simulated stress ranges caused by the maximum total moment (M_T)
L = 150 m, U = 360 T/hr., dia = 25 mm

section number	centroidal simulated stress ranges based on F and F_L			centroidal simulated and actual stress ranges			outer bar simulated and actual stress ranges		
	S_{RHT}	S_{RHL}	D_{SH}	S_{rh}	f_{srh}	D_{fh}	S_{rhe}	f_{srhe}	D_{fhe}
116	83.24	85.10	2.24	85.10	81.64	4.24	94.15	89.81	4.84
117	77.44	79.27	2.36	79.27	75.53	4.95	89.39	84.08	6.31
118	70.35	71.33	1.39	71.33	70.25	1.54	78.68	77.49	1.53
119	65.78	66.69	1.39	66.69	65.51	1.80	74.72	73.36	1.85
120	61.64	62.42	1.26	62.42	61.42	1.64	69.44	68.20	1.81
121	57.79	58.48	1.19	58.48	56.83	2.91	65.92	63.97	3.06
122	54.04	54.52	0.90	54.52	53.61	1.71	60.95	59.86	1.82
123	50.89	51.30	0.80	51.30	50.02	2.56	58.01	56.53	2.63
124	48.56	48.79	0.48	48.79	48.56	0.48	55.76	55.41	0.65
125	45.47	45.82	0.77	45.82	44.75	2.40	51.93	50.70	2.43

Table (7f) - Actual and simulated stress ranges caused by the average total moment, $M_H = 0.5\ (M_T + M_D)$
L = 15.0 m, U = 360 T/hr., dia = 25 mm

Table (8) - Beam details for 15.0 m span and loading frequency, U = 180 and 90 T/hr. Bar dia = 25 mm

section number	initial steel stress	required beam depth	actual beam depth	beam width	beam height	total number of bars	reinf. ratio (%)	max. shear stress	various centroidal stresses			various outer bar stresses		
	f_{si}	d_{req}	d	b	h	N_b	R_R	v	f_{sa}	f_{sh}	f_{sd}	f_{sae}	f_{she}	f_{sde}
126	410.0	822.5	862.0	250	950	11	2.51	1.93	380.8	298.4	220.7	390.7	325.8	240.3
127	380.0	827.5	857.5	250	950	12	2.75	1.94	354.1	276.0	204.5	362.6	304.6	225.1
128	350.0	862.9	911.9	250	1000	12	2.58	1.83	328.7	260.4	194.0	343.6	285.4	212.2
129	330.0	892.1	905.3	250	1000	13	2.82	1.85	307.3	243.1	181.4	340.5	270.2	201.2
130	310.0	904.3	954.3	250	1050	13	2.67	1.76	290.1	230.1	172.4	321.2	254.1	190.0
131	290.0	919.4	949.1	250	1050	14	2.90	1.77	272.5	216.0	162.0	305.6	241.6	180.8
132	272.0	935.9	944.4	250	1050	15	3.12	1.78	257.0	203.9	152.5	291.6	230.7	172.1
133	250.0	959.9	993.6	250	1100	15	2.96	1.70	243.2	194.0	146.1	273.8	217.9	163.8
134	230.0	986.6	988.6	250	1100	16	3.18	1.71	230.0	182.8	137.3	261.7	207.4	155.5

Table (8a): L = 15.0 m, U = 180 and 90 T/hr., dia = 25 mm

section number	various total moment values			max. shear	various max. concrete strains			various strain factors and their relative difference						
	M_T	M_H	M_D	V_T	e_{ca}	e_{ch}	e_{cd}	S_{FT}	S_{FH}	S_{FD}	D_{Sf}	d_{pt}	d_{ph}	d_{pd}
126	1432.4	1147.9	863.4	415.5	2.49	1.31	0.90	1.099	1.092	1.089	0.89	87.92	84.77	84.95
127	1432.4	1147.9	863.4	415.5	2.09	1.28	0.88	1.116	1.104	1.101	1.43	92.50	88.89	89.09
128	1440.9	1156.4	871.9	417.8	1.56	1.13	0.79	1.097	1.096	1.094	0.35	88.09	89.36	89.50
129	1440.9	1156.4	871.9	417.8	1.54	1.11	0.78	1.115	1.112	1.109	0.58	94.70	95.32	95.53
130	1449.3	1164.8	880.3	420.0	1.34	0.99	0.71	1.107	1.104	1.102	0.46	95.67	95.89	96.04
131	1449.3	1164.8	880.3	420.0	1.32	0.98	0.70	1.121	1.118	1.116	0.51	100.95	101.24	101.44
132	1449.3	1164.8	880.3	420.0	1.31	0.97	0.69	1.135	1.131	1.128	0.54	105.58	105.93	106.16
133	1457.7	1173.2	888.8	422.3	1.16	0.88	0.63	1.126	1.123	1.121	0.44	106.41	106.65	106.82
134	1457.7	1173.2	888.8	422.3	1.15	0.86	0.62	1.138	1.135	1.132	0.46	110.67	110.91	111.11

Table (8b): L = 15.0 m, U = 180 and 90 T/hr., dia = 25 mm

sec.	section moduli based on centroidal stresses and their relative differences								section moduli based on outer bar stresses and their relative differences							
no.	Z_T	Z_{TH}	Z_D	Z_L	Z_{LH}	D_{Z1}	D_{Z2}	D_{Z3}	Z'_T	Z'_{TH}	Z'_D	Z'_L	Z'_{LH}	D'_{Z1}	D'_{Z2}	D'_{Z3}
126	3.761	3.847	3.912	3.554	3.661	4.00	2.26	3.01	3.666	3.523	3.593	3.784	3.329	4.05	4.05	13.65
127	4.045	4.159	4.222	3.804	3.980	4.37	2.82	4.63	3.950	3.768	3.836	4.136	3.576	4.82	4.82	15.65
128	4.384	4.441	4.494	4.225	4.288	2.51	1.32	1.50	4.193	4.052	4.109	4.329	3.888	3.47	3.47	11.33
129	4.688	4.757	4.806	4.518	4.615	2.52	1.48	2.14	4.232	4.279	4.333	4.085	4.121	2.40	1.12	0.89
130	4.996	5.063	5.106	4.835	4.934	2.21	1.34	2.04	4.512	4.585	4.633	4.337	4.442	2.67	1.61	2.42
131	5.318	5.392	5.433	5.150	5.268	2.16	1.39	2.31	4.742	4.822	4.869	4.558	4.682	2.68	1.68	2.70
132	5.639	5.712	5.774	5.442	5.528	2.39	1.29	1.57	4.970	5.050	5.116	4.759	4.855	2.95	1.61	2.01
133	5.993	6.047	6.081	5.860	5.942	1.47	0.90	1.39	5.324	5.385	5.426	5.172	5.261	1.92	1.15	1.71
134	6.337	6.417	6.473	6.135	6.249	2.15	1.27	1.85	5.571	5.656	5.717	5.357	5.475	2.63	1.54	2.21

Table (8c): L = 15.0 m, U = 180 and 90 T/hr., dia = 25 mm

section number	neutral axis depth ratios			lever arm effective depth ratios				
	R_T	R_H	R_D	j_T	j_H	j_D	j_L	j_{LH}
126	0.465	0.467	0.448	0.808	0.823	0.838	0.763	0.784
127	0.499	0.481	0.462	0.801	0.820	0.833	0.753	0.785
128	0.487	0.464	0.449	0.816	0.828	0.838	0.787	0.799
129	0.500	0.478	0.462	0.811	0.824	0.833	0.782	0.799
130	0.481	0.464	0.451	0.820	0.832	0.839	0.794	0.810
131	0.493	0.476	0.463	0.815	0.827	0.833	0.790	0.808
132	0.504	0.487	0.475	0.811	0.822	0.831	0.783	0.795
133	0.488	0.475	0.464	0.819	0.827	0.832	0.801	0.812
134	0.499	0.486	0.476	0.816	0.826	0.833	0.790	0.804

Table (8d): L = 15.0 m, U = 180 and 90 T/hr., dia = 25 mm

section	live load modulus	strain factor	combined load modulus	centroidal simulated stress ranges based on F and F_L			centroidal simulated and actual stress ranges			outer bar simulated and actual stress ranges			fatigue limit
number	F_L	S_F	F	S_{RT}	S_{RL}	D_S	S_r	f_{sr}	D_f	S_{re}	f_{sre}	D_{fe}	S_e
126	3.554	1.094	3.837	152.63	160.10	4.89	160.10	160.10	0.00	149.89	150.38	- 0.32	82.19
127	3.804	1.108	4.134	142.01	149.57	5.33	149.57	149.57	0.00	137.00	137.58	- 0.42	87.23
128	4.225	1.096	4.439	130.59	134.67	3.12	134.67	134.67	0.00	131.36	131.44	- 0.06	91.48
129	4.518	1.112	4.747	122.12	125.93	3.13	125.93	125.93	0.00	139.12	139.30	- 0.12	95.10
130	4.835	1.105	5.051	114.52	117.69	2.76	117.69	117.69	0.00	130.45	131.19	- 0.56	98.79
131	5.150	1.119	5.376	107.58	110.49	2.71	110.49	110.49	0.00	124.05	124.82	- 0.62	101.84
132	5.442	1.132	5.706	101.51	104.55	2.99	104.55	104.55	0.00	118.77	119.56	- 0.66	104.72
133	5.860	1.123	6.037	95.32	97.09	1.86	97.09	97.09	0.00	109.42	110.01	- 0.55	107.45
134	6.135	1.135	6.405	90.29	92.74	2.71	92.74	92.74	0.00	105.62	106.22	- 0.57	110.20

Table (8e) - Actual and simulated stress ranges caused by the maximum total moment (M_T)
L = 15.0 m, U = 180 amd 90 T/hr., dia = 25 mm

section number	centroidal simulated stress ranges based on F and F_L			centroidal simulated and actual stress ranges			outer bar simulated and actual stress ranges		
	S_{RHT}	S_{RHL}	D_{SH}	S_{rh}	f_{srh}	D_{fh}	S_{rhe}	f_{srhe}	D_{fhe}
126	78.48	80.05	2.00	80.05	77.71	3.01	88.62	85.45	3.71
127	73.19	74.79	2.18	74.79	71.48	4.63	84.51	79.55	6.23
128	66.50	67.34	1.26	67.34	66.34	1.50	74.26	73.17	1.49
129	62.18	62.97	1.26	62.97	61.65	2.14	70.61	69.03	2.29
130	58.20	58.84	1.10	58.84	57.66	2.04	65.44	64.05	2.18
131	54.66	55.25	1.08	55.25	54.00	2.31	62.25	60.77	2.45
132	51.66	52.28	1.20	52.28	51.47	1.57	59.62	58.60	1.74
133	48.19	48.55	0.74	48.55	47.88	1.39	54.89	54.09	1.49
134	45.88	46.37	1.08	46.37	45.53	1.85	52.99	51.96	1.98

Table (8f) - Actual and simulated stress ranges caused by the average total moment, $M_H = 0.5\ (M_T + M_D)$
L = 15.0 m, U = 180 and 90 T/hr., dia = 25 mm

Table (9) - Beam details for 17.5 m span, with all values of the loading frequency Bar dia = 25 mm

section number	initial steel stress	required beam depth	actual beam depth	beam width	beam height	total number of bars	reinf. ratio (%)	max. shear stress	various centroidal stresses			various outer bar stresses		
	f_{si}	d_{req}	d	b	h	N_b	R_R	v	f_{sa}	f_{sh}	f_{sd}	f_{sae}	f_{she}	f_{sde}
210	410.0	880.3	965.2	300	1050	13	2.20	1.69	389.7	313.7	239.2	398.0	337.1	256.5
211	380.0	885.7	961.1	300	1050	14	2.38	1.69	365.9	293.6	224.0	373.4	318.1	242.2
212	350.0	924.7	957.5	300	1050	15	2.56	1.70	345.9	275.5	210.7	352.4	300.9	229.6
213	340.0	950.2	956.8	300	1050	16	2.74	1.70	326.1	261.5	199.1	343.6	288.7	219.3
214	320.0	962.5	1005.3	300	1100	16	2.60	1.63	308.8	248.0	190.7	339.7	272.1	208.9
215	305.0	973.5	1000.7	300	1100	17	2.78	1.64	293.3	235.8	180.9	326.0	261.3	200.1
216	280.0	995.7	996.0	300	1100	18	2.96	1.64	279.4	224.3	171.7	313.5	250.9	191.6
217	267.0	1009.4	1046.0	300	1150	18	2.82	1.58	265.1	214.3	164.9	295.3	238.1	182.9
218	260.0	1017.7	1042.3	300	1150	19	2.98	1.58	252.7	204.4	157.2	283.9	229.0	175.8
219	250.0	1030.5	1038.9	300	1150	20	3.15	1.59	241.6	195.0	149.9	273.6	220.2	169.0

Table (9a): L = 17.5 m, all values of U, dia = 25 mm

section	various total moment values			max. shear	various max. concrete strains			various strain factors and their relative difference						
number	M_T	M_H	M_D	V_T	e_{ca}	e_{ch}	e_{cd}	S_{FT}	S_{FH}	S_{FD}	D_{Sf}	d_{pt}	d_{ph}	d_{pd}
210	1983.1	1614.8	1246.4	488.5	2.32	1.25	0.89	1.076	1.074	1.072	0.38	84.81	82.50	82.61
211	1983.1	1614.8	1246.4	488.5	2.01	1.23	0.88	1.088	1.083	1.081	0.64	88.93	86.29	86.41
212	1983.1	1614.8	1246.4	488.5	1.75	1.20	0.86	1.101	1.092	1.089	1.03	92.24	89.60	89.74
213	1983.1	1614.8	1246.4	488.5	1.64	1.19	0.85	1.106	1.104	1.101	0.43	93.19	94.54	94.73
214	1996.9	1628.6	1260.2	491.6	1.43	1.07	0.78	1.100	1.097	1.095	0.45	94.73	95.01	95.15
215	1996.9	1628.6	1260.2	491.6	1.41	1.06	0.77	1.111	1.108	1.106	0.50	99.28	99.54	99.72
216	1996.9	1628.6	1260.2	491.6	1.40	1.05	0.76	1.122	1.118	1.116	0.54	103.33	103.61	103.82
217	2010.7	1642.3	1274.0	494.8	1.24	0.95	0.70	1.114	1.111	1.109	0.42	103.97	104.18	104.34
218	2010.7	1642.3	1274.0	494.8	1.23	0.94	0.69	1.123	1.121	1.118	0.45	107.70	107.94	108.12
219	2010.7	1642.3	1274.0	494.8	1.22	0.93	0.68	1.132	1.129	1.127	0.46	111.08	111.35	111.55

Table (9b): L = 17.5 m, all values of U, dia = 25 mm

sec.	section moduli based on centroidal stresses and their relative differences								section moduli based on outer bar stresses and their relative differences							
no.	Z_T	Z_{TH}	Z_D	Z_L	Z_{LH}	D_{Z1}	D_{Z2}	D_{Z3}	Z'_T	Z'_{TH}	Z'_D	Z'_L	Z'_{LH}	D'_{Z1}	D'_{Z2}	D'_{Z3}
210	5.089	5.147	5.212	4.894	4.940	2.41	1.15	0.95	4.982	4.791	4.860	5.204	4.572	3.99	3.99	13.83
211	5.420	5.499	5.564	5.193	5.289	2.66	1.45	1.86	5.311	5.076	5.146	5.615	4.850	4.64	4.64	15.77
212	5.734	5.860	5.915	5.451	5.682	3.16	2.21	4.24	5.627	5.367	5.429	5.996	5.166	4.84	4.84	16.05
213	6.081	6.176	6.261	5.798	5.904	2.97	1.57	1.83	5.771	5.594	5.685	5.923	5.307	3.17	3.17	11.61
214	6.467	6.567	6.607	6.240	6.434	2.17	1.55	3.10	5.878	5.985	6.033	5.632	5.825	2.63	1.8	3.44
215	6.808	6.907	6.966	6.554	6.714	2.32	1.46	2.45	6.125	6.233	6.299	5.850	6.018	2.83	1.76	2.87
216	7.148	7.259	7.339	6.844	7.000	2.67	1.56	2.28	6.370	6.490	6.576	6.047	6.214	3.22	1.88	2.76
217	7.584	7.664	7.727	7.349	7.456	1.89	1.06	1.45	6.808	6.897	6.966	6.553	6.670	2.31	1.30	1.79
218	7.958	8.036	8.104	7.717	7.812	1.84	0.99	1.23	7.084	7.172	7.246	6.819	6.928	2.29	1.25	1.59
219	8.321	8.424	8.497	8.034	8.183	2.11	1.24	1.85	7.348	7.459	7.538	7.042	7.197	2.58	1.50	2.20

Table (9c): L = 17.5 m, all values of U, dia = 25 mm

section number	neutral axis depth ratios			lever arm effective depth ratios				
	R_T	R_H	R_D	j_T	j_H	j_D	j_L	j_{LH}
210	0.427	0.444	0.428	0.826	0.834	0.844	0.795	0.800
211	0.452	0.456	0.439	0.821	0.830	0.840	0.786	0.799
212	0.484	0.466	0.450	0.813	0.829	0.837	0.773	0.804
213	0.501	0.477	0.461	0.809	0.823	0.835	0.772	0.787
214	0.481	0.463	0.449	0.819	0.832	0.837	0.790	0.815
215	0.491	0.473	0.460	0.815	0.827	0.835	0.785	0.804
216	0.500	0.482	0.470	0.812	0.825	0.834	0.777	0.795
217	0.484	0.470	0.459	0.821	0.829	0.836	0.795	0.807
218	0.493	0.479	0.468	0.819	0.827	0.834	0.794	0.804
219	0.501	0.488	0.477	0.816	0.826	0.833	0.788	0.802

Table (9d): L = 17.5 m, all values of U, dia = 25 mm

section	live load modulus	strain factor	combined load modulus	centroidal simulated stress ranges based on F and F_L			centroidal simulated and actual stress ranges			outer bar simulated and actual stress ranges			fatigue limit
number	F_L	S_F	F	S_{RT}	S_{RL}	D_S	S_r	f_{sr}	D_f	S_{re}	f_{sre}	D_{fe}	S_e
210	4.894	1.074	5.147	146.12	150.53	3.02	150.53	150.53	0.00	141.34	141.56	- 0.16	76.86
211	5.193	1.085	5.492	137.07	141.87	3.50	141.87	141.87	0.00	130.90	131.20	- 0.23	81.57
212	5.451	1.095	5.825	129.76	135.14	4.15	135.14	135.14	0.00	122.50	122.87	- 0.30	85.74
213	5.798	1.104	6.171	122.29	127.06	3.90	127.06	127.06	0.00	124.25	124.37	- 0.10	89.14
214	6.240	1.098	6.537	114.74	118.05	2.89	118.05	118.05	0.00	130.05	130.81	- 0.59	92.57
215	6.554	1.109	6.887	109.05	112.41	3.08	112.41	112.41	0.00	125.12	125.93	- 0.65	95.48
216	6.844	1.119	7.244	103.96	107.64	3.54	107.64	107.64	0.00	120.98	121.82	- 0.70	98.26
217	7.349	1.112	7.655	97.77	100.25	2.53	100.25	100.25	0.00	111.81	112.42	- 0.55	101.14
218	7.717	1.121	8.031	93.17	95.47	2.47	95.47	95.47	0.00	107.40	108.03	- 0.59	103.48
219	8.034	1.130	8.409	89.17	91.69	2.83	91.69	91.69	0.00	103.98	104.62	- 0.61	105.73

Table (9e) - Actual and simulated stress ranges caused by the maximum total moment (M_T)
L = 17.5 m, all values of U, dia = 25 mm

section number	centroidal simulated stress ranges based on F and F_L			centroidal simulated and actual stress ranges			outer bar simulated and actual stress ranges		
	S_{RHT}	S_{RHL}	D_{SH}	S_{rh}	f_{srh}	D_{fh}	S_{rhe}	f_{srhe}	D_{fhe}
210	74.56	75.27	0.95	75.27	74.56	0.95	81.35	80.57	0.97
211	70.00	70.93	1.33	70.93	69.64	1.86	77.72	75.94	2.34
212	66.52	67.57	1.58	67.57	64.82	4.24	75.17	71.30	5.43
213	62.60	63.53	1.49	63.53	62.39	1.83	70.66	69.40	1.81
214	58.39	59.03	1.08	59.03	57.25	3.10	65.26	63.23	3.21
215	55.56	56.20	1.16	56.20	54.86	2.45	62.81	61.21	2.61
216	53.11	53.82	1.33	53.82	52.62	2.28	60.75	59.27	2.49
217	49.66	50.12	0.94	50.12	49.41	1.45	56.10	55.22	1.58
218	47.30	47.73	0.92	47.73	47.15	1.23	53.90	53.17	1.37
219	45.37	45.85	1.05	45.85	45.02	1.85	52.19	51.18	1.97

Table (9f) - Actual and simulated stress ranges caused by the average total moment, $M_H = 0.5\ (M_T + M_D)$
L = 17.5 m, all values of U, dia = 25 mm

Table (10) - Beam details for 20.0 m span, with all values of the loading frequency Bar dia = 25 mm

section number	initial steel stress	required beam depth	actual beam depth	beam width	beam height	total number of bars	reinf. ratio (%)	max. shear stress	various centroidal stresses			various outer bar stresses		
	f_{si}	d_{req}	d	b	h	N_b	R_R	v	f_{sa}	f_{sh}	f_{sd}	f_{sae}	f_{she}	f_{sde}
310	430.0	968.1	1121.8	350	1200	14	1.75	1.44	406.5	336.7	264.2	412.8	342.4	277.6
311	400.0	930.6	1117.5	350	1200	15	1.88	1.44	382.9	316.9	249.2	388.9	335.5	263.5
312	380.0	945.0	1113.8	350	1200	16	2.01	1.45	362.7	299.1	235.0	368.2	318.6	250.0
313	350.0	987.2	1110.4	350	1200	17	2.15	1.45	346.5	282.9	222.5	351.5	303.2	238.1
314	340.0	1014.9	1110.4	350	1200	18	2.27	1.45	329.3	269.4	211.6	342.6	290.2	227.7
315	320.0	1028.5	1105.5	350	1200	19	2.41	1.46	313.9	257.2	201.8	340.3	279.3	218.8
316	310.0	1036.4	1101.4	350	1200	20	2.55	1.46	300.7	245.7	192.5	329.8	268.9	210.3
317	300.0	1045.1	1097.7	350	1200	21	2.68	1.47	288.3	235.7	184.6	318.5	259.8	203.1
318	280.0	1064.8	1094.4	350	1200	22	2.82	1.47	276.5	226.1	177.1	307.6	250.9	196.2
319	270.0	1076.4	1091.3	350	1200	23	2.96	1.48	265.9	217.8	170.9	297.8	243.3	190.6
320	260.0	1088.9	1090.8	350	1200	24	3.09	1.48	255.5	209.9	165.0	286.9	235.9	185.1
321	250.0	1102.8	1137.9	350	1250	24	2.96	1.43	244.9	201.1	158.5	274.2	224.7	176.8

Table (10a): L = 20.0 m, all values of U, dia = 25 mm

section number	various total moment values			max. shear	various max. concrete strains			various strain factors and their relative difference						
	M_T	M_H	M_D	V_T	e_{ca}	e_{ch}	e_{cd}	S_{FT}	S_{FH}	S_{FD}	D_{Sf}	d_{pt}	d_{ph}	d_{pd}
310	2676.9	2215.4	1754.0	564.2	2.07	1.14	0.85	1.0502	1.0504	1.051	0.04	78.22	76.27	77.05
311	2676.9	2215.4	1754.0	564.2	1.84	1.12	0.84	1.058	1.059	1.058	0.11	82.50	80.97	81.02
312	2676.9	2215.4	1754.0	564.2	1.64	1.10	0.82	1.067	1.065	1.064	0.25	86.25	84.47	84.54
313	2676.9	2215.4	1754.0	564.2	1.47	1.08	0.81	1.075	1.071	1.070	0.50	89.56	87.59	87.66
314	2676.9	2215.4	1754.0	564.2	1.38	1.06	0.795	1.078	1.077	1.076	0.22	89.61	90.39	90.46
315	2676.9	2215.4	1754.0	564.2	1.37	1.05	0.786	1.088	1.086	1.084	0.34	94.54	94.80	94.90
316	2676.9	2215.4	1754.0	564.2	1.35	1.04	0.78	1.097	1.094	1.093	0.38	98.64	98.81	98.93
317	2676.9	2215.4	1754.0	564.2	1.34	1.03	0.77	1.105	1.102	1.100	0.40	102.28	102.47	102.61
318	2676.9	2215.4	1754.0	564.2	1.32	1.02	0.762	1.113	1.110	1.108	0.43	105.61	105.83	105.99
319	2676.9	2215.4	1754.0	564.2	1.31	1.01	0.756	1.120	1.117	1.115	0.46	108.67	108.92	109.10
320	2676.9	2215.4	1754.0	564.2	1.29	1.00	0.75	1.123	1.124	1.122	0.21	109.24	111.77	111.96
321	2697.9	2236.4	1775.0	568.4	1.17	0.92	0.69	1.120	1.117	1.115	0.39	112.13	112.32	112.47

Table (10b): L = 20.0 m, all values of U, dia = 25 mm

sec.	section moduli based on centroidal stresses and their relative differences								section moduli based on outer bar stresses and their relative differences							
no.	Z_T	Z_{TH}	Z_D	Z_L	Z_{LH}	D_{Z1}	D_{Z2}	D_{Z3}	Z'_T	Z'_{TH}	Z'_D	Z'_L	Z'_{LH}	D'_{Z1}	D'_{Z2}	D'_{Z3}
310	6.586	6.580	6.638	6.489	6.369	0.88	0.09	1.88	6.485	6.470	6.318	6.827	7.123	2.64	0.22	4.33
311	6.991	6.990	7.038	6.903	6.813	0.69	0.02	1.33	6.884	6.603	6.655	7.364	6.410	4.25	4.25	14.88
312	7.380	7.408	7.465	7.224	7.200	1.15	0.38	0.32	7.270	6.954	7.016	7.808	6.731	4.54	4.54	16.00
313	7.725	7.830	7.883	7.440	7.634	2.05	1.36	2.60	7.615	7.308	7.367	8.136	7.091	4.20	4.20	14.73
314	8.129	8.223	8.288	7.843	7.987	1.96	1.16	1.85	7.813	7.634	7.705	8.027	7.378	2.34	2.34	8.80
315	8.527	8.612	8.692	8.228	8.321	1.94	1.01	1.13	7.867	7.931	8.016	7.598	7.622	1.90	0.81	0.32
316	8.902	9.016	9.113	8.525	8.665	2.38	1.29	1.64	8.116	8.239	8.341	7.722	7.874	2.76	1.51	1.97
317	9.285	9.401	9.502	8.900	9.037	2.33	1.25	1.54	8.404	8.528	8.634	7.997	8.149	2.75	1.49	1.89
318	9.683	9.799	9.904	9.289	9.422	2.28	1.20	1.43	8.702	8.829	8.938	8.284	8.434	2.72	1.46	1.81
319	10.068	10.172	10.263	9.717	9.842	1.93	1.03	1.28	8.987	9.105	9.204	8.603	8.748	2.41	1.31	1.68
320	10.476	10.557	10.631	10.194	10.284	1.48	0.77	0.88	9.330	9.390	9.476	9.065	9.076	1.56	0.64	0.13
321	11.018	11.122	11.198	10.686	10.839	1.64	0.95	1.43	9.839	9.954	10.039	9.476	9.640	2.03	1.17	1.73

Table (10c): L = 20.0 m, all values of U, dia = 25 mm

section number	neutral axis depth ratios			lever arm effective depth ratios				
	R_T	R_H	R_D	j_T	j_H	j_D	j_L	j_{LH}
310	0.366	0.404	0.392	0.854	0.852	0.860	0.842	0.825
311	0.386	0.414	0.401	0.850	0.848	0.854	0.839	0.827
312	0.411	0.423	0.411	0.844	0.846	0.852	0.826	0.822
313	0.438	0.433	0.420	0.834	0.843	0.849	0.803	0.822
314	0.456	0.441	0.429	0.829	0.839	0.845	0.799	0.815
315	0.465	0.449	0.438	0.827	0.835	0.843	0.798	0.807
316	0.473	0.458	0.447	0.823	0.834	0.843	0.788	0.802
317	0.481	0.466	0.455	0.821	0.831	0.840	0.787	0.799
318	0.488	0.474	0.463	0.819	0.829	0.838	0.786	0.797
319	0.496	0.481	0.469	0.817	0.826	0.833	0.789	0.799
320	0.502	0.488	0.476	0.815	0.823	0.829	0.793	0.802
321	0.489	0.477	0.467	0.822	0.830	0.836	0.797	0.809

Table (10d): L = 20.0 m, all values of U, dia = 25 mm

section	live load modulus	strain factor	combined load modulus	centroidal simulated stress ranges based on F and F_L			centroidal simulated and actual stress ranges			outer bar simulated and actual stress ranges			fatigue limit
number	F_L	S_F	F	S_{RT}	S_{RL}	D_S	S_r	f_{sr}	D_f	S_{re}	f_{sre}	D_{fe}	S_e
310	6.369	1.050	6.580	142.58	144.90	1.63	144.90	142.22	1.88	138.02	135.19	2.10	69.89
311	6.813	1.059	6.990	133.75	135.46	1.28	135.46	133.69	1.33	127.25	125.33	1.53	74.53
312	7.200	1.065	7.408	126.38	128.17	1.42	128.17	127.76	0.32	118.54	118.21	0.28	79.00
313	7.440	1.073	7.804	120.52	124.04	2.92	124.04	124.04	0.00	113.26	113.44	- 0.16	82.93
314	7.843	1.077	8.208	114.48	117.67	2.79	117.67	117.67	0.00	114.92	114.97	- 0.04	86.37
315	8.228	1.086	8.609	109.14	112.16	2.77	112.16	112.16	0.00	121.37	121.47	- 0.08	89.29
316	8.525	1.095	9.007	104.72	108.26	3.38	108.26	108.26	0.00	118.90	119.52	- 0.52	92.10
317	8.900	1.103	9.393	100.38	103.70	3.31	103.70	103.70	0.00	114.76	115.40	- 0.56	94.46
318	9.289	1.110	9.793	96.24	99.36	3.24	99.36	99.36	0.00	110.74	111.40	- 0.59	96.74
319	9.717	1.118	10.165	92.43	94.97	2.76	94.97	94.97	0.00	106.59	107.27	- 0.64	98.61
320	10.194	1.124	10.554	88.66	90.54	2.12	90.54	90.54	0.00	102.18	101.81	0.36	100.42
321	10.686	1.118	11.108	84.37	86.36	2.36	86.36	86.36	0.00	96.86	97.39	- 0.55	103.15

Table (10e) - Actual and simulated stress ranges caused by the maximum total moment (M_T)
L = 20.0 m, all values of U, dia = 25 mm

section number	centroidal simulated stress ranges based on F and F_L			centroidal simulated and actual stress ranges			outer bar simulated and actual stress ranges		
	S_{RHT}	S_{RHL}	D_{SH}	S_{rh}	f_{srh}	D_{fh}	S_{rhe}	f_{srhe}	D_{fhe}
310	72.45	72.45	0.00	72.45	72.45	0.00	64.79	64.79	0.00
311	67.73	67.73	0.00	67.73	67.73	0.00	71.99	71.99	0.00
312	64.09	64.09	0.00	64.09	64.09	0.00	68.58	68.56	0.03
313	61.39	62.02	1.03	62.02	60.45	2.60	67.13	65.07	3.16
314	58.27	58.84	0.98	58.84	57.77	1.85	63.69	62.54	1.84
315	55.54	56.08	0.97	56.08	55.45	1.13	61.28	60.54	1.22
316	53.49	54.13	1.19	54.13	53.25	1.64	59.65	58.61	1.78
317	51.25	51.85	1.17	51.85	51.06	1.54	57.58	56.63	1.69
318	49.12	49.68	1.14	49.68	48.98	1.43	55.58	54.71	1.59
319	47.03	47.49	0.97	47.49	46.89	1.28	53.51	52.75	1.45
320	44.94	45.27	0.74	45.27	44.87	0.88	51.28	50.84	0.87
321	42.83	43.18	0.82	43.18	42.57	1.43	48.60	47.87	1.53

Table (10f) - Actual and simulated stress ranges caused by the average total moment, $M_H = 0.5\ (M_T + M_D)$
L = 20.0 m, all values of U, dia = 25 mm

Table (11) - Beam details for 25.0 m span, with all values of the loading frequency Bar dia = 25 mm

section number	initial steel stress	required beam depth	actual beam depth	beam width	beam height	total number of bars	reinf. ratio (%)	max. shear stress	various centroidal stresses			various outer bar stresses		
	f_{si}	d_{req}	d	b	h	N_b	R_R	v	f_{sa}	f_{sh}	f_{sd}	f_{sae}	f_{she}	f_{sde}
410	430.0	1087.0	1422.2	450	1500	18	1.38	1.16	408.5	353.0	293.5	412.9	355.5	304.0
411	400.0	1043.5	1418.7	450	1500	19	1.46	1.16	389.7	337.6	279.3	394.0	341.9	290.5
412	380.0	1060.2	1415.5	450	1500	20	1.54	1.17	374.5	322.7	267.0	378.6	337.1	278.7
413	360.0	1087.6	1412.6	450	1500	21	1.62	1.17	359.8	308.8	255.7	363.6	323.7	267.9
414	350.0	1109.6	1410.0	450	1500	22	1.70	1.17	346.8	295.4	244.2	350.3	310.7	256.7
415	340.0	1141.9	1409.4	450	1500	23	1.78	1.17	333.2	283.5	235.5	342.0	299.1	248.3
416	330.0	1149.5	1406.8	450	1500	24	1.86	1.17	320.7	273.0	225.9	339.6	288.9	238.9
417	310.0	1166.8	1403.2	450	1500	25	1.94	1.18	309.4	263.8	217.8	329.2	280.4	231.5
418	300.0	1177.0	1399.9	450	1500	26	2.03	1.18	299.5	254.8	211.2	320.2	272.2	225.4
419	290.0	1188.1	1396.8	450	1500	27	2.11	1.18	289.0	246.2	203.7	310.3	264.1	218.3
420	285.0	1194.3	1393.9	450	1500	28	2.19	1.19	280.7	238.9	197.5	302.7	257.3	212.6

Table (11a): L = 25.0 m, all values of U, dia = 25 mm

section number	various total moment values			max. shear	various max. concrete strains			various strain factors and their relative difference						
	M_T	M_H	M_D	V_T	e_{ca}	e_{ch}	e_{cd}	S_{FT}	S_{FH}	S_{FD}	D_{Sf}	d_{pt}	d_{ph}	d_{pd}
410	4517.1	3867.9	3218.8	743.6	1.67	1.09	0.81	1.034	1.036	1.036	0.16	77.84	77.84	77.34
411	4517.1	3867.9	3218.8	743.6	1.53	1.00	0.80	1.039	1.040	1.040	0.12	81.35	80.08	80.66
412	4517.1	3867.9	3218.8	743.6	1.42	0.98	0.79	1.043	1.0444	1.0440	0.12	84.50	83.65	83.68
413	4517.1	3867.9	3218.8	743.6	1.31	0.97	0.77	1.0479	1.0482	1.0476	0.05	87.36	86.39	86.41
414	4517.1	3867.9	3218.8	743.6	1.21	0.95	0.76	1.053	1.052	1.051	0.16	89.96	88.89	88.92
415	4517.1	3867.9	3218.8	743.6	1.14	0.94	0.75	1.0551	1.0550	1.054	0.07	90.58	91.18	91.21
416	4517.1	3867.9	3218.8	743.6	1.13	0.93	0.74	1.059	1.0582	1.0575	0.14	93.24	93.29	93.32
417	4517.1	3867.9	3218.8	743.6	1.12	0.92	0.735	1.064	1.0632	1.0625	0.15	96.82	96.86	96.90
418	4517.1	3867.9	3218.8	743.6	1.11	0.91	0.729	1.069	1.068	1.067	0.17	100.12	100.18	100.22
419	4517.1	3867.9	3218.8	743.6	1.09	0.90	0.721	1.074	1.073	1.072	0.18	103.20	103.26	103.31
420	4517.1	3867.9	3218.8	743.6	1.08	0.89	0.715	1.078	1.077	1.076	0.18	106.08	106.14	106.20

Table (11b): L = 25.0 m, all values of U, dia = 25 mm

sec.	section moduli based on centroidal stresses and their relative differences								section moduli based on outer bar stresses and their relative differences							
no.	Z_T	Z_{TH}	Z_D	Z_L	Z_{LH}	D_{Z1}	D_{Z2}	D_{Z3}	Z'_T	Z'_{TH}	Z'_D	Z'_L	Z'_{LH}	D'_{Z1}	D'_{Z2}	D'_{Z3}
410	11.058	10.959	10.966	11.293	10.921	0.91	0.91	3.41	10.941	10.879	10.587	11.931	12.601	3.35	0.57	5.62
411	11.590	11.459	11.523	11.760	11.149	1.15	1.15	5.48	11.466	11.312	11.080	12.550	12.625	3.48	1.36	0.60
412	12.062	11.986	12.057	12.075	11.646	0.64	0.64	3.69	11.933	11.476	11.549	13.002	11.125	3.98	3.98	16.88
413	12.556	12.524	12.588	12.477	12.216	0.51	0.26	2.14	12.425	11.948	12.016	13.569	11.623	3.99	3.99	16.73
414	13.024	13.093	13.179	12.656	12.683	1.19	0.53	0.21	12.893	12.449	12.538	13.869	12.027	3.57	3.57	15.32
415	13.555	13.642	13.666	13.287	13.527	0.82	0.65	1.80	13.207	12.931	12.961	13.856	12.780	2.13	2.13	8.42
416	14.087	14.166	14.249	13.700	13.769	1.15	0.56	0.50	13.302	13.387	13.474	12.893	12.972	1.29	0.64	0.61
417	14.600	14.664	14.776	14.181	14.133	1.21	0.44	0.34	13.719	13.792	13.906	13.277	13.251	1.36	0.53	0.20
418	15.082	15.179	15.240	14.703	14.883	1.05	0.65	1.23	14.107	14.211	14.280	13.698	13.882	1.22	0.74	1.34
419	15.630	15.712	15.803	15.219	15.273	1.10	0.52	0.36	14.556	14.646	14.742	14.113	14.184	1.28	0.62	0.50
420	16.092	16.193	16.297	15.605	15.698	1.27	0.63	0.60	14.923	15.033	15.141	14.409	14.517	1.46	0.73	0.75

Table (11c): L = 25.0 m, all values of U, dia = 25 mm

section number	neutral axis depth ratios			lever arm effective depth ratios				
	R_T	R_H	R_D	j_T	j_H	j_D	j_L	j_{LH}
410	0.314	0.344	0.356	0.880	0.872	0.872	0.899	0.869
411	0.330	0.371	0.364	0.876	0.865	0.870	0.889	0.842
412	0.346	0.378	0.371	0.868	0.862	0.867	0.869	0.838
413	0.366	0.385	0.377	0.862	0.859	0.864	0.857	0.838
414	0.390	0.392	0.384	0.855	0.859	0.865	0.831	0.832
415	0.407	0.398	0.390	0.852	0.858	0.859	0.835	0.850
416	0.413	0.404	0.397	0.850	0.855	0.860	0.827	0.831
417	0.419	0.410	0.403	0.848	0.852	0.858	0.824	0.821
418	0.425	0.416	0.408	0.844	0.850	0.853	0.823	0.833
419	0.431	0.422	0.415	0.844	0.849	0.854	0.822	0.825
420	0.436	0.427	0.420	0.840	0.845	0.851	0.815	0.819

Table (11d): L = 25.0 m, all values of U, dia = 25 mm

section	live load modulus	strain factor	combined load modulus	centroidal simulated stress ranges based on F and F_L			centroidal simulated and actual stress ranges			outer bar simulated and actual stress ranges			fatigue limit
number	F_L	S_F	F	S_{RT}	S_{RL}	D_S	S_r	f_{sr}	D_f	S_{re}	f_{sre}	D_{fe}	S_e
410	10.921	1.036	10.959	118.68	118.89	0.17	118.89	114.97	3.41	113.09	108.82	3.92	61.17
411	11.149	1.040	11.459	114.88	116.46	1.37	116.46	110.40	5.48	109.87	103.46	6.20	65.63
412	11.646	1.044	11.986	109.91	111.49	1.44	111.49	107.52	3.69	104.11	99.85	4.26	69.53
413	12.216	1.048	12.524	104.98	106.29	1.25	106.29	104.06	2.14	98.05	95.69	2.46	73.10
414	12.656	1.052	13.093	100.77	102.59	1.81	102.59	102.59	0.00	93.56	93.61	- 0.06	76.78
415	13.287	1.055	13.610	96.36	97.72	1.41	97.72	97.72	0.00	93.70	93.70	- 0.005	79.55
416	13.700	1.058	14.166	92.98	94.77	1.93	94.77	94.77	0.00	100.46	100.70	- 0.24	82.67
417	14.133	1.063	14.664	90.20	91.87	1.84	91.87	91.56	0.34	97.87	97.79	0.08	85.12
418	14.703	1.068	15.161	86.74	88.31	1.81	88.31	88.31	0.00	94.52	94.78	- 0.28	87.11
419	15.219	1.073	15.712	83.82	85.31	1.78	85.31	85.31	0.00	91.72	92.00	- 0.30	89.45
420	15.605	1.077	16.193	81.44	83.20	2.16	83.20	83.20	0.00	89.83	90.11	- 0.31	91.35

Table (11e) - Actual and simulated stress ranges caused by the maximum total moment (M_T)
L = 25.0 m, all values of U, dia = 25 mm

section number	centroidal simulated stress ranges based on F and F_L			centroidal simulated and actual stress ranges			outer bar simulated and actual stress ranges		
	S_{RHT}	S_{RHL}	D_{SH}	S_{rh}	f_{srh}	D_{fh}	S_{rhe}	f_{srhe}	D_{fhe}
410	59.44	59.44	0.00	59.44	59.44	0.00	51.52	51.52	0.00
411	58.23	58.23	0.00	58.23	58.23	0.00	51.42	51.42	0.00
412	55.74	55.74	0.00	55.74	55.74	0.00	58.35	58.35	0.00
413	53.14	53.14	0.00	53.14	53.14	0.00	55.85	55.85	0.00
414	51.19	51.30	0.21	51.30	51.19	0.21	54.17	52.98	0.35
415	48.66	48.86	0.41	48.86	47.99	1.80	51.71	50.80	1.80
416	47.15	47.38	0.50	47.38	47.15	0.50	50.31	50.04	0.54
417	45.93	45.93	0.00	45.93	45.93	0.00	49.02	48.99	0.06
418	43.92	44.15	0.53	44.15	43.62	1.23	47.35	46.76	1.26
419	42.50	42.66	0.36	42.66	42.50	0.36	45.96	45.77	0.41
420	41.35	41.60	0.60	41.60	41.35	0.60	45.01	44.72	0.65

Table (11f) - Actual and simulated stress ranges caused by the average total moment, $M_H = 0.5\ (M_T + M_D)$

L = 25.0 m, all values of U, dia = 25 mm

Table (12) - Beam details for 27.5 m span, with all values of the loading frequency
Bar dia = 25 mm

section number	initial steel stress	required beam depth	actual beam depth	beam width	beam height	total number of bars	reinf. ratio (%)	max. shear stress	various centroidal stresses			various outer bar stresses		
	f_{si}	d_{req}	d	b	h	N_b	R_R	v	f_{sa}	f_{sh}	f_{sd}	f_{sae}	f_{she}	f_{sde}
511	400.0	1099.2	1569.8	500	1650	21	1.31	1.08	399.4	351.2	299.5	403.3	353.6	309.8
512	390.0	1107.4	1566.9	500	1650	22	1.38	1.08	384.4	337.7	286.9	388.2	341.8	297.7
513	370.0	1129.9	1564.2	500	1650	23	1.44	1.08	370.3	325.0	274.7	373.9	338.3	285.9
514	360.0	1146.9	1561.8	500	1650	24	1.51	1.09	357.8	312.3	264.2	361.1	326.0	275.7
515	350.0	1170.4	1559.5	500	1650	25	1.57	1.09	346.4	301.1	255.2	349.5	315.2	267.0
516	340.0	1205.2	1558.8	500	1650	26	1.64	1.09	334.3	290.2	246.5	341.9	304.5	258.5
517	330.0	1213.4	1556.5	500	1650	27	1.70	1.09	323.7	280.8	238.0	340.1	295.3	250.2
518	320.0	1222.5	1553.2	500	1650	28	1.77	1.09	313.6	271.2	230.6	331.2	286.3	243.3
519	310.0	1232.5	1550.2	500	1650	29	1.84	1.09	303.8	263.5	222.9	322.1	279.1	236.0
520	300.0	1243.4	1547.3	500	1650	30	1.90	1.10	294.3	254.9	216.6	313.1	271.0	230.1

Table (12a): L = 27.5 m, all values of U, dia = 25 mm

section number	various total moment values			max. shear	various max. concrete strains			various strain factors and their relative difference						
	M_T	M_H	M_D	V_T	e_{ca}	e_{ch}	e_{cd}	S_{FT}	S_{FH}	S_{FD}	D_{Sf}	d_{pt}	d_{ph}	d_{pd}
511	5712.8	4973.9	4235.0	848.5	1.50	1.03	0.80	1.033	1.0344	1.0345	0.16	80.22	80.22	79.77
512	5712.8	4973.9	4235.0	848.5	1.40	0.96	0.79	1.036	1.037	1.038	0.13	83.14	82.03	82.57
513	5712.8	4973.9	4235.0	848.5	1.30	0.94	0.78	1.040	1.0410	1.0407	0.12	85.81	85.12	85.14
514	5712.8	4973.9	4235.0	848.5	1.22	0.93	0.77	1.043	1.044	1.043	0.04	88.25	87.49	87.50
515	5712.8	4973.9	4235.0	848.5	1.13	0.92	0.76	1.047	1.0466	1.0462	0.10	90.50	89.67	89.69
516	5712.8	4973.9	4235.0	848.5	1.08	0.91	0.75	1.049	1.049	1.0487	0.05	91.17	91.70	91.72
517	5712.8	4973.9	4235.0	848.5	1.06	0.90	0.74	1.0522	1.0516	1.051	0.10	93.51	93.58	93.60
518	5712.8	4973.9	4235.0	848.5	1.05	0.885	0.73	1.0563	1.0557	1.055	0.11	96.79	96.82	96.84
519	5712.8	4973.9	4235.0	848.5	1.04	0.877	0.724	1.060	1.0595	1.0590	0.12	99.82	99.85	99.88
520	5712.8	4973.9	4235.0	848.5	1.03	0.868	0.718	1.064	1.0633	1.0626	0.13	102.66	102.70	102.73

Table (12b): L = 27.5 m, all values of U, dia = 25 mm

sec.	section moduli based on centroidal stresses and their relative differences								section moduli based on outer bar stresses and their relative differences							
no.	Z_T	Z_{TH}	Z_D	Z_L	Z_{LH}	D_{Z1}	D_{Z2}	D_{Z3}	Z'_T	Z'_{TH}	Z'_D	Z'_L	Z'_{LH}	D'_{Z1}	D'_{Z2}	D'_{Z3}
511	14.304	14.163	14.142	14.788	14.285	1.14	0.99	3.52	14.165	14.066	13.671	15.803	16.856	3.62	0.71	6.66
512	14.862	14.727	14.761	15.158	14.532	0.92	0.92	4.31	14.717	14.551	14.226	16.335	16.746	3.46	1.14	2.52
513	15.426	15.304	15.415	15.456	14.696	0.80	0.80	5.17	15.278	14.701	14.813	16.789	14.090	3.93	3.93	19.15
514	15.969	15.926	16.029	15.799	15.362	0.64	0.27	2.84	15.820	15.256	15.361	17.303	14.684	3.70	3.70	17.83
515	16.491	16.517	16.592	16.208	16.099	0.61	0.16	0.67	16.344	15.782	15.860	17.909	15.346	3.56	3.56	16.70
516	17.090	17.137	17.180	16.836	16.892	0.53	0.27	0.33	16.710	16.333	16.382	17.726	16.057	2.31	2.31	10.39
517	17.648	17.714	17.794	17.240	17.270	0.83	0.38	0.17	16.797	16.844	16.929	16.432	16.378	0.78	0.28	0.32
518	18.218	18.342	18.367	17.804	18.203	0.82	0.68	2.24	17.247	17.375	17.408	16.804	17.190	0.93	0.74	2.30
519	18.806	18.879	19.002	18.264	18.205	1.05	0.39	0.33	17.738	17.819	17.944	17.173	17.135	1.16	0.46	0.22
520	19.414	19.517	19.556	19.019	19.292	0.73	0.53	1.44	18.247	18.356	18.404	17.813	18.082	0.86	0.59	1.51

Table (12c): L = 27.5 m, all values of U, dia = 25 mm

section number	neutral axis depth ratios			lever arm effective depth ratios				
	R_T	R_H	R_D	j_T	j_H	j_D	j_L	j_{LH}
511	0.306	0.338	0.349	0.884	0.875	0.874	0.914	0.883
512	0.321	0.361	0.355	0.878	0.870	0.872	0.896	0.858
513	0.337	0.367	0.361	0.874	0.866	0.873	0.875	0.832
514	0.355	0.373	0.367	0.868	0.865	0.871	0.859	0.835
515	0.376	0.379	0.372	0.862	0.863	0.867	0.847	0.841
516	0.392	0.384	0.378	0.859	0.862	0.864	0.846	0.849
517	0.397	0.389	0.383	0.855	0.859	0.863	0.836	0.837
518	0.402	0.395	0.388	0.853	0.859	0.860	0.834	0.853
519	0.407	0.400	0.394	0.852	0.856	0.861	0.828	0.825
520	0.412	0.405	0.399	0.852	0.857	0.858	0.835	0.847

Table (12d): L = 27.5 m, all values of U, dia = 25 mm

section	live load modulus	strain factor	combined load modulus	centroidal simulated stress ranges based on F and F_L			centroidal simulated and actual stress ranges			outer bar simulated and actual stress ranges			fatigue limit
number	F_L	S_F	F	S_{RT}	S_{RL}	D_S	S_r	f_{sr}	D_f	S_{re}	f_{sre}	D_{fe}	S_e
511	14.285	1.034	14.163	103.90	103.45	0.43	103.90	99.94	3.97	97.80	93.51	4.58	59.27
512	14.532	1.037	14.727	101.02	101.70	0.67	101.70	97.50	4.31	94.95	90.47	4.95	63.26
513	14.696	1.041	15.304	98.56	100.56	2.03	100.56	95.61	5.17	93.28	88.03	5.97	67.15
514	15.362	1.044	15.926	94.50	96.20	1.80	96.20	93.54	2.84	88.22	85.41	3.29	70.52
515	16.099	1.047	16.517	90.63	91.79	1.28	91.79	91.18	0.67	83.12	82.52	0.73	73.38
516	16.836	1.049	17.135	86.90	87.78	1.01	87.78	87.78	0.00	83.37	83.37	0.00	76.19
517	17.240	1.052	17.714	84.50	85.72	1.45	85.72	85.72	0.00	89.91	89.94	- 0.03	78.94
518	17.804	1.056	18.293	81.73	83.00	1.56	83.00	83.00	0.00	87.76	87.95	- 0.21	81.22
519	18.205	1.060	18.879	79.73	81.18	1.82	81.18	80.91	0.33	86.15	86.05	0.11	83.62
520	19.019	1.063	19.485	76.63	77.70	1.40	77.70	77.70	0.00	82.77	82.96	- 0.24	85.56

Table (12e) - Actual and simulated stress ranges caused by the maximum total moment (M_T)
L = 27.5 m, all values of U, dia = 25 mm

section number	centroidal simulated stress ranges based on F and F_L			centroidal simulated and actual stress ranges			outer bar simulated and actual stress ranges		
	S_{RHT}	S_{RHL}	D_{SH}	S_{rh}	f_{srh}	D_{fh}	S_{rhe}	f_{srhe}	D_{fhe}
511	51.73	51.73	0.00	51.73	51.73	0.00	43.84	43.84	0.00
512	50.85	50.85	0.00	50.85	50.85	0.00	44.13	44.13	0.00
513	50.28	50.28	0.00	50.28	50.28	0.00	52.44	52.44	0.00
514	48.10	48.10	0.00	48.10	48.10	0.00	50.32	50.32	0.00
515	45.90	45.90	0.00	45.90	45.90	0.00	48.18	48.18	0.06
516	43.77	43.89	0.26	43.89	43.74	0.33	46.17	46.02	0.33
517	42.79	42.86	0.17	42.86	42.79	0.17	45.20	45.11	0.18
518	41.33	41.50	0.41	41.50	40.59	2.24	43.95	42.98	2.24
519	40.59	40.59	0.00	40.59	40.59	0.00	43.14	43.12	0.05
520	38.71	38.85	0.37	38.85	38.30	1.44	41.46	40.86	1.45

Table (12f) - Actual and simulated stress ranges caused by the average total moment, $M_H = 0.5\ (M_T + M_D)$
L = 27.5 m, all values of U, dia = 25 mm

CHAPTER 5

ANALYSIS OF FATIGUE CUMULATIVE DAMAGE

In this study, fatigue life has been estimated by using Palmgren - Miner's equation (Eq. 5.1) and Inoue - Nakagawa's equation (Eq. 5.2) :

$$\sum \frac{n_i}{N_i} = 1.0 \qquad \ldots\ (5.1)$$

$$\sum \frac{n_i}{\sqrt{N_{SC}\ N_i}} = 1.0 \qquad \ldots\ (5.2)$$

where:

n_i = number of cycles applied at stress range S_i
$N_{SC} = \sum n_i$
N_i = number of cycles to failure at stress range S_i

It has been shown, in Chapter (2), that for the fatigue of straight hot rolled reinforcing bars, the adopted relationship to represent the S- N curve has the form :

$$\log N = A_N - 200\ (10^{-5}) f_{min} - 591\ (10^{-5}) f_r \qquad \ldots\ (5.3)$$

where, A_N is a numerical constant which depends on the bar size and characteristics, f_{min} is the stress caused by the bridge dead loads in N/mm^2 and f_r is the stress range in N/mm^2. Eq. (5.3) is applicable for all stress ranges above the bars' fatigue limit (f_f) which is given, in Chapter (2), by :

$$f_f = 161.5 - 0.33\ f_{min} \qquad \ldots\ (5.4)$$

If we define a dimensionless damage ratio D, at a number of cycles j, such that (D = 0) for the virgin material (j = 0) and (D = 1) at failure, then D at any stage j can be given by :

$$D_m = \sum \frac{n_j}{N_j}$$

$$D_n = \sum \frac{n_j}{\sqrt{N_{SC} N_j}}$$

where D_m and D_n are damage ratios based on Equations (5.1) and (5.2) respectively.

From the above definition of the damage ratio based on Palmgren - Miner's relationship (D_m), we see that the relationship is linear. This leads to the conclusion that we can form a summation of the damage from a series of loading, at different stress ranges, by simple addition. Thus if we have n_1 cycles of a stress range S_1 and n_2 cycles of a stress range S_2, etc., the damage will be obtained by their combination. If such a series of loading is itself repeated, say K times, the total damage will simply be K times the damage of one series.

However, this linear relationship does not hold, if we apply the Inoue - Nakagawa's relationship (Eq. 5.2). If we examine the derivation of the Inoue - Nakagawa's relationship (given in App. A), we note that the damage sum at failure is derived by taking the square root of the following equation:

$$\frac{1}{N_{SC}} \left[\sum \frac{n_i}{\sqrt{N_i}} \right]^2 = 1.0$$

Let us now define the damage ratio based on Inoue - Nakagawa's relationship (D_n) by :

$$D_n = \frac{1}{N_{SC}} \left[\sum \frac{n_j}{\sqrt{N_j}} \right]^2$$

If we have n_1 cycles of a stress range S_1 and n_2 cycles of a stress range S_2, etc., and the series of loading is itself repeated for K times, then we conclude from the above form for D_n that the total damage will simply be K times the damage of one series. For this reason, the last form of the damage ratio based on Inoue - Nakagawa's relationship (D_n) has been adopted in this study.

Therefore, since it has been assumed in Chapter (3) that the traffic model is repeatable every week, then it follows that the damage caused in K weeks is simply K multiplied by the damage per week.

Consequently, the bridge life is given by :

$$\text{Life in years} = \frac{1}{N_w \times D_w}$$

where D_w is the amount of damage per week, and N_w is the average number of weeks in one year, taken over a period of four years to include the effect of the leap years :

$$N_w = 0.25\ (3 \times 365 + 366)/7 = 52.179 \text{ weeks/year}$$

The procedure used to estimate D_w is given in the following sections.

5.1 Simulation of Stress Spectrum

As discussed in Chapter (4), the stress spectrum has been simulated as follows :

a- The section modulus F_L is taken as :

F_L = the minimum of Z_L and Z_{LH} , which are defined as :

$$Z_L = \frac{M_L}{f_{sa} - f_{sd}}$$

$$Z_{LH} = \frac{M_{LH}}{f_{sh} - f_{sd}}$$

where :

M_L = the maximum live load moment (including impact)
$M_{LH} = 0.5\ M_L$
f_{sa} , f_{sh} , f_{sd} = the stresses caused by the maximum total moment ($M_T = M_L + M_D$, where M_D is the dead load moment), the average total moment ($M_H = 0.5\ M_L + M_D$) and the dead load moment (M_D) respectively. These stresses correspond to the strains at the centre of the tensile force (T).

(F_L rounded to two decimal places).

b- The strain factor S_F is taken as :

S_F = the maximum of S_{FH} and $0.5\ (S_{FT} + S_{FD})$

where S_{FT} , S_{FH} and S_{FD} are the ratios, of the outer bar strain to the strain at the centre of the tensile force, which correspond to the maximum total moment (M_T), the average total moment (M_H) and the dead load moment (M_D) respectively.

(S_F rounded to three decimal places).

c- The stress range in the outer bar is simulated as :

1 - $$S'_r = \frac{\text{live load moment at mid span (including impact)}}{\text{section modulus } (F_L)}$$

where S'_r is the stress range resulting from the total centroidal stress which corresponds to the strain at the centre of the total tensile force.

2 - From the total centroidal stress ($f'_{ss} = S'_r + f_{sd}$), the corresponding strain e'_{ss} is calculated.

3 - From the outer bar strain ($e'_{sse} = e'_{ss} \times S_F$), the outer bar stress f'_{sse} is calculated.

4 - Finally, the stress range in the outer bar is :

$$S'_{re} = f'_{sse} - f_{sde}$$

where f_{sde} is the total outer bar stress caused by the dead load moment (M_D).

(Both f_{sd} and f_{sde} values are rounded to one decimal place).

The aforementioned procedure implies that, for each beam section, four parameters are needed (i.e. F_L , S_F , f_{sd} and f_{sde}). Values of these parameters for the various combinations of the bridge span (L) and the loading frequency (U), are given at the end of this chapter.

5.2 Cycle Counting Methods

In order to use any complex stress spectrum, in conjunction with standard constant amplitude data, to estimate the fatigue life, the stress spectrum must be reduced to a series of equivalent cycles or half cycles (ranges). This process is known as cycle counting. A large number of counting methods have been proposed, but two are the most useful. The two methods are the range - mean and the rainflow counting methods (50, 51).

5.2.1 Range - Mean Method

In this method, the range between successive turning points (local maximum or minimum) and the mean of their two values are recorded, but noting that only ranges,exceeding a specified gate level, are counted (Figure 5.1). This is because a small range may break the continuity of a much larger range and convert it to small ranges all of them below the fatigue limit. The introduction of a gate level allows the consideration of a turning value only if it is greater than the specified gate from the last turning value (50, 51).

It is difficult to define an optimum value of the gate level. if, for example, in Figure (5.1) the gate level is greater than the range of B - C, the stress spectrum is divided into four ranges; R_1 , R_2 , R_3 and R_4. If a smaller gate, less than B - C, had been used then three small ranges A - B, B - C and C - D would have been included instead of the larger range from A - D.

For metals, the relationship between the number of cycles to failure N and the stress range S can be approximated (7) by ;

$$NS^q = K$$

where K and q are constants which depend upon the material concerned and the design detail. Since q ranges approximately from a value of 3 to 10, then if an interrupted large range is broken into n smaller ranges, the total damage for the n ranges may be less than that for the single large range. This is because of the fact that stress range S is raised to a power q greater than unity. This means that decreasing the gate level may result in more events being counted but with less total damage resulting. Also, if we increase the gate level, this may result in fewer events but more damage.

As a result, the only sensible way would seem to be to try several gate levels and use that value which gives the maximum predicted damage (50, 51). Even with such a value of the gate level, there is no certainty that the predicted amount of damage is absolutely conservative, because its value is obtained by excluding a large number of small cycles which none the less may be damaging. This suggests that the predicted damage may be non - conservative (50).

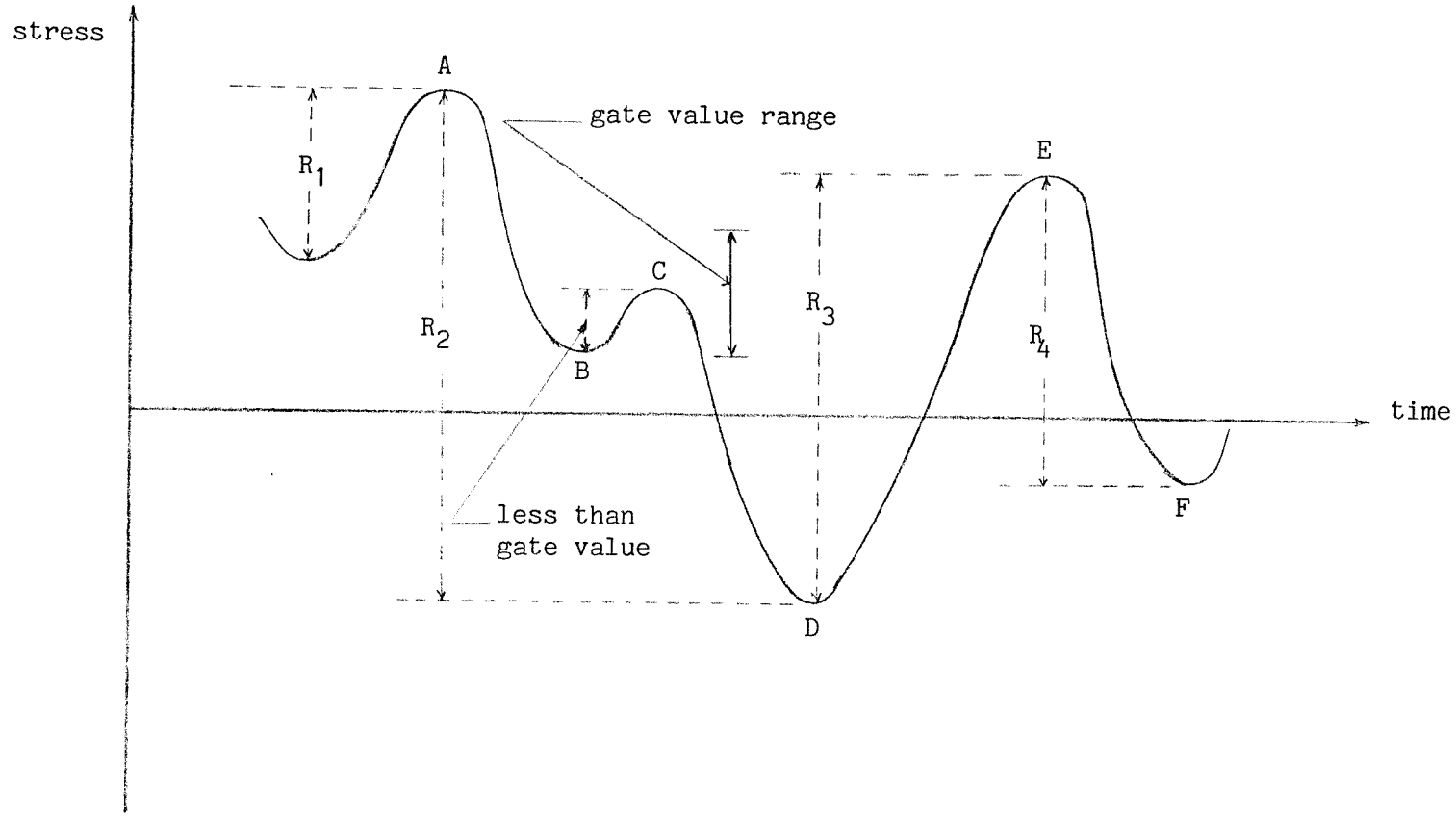

Figure (5.1) - Stress spectrum divided into ranges R_1 , R_2 , R_3 and R_4

5.2.2 Rainflow Method

This method, proposed by Endo et al (52), counts cycles and half cycles. In this outstanding technique, the counting is performed on the basis of the stress - strain behaviour of the material.

Figure (5.2) illustrates the relationship between the stress - strain behaviour and the counting method. It is important to note that when a large range, for example A - D is interrupted by a smaller one B - C - B', the coordinates of B' and B are very close on the stress - strain curve. This indicates that the material acts as if the large range was uninterrupted and there is a complete cycle B - C - B'. The rainflow method performs the counting in the same way as the material reacts to loading cycles. Thus, this method is superior to all others because it is the only one which reflects material behaviour (7,50,51).

For this method to be applied, the ordered sequence of peaks and troughs of the strain is the most suitable characteristic for the counting. However, the sequence of the stress may be used as an alternative without serious errors (52). The rainflow method has three alternative procedures, each of which gives the same results for the number and magnitude of counted cycles.

In all procedures, the first point in the spectrum is effectively defined by the next point. If the next point is a peak, then the origin is a trough and vice versa.

5.2.2.1 First Procedure - Rainflow

This procedure, which is the most well known, uses the simulation of rainflow on fictive multifarious overlapped pagoda roofs (Fig. 5.3). For this we turn the strain (or stress) spectrum through (90°), so that the time axis is vertical. The strain (or stress) spectrum becomes the imagined series of pagoda roofs, as in Figure 5.3. This figure shows part of a strain spectrum and the corresponding strain - stress loop. Further, we imagine that each turning point 1, 2, 3, etc., is the origin of a flow of rain.

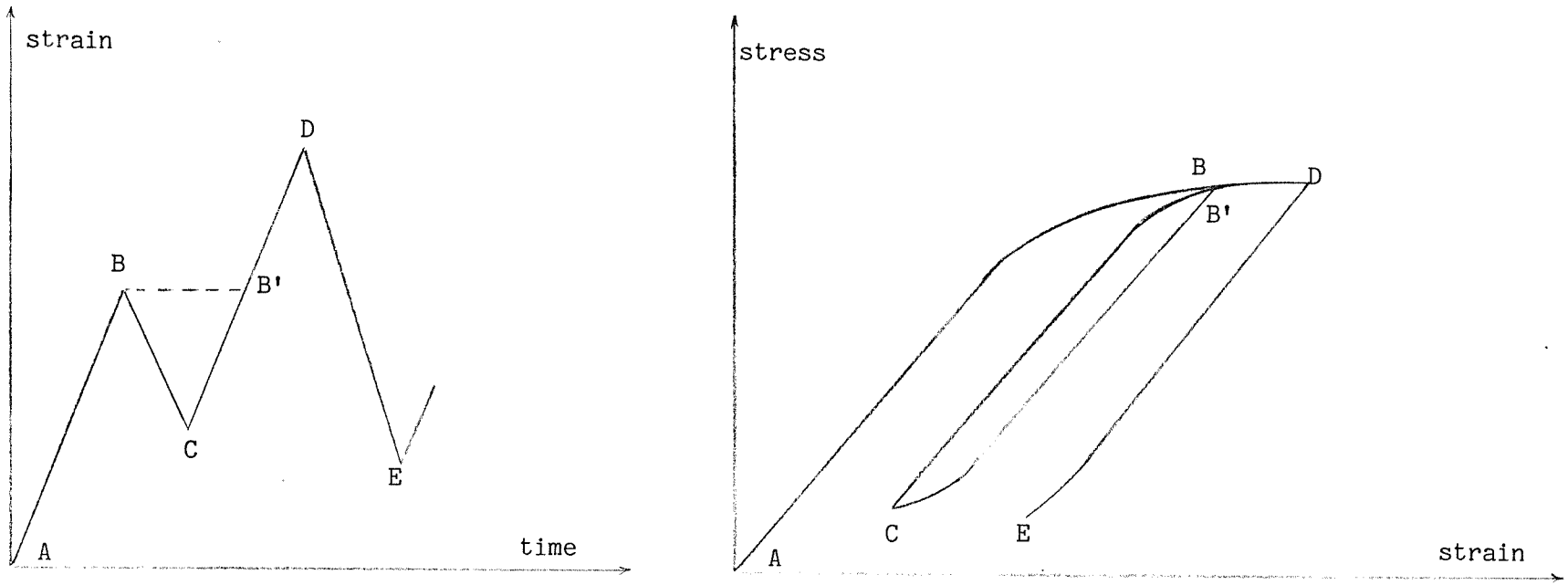

Figure (5.2) - Strain spectrum and the corresponding stress-strain behaviour

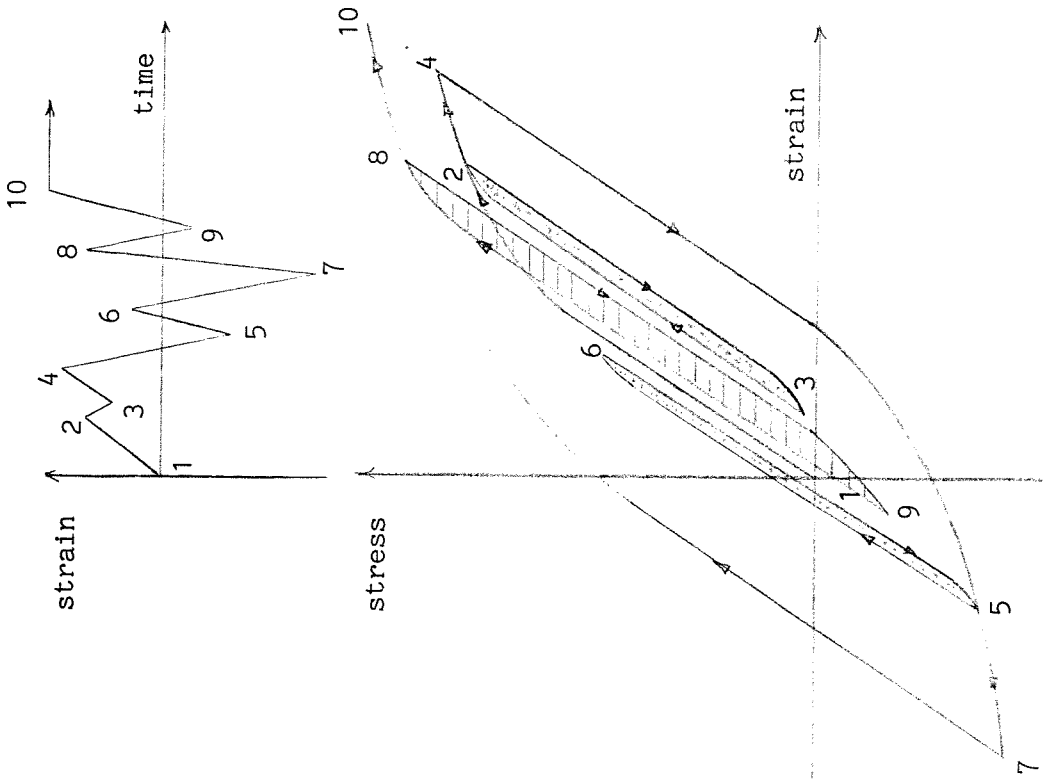

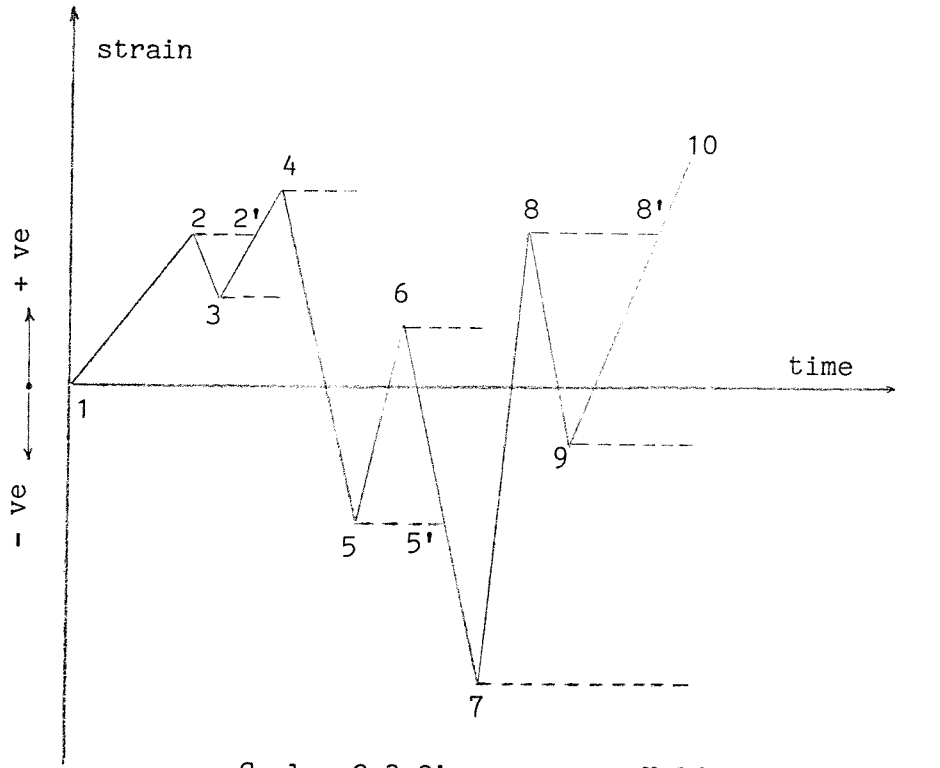

Cycles 2-3-2'
8-9-8'
5-6-5'

Half cylces 1-2-4
4-5-7
7-8-10

Figure (5.3) - Rainflow procedure and its conformity with the strain-stress behaviour

Let us consider the first rainflow beginning at the first point (point 1), which is considered a trough point since it is followed by a peak point. This flow runs down the roof, (segment 1 - 2), until it reaches point (2), then it falls down until it meets a larger roof (3 - 4), when it again flows down the roof away from its origin (point 1).

This flow continues to fall down to the lower roofs unless it comes opposite a trough more negative than the trough from which it started. In the present case, the flow has started from the trough point (1) and so it has to stop opposite the trough point (5) since this is more negative than the starting point.

When a flow stops, we count one half cycle from its origin to its end point. Thus, as a result, one half cycle (1 - 4) has been counted.

A second flow starts from the peak point (2) and continues down the roof (segment 2 - 3) until it reaches point (3), then it falls vertically towards the lower roofs unless it comes opposite a peak more positive than the peak from which it started.

In this case, the flow has started from the peak point (2) and has to stop opposite the peak point (4) which is more positive than the starting point. This gives another half cycle (2 - 3).

The third flow starts from the trough point (3) and continues down the roof (3- 4) until it meets the first flow (originating from point 1) at point (2') where it has to stop, giving another half cycle (3 - 2').

This procedure continues with a flow from each turning point. Each flow continues to fall down to the lower roofs unless it meets one of the following two conditions :

a - the rain is to stop when it meets another flow originating from a preceding point.

b - the rain originating from a peak is to stop, if it comes opposite a following peak more positive than the peak from which it started (or a trough more negative than the trough from which it started).

By tracing the flow from each turning point, the spectrum will be analysed, with every part of it counted once and only once (7, 50, 51, 52). The values of the strain (or stress) at the starting point of each flow and at its end point define the magnitude of the strain (or stress) range.

It is worth noting that if a flow stops because of the first condition a (meeting a previous flow), then there is always an equivalent flow which stops because of the second condition b (larger peaks or smaller troughs). Both flows make one complete cycle. For example, the half cycles (3 - 2') and (2 - 3) make a complete cycle. This cycle can be compared with the corresponding cycle in the strain - stress loop (52).

5.2.2.2 Second Procedure, Maximum - Minimum

We consider Figure 5.4, which shows part of a strain spectrum. This process is concerned with dividing the spectrum down into a series of short segments, based upon the values of the peaks and troughs, to evaluate the number and magnitude of cycles. The counting by the maximum - minimum procedure is performed as follows :

a - We determine the absolute maximum and absolute minimum (points 34 and 17) of the spectrum under consideration. The maximum and minimum points and the two end points divide the spectrum into front, middle and rear parts, denoted by F, M and R (see Fig. 5.4).

b - If the end of part F is bounded by a minimal value, then we next look for the maximum value in that part, in this case point 14 (if it was bounded by a maximal value, we would look for the minimum).

For the section of part F bounded by the starting point and the maximum point 14 (or minimum), we determine the minimum point 7 (or maximum).

This forms the basis for a further subdivision of the section and we proceed towards the starting point, until the section considered has reduced to the first segment (0 - 1).

c - We repeat the subdivision process as above on the rear part R proceeding towards the end point (39). Since part R is bounded by the absolute maximum (point 34), then we first determine its minimum point (35).

Now section (35 - 39) is bounded by a minimum point, hence we determine the maximum within the segment (point 38).

Steps a, b and c evaluate the half cycles which are marked by H in Fig. 5.4, noting that the middle part M constitutes one half cycle by itself.

Figure (5.4) : Maximum-minimum procedure

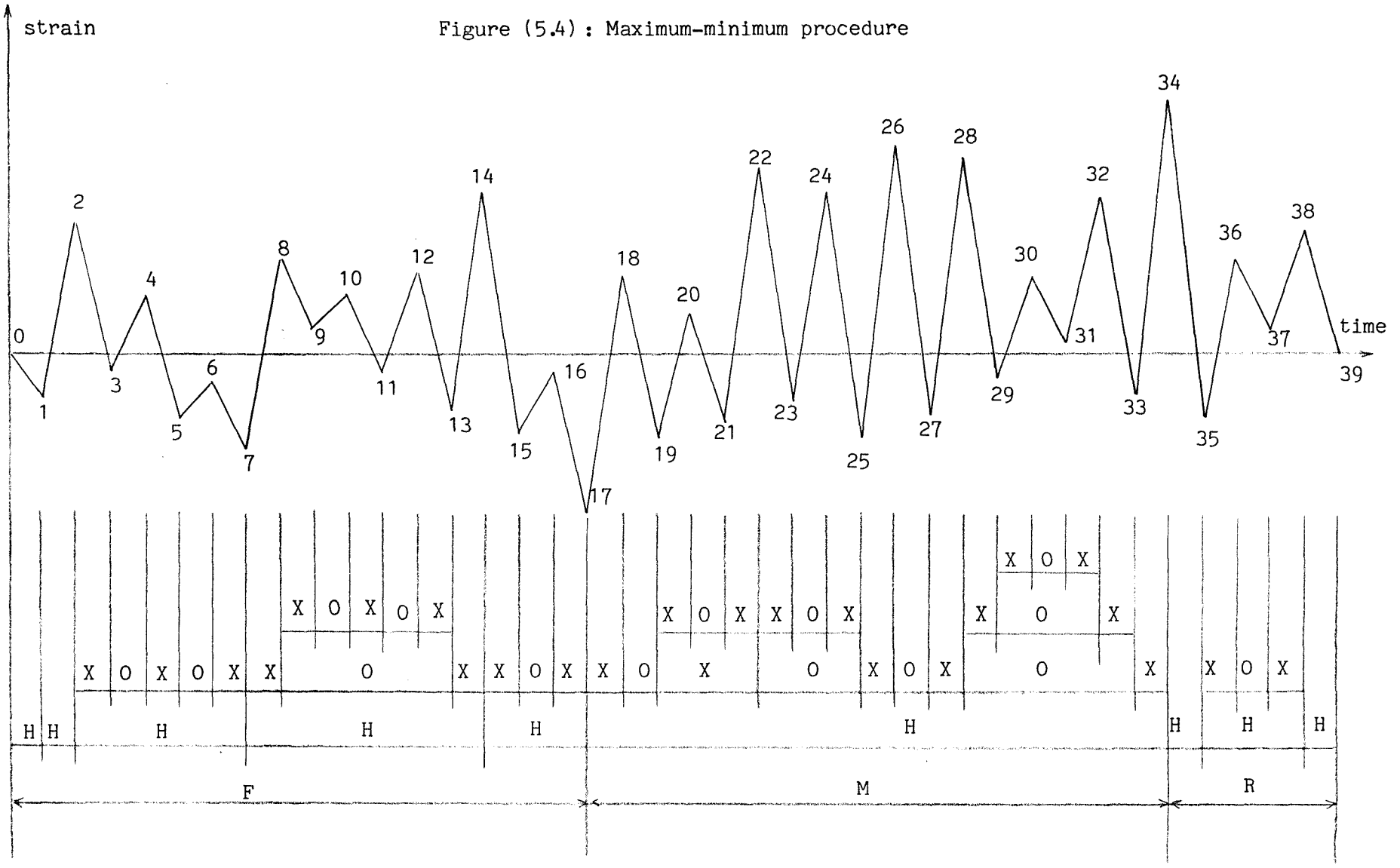

d - To determine the full cycles, the aforementioned procedure has to be applied again to all sections marked by H. In the application to any section, the end points for that section should be disregarded in the process of determining the maximum and minimum internal points for that section.

At the end of this process, the full cycles are determined by picking out ranges whose serial numbers within the section H are even (these are marked O in Fig. 5.4). All ranges with odd serial numbers (marked X in Fig. 5.4) are not counted.

To illustrate this, let us consider the section H represented by the middle part M. If we disregard its end points (17, 34), then its maximum is point (26), while point (25) represents its minimum. Now the local front section (17 - 25) of this middle part M is bounded by a minimum point (25). It will be seen that point (22) represents its maximum and determines the next subdivision. The new section (17 - 22) is bounded by a maximum point (22) and its own minimum is now given by point (19), remembering that we always disregard the starting point. This now establishes the next subdivision, which is itself subdivided by the maximum internal point (18) which concludes the division of this front part of the middle section M.

The local rear section (26 - 34) of the middle part M can be analysed now, in a similar way. Thus the first round of the full cycles of the middle section can be extracted by picking out ranges (18 - 19), (22 - 25), (26 - 27) and (28 - 33). All these ranges (marked O in Fig. 5.4) have even serial number within the middle part M. As mentioned earlier, odd numbered ranges (marked X in Fig. 5.4) are disregarded.

e - We apply step d to all ranges marked O and X, for as many times as required, to define completely all the full cycles counted by this procedure.

5.2.2.3 Third Procedure - Pattern Classification

This procedure is performed by considering three successive ranges from the complex strain (or stress) spectrum, which can then be compared and as a result classified into four basic shapes or patterns (Figure 5.5).

Type a shows that the second range (2 - 3) of the three is smaller than the first range (1 - 2), whilst the third range (3 - 4) is larger than the second range (2 - 3). This pattern is named the decrease- increase type or simply D - I type.

The names given to the other patterns follow from this idea of comparing the second with the first range and the third with the second range.

As shown in Fig. 5.5, the decrease - increase type, D - I, corresponds to one closed hysteresis loop which is between (2) and (3) and one half cycle between (1) and (4). Accordingly, we can count the cycle (2 - 3) and eliminate the intermediate points (2) and (3) by joining (1) and (4) by a line. We then consider in the same way the type of pattern produced by the then remaining points (1) and (4) and the next two points (5) and (6).

In case of I - I type, that is each successive range is greater than its predecessor, ranges (1 - 2) and (2 - 3) always correspond to one half cycle irrespective of the following range (3 - 4). Accordingly, we can count the two half cycles (1 - 2) and (2 - 3) and eliminate points (1) and (2). Whence points (3, 4, 5, 6) are to be considered next.

In case of the increase - decrease type, I - D, the first range (1 - 2) is always one half cycle. Whether range (2 - 3) is one cycle or one half cycle, this cannot be determined from the first pattern (1 - 2 - 3 - 4). Therefore the next pattern (2 - 3 - 4 - 5) has to be considered after counting the half cycle (1 - 2) and eliminating point (1).

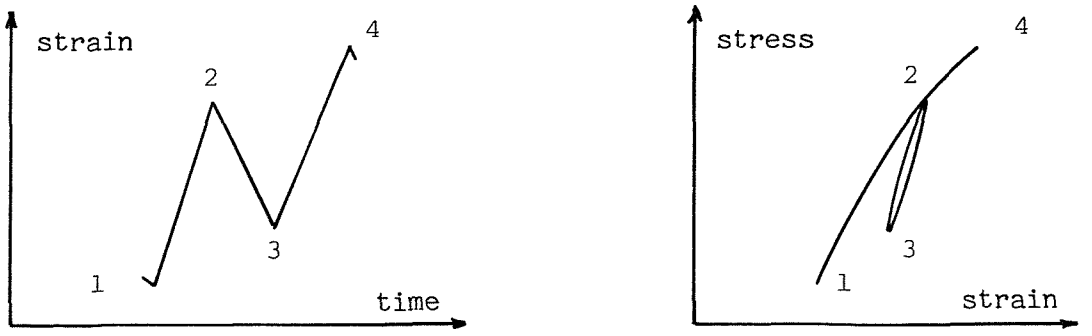

(a) D-I type

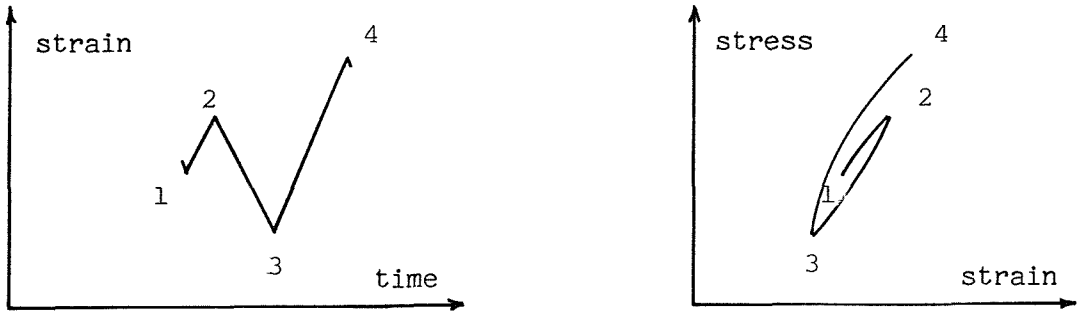

(b) I-I type

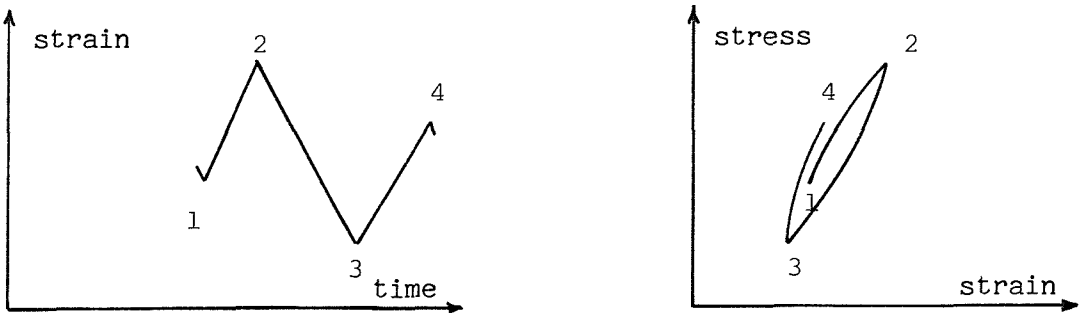

(c) I-D type

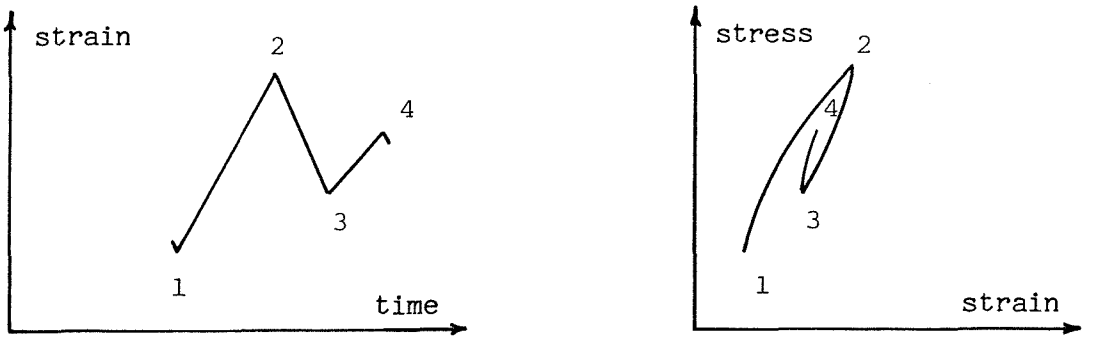

(d) D-D type

Figure (5.5)

Pattern Classification Procedure
Left: Strain vs. time
Right: Stress vs. strain

In case of the decrease - decrease type, D - D, nothing can be determined without considering the next pattern (2 - 3 - 4 - 5). Point (1) has to be kept aside temporarily, while considering the next pattern (2 - 3 - 4 - 5). It should be noted that since the first pattern (1 - 2 - 3 - 4) is of D - D type, i.e. the range (3 - 4) is smaller than the range (2 - 3), then the next pattern (2 - 3 - 4 - 5) is accordingly either of D - I or D - D type.

If the type of the pattern (2 - 3 - 4 - 5) is D - I, then as shown earlier, points (3) and (4) are to be eliminated after counting the cycle (3 - 4). Whence, point (1) has to be considered now by examining the pattern (1 - 2 - 5 - 6).

If the pattern (2 - 3 - 4 - 5) is also D - D, then point (2) has to be kept aside with point (1). These two points have to be considered, immediately after two following points have been eliminated.

If it happens that the pattern (3 - 4 - 5 - 6) is also of D - D type, then we will be in a situation where more than two points (1, 2, 3) have to be kept aside. Later, these points have to be considered, starting with the last point which has been kept aside (point 3).

If this procedure is applied to the spectrum shown in Figure 5.6, which is exactly similar to that shown in Fig. 5.4, then the first pattern (0 - 1 - 2 - 3) has an I - D type. Therefore, range (0 - 1) is a half cycle range. After eliminating point (0), the next pattern (1 - 2 - 3 - 4) has a D - D type, so that the next point (5) has to be considered, keeping aside point (1). Pattern (2 - 3 - 4 - 5) has a D - I type which means that range (3 - 4) is a full cycle range.

Since point (1) has been kept aside, then the next pattern to be considered, after eliminating points (3) and (4) and recalling point (1), is (1 - 2 - 5 - 6) whose type is I - D. Hence range (1 - 2) is a half cycle range. After eliminating point (1), the next pattern (2 - 5 - 6 - 7) has a D - I type and range (5 - 6) is a full cycle range. After eliminating points (5) and (6), the next pattern (2 - 7 - 8 - 9) has a D - D type, meaning that point (2) has to be kept aside when considering the next pattern (7 - 8 - 9 - 10) whose type is D - D. This means that we have now two points to be kept

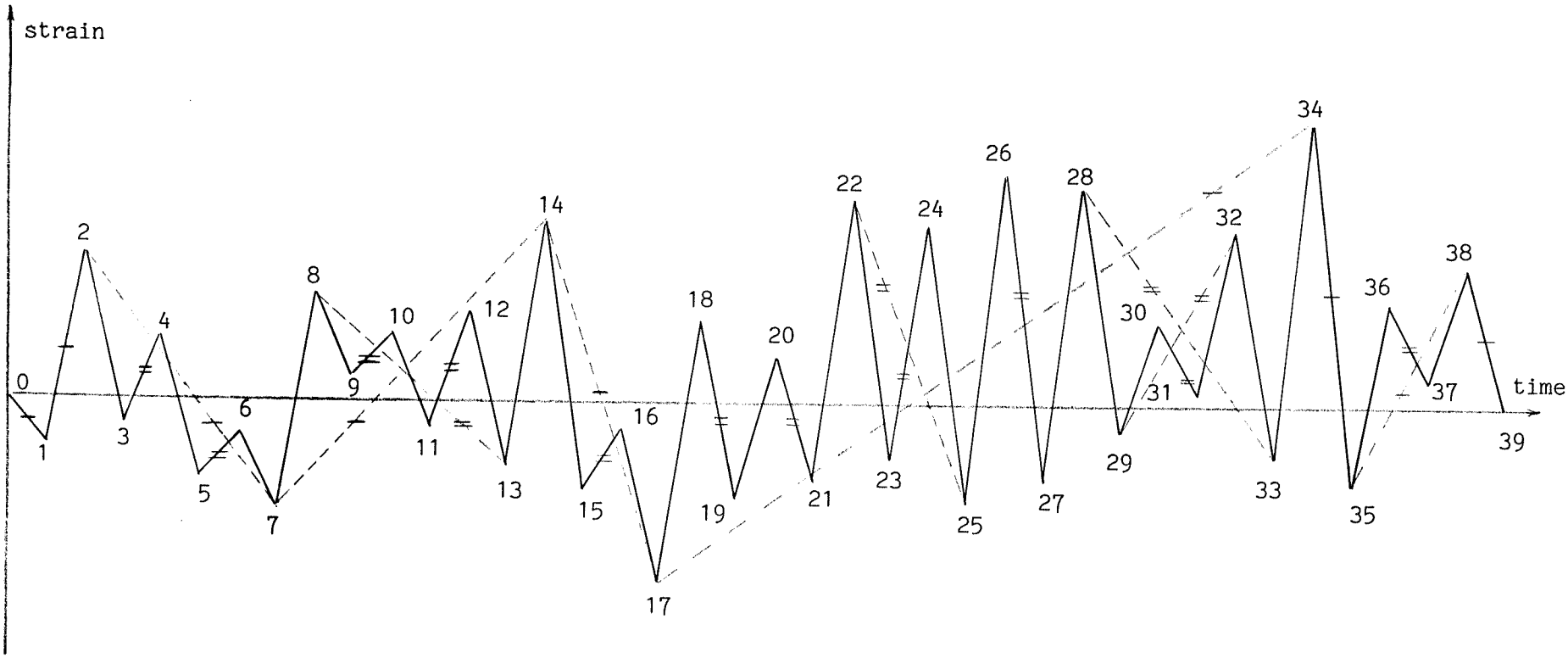

Figure (5.6) - Pattern classification procedure

aside (point 2 and 7). The next pattern (8 - 9 - 10 - 11) has a D - I type, hence range (9 - 10) is a full cycle range. After eliminating points (9) and (10), and recalling points (2) and (7), the next pattern (2 - 7 - 8 - 11) has a D - D type. Point (2) has to be kept aside again and the next pattern (7 - 8 - 11 - 12) has a D - D type. Whence point (7) has to be kept aside again, with point (2). The next pattern (8 - 11 - 12 - 13) has a D - I type, giving the range (11 - 12) as a full cycle range. By eliminating points (11) and (12) and recalling points (2) and (7), the next pattern will be (2 - 7 - 8 - 13) whose type is D - D. Again, point (2) has to be kept aside and the next pattern (7 - 8 - 13 - 14) has a D - I type. Hence the range (8 - 13) is a full cycle range. After eliminating points (8) and (13) and recalling point (2), the next pattern will be (2 - 7 - 14 - 15) whose type is I - D, and so on.

In Fig. 5.6, lines marked with (=) and (-) represent the full cycle and half cycle ranges respectively.

5.3 Computer Program

The computer program which simulates the stress spectrum is similar to that used to simulate the moment spectrum (Section 3.6). The only difference is that, from the stored live load moment values the corresponding stress range values in the outer bar are simulated (as described in Section 5.1) and stored.

In this study, the rainflow method has been adopted to perform the stress cycle counting. After examining an existing computer program constructed to perform the cycle counting, for airframe structures, by the first procedure (rainflow procedure - Section 5.2.2.1), the author has chosen to write another program, based on the third procedure (pattern classification procedure - Section 5.2.2.3). This is because it is believed that such program would be simpler in construction and faster in execution than the alternative one based on the first procedure. The flow chart of this Program is given in Figure 5.7 and the full listing is given in Appendix B.

The amount of the damage per week (D_w) has been computed by adding the damage caused by the successive counted cycles on a cycle to cycle base.

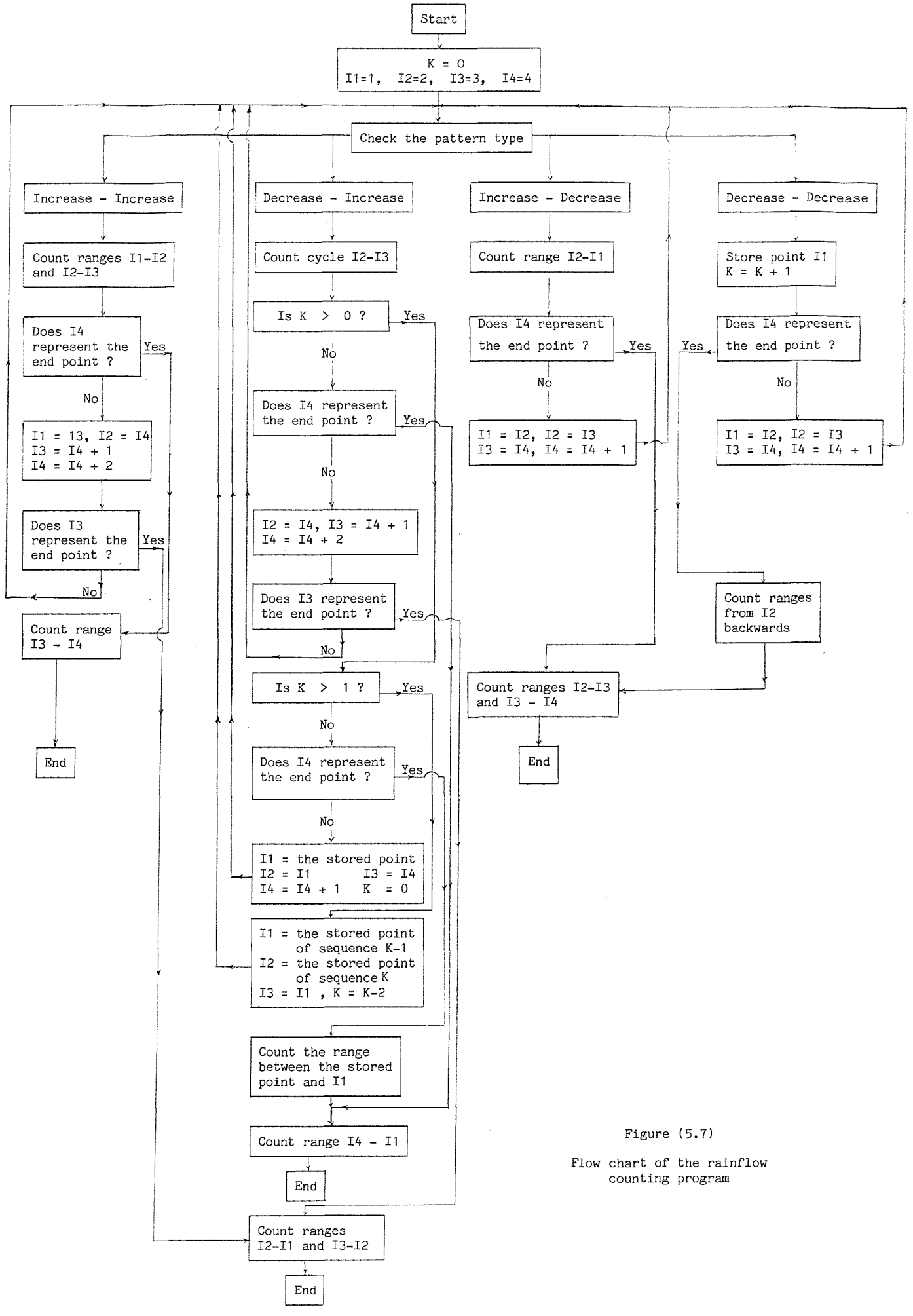

Figure (5.7)

Flow chart of the rainflow counting program

5.4 Tables of Stress Simulation Parameters

bar dia (mm)	section number	section modulus KN.M/(N/mm²)	strain factor	centroidal and outer bar dead load stresses N/mm²	
		F_L	S_F	f_{sd}	f_{sde}
32	12	3.71	1.085	212.5	229.3
	13	4.18	1.104	188.9	207.9
	14	4.56	1.097	178.9	195.7
	15	4.86	1.090	170.2	185.2
	16	5.45	1.107	154.2	170.3
	17	5.84	1.101	147.2	161.7
25	117	3.80	1.108	204.5	225.1
	118	4.22	1.096	194.0	212.2
	119	4.51	1.112	181.4	201.2
	120	4.82	1.105	172.4	190.0
	121	5.14	1.119	162.0	180.8
	122	5.50	1.111	154.6	171.4
	123	5.85	1.123	146.1	163.8

Table 1 - Stress simulation parameters for
L = 15.0 m and U = 360 T/hr.

bar dia (mm)	section number	section modulus KN.M/(N/mm²)	strain factor	centroidal and outer bar dead load stresses N/mm²	
		F_L	S_F	f_{sd}	f_{sde}
32	110	3.71	1.085	212.5	229.3
	111	4.18	1.104	188.9	207.9
	112	4.56	1.097	178.9	195.7
	113	4.86	1.090	170.2	185.2
	114	5.45	1.107	154.2	170.3
25	127	3.80	1.108	204.5	225.1
	128	4.22	1.096	194.0	212.2
	129	4.51	1.112	181.4	201.2
	130	4.82	1.105	172.4	190.0
	131	5.14	1.119	162.0	180.8
	132	5.44	1.132	152.5	172.1
	133	5.85	1.123	146.1	163.8

Table 2 - Stress simulation parameters for
L = 15.0 m and U = 180 and 90 T/hr.

bar dia (mm)	section number	section modulus KN.M/(N/mm²)	strain factor	centroidal and outer bar dead load stresses N/mm²	
		F_L	S_F	f_{sd}	f_{sde}
32	21	5.04	1.051	234.9	246.5
	22	5.43	1.070	211.6	225.7
	23	6.00	1.084	193.6	209.4
	24	6.42	1.079	185.0	199.3
	25	6.94	1.092	169.6	185.0
	26	7.43	1.087	162.7	176.5
25	211	5.19	1.085	224.0	242.2
	212	5.45	1.095	210.7	229.6
	213	5.80	1.104	199.1	219.3
	214	6.24	1.098	190.7	208.9
	215	6.55	1.109	180.9	200.1
	216	6.84	1.119	171.7	191.6
	217	7.35	1.112	164.9	182.9
	218	7.72	1.121	157.2	175.8

Table 3 - Stress simulation parameters for
L = 17.5 m and all values of U

bar dia (mm)	section number	section modulus KN.M/(N/mm²)	strain factor	centroidal and outer bar dead load stresses N/mm²	
		F_L	S_F	f_{sd}	f_{sde}
32	31	6.66	1.037	249.9	259.0
	32	7.36	1.043	226.9	236.5
	33	7.89	1.055	208.8	220.1
	34	8.55	1.067	193.8	206.4
	35	9.26	1.077	180.9	194.5
	36	9.81	1.086	168.9	183.1
25	311	6.81	1.059	249.2	263.5
	312	7.20	1.065	235.0	250.0
	313	7.44	1.073	222.5	238.1
	314	7.84	1.077	211.6	227.7
	315	8.23	1.086	201.8	218.8
	316	8.53	1.095	192.5	210.3
	317	8.90	1.103	184.6	203.1
	318	9.29	1.110	177.1	196.2
	319	9.72	1.118	170.9	190.6

Table 4 - Stress simulation parameters for
L = 20.0 m and all values of U

bar dia (mm)	section number	section modulus KN.M/(N/mm²)	strain factor	centroidal and outer bar dead load stresses N/mm²	
		F_L	S_F	f_{sd}	f_{sde}
32	42	11.73	1.032	270.1	278.6
	43	12.53	1.039	251.8	261.6
	44	13.23	1.046	235.5	246.3
	45	13.93	1.053	220.8	232.3
	46	14.70	1.059	207.9	220.0
25	411	11.15	1.0401	279.3	290.5
	412	11.65	1.044	267.0	278.7
	413	12.22	1.048	255.7	267.9
	414	12.66	1.052	244.2	256.7
	415	13.29	1.055	235.5	248.3
	416	13.70	1.058	225.9	238.9
	417	14.13	1.063	217.8	231.5
	418	14.70	1.068	211.2	225.4
	419	15.22	1.073	203.7	218.3

Table 5 - Stress simulation parameters for
L = 25.0 m and all values of U

bar dia (mm)	section number	section modulus KN.M/(N/mm²)	strain factor	centroidal and outer bar dead load stresses N/mm²	
		F_L	S_F	f_{sd}	f_{sde}
32	52	14.30	1.026	294.1	301.6
	53	14.95	1.028082	274.2	281.9
	54	16.11	1.034135	257.8	266.6
	55	16.91	1.040	243.5	253.2
	56	17.85	1.045	230.6	240.8
25	512	14.53	1.037644	286.9	297.7
	513	14.70	1.041	274.7	285.9
	514	15.36	1.044	264.2	275.7
	515	16.10	1.047	255.2	267.0
	516	16.84	1.049	246.5	258.5
	517	17.24	1.052	238.0	250.2
	518	17.80	1.056	230.6	243.3
	519	18.20	1.060	222.9	236.0

Table 6 - Stress simulation parameters for
L = 27.5 m and all values of U

CHAPTER 6

RESULTS AND DISCUSSION

6.1 The Variation of The Bridge Fatigue Life with The Section Modulus

Fatigue lives, for the different combinations of the loading frequency (U) and the bridge span (L) , have been calculated and are given in tables and graphs at the end of this chapter. As mentioned in Chapter (5), fatigue life has been estimated by using two theories (i.e. Palmgren - Miner's theory and Inoue - Nakagawa's theory). The first theory is widely accepted by designers and researchers and it is currently adopted and used extensively in the prediction of fatigue lives of general structures. Consequently in this study, the relationship between the fatigue life and the section modulus is based on values predicted by this theory.

Fatigue lives have been predicted also by using the second theory (Inoue - Nakagawa's theory) only for the purpose of comparison. As can be seen from the fatigue life tables, the two values are very close and the agreement is very good.

For 15.0, 17.5 and 20.0 m spans, Log(life) value increases consistently with increasing the section modulus F_L. But for 25.0 and 27.5 m spans, the relationship ceases to be a smooth curve of single curvature and a form of 'kink' develops.

To explain this behaviour, let us examine the variation of M_e , the limiting value of the live load moment, including impact, which gives an outer bar stress range equivalent to the endurance limit, S_e . To do this, we have to investigate first the relation between the total centroidal stress, f'_{ss} , which corresponds to the strain at the centre of the tensile force, and the total outer bar stress, f'_{sse} , as follows:

Case (1)

If the centroidal stress (f'_{ss}) and the corresponding outer bar stress (f'_{sse}) both fall on the same linear segment of the stress - strain curve, Fig. 6.1 (let us assume now it is the second linear segment), then the difference between the two stresses is :

$$f'_{sse} - f'_{ss} = (S_F\, e'_{ss} - e'_{ss})\, E' = E'\, e'_{ss}\, (S_F - 1)$$

Where e'_{ss} is the centroidal strain and S_F is the strain factor, which is the ratio of the outer bar strain(e'_{sse}) to the centroidal strain (e'_{ss}) and E' is the slope of the second linear segment of the stress - strain curve. Hence :

$$f'_{ss} = f'_{sse} - E'e'_{ss}\, (S_F - 1) \qquad \ldots.(6.1)$$

Equation (6.1) represents a general relationship between the centroidal and outer bar stresses, in terms of the centroidal strain(e'_{ss}),the strain factor (S_F) and the slope of the stress - strain curve for the steel.

If we consider the limiting outer bar stress (denoted by f_{sel}) which gives a stress range equivalent to the endurance limit (S_e), then any lower stress will not affect the fatigue life. The endurance limit (S_e) is given in Chapter (2) by :

$$S_e = 161.5 - 0.33\, f_{sde}$$

where f_{sde} is the dead load outer bar stress. Hence the limiting outer bar stress (f_{sel}) is :

$$f_{sel} = S_e + f_{sde} = 161.5 + 0.67\, f_{sde}$$

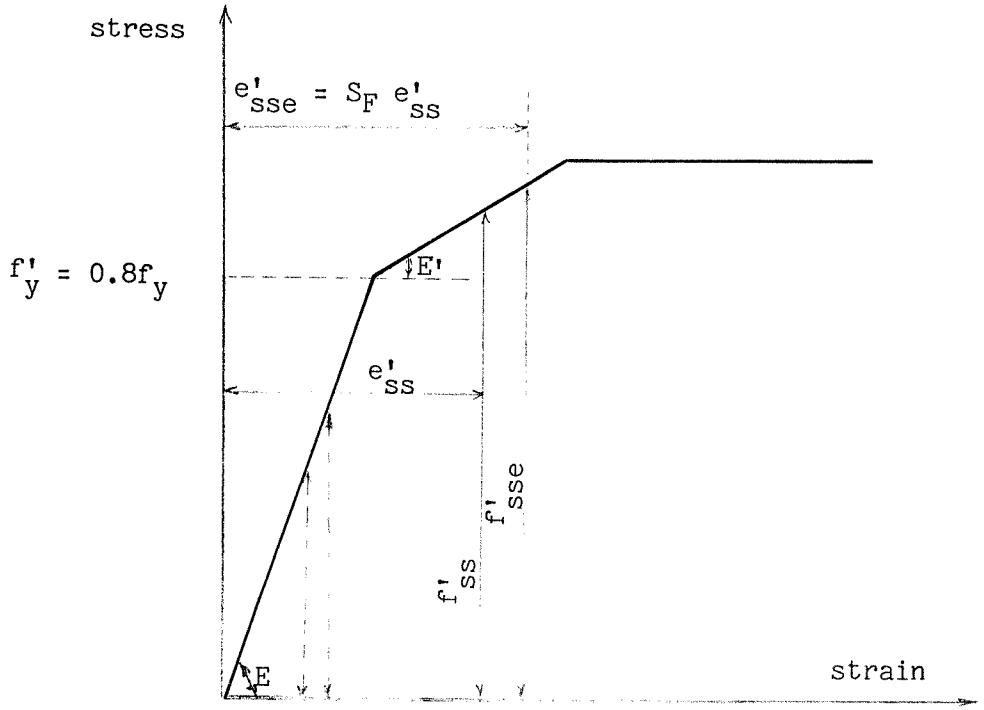

case (1)

f'_{ss} and $f'_{sse} \geq 0.8f_y$

or

f'_{ss} and $f'_{sse} < 0.8f_y$

$f_y = 425\ N/mm^2$

$f'_y = 340\ N/mm^2$

Figure (6.1) - The 'outer bar stress - centroidal stress' relationship for case (1)

Hence it follows from the general Equation (6.1) that the limiting centroidal stress, below which stresses are not effective,is :

$$f_{sl} = f_{sel} - E' e_{sl} (S_F - 1)$$

or

$$f_{sl} = 161.5 + 0.67 f_{sde} - E' e_{sl} (S_F - 1) \quad ....(6.2)$$

where e_{sl} is the centroidal strain which corresponds to the centroidal stress f_{sl}.

The live load modulus (F_L) is taken in Chapter (4) to represent the section through all loading stages. Thus the centroidal stress range S'_r is simulated by the following equation :

$$S'_r = M'_L/F_L$$

where M'_L is the live load moment (including impact). Consequently the relation between the limiting moment value M_e and the limiting centroidal stress f_{sl} can be written as :

$$f_{sl} - f_{sd} = M_e/F_L$$

Hence $M_e = F_L (f_{sl} - f_{sd})$

where f_{sd} is the centroidal dead load stress.

If we now substitute f_{sl} by the expression given in Eq. 6.2, we get:

$$M_e = F_L (161.5 + 0.67 f_{sde} - E' e_{sl} (S_F - 1) - f_{sd}) \quad ...(6.3)$$

For all beam sections in this study, the outer bar dead load stress f_{sde} is less than $(0.8\ f_y)$, i.e. f_{sde} falls on the first linear segment of the stress - strain curve (Fig. 6.1). Whence, the outer bar and centroidal dead load stresses (f_{sde} and f_{sd}) are related by :

$$f_{sde} = E\ e_{sde} = E\ S_F\ e_{sd} = S_F\ f_{sd}$$

where e_{sde} , e_{sd} are the dead load outer bar and centroidal strains and E is Young's modulus.

Substituting f_{sde} in Eq. 6.3 gives :

$$M_e = F_L\ (161.5 + 0.67\ S_F\ f_{sd} - E'e_{sl}(S_F - 1) - f_{sd})$$

or

$$M_e = F_L\ (161.5 - f_{sd}\ (1 - 0.67\ S_F) - E'e_{sl}(S_F - 1)) \quad ....(6.4)$$

This equation is valid when both the outer bar and centroidal stresses fall on the second linear segment, of the stress - strain curve, whose slope is E'.

If both stresses fall on the first linear segment, whose slope is E, then Eq. 6.4 will still be valid if we replace E' by E.

The strain factor (S_F) is, by definition, greater than unity and all the strain factors (S_F) in this study are smaller than (1/0.67 = 1.5). Thus for this case, case (1), as we move from one beam section to the next larger section (with lower stresses), the section modulus (F_L) increases. Thus both the centroidal dead load stress f_{sd} and the centroidal strain e_{sl} decrease. At the same time, the variation in the strain factor, from one section to the next, is very small (as can be seen from the design tables at the end of Chapter 4). Therefore, it is concluded from Eq. 6.4 that the limiting moment value M_e increases with increasing the section modulus (F_L). This means that for case (1), as the modulus F_L increases, the limiting value M_e increases. Consequently the number of effective cycles decreases and the fatigue life increases.

Case (2)

If the centroidal stress f'_{ss} and the corresponding outer bar stress f'_{sse} are on different linear segments of the stress - strain curve (Fig. 6.2), then the difference between the two stresses is :

$$f'_{sse} - f'_{ss} = (f'_y/E' - f'_y/E + e'_{ss} S_F)E' - e'_{ss} E$$

$$= f'_y - E' f'_y/E + e'_{ss} E'S_F - e'_{ss} E$$

Noting that, $E = 5.71 E'$, we see that:

$$f'_{sse} - f'_{ss} = f'_y - f'_y/5.71 + e'_{ss} E' S_F - e'_{ss} E$$

$$= 4.71 f'_y/5.71 + e'_{ss} E' S_F - 5.71 e'_{ss} E'$$

Hence the centroidal stress is given by :

$$f'_{ss} = f'_{sse} - 4.71 f'_y/5.71 - e'_{ss} E' S_F + 5.71 e'_{ss} E' \quad ...(6.5)$$

Similarly to case (1), the limiting outer bar stress f_{sel} below which stresses do not affect the fatigue life is :

$$f_{sel} = 161.5 + 0.67 f_{sde}$$

Furthermore, the limiting centroidal stress f_{sl} below which stresses do not affect the fatigue life, can be obtained from Eq. 6.5 by substituting f'_{sse} by f_{sel} and e'_{ss} by e_{sl}. Hence it follows that the limiting centroidal stress can be expressed as :

$$f_{sl} = 161.5 + 0.67 f_{sde} - 4.71 f'_y/5.71 - e_{sl} E' S_F + 5.71 e_{sl} E'$$

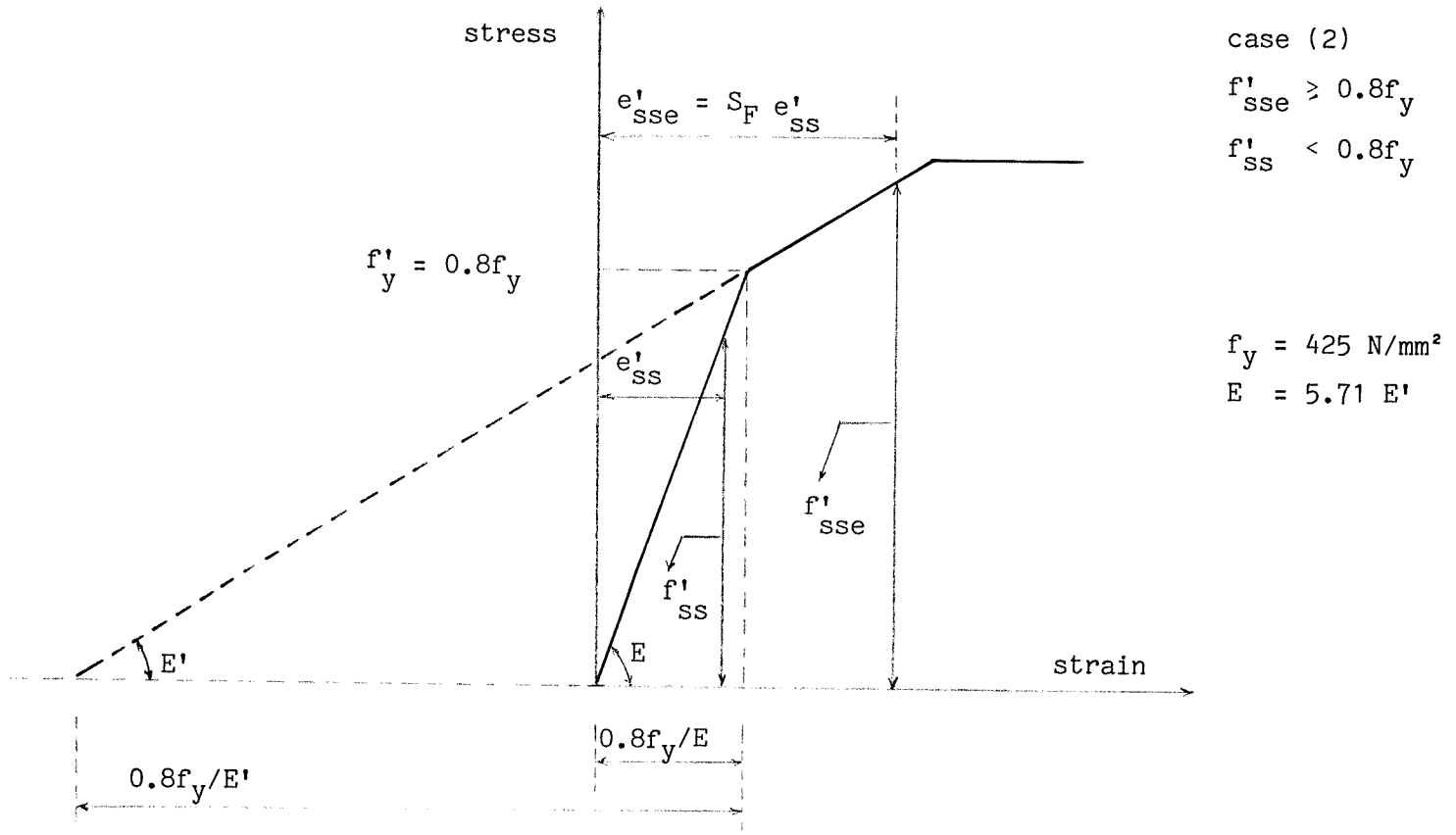

Figure (6.2) - The 'outer bar stress - centroidal stress' relationship for case (2)

Similarly to case (1), the limiting live load moment value M_e is given by :

$$M_e = F_L (f_{sl} - f_{sd})$$

Also, the outer bar dead load stress (f_{sde}) is given by, $f_{sde} = S_F f_{sd}$. By substituting for f_{sl} and f_{sde} we get the following equation for M_e :

$$M_e = F_L (161.5 + 0.67 S_F f_{sd} - 4.71 f'_y/5.71 - e_{sl} E' S_F + 5.71 e_{sl} E' - f_{sd})$$

For this case, case (2), the centroidal and outer bar stresses are assumed to fall on different linear segments of the stress - strain curve. It therefore follows that the limiting centroidal stress (f_{sl}) falls on the first linear segment whose slope is E. Hence f_{sl} can be evaluated by :

$$f_{sl} = E\, e_{sl} = 5.71\, E'\, e_{sl} \qquad f_{sl} < f'_y$$

Substituting and rearranging, we get :

$$M_e = F_L [161.5 - f_{sd} (1 - 0.67 S_F) - E' e_{sl} (S_F - 1)] + 4.71 F_L [f_{sl} - f'_y]/5.71$$

.... part 1
.... part 2
.... (6.6)

Part 1 of Eq. 6.6 is exactly similar to Eq. 6.4 of case (1). Hence as concluded earlier, when the modulus F_L increases, part 1 increases also. However for this case, the limiting centroidal stress (f_{sl}) falls on the first linear segment of the stress - strain curve, i.e. $f_{sl} < f'_y$. Thus, part 2 of Eq. 6.6 is always negative. Consequently for case (2), as the equation contains a part with positive slope and a part with negative slope, there is no certainty that the limiting moment value M_e increases consistently with the increasing modulus F_L , as it does for case (1).

If we consider the short spans (15.0, 17.5 and 20.0 m), the dead load stresses are low enough to keep the limiting total outer bar stress ($f_{sel} = S_e + f_{sde} = 161.5 + 0.67\ f_{sde}$), in all sections, less than the change point f'_y. Therefore all sections are controlled by the equation relevant to case (1) (Eq. 6.4 and Fig. 6.1). Accordingly, the fatigue life increases consistently with increasing the section modulus.

However, for the longer spans (25.0 and 27.5 m), where the section depths are increased to comply with the deflection requirement, the dead load stress for some sections is high enough to push the limiting total outer bar stress (f_{sel}) over the change point ($f'_y = 0.8 f_y$). If the corresponding centroidal stress (f_{sl}) is also over ($0.8\ f_y$) (as is the case for the highly stressed sections), then case (1) will govern the behaviour of the limiting moment value (M_e). As a result, it increases with the increasing modulus (F_L).

As we move to the sections with lower stresses, we get some sections whose limiting outer bar stress (f_{sel}) is still higher than ($0.8\ f_y$), but the corresponding centroidal stress (f_{sl}) is less than this value. For such sections the limiting moment value (M_e) is defined by the equation relevant to case (2) (Eq. 6.6 and Fig. 6.2). Consequently part 2 of Eq. 6.6 will decide whether the limiting moment value (M_e) for such a section is higher or lower than its value for the next more highly stressed section.

Table (6.1) gives the details of the sections governed by case (2) compared with the more highly stressed sections next to them. From this table, it appears that for the sections reinforced with 32 mm bars and governed by case (2), the absolute value of the negative part 2 is, relatively, not large enough to reverse the sign of the gradient $\Delta M_e/\Delta F_L$, and hence ΔLog(life)/ ΔF_L, but it is sufficient to decrease its value in comparison to the other intervals. For the similar sections reinforced with 25 mm bars, the absolute value of the negative part 2 is, relatively, large enough to reverse the sign of the gradient ΔLog(life)/ ΔF_L.

bar dia (mm)	section number	limiting outer bar and centroidal stress ranges, in N/mm²		section modulus (F_L) KN.M/(N/mm²)	limiting live load moment, M_e, in KN.M			
					case (1)	case (2)		
		f_{sel}	f_{sl}		M_e (Eq.6.4)	Part (1) (Eq.6.6)	Part (2) (Eq.6.6)	M_e (Eq.6.6)
32	42	348.17	346.07	11.73	892.5	N/A	N/A	N/A
	43	336.76	324.12	12.53	906.6	N/A	N/A	N/A
	53	350.36	348.45	14.95	1110.0	N/A	N/A	N/A
	54	340.12	329.48	16.11	N/A	1294.1	- 139.7	1154.4
25	412	348.23	345.37	11.65	913.0	N/A	N/A	N/A
	413	340.99	329.82	12.22	N/A	1008.6	- 102.5	906.1
	514	346.22	343.45	15.36	1218.7	N/A	N/A	N/A
	515	340.39	326.86	16.10	N/A	1330.2	- 174.4	1155.8

Table (6.1) - Sections for which, the limiting outer bar and centroidal stresses (f_{sel}, f_{sl}) are slightly higher or lower than the change point (f'_y = 340 N/mm²)

6.2 Sections with Low Stresses in The Reinforcement

For the sections listed in Table (6.2a), it is interesting to note that they might be capable of carrying the design load even after the failure of their outer layer of bars. The new stresses in the remaining bars, under full design load, which we will call the 'revised' bar stresses, will still be less than the yield value, and therefore the section will remain intact.

The revised centroidal stress f'_{sa} can be estimated approximately from:

$$f'_{sa} = f_{sa} \times \frac{N_b}{N_b - n_b}$$

where:

N_b = the total number of bars in the section.
n_b = the number of bars in the outer layer.

The actual values of f'_{sa} are higher than those estimated by the above formula and shown in Table (6.2a), due to the decrease in the lever arm which results from the failure of the outer layer of bars.

For some sections (16, 121, 131, 130, 216, 215, 317 and 419), the revised centroidal stresses (f'_{sa}) are high enough to make their remaining reinforcement yield under the maximum probable moment M_p (Sections 3.7 and 4.8). This can be seen by comparing these sections, after the failure of their outer layer, with the highly stressed sections whose behaviour under the maximum probable moments (M_p) has been investigated in Chapter (4). Table (6.2b) shows this comparison, and it is clear that these sections are not capable of resisting the maximum probable moment (M_p).

bar dia (mm)	section number	total number of bars	number of bars in one layer	maximum centroidal stresses before and after the outer layer failure, in N/mm²	
		N_b	n_b	f_{sa}	f'_{sa}
32	17	9	3	250.0	375.0
	16	9	3	264.5	396.8
	114	9	3	258.2	387.3
	26	11	4	261.8	411.4
	36	14	5	262.9	409.0
25	123	15	4	248.7	339.1
	122	14	4	263.6	369.0
	121	14	4	279.0	390.6
	133	15	4	243.2	331.6
	132	15	4	257.0	350.5
	131	14	4	272.5	381.5
	130	13	4	290.1	419.0
	218	19	5	252.7	343.0
	217	18	5	265.1	367.1
	216	18	5	279.4	386.9
	215	17	5	293.3	415.5
	319	23	6	265.9	359.7
	318	22	6	276.5	380.2
	317	21	6	288.3	403.6
	419	27	8	289.0	410.7

Table (6.2a) - Approximate revised centroidal stresses for the sections with low stresses, after the failure of their outer layer of bars

Span (m)	serial number of the section with failed outer layer (section a)	revised centroidal stress for section (a) under design load (f'_{sa}) (N/mm^2)	serial number of the highly stressed section (section b)	centroidal stress for section (b) under design load (f_{sa}) (N/mm^2)	centroidal stress for section (b) under M_p (f_{sp}) (N/mm^2)	outer bar stress for section (b) under M_p (f_{spe}) (N/mm^2)
15.0	16	396.8	11	395.8	425.6	433.2
15.0	121	390.6	116	390.9	422.7	437.0
15.0	131	381.5	126	380.8	422.7	437.0
15.0	130	419.0	126	380.8	422.7	437.0
17.5	216	386.9	210	389.7	413.0	423.1
17.5	215	415.5	210	389.7	413.0	423.1
20.0	317	403.6	310	406.5	421.4	428.5
25.0	419	410.7	410	408.5	421.4	426.2

Table (6.2b)- Comparison between the sections with failed outer layer and the highly stressed sections

For the remaining sections (i.e. 17, 114, 26, 36, 123, 122, 133, 132, 218, 217, 319 and 318), fatigue life after the failure of their outer layer seems to be less than 0.5 per cent of the life before the first failure. This is clearly too small to be of practical value. This effect can be seen by comparing these sections, after the failure of their outer layer, with other sections (12, 110, 21, 31, 118, 117, 128, 127, 212, 211, 312 and 311) in the fatigue life tables given at the end of this chapter.

As an example, let us compare section (318) with section (311) in Table (4c) page (297). For the latter, the fatigue life is about 5.7 years which results from a total centroidal stress of about 385 N/mm^2. For section (318), the fatigue life of the outer layer of bars is about 1205 years. For this section, the approximate revised centroidal stress , after the failure of the outer layer of bars, is given in Table (6.2a) to be about 380 N/mm^2. By comparing this revised stress with the stress for section (311), we conclude that the fatigue life of section (318) after the failure of its outer layer of bars would be only around 0.5 per cent of the life before this failure.

Therefore, fatigue lives for the sections under consideration are taken to be defined by the stage of the outer layer failure.

6.3 Curve Fitting

Two methods to fit a curve to a certain data have been used. The first is the standard least squares method (Appendix C), whilst the second one is derived by the author to ensure a 'safe' result, as shown in the following section.

6.3.1 Safe Curve Method

The least squares method fits a curve with deviations above and below it. Such fitting is not appropriate for design data, if a safe design is required.

If we have n linear equations connecting a set of m unknowns, say X_1, X_2,...., X_m with n > m, the residuals for a 'safe curve', Fig. (6.3), with all deviations above it are always negative or zero (non-positive):

$$r_i = \sum_{j=1}^{m} a_{ij} X_j - b_i \leq 0 \qquad i = 1, 2, \ldots, n$$

This method is a process for finding the values for X_1, X_2, ..., X_m which will make the sum of the deviations as numerically small as possible i.e.

$$G = \sum_{i=1}^{n} (-r_i) > 0$$

Finding the values for X_1, X_2 ,.., X_m which minimize G and satisfy the conditions of non-positive residuals is a standard linear programming problem (53), whose solution is easily derived.

If we have to fit a pth degree polynomial to a certain data :

$$y = a_0 + a_1 x + a_2 x^2 + \ldots\ldots + a_p x^p$$

then, the above equation is still linear in the unknown parameters a_j.

In this case the constraints are :

$$a_0 + a_1 x_i + a_2 x_i^2 + \ldots\ldots + a_p x_i^p \leq y_i \qquad i = 1, 2, \ldots, n$$

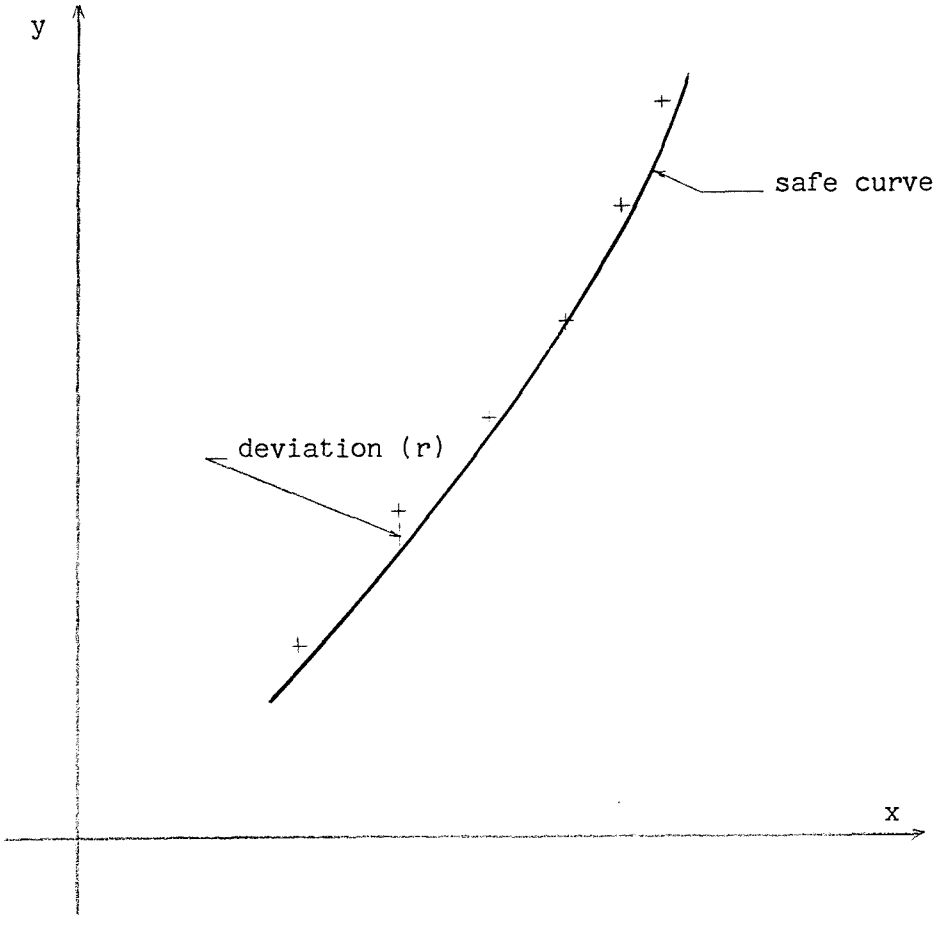

Figure (6.3) - Curve fitting by the safe curve method

While the objective function G is :

$$G = \sum_{i=1}^{n} (-r_i)$$

$$G = \sum_{1}^{n} y_i - (na_0 + a_1 \sum_{1}^{n} x_i + a_2 \sum_{1}^{n} x_i^2 + \ldots + a_p \sum_{1}^{n} x_i^p)$$

or simply :

$$G = -(na_0 + a_1 \sum_{1}^{n} x_i + a_2 \sum_{1}^{n} x_i^2 + \ldots + a_p \sum_{1}^{n} x_i^p)$$

In this study, the E04MBF subroutine (App. D) of the NAG Library has been used to find the safe second degree polynomial curve for the Section modulus F_L - Log (life) data. This subroutine solves linear programming problems or finds a feasible point for such problems. An initial estimate of the solution must be supplied by the user. This has been estimated from the relevant least squares curve coefficients, which have been obtained by another subroutine G02CJF (App. C).

6.4 Log (life) - F_L Safe Curves

To establish a graphical relationship, the least squares curves have been found to provide an initial estimate for the required safe curves (as explained in Sec. 6.3.1) and to provide a comparison between the two sets of curves.

The first computer run has been made to find the least squares second degree polynomials (i.e. $y = T_0 + T_1x + T_2x^2$), by giving the same weight for all points. The resulting curves for 15.0, 17.5 and 20.0 m spans are satisfactory except for the combination of L = 15.0 m and U = 360 T/hr. where the point related to section (17) seems to be relatively far from the fitted curve. Examining this point, in the fatigue life tables at the end of this chapter, reveals that its corresponding fatigue life is based on one effective cycle per week only, and therefore it is believed acceptable to disregard this point, and find the best fit for the remaining points related to L = 15.0 m and U = 360 T/hr.

For 25.0 and 27.5 m spans, the resulting curves cannot be considered satisfactory, which is due to the presence of some points at which, the gradient ΔLog(life)/ ΔF_L is either negative or small (Sec.6.1). Consequently, a second run has been made for these spans, with some points given certain weights to bring them back to the general behaviour of the remaining points.

Weight values have been estimated visually and are given in Table (6.3) which also gives a comparison between the first and second run.

Since any stress range smaller than the endurance limit (S_e) is assumed not to cause any damage, there is a certain section modulus value, beyond which the fatigue life is theoretically infinite. For this, two other forms of curves have been tried :

$$\text{Log(life)} = T_0 + \frac{T_1}{F_{LC} - F_L} + \frac{T_2}{(F_{LC} - F_L)^2}$$

$$\text{Log(life)} = T_0 + \frac{T_1}{\ln F_{LC} - \ln F_L} + \frac{T_2}{(\ln F_{LC} - \ln F_L)^2}$$

where F_{LC} is a critical value of the section modulus.

For each combination of U and L, three values of F_{LC} have been tried. They are taken around that section modulus value, shown in the design tables (Chapter 4), which makes the maximum stress range S_{re} nearly equal to the endurance limit (S_e). Table (6.4) shows these three values for the different combinations of U and L.

A third run has been made to find the least squares fit for these two forms, using the weighted values of the points, but as can be seen from Table (6.5), the new forms do not generally give a better fit than the second degree polynomial which has the advantage of a simpler form. For this, the two new forms have been disregarded.

The coefficients T_0, T_1, T_2 values of the least squares second degree polynomial have been used as the initial estimate for the required coefficients of the safe curves.

The coefficients T_0, T_1, T_2 values for the safe curves are given in Table (6.6), which also shows the deviation between the original weighted Log(life) values and the corresponding values interpolated from the safe curves. These deviations for the fatigue life interval, 25 yrs $\lesssim$ life $\lesssim$ 400 yrs, are reasonably small for 15.0, 17.5 and 20.0 m spans, but are not so for the two longer spans due to the presence of the odd points, as discussed earlier.

Even with these odd points, the sums of squares of the residuals seem to be adequately small and consequently, it has not been thought necessary to try polynomials with higher degrees.

Notes Regarding Tables (6.3, 6.4, 6.5 and 6.6) :

y = Log(life), where 'life' is the fatigue life of the bridge, in years, estimated by the Palmgren - Miner's theory.

w = the weight given to some odd points to improve the curve fitting ($0 < w < 1$).

$y_w = y \times w$

T_0 , T_1 , T_2 = polynomial coefficients for the curve :

$$y = T_0 + T_1 F_L + T_2 F_L^2$$

r_i = $T_0 + T_1 F_{Li} + T_2 F_{Li}^2 - y_i$, $(\sum r_i^2)$ is based on the original 'y' values, while $(\sum r_i^2)_P$ is based on the weighted values 'y_w'. Both $(\sum r_i^2)$ and $(\sum r_i^2)_P$ are for the least squares fit.

F_{LC1}, F_{LC2}, F_{LC3} = the section modulus values taken near the point, where the outer bar stress range (S_{re}) is equivalent to the endurance limit (S_e). F_{LC} is one of these 3 values which gives the best least squares fit for :

$$y_V = T_0 + \frac{T_1}{F_{LC} - F_L} + \frac{T_2}{(F_{LC} - F_L)^2}$$

and

$$y_L = T_0 + \frac{T_1}{\ln F_{LC} - \ln F_L} + \frac{T_2}{(\ln F_{LC} - \ln F_L)^2}$$

$(\sum r_i^2)_V$ = $(\sum r_i^2)$ resulting from the least squares fit of y_V , using the weighted values y_w .

$(\sum r_i^2)_L$ = $(\sum r_i^2)$ resulting from the least squares fit of y_L , using the weighted values y_w .

$(\sum r_i^2)_S$ = $(\sum r_i^2)$ resulting from the safe curve polynomial fit, using the weighted values y_w .

R_y = the largest value of (y_d/y_e), where y_d is the real value, while y_e is the corresponding interpolated value (y_e = Log(life) = $T_0 + T_1F_L + T_2F_L^2$)

R'_y = R_y value taken over the interval $(1.398 \leq y_e \leq 2.602)$ which corresponds to (25 yrs. $\leq$ fatigue life $\leq$ 400 yrs.)

dia (mm)	L (m)	U (T/hr.)	section number	y	y_w	w	$(\sum r_i^2)$	$(\sum r_i^2)_P$
32	25.0	90	42	1.627	1.464	0.90	0.0377	0.0207
		180	42	1.338	1.204	0.90	0.0277	0.0155
		360	42	1.054	0.896	0.85	0.0173	0.0067
	27.5	90	53	2.114	1.903	0.90	0.1021	0.0242
		180	53	1.812	1.540	0.85	0.1058	0.0132
		360	53	1.514	1.211	0.80	0.1186	0.0109
25	25.0	90	412	1.733	1.473	0.85	0.0982	0.0386
			413	1.726	1.640	0.95		
		180	412	1.439	1.151	0.80	0.1086	0.0503
			413	1.432	1.289	0.90		
		360	412	1.158	0.869	0.75	0.1121	0.0461
			413	1.149	0.977	0.85		
	27.5	90	513	2.110	1.899	0.90	0.3482	0.0693
			514	2.636	2.241	0.85		
		180	513	1.809	1.538	0.85	0.3787	0.0521
			514	2.376	1.901	0.80		
		360	513	1.512	1.210	0.80	0.4180	0.0511
			514	2.093	1.570	0.75		

Table (6.3) - Weight values and their effect in improving the curve fitting

		dia = 32 mm			dia = 25 mm		
L(m)	U (T/hr.)	F_{LC1}	F_{LC2}	F_{LC3}	F_{LC1}	F_{LC2}	F_{LC3}
15.0	90 and 180	5.85	5.80	5.75	6.05	6.00	5.95
	360	6.30	6.20	6.10	6.15	6.10	6.05
17.5	all values	7.90	7.75	7.60	7.95	7.85	7.75
20.0	all values	10.30	10.20	10.10	10.40	10.30	10.20
25.0	all values	15.70	15.60	15.50	15.45	15.30	15.15
27.5	all values	18.75	18.65	18.55	18.60	18.45	18.30

Table (6.4) - Critical values of the section modulus in KN.M/(N/mm^2)

L(m)	U(T/hr.)	T_0	T_1	T_2	$(\sum r_i^2)_P$	F_{LC}	$(\sum r_i^2)_V$	$(\sum r_i^2)_L$
15.0	90	1.1046	- 1.1799	0.2825	0.0044	5.85	0.0016	0.0015
	180	2.2399	- 1.8424	0.3586	0.0022	5.85	0.0014	0.0013
	360	1.6402	- 1.6838	0.3389	0.0022	6.10	0.0000	0.0000
17.5	90	6.1572	- 2.7015	0.3223	0.0035	7.90	0.0372	0.0360
	180	7.2829	- 3.2026	0.3663	0.0029	7.90	0.0236	0.0226
	360	7.2249	- 3.2645	0.3701	0.0062	7.90	0.0292	0.0281
20.0	90	- 0.8025	- 0.2920	0.0791	0.0037	10.30	0.1561	0.1533
	180	0.0245	- 0.5988	0.1000	0.0045	10.30	0.1382	0.1355
	360	1.8587	- 1.1633	0.1373	0.0067	10.30	0.0950	0.0927
25.0	90	15.2982	- 2.7594	0.1344	0.0207	15.50	0.0096	0.0097
	180	22.5725	- 3.9455	0.1808	0.0155	15.50	0.0133	0.0134
	360	26.5797	- 4.6340	0.2082	0.0067	15.50	0.0087	0.0088
27.5	90	4.3355	- 0.8372	0.0446	0.0242	18.75	0.0371	0.0369
	180	10.9521	- 1.7591	0.0752	0.0132	18.75	0.0177	0.0175
	360	18.8705	- 2.8230	0.1095	0.0109	18.75	0.0109	0.0108

Table (6.5a) - Least squares fits for the weighted points
Bar dia = 32 mm

L(m)	U(T/hr.)	T_0	T_1	T_2	$(\sum r_i^2)_P$	F_{LC}	$(\sum r_i^2)_V$	$(\sum r_i^2)_L$
15.0	90	1.1545	-1.1382	0.2659	0.0062	6.05	0.1928	0.1899
	180	2.1760	- 1.7311	0.3321	0.0064	6.05	0.1704	0.1677
	360	2.4801	- 2.0230	0.3679	0.0082	6.15	0.0779	0.0755
17.5	90	3.9147	- 1.8594	0.2404	0.0022	7.95	0.3085	0.3046
	180	5.0202	- 2.3375	0.2809	0.0016	7.95	0.2725	0.2688
	360	4.9282	- 2.4033	0.2865	0.0053	7.95	0.2250	0.2215
20.0	90	- 0.0078	- 0.4966	0.0887	0.0069	10.40	0.0727	0.0708
	180	1.2273	- 0.8979	0.1149	0.0104	10.40	0.0511	0.0494
	360	3.5607	- 1.5606	0.1564	0.0025	10.40	0.0538	0.0522
25.0	90	11.1531	- 2.0211	0.1019	0.0386	15.45	0.3450	0.3432
	180	12.9902	- 2.3804	0.1169	0.0503	15.45	0.3648	0.3630
	360	16.4702	- 2.9914	0.1415	0.0461	15.45	0.2969	0.2952
27.5	90	20.7833	- 2.7876	0.1021	0.0693	18.60	0.1186	0.1182
	180	21.8843	- 3.0018	0.1100	0.0521	18.60	0.1242	0.1236
	360	29.5201	- 4.0243	0.1428	0.0511	18.60	0.0833	0.0829

Table (6.5b) - Least squares fit for the weighted points
Bar dia = 25 mm

L(m)	U(T/hr.)	T_0	T_1	T_2	$(\sum r_i^2)_S$	R_y	R'_y
15.0	90	2.5000	- 1.7926	0.3475	0.0105	1.0496	1.0496
	180	2.8911	- 2.1267	0.3885	0.0036	1.0347	1.0347
	360	2.4655	- 2.0450	0.3770	0.0044	1.0461	1.0461
17.5	90	4.8288	- 2.2477	0.2837	0.0136	1.0344	1.0057
	180	6.6350	- 2.9907	0.3488	0.0060	1.0765	1.0000
	360	5.4639	- 2.6648	0.3192	0.0225	1.1084	1.0000
20.0	90	- 1.9993	- 0.0197	0.0635	0.0110	1.1383	1.0129
	180	- 0.6710	- 0.4424	0.0910	0.0101	1.1790	1.0182
	360	1.5827	- 1.0971	0.1330	0.0105	1.2216	1.0000
25.0	90	27.7357	- 4.6360	0.2043	0.0770	1.0787	1.0783
	180	33.9852	- 5.6695	0.2451	0.0613	1.0880	1.0880
	360	34.1278	- 5.7743	0.2507	0.0268	1.0678	1.0678
27.5	90	8.5840	- 1.3956	0.0626	0.0438	1.1168	1.1168
	180	14.4727	- 2.2180	0.0899	0.0248	1.1032	1.0000
	360	21.2637	- 3.1416	0.1198	0.0188	1.1244	1.0121

Table (6.6a) - Safe curves for the weighted points
Bar dia = 32 m

L(m)	U(T/hr.)	T_0	T_1	T_2	$(\sum r_i^2)_S$	R_y	R'_y
15.0	90	1.0767	- 1.0866	0.2574	0.0161	1.0437	1.0437
	180	1.4746	- 1.4063	0.2941	0.0218	1.0395	1.0359
	360	3.5328	- 2.4807	0.4149	0.0227	1.1467	1.0410
17.5	90	3.4265	- 1.6978	0.2269	0.0055	1.0175	1.0150
	180	5.2571	- 2.4214	0.2877	0.0043	1.0438	1.0109
	360	5.6358	- 2.6343	0.3043	0.0137	1.0943	1.0174
20.0	90	- 1.3006	- 0.1935	0.0708	0.0160	1.1403	1.0137
	180	1.0858	- 0.8597	0.1119	0.0199	1.1116	1.0200
	360	4.1925	- 1.7197	0.1660	0.0059	1.0579	1.0169
25.0	90	15.0023	- 2.5967	0.1227	0.1157	1.0827	1.0702
	180	15.4715	- 2.7481	0.1299	0.1197	1.0939	1.0939
	360	15.2588	- 2.8131	0.1346	0.1038	1.1849	1.0732
27.5	90	28.5973	- 3.8069	0.1346	0.1748	1.1857	1.1857
	180	31.1899	- 4.1902	0.1473	0.1387	1.1941	1.1941
	360	39.3631	- 5.2707	0.1817	0.1361	1.2411	1.0979

Table (6.6b) - Safe curves for the weighted points
Bar dia = 25 mm

6.5 The Centroidal Stress Range Giving a (100) Yrs. Fatigue Life

Table (6.7) gives, for each combination of U and L, the design value (corresponding to the design maximum live load moment, including impact) of the centroidal stress range f_{sr100} which is needed to produce a design fatigue life of (100) years. These values have been interpolated from the fitted curves.

For each specific loading frequency U, the stress range for the 100 yrs. fatigue life (f_{sr100}) decreases with increasing span. This is because dead load stresses (f_{sde}) are higher for the longer spans. Whence the endurance limit ($S_e = 161.5 - 0.33\ f_{sde}$) decreases with increasing dead load stresses (f_{sde}), allowing smaller ranges to be effective. Also, since the number of stress cycles to failure (N) is given by Eq. (5.3) as : $N = A_N - 200\ (10^{-5})\ f_{min} - 591\ (10^{-5})\ f_r$ then, if the dead load stress (f_{min}) increases, N decreases and this allows the stress cycles to be more damaging. Consequently, to get the same design fatigue life, the stress range f_{sr100} tends to be smaller.

As we move from the small spans 15.0, 17.5 and 20.0 m to the larger ones, 25.0 and 27.5 m, there is a relatively large decrease in the stress range f_{sr100} value. This is because of the relatively large dead load stresses associated with the long spans, and is caused by the need to increase the beam section depth to meet the deflection requirement.

For all spans, the ratio of the stress range for the (100) yrs. fatigue life to the yield stress (f_{sr100}/f_y), ranges approximately between (0.20) and (0.27).

Finally, the stress range f_{sr100} decreases as the bar diameter decreases. This is also due to the larger dead load stresses associated with small bars.

Notes Regarding Table (6.7)

F_{L100} = the required section modulus, to give a design fatigue life of (100) yrs., estimated from the safe life curve, in $KN.M/(N/mm^2)$.

F'_{L100} = as above, but estimated from the least squares curve, in $KN.M/(N/mm^2)$.

f_{sr100} = M_L/F_{L100} , where M_L is the maximum live load moment including impact, in KN.M.

		dia = 32 mm					dia = 25 mm				
L(m)	U(T/hr.)	$F_{L100}(a)$	$F'_{L100}(b)$	a/b	f_{sr100}	f_{sr100}/f_y	$F_{L100}(a)$	$F'_{L100}(b)$	a/b	f_{sr100}	f_{sr100}/f_y
15.0	90	4.863	4.833	1.0062	117.00	0.275	4.947	4.926	1.0043	115.02	0.271
	180	5.017	5.004	1.0026	113.41	0.267	5.129	5.109	1.0039	110.93	0.261
	360	5.186	5.174	1.0023	115.73	0.272	5.280	5.250	1.0057	113.66	0.267
17.5	90	6.353	6.351	1.0003	115.96	0.273	6.519	6.511	1.0012	113.01	0.266
	180	6.543	6.537	1.0009	112.59	0.265	6.736	6.722	1.0021	109.37	0.257
	360	6.737	6.720	1.0025	109.35	0.257	6.933	6.909	1.0035	106.26	0.250
20.0	90	8.091	8.078	1.0016	114.06	0.268	8.333	8.319	1.0017	110.75	0.261
	180	8.369	8.353	1.0019	110.28	0.259	8.629	8.597	1.0037	106.95	0.252
	360	8.612	8.592	1.0023	107.16	0.252	8.868	8.851	1.0019	104.07	0.245
25.0	90	13.011	12.803	1.0162	99.79	0.235	13.018	12.837	1.0141	99.74	0.235
	180	13.376	13.207	1.0128	97.07	0.228	13.436	13.287	1.0112	96.63	0.227
	360	13.624	13.535	1.0066	95.30	0.224	13.728	13.647	1.0059	94.58	0.223
27.5	90	15.528	15.363	1.0107	95.17	0.224	15.659	15.197	1.0304	94.37	0.222
	180	16.020	15.910	1.0069	92.25	0.217	16.237	15.970	1.0167	91.01	0.214
	360	16.440	16.368	1.0044	89.89	0.212	16.691	16.505	1.0113	88.54	0.208

Table (6.7) - The centroidal stress ranges giving a (100) years fatigue life

6.6 The Effect of The Section Modulus Definition on The Predicted Fatigue Life

As mentioned earlier, in Chapter (4), the section modulus has been defined as : F_{L1} = the minimum of Z_L and Z_{LH} , where Z_L and Z_{LH} are the live load moduli corresponding to the maximum live load moment (M_L) and the average live load moment ($\frac{1}{2}$ M_L) respectively.

In order to investigate the effect of the modulus value (F_L) on the bridge fatigue life, separate runs have been made for L = 15.0 m and U = 90 T/hr. with F_L value defined as : F_{L2} = the maximum of Z_L and Z_{LH} .

The results shown in Table (6.8) reveal that,for section (111) (as an example), the variation in the modulus value is as small as 3.59 percent, but the difference in fatigue lives is as high as 33 percent. This is mainly because increasing the modulus value results in decreasing the values of the simulated stress ranges. As a result, more stress ranges would be smaller than the endurance limit value.

The idea of excluding all stress ranges lower than a certain endurance limit, in the damage sum, has been criticised by many researchers as a major defect in the linear damage sum rule (10). Also, in reality, the endurance limit value decreases with an increasing number of cycles (3). Until now, there has been no common practice to deal with these two points. It is likely that considerably more work will need to be done before significant progress can be made in this field for both steel in general, and for reinforcing steel in particular.

But, let us now consider the effect of defining the modulus F_L on the interpolated section modulus value which gives a certain design fatigue life (say 25, 50, 100 and 200 years).

section number	section modulus F_L KN.M/(N/mm²)	fatigue life in years		centroidal and outer bar simulated stresses (N/mm²)		outer bar stress range (N/mm²)	fatigue limit (N/mm²)	total number of cycles and effective cycles, per week		$Log(life)_m$
		$(life)_m$	$(life)_n$	f_{ss}	f_{sse}	S_{re}	S_e	N_c	N_{ec}	
110	3.86	5.16	5.18	359.9	366.7	137.36	85.83	25227	2696	0.713
111	4.33	15.94	16.01	320.3	342.4	134.49	92.89	25227	902	1.202
112	4.66	47.47	47.62	301.0	330.2	134.50	96.92	25227	313	1.676
113	4.96	161.81	162.09	284.9	310.6	125.36	100.38	25227	94	2.209
114	5.58	1458.93	1459.44	256.2	283.6	113.28	105.30	25227	11	3.164

Table (6.8a) - Bridge fatigue lives for L = 15.0 m and U = 90 T/hr., which are based on a modulus defined as: F_L = the maximum of Z_L and Z_{LH}
Bar dia = 32 mm

section number	section modulus F_L KN.M/(N/mm²)	fatigue life in years		centroidal and outer bar simulated stresses (N/mm²)		outer bar stress range (N/mm²)	fatigue limit (N/mm²)	total number of cycles and effective cycles, per week		$Log(life)_m$
		$(life)_m$	$(life)_n$	f_{ss}	f_{sse}	S_{re}	S_e	N_c	N_{ec}	
127	3.98	5.76	5.79	347.5	354.7	129.60	87.22	25227	2420	0.760
128	4.28	13.67	13.73	326.9	343.2	131.01	91.47	25227	1055	1.136
129	4.60	30.21	30.32	305.1	339.3	138.06	95.10	25227	488	1.480
130	4.91	96.74	96.95	288.3	318.6	128.55	98.80	25227	156	1.986
131	5.27	282.99	283.36	270.0	302.1	121.29	101.84	25227	55	2.452
132	5.53	920.78	921.42	255.4	289.1	117.00	104.71	25227	17	2.964

Table (6.8b) - Bridge fatigue lives for L = 15.0 m and U = 90 T/hr., which are based on a modulus defined as: F_L = the maximum of Z_L and Z_{LH}
Bar dia = 25 mm

Curve fitting has been carried out to find the least squares and safe curves for F_{L2} - Log (life) data. From these curves, the section modulus values which give a design fatigue life of 25, 50, 100 and 200 yrs. have been interpolated and compared with the corresponding values based on F_{L1} data. Fortunately, the maximum deviation between the two values (Table 6.9) is only around 1.0 percent. Consequently, the difference between the centroidal total stresses is expected to be less than half that. This is because, for all our sections, the centroidal stress range is not more than 50 percent of the total stress.

Since the deviations shown in Table (6.9) are quite small, it is believed that it is reasonable to define the section modulus as : F_L = the minimum of Z_L and Z_{LH} , which gives more conservative results.

Some calculations have been made, and given in Appendix E, to breakdown the variation in the fatigue lives which results from an increase in the section modulus value. This variation has two components. The first is caused by the increase in the section modulus itself, which results in reducing all the stress range values. The second and the most important component is caused by excluding more stress ranges because they become less than the endurance limit.

These calculations reveal that, for section 111 (as an example), a difference of 3.59 percent in the section modulus value gives a 33 percent difference in the fatigue life. Out of this figure, about 28 percent difference results from the cycles excluded becauses they become lower than the endurance limit, while about only 5 percent is due to the change in the stress range values.

As mentioned earlier, there are some cases where stress ranges in the outer bar are lower than the centroidal stress ranges. Even for such cases, fatigue life is considered to be controlled by the outer layer of bars, because the endurance limit (S_e) for this layer is smaller than the corresponding values for the other layers ($S_e = 161.5 - 0.33\, f_{min}$, where f_{min} is the dead load stress).

dia (mm)	design fatigue life (yrs.)	least squares polynomial			safe life polynomial		
		F_{L1}	F_{L2}	F_{L2}/F_{L1}	F_{L1}	F_{L2}	F_{L2}/F_{L1}
32	25	4.412	4.443	1.0070	4.446	4.489	1.0097
	50	4.631	4.662	1.0067	4.665	4.712	1.0101
	100	4.833	4.867	1.0070	4.863	4.915	1.0107
	200	5.020	5.061	1.0082	5.046	5.102	1.0111
25	25	4.485	4.515	1.0067	4.499	4.536	1.0082
	50	4.715	4.739	1.0051	4.733	4.764	1.0065
	100	4.926	4.948	1.0045	4.947	4.976	1.0059
	200	5.122	5.145	1.0045	5.146	5.174	1.0054

	dia (mm)	least squares polynomial			safe life polynomial		
		T_0	T_1	T_2	T_0	T_1	T_2
F_{L1}	32	1.1046	-1.1799	0.2825	2.5000	-1.7926	0.3475
	25	1.1545	-1.1382	0.2659	1.0767	-1.0866	0.2574
F_{L2}	32	-0.4813	-0.4893	0.2053	1.8391	-1.4793	0.3077
	25	0.1245	-0.7269	0.2235	0.2461	-0.7639	0.2244

Table (6.9)

Section modulus values [in KN.M/(N/mm²)]
giving a certain design fatigue life, based on
two different criteria, with some information
about the related curve fittings
L = 15.0 m, U = 90 T/hr.

F_{L1} = min. of (Z_L , Z_{LH}), F_{L2} = max. of (Z_L , Z_{LH})

Values of the stress range (S_{re}) and the endurance limit (S_e), based on the rounded parameters; F_L, S_F, f_{sd} and f_{sde} , are given in the fatigue life tables at the end of this chapter. These are very slightly different from the corresponding values, based on the unrounded parameters, which are given in the design tables at the end of Chapter (4).

6.7 Recommendation for Future Work

The work reported in this thesis has attempted to provide a method of assessing the required section properties, specifically section modulus, of simply supported reinforced concrete bridge beams to provide a minimum life when the bridge carries a statistically specified traffic load. The basis of the analysis is the use of what are believed to be the best available theories for the fatigue behaviour of hot rolled steel reinforcement under high cycle-low amplitude conditions.

In the course of the work the question of the effects of a small number of high amplitude loadings was briefly referred to. Little information appears to exist of the effects of such loadings.

However, the importance of the latter type is increasing as a result of the move toward using the materials in a more economical way, which results in lighter and more slender structures, with a higher risk of fatigue failure (16). Consequently, many aspects of this type of fatigue which are unrevealed need thorough investigations.

6.8 Fatigue Life Curves and Tables

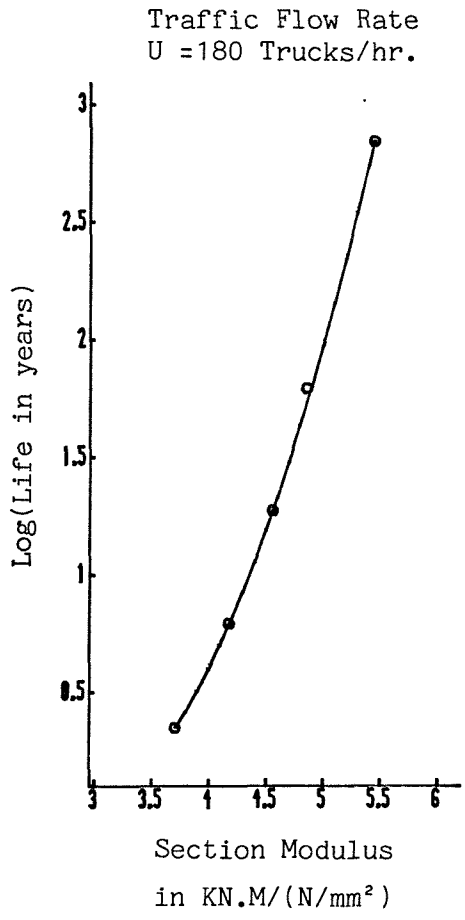

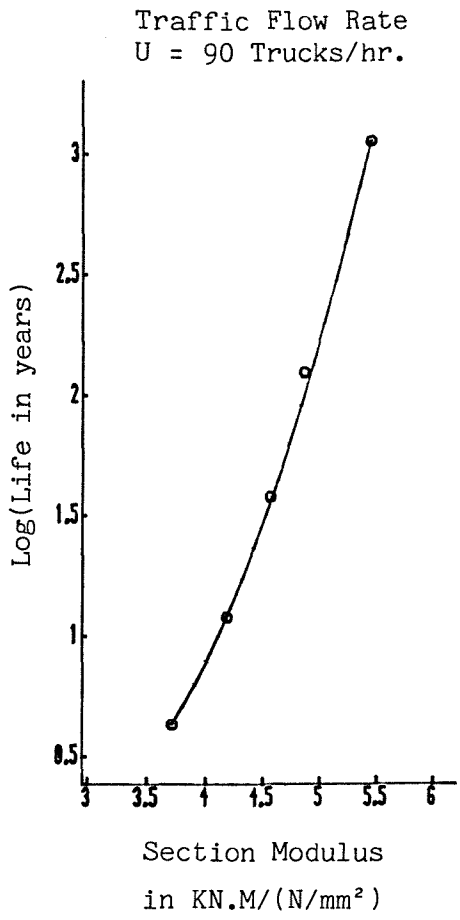

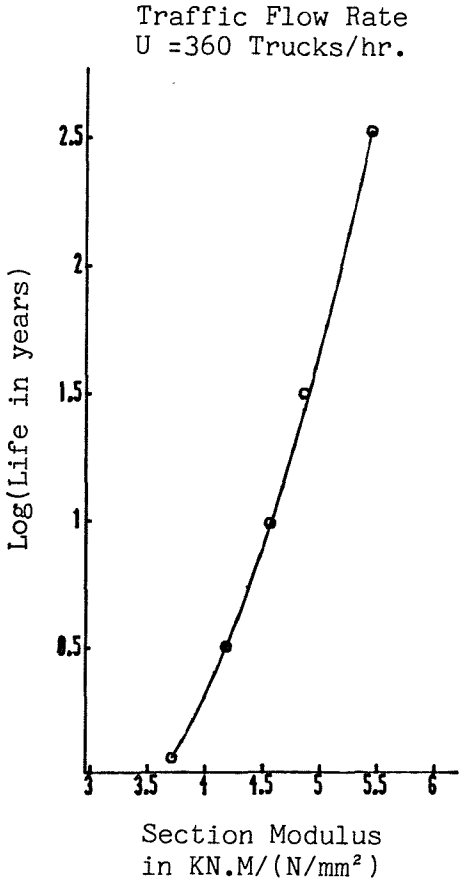

Figure (1)

Section Modulus (F_L) - Log(Life)
Curve for Span = 15.0 m

Bar dia = 32 mm

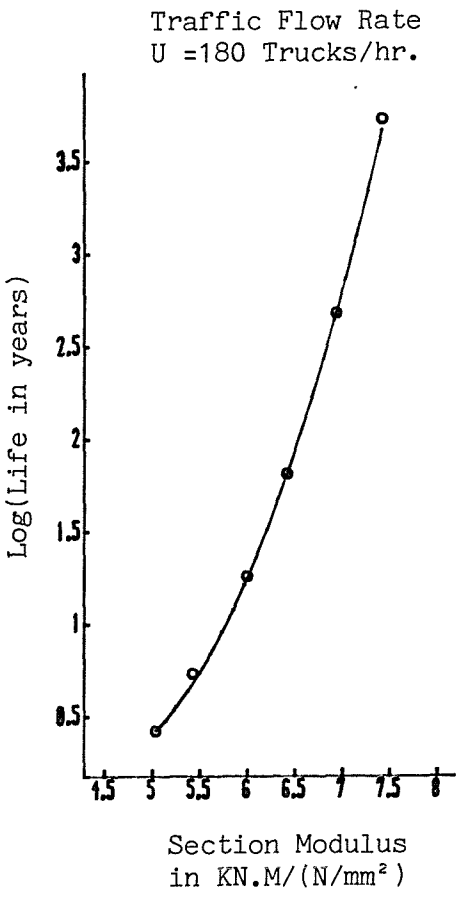

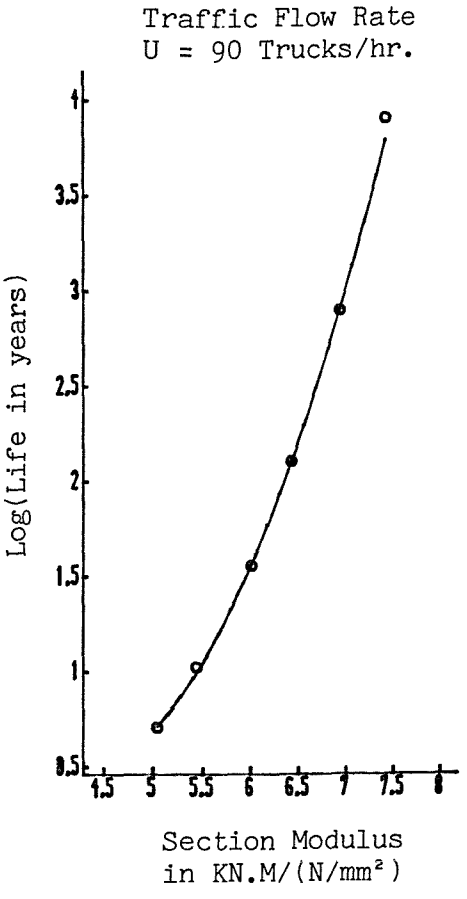

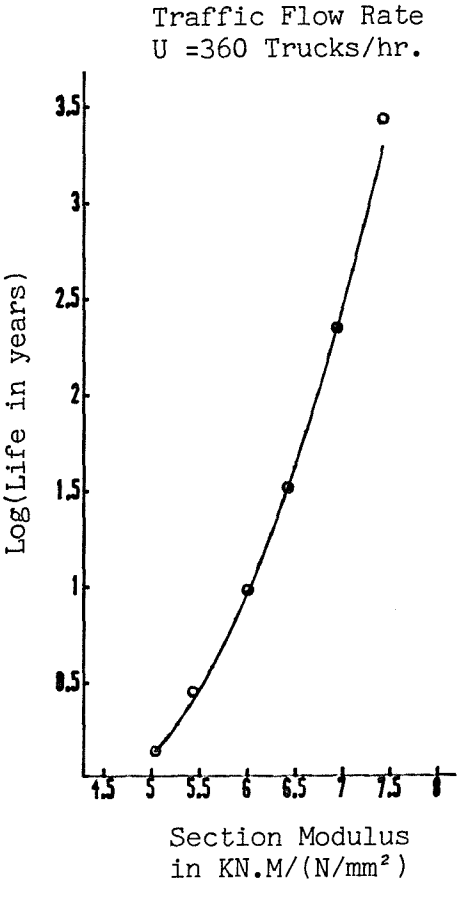

Figure (2)

Section Modulus (F_L) - Log(Life)
Curve for Span = 17.5 m
Bar dia = 32 mm

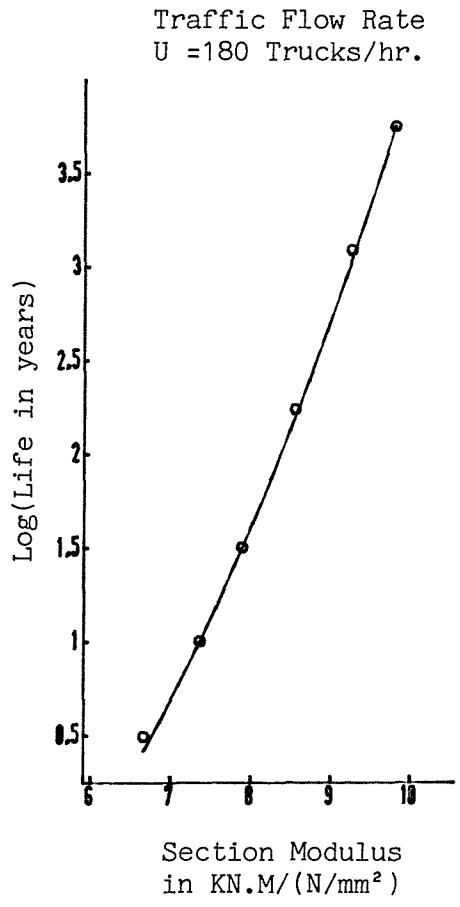

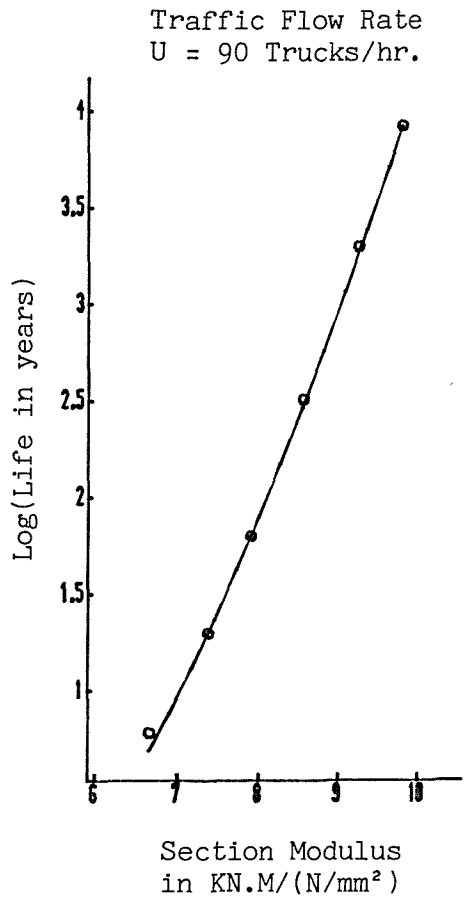

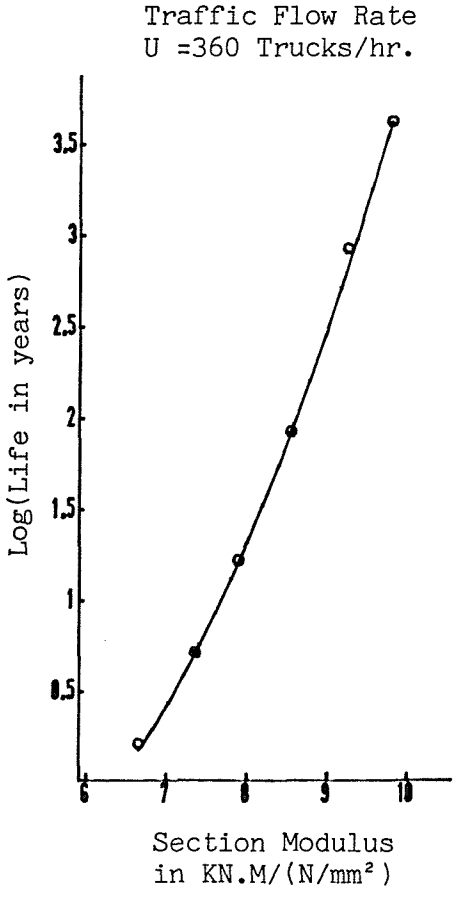

Figure (3)

Section Modulus (F_L) - Log(Life)
Curve for Span = 20.0 m
Bar dia = 32 mm

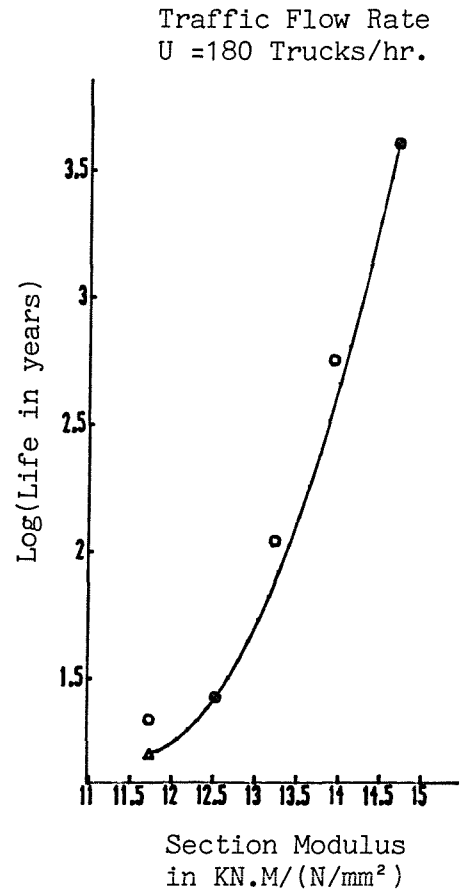

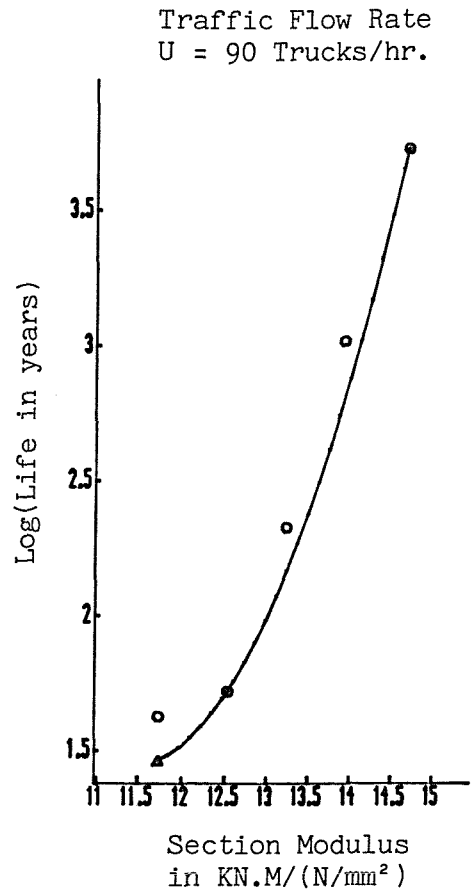

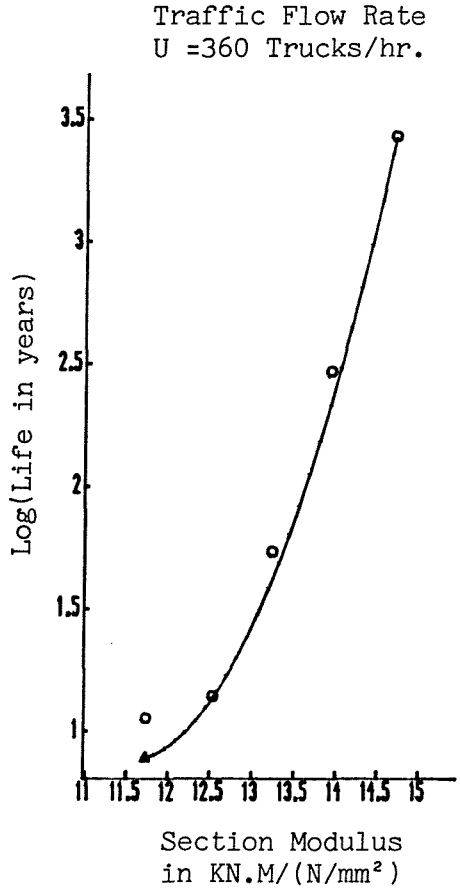

Figure (4)

Section Modulus (F_L) - Log(Life)
Curve for Span = 25.0 m
Bar dia = 32 mm

o represents original points
Δ represents weighted points

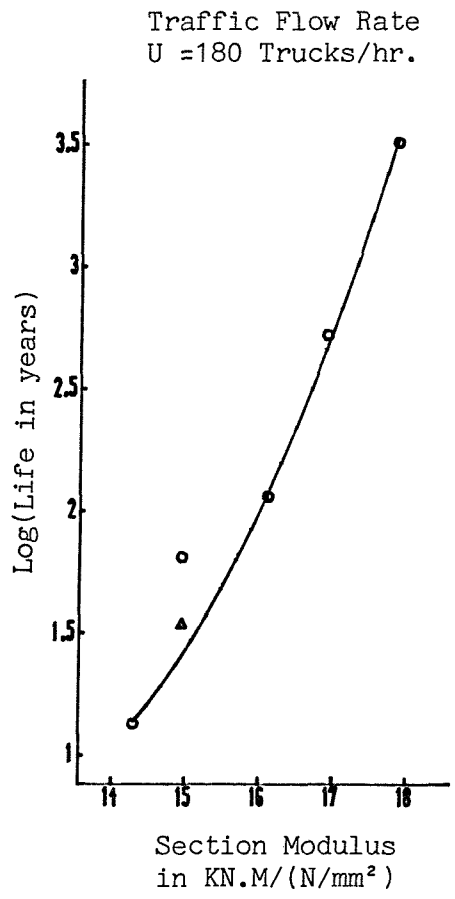

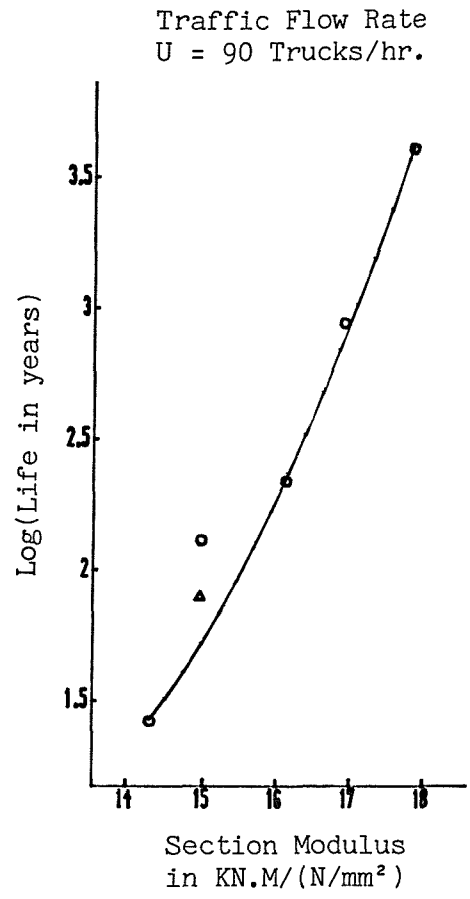

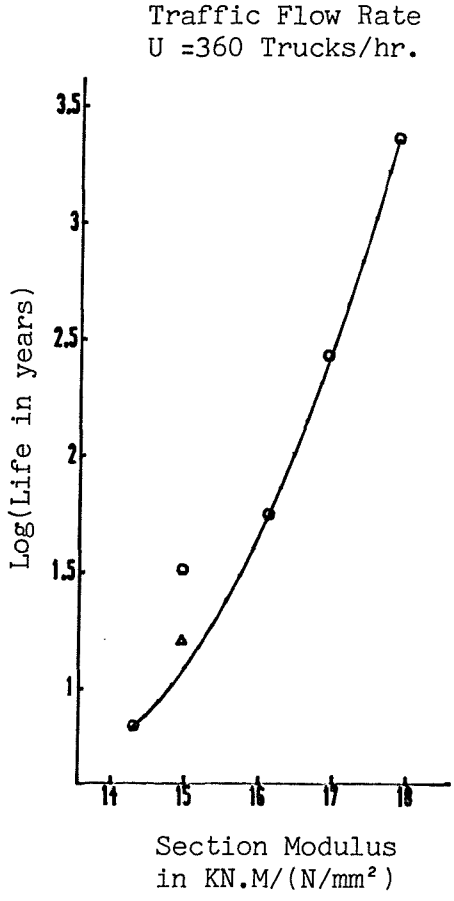

Figure (5)

Section Modulus (F_L) - Log(Life)
Curve for Span = 27.5 m
Bar dia = 32 mm

o represents original points
Δ represents weighted points

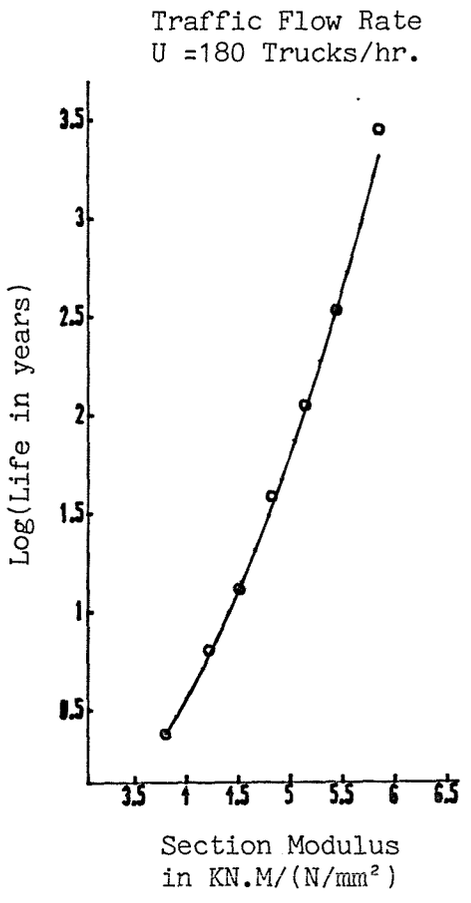

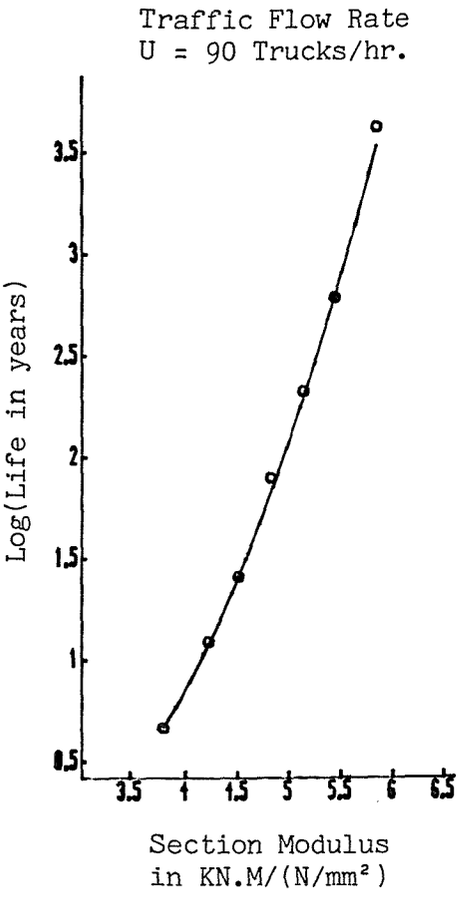

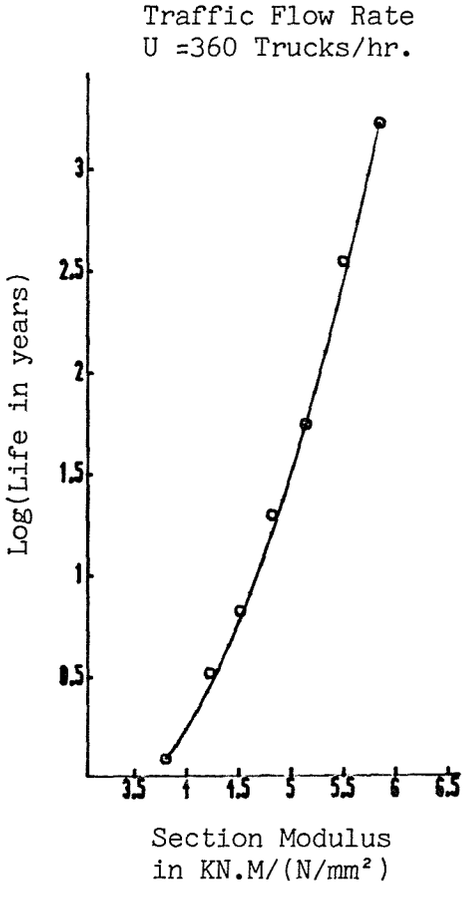

Figure (6)

Section Modulus (F_L) - Log(Life)
Curve for Span = 15.0 m
Bar dia = 25 mm

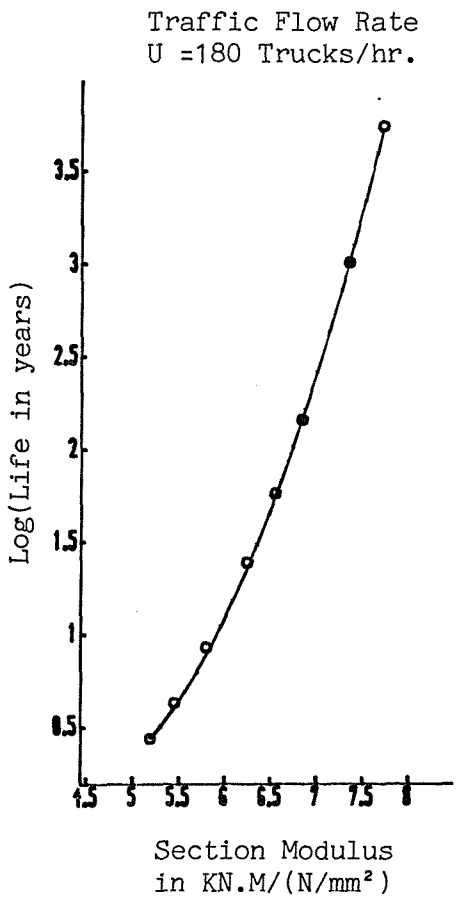

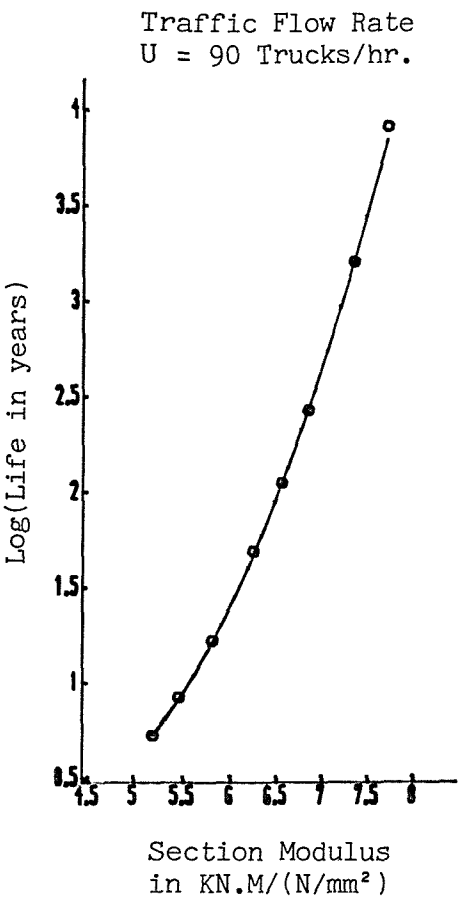

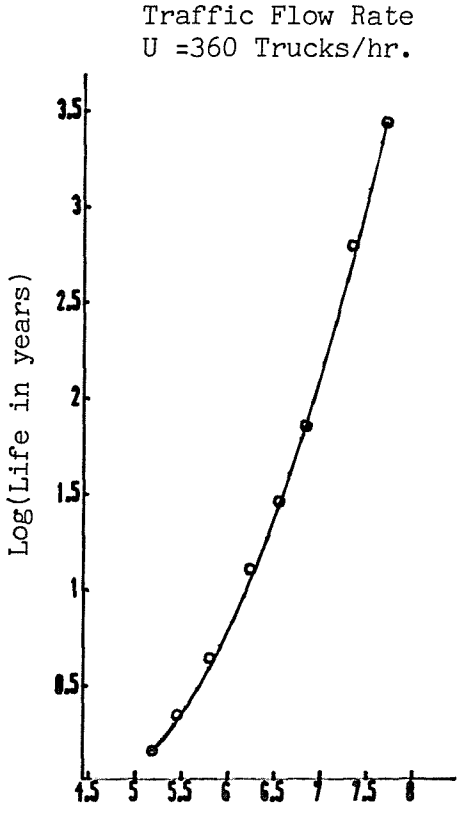

Figure (7)

Section Modulus (F_L) - Log(Life)
Curve for Span = 17.5 m
Bar dia = 25 mm

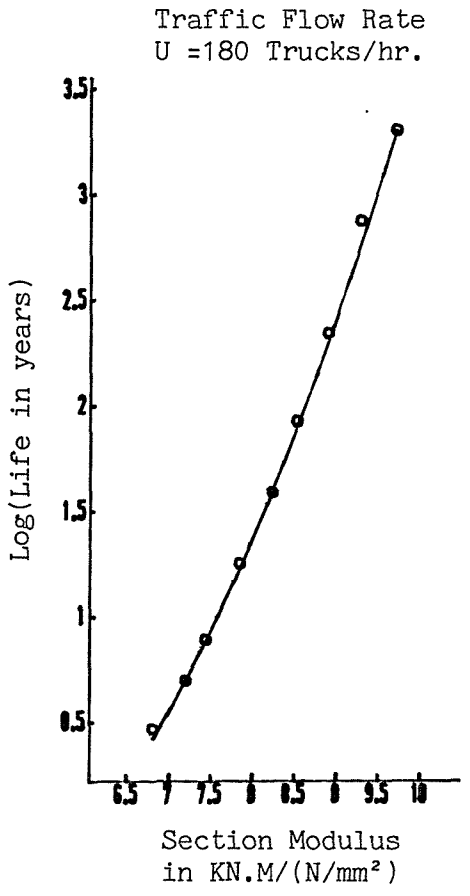

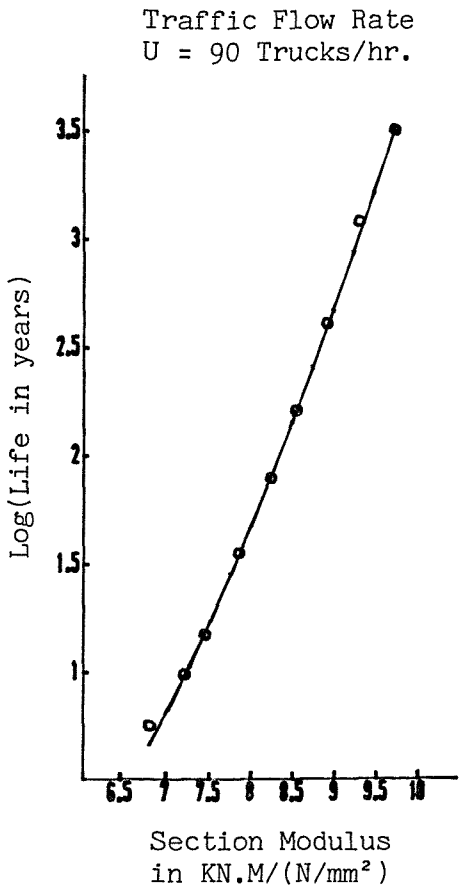

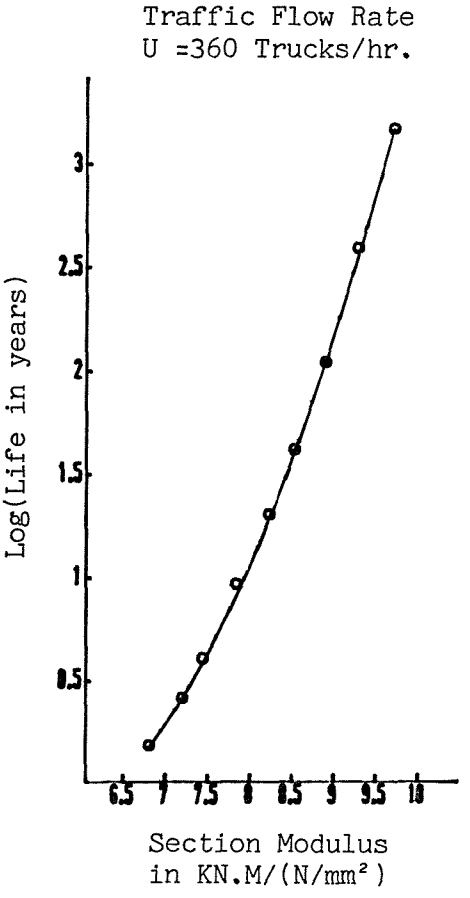

Figure (8)

Section Modulus (F_L) - Log(Life)
Curve for Span = 20.0 m
Bar dia = 25 mm

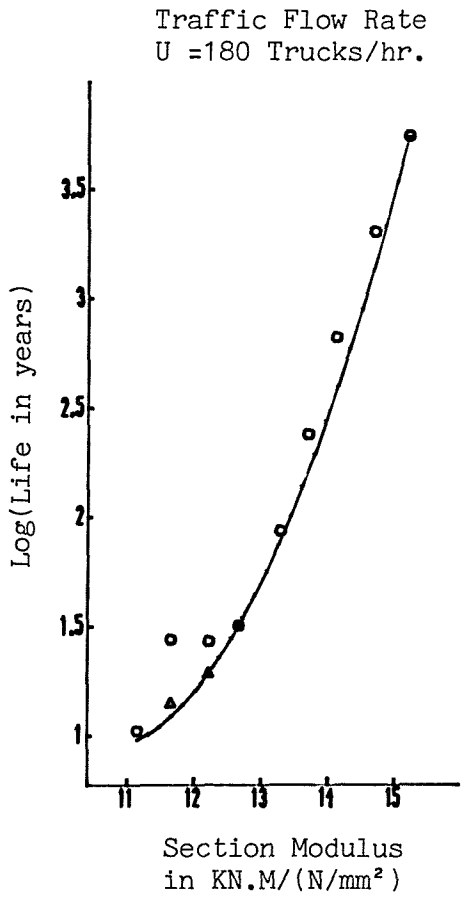

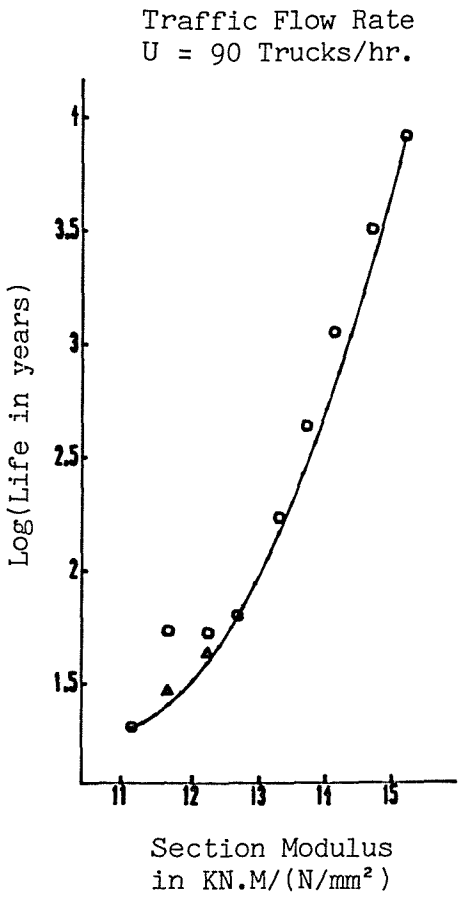

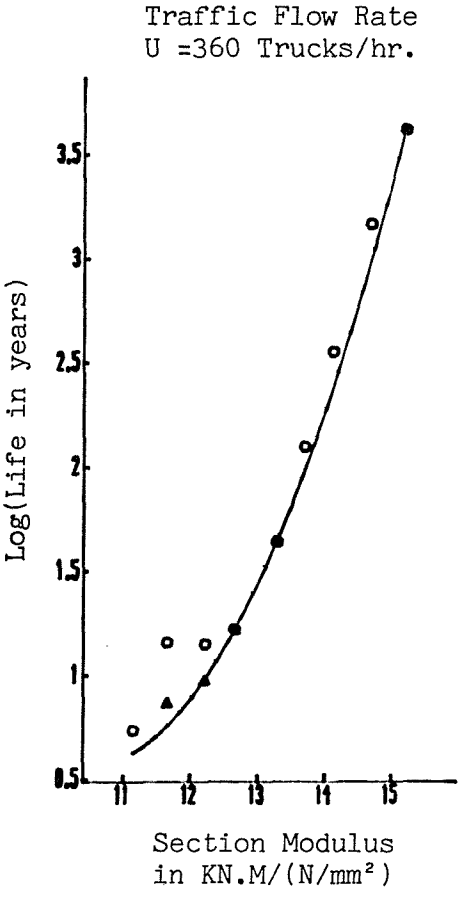

Figure (9)

Section Modulus (F_L) - Log(Life)
Curve for Span = 25.0 m
Bar dia = 25 mm

o represents original points
Δ represents weighted points

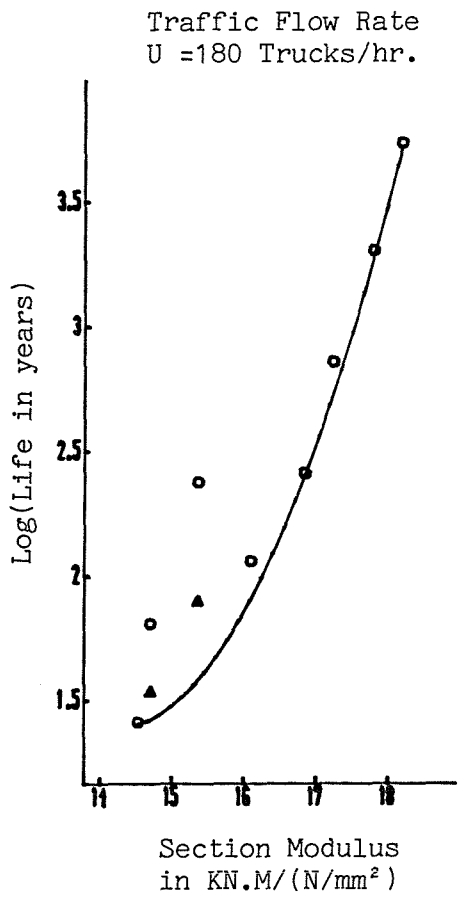

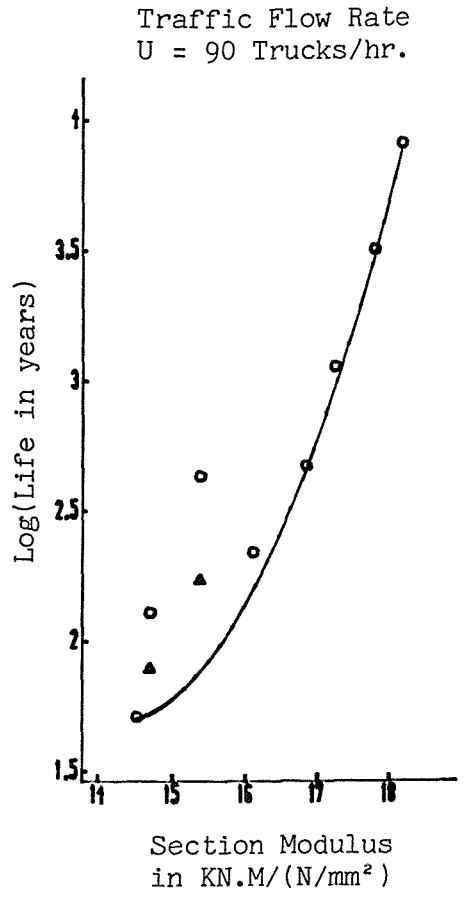

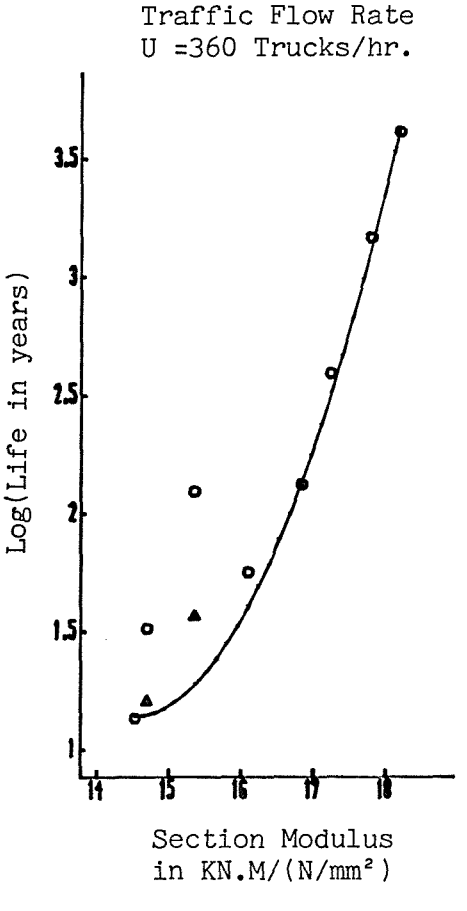

Figure (10)

Section Modulus (F_L) - Log(Life)
Curve for Span = 27.5 m
Bar dia = 25 mm

o represents original points
Δ represents weighted points

Table (1) - Bridge fatigue lives for loading frequency, U = 90 T/hr.
Bar dia = 32 mm

section number	section modulus F_L KN.M/(N/mm²)	fatigue life in years		centroidal and outer bar simulated stresses (N/mm²)		outer bar stress range (N/mm²)	fatigue limit (N/mm²)	total number of cycles and effective cycles, per week		Log(life)_m
		$(\text{life})_m$	$(\text{life})_n$	f_{ss}	f_{sse}	S_{re}	S_e	N_c	N_{ec}	
110	3.71	4.29	4.31	365.9	373.1	143.83	85.83	25227	3198	0.632
111	4.18	11.98	12.04	325.0	343.3	135.40	92.89	25227	1191	1.078
112	4.56	37.82	37.95	303.7	333.1	137.43	96.92	25227	391	1.578
113	4.86	124.11	124.36	287.3	313.1	127.93	100.38	25227	122	2.094
114	5.45	1124.85	1125.46	258.6	286.3	115.97	105.30	25227	14	3.051

Table (1a) - Bridge fatigue lives
L = 15.0 m, U = 90 T/hr., dia = 32 mm

section number	section modulus F_L KN.M/(N/mm²)	fatigue life in years		centroidal and outer bar simulated stresses (N/mm²)		outer bar stress range (N/mm²)	fatigue limit (N/mm²)	total number of cycles and effective cycles, per week		Log(life)_m
		$(\text{life})_m$	$(\text{life})_n$	f_{ss}	f_{sse}	S_{re}	S_e	N_c	N_{ec}	
21	5.04	5.09	5.10	381.1	386.2	139.70	80.16	14583	2831	0.707
22	5.43	10.54	10.58	347.3	352.0	126.25	87.02	14583	1369	1.023
23	6.00	36.01	36.11	316.4	340.5	131.12	92.40	14583	416	1.556
24	6.42	126.96	127.18	299.7	323.4	124.13	95.73	14583	121	2.104
25	6.94	783.60	784.28	275.8	301.1	116.12	100.45	14583	20	2.894
26	7.43	7962.14	7962.30	261.9	284.6	108.13	103.26	14583	2	3.901

Table (1b) - Bridge fatigue lives
L = 17.5 m, U = 90 T/hr., dia = 32 mm

section number	section modulus F_L KN.M/(N/mm²)	fatigue life in years		centroidal and outer bar simulated stresses (N/mm²)		outer bar stress range (N/mm²)	fatigue limit (N/mm²)	total number of cycles and effective cycles, per week		Log(life)_m
		$(\text{life})_m$	$(\text{life})_n$	f_{ss}	f_{sse}	S_{re}	S_e	N_c	N_{ec}	
31	6.66	6.06	6.07	388.5	392.5	133.47	76.03	14610	2472	0.782
32	7.36	19.80	19.84	352.3	355.4	118.88	83.46	14610	752	1.297
33	7.89	63.06	63.19	325.8	340.7	120.55	88.87	14610	242	1.800
34	8.55	321.82	322.24	301.7	322.0	115.56	93.39	14610	48	2.508
35	9.26	1980.40	1981.51	280.6	302.2	107.67	97.32	14610	8	3.297
36	9.81	8335.86	8336.01	263.0	285.60	102.49	101.08	14610	2	3.921

Table (1c) - Bridge fatigue lives
L = 20.0 m, U = 90 T/hr., dia = 32 mm

section number	section modulus F_L KN.M/(N/mm²)	fatigue life in years		centroidal and outer bar simulated stresses (N/mm²)		outer bar stress range (N/mm²)	fatigue limit (N/mm²)	total number of cycles and effective cycles, per week		Log(life)_m
		$(\text{life})_m$	$(\text{life})_n$	f_{ss}	f_{sse}	S_{re}	S_e	N_c	N_{ec}	
42	11.73	42.36	42.45	380.8	384.0	105.40	69.56	14584	357	1.627
43	12.53	52.53	52.55	355.4	358.4	96.75	75.17	14584	303	1.720
44	13.23	212.98	213.16	333.6	341.6	95.28	80.22	14584	73	2.328
45	13.93	1039.78	1040.51	314.0	330.7	98.35	84.84	14584	15	3.017
46	14.70	5380.01	5381.03	296.2	313.7	93.70	88.90	14584	3	3.731

Table (1d) - Bridge fatigue lives
L = 25.0 m, U = 90 T/hr., dia = 32 mm

section number	section modulus F_L KN.M/(N/mm²)	fatigue life in years		centroidal and outer bar simulated stresses (N/mm²)		outer bar stress range (N/mm²)	fatigue limit (N/mm²)	total number of cycles and effective cycles, per week		Log(life)_m
		$(\text{life})_m$	$(\text{life})_n$	f_{ss}	f_{sse}	S_{re}	S_e	N_c	N_{ec}	
52	14.30	26.42	26.47	397.4	400.5	98.89	61.97	14597	571	1.422
53	14.95	129.98	130.15	373.1	375.7	93.75	68.47	14597	118	2.114
54	16.11	218.61	218.65	349.5	351.9	85.29	73.52	14597	75	2.340
55	16.91	877.44	877.84	330.9	340.7	87.52	77.94	14597	18	2.943
56	17.85	4063.07	4063.84	313.4	327.5	86.69	82.04	14597	4	3.609

Table (1e) - Bridge fatigue lives
L = 27.5 m, U = 90 T/hr., dia = 32 mm

Table (2) - Bridge fatigue lives for loading frequency, U = 180 T/hr.
Bar dia = 32 mm

section number	section modulus F_L KN.M/(N/mm²)	fatigue life in years		centroidal and outer bar simulated stresses (N/mm²)		outer bar stress range (N/mm²)	fatigue limit (N/mm²)	total number of cycles and effective cycles, per week		Log(life)_m
		$(\text{life})_m$	$(\text{life})_n$	f_{ss}	f_{sse}	S_{re}	S_e	N_c	N_{ec}	
110	3.71	2.23	2.24	365.9	373.1	143.83	85.83	48778	6140	0.348
111	4.18	6.18	6.21	325.0	343.3	135.40	92.89	48778	2300	0.791
112	4.56	18.66	18.72	303.7	333.1	137.43	96.92	48778	794	1.271
113	4.86	61.82	61.93	287.3	313.1	127.93	100.38	48778	247	1.791
114	5.45	689.92	690.29	258.6	286.3	115.97	105.30	48778	23	2.839

Table (2a) - Bridge fatigue lives
L = 15.0 m, U = 180 T/hr., dia = 32 mm

section number	section modulus F_L KN.M/(N/mm²)	fatigue life in years		centroidal and outer bar simulated stresses (N/mm²)		outer bar stress range (N/mm²)	fatigue limit (N/mm²)	total number of cycles and effective cycles, per week		Log(life)_m
		$(\text{life})_m$	$(\text{life})_n$	f_{ss}	f_{sse}	S_{re}	S_e	N_c	N_{ec}	
21	5.04	2.64	2.65	381.1	386.2	139.70	80.16	28258	5449	0.422
22	5.43	5.40	5.42	347.3	352.0	126.25	87.02	28258	2669	0.732
23	6.00	18.13	18.18	316.4	340.5	131.12	92.40	28258	827	1.258
24	6.42	64.74	64.83	299.7	323.4	124.13	95.73	28258	239	1.811
25	6.94	477.22	477.61	275.8	301.1	116.12	100.45	28258	33	2.679
26	7.43	5319.50	5319.59	261.9	284.6	108.13	103.26	28258	3	3.726

Table (2b) - Bridge fatigue lives
L = 17.5 m, U = 180 T/hr., dia = 32 mm

section number	section modulus F_L KN.M/(N/mm²)	fatigue life in years		centroidal and outer bar simulated stresses (N/mm²)		outer bar stress range (N/mm²)	fatigue limit (N/mm²)	total number of cycles and effective cycles, per week		Log(life)_m
		$(\text{life})_m$	$(\text{life})_n$	f_{ss}	f_{sse}	S_{re}	S_e	N_c	N_{ec}	
31	6.66	3.12	3.12	388.5	392.5	133.47	76.03	28360	4803	0.494
32	7.36	10.04	10.07	352.3	355.4	118.88	83.46	28360	1482	1.002
33	7.89	31.86	31.91	325.8	340.7	120.55	88.87	28360	480	1.503
34	8.55	172.88	173.08	301.7	322.0	115.56	93.39	28360	90	2.238
35	9.26	1224.34	1224.97	280.6	302.2	107.67	97.32	28360	13	3.088
36	9.81	5568.56	5568.64	263.0	285.6	102.49	101.08	28360	3	3.746

Table (2c) - Bridge fatigue lives
L = 20.0 m, U = 180 T/hr., dia = 32 mm

section number	section modulus F_L KN.M/(N/mm²)	fatigue life in years		centroidal and outer bar simulated stresses (N/mm²)		outer bar stress range (N/mm²)	fatigue limit (N/mm²)	total number of cycles and effective cycles, per week		Log(life)_m
		$(\text{life})_m$	$(\text{life})_n$	f_{ss}	f_{sse}	S_{re}	S_e	N_c	N_{ec}	
42	11.73	21.76	21.80	380.8	384.0	105.40	69.56	28275	695	1.338
43	12.53	26.59	26.60	355.4	358.4	96.75	75.17	28275	599	1.425
44	13.23	110.00	110.08	333.6	341.6	95.28	80.22	28275	142	2.041
45	13.93	563.07	563.45	314.0	330.7	98.35	84.84	28275	28	2.751
46	14.70	4021.85	4022.45	296.2	313.7	93.70	88.90	28275	4	3.604

Table (2d) - Bridge fatigue lives
L = 25.0 m, U = 180 T/hr., dia = 32 mm

section number	section modulus F_L KN.M/(N/mm²)	fatigue life in years		centroidal and outer bar simulated stresses (N/mm²)		outer bar stress range (N/mm²)	fatigue limit (N/mm²)	total number of cycles and effective cycles, per week		Log(life)_m
		$(\text{life})_m$	$(\text{life})_n$	f_{ss}	f_{sse}	S_{re}	S_e	N_c	N_{ec}	
52	14.30	13.45	13.48	397.4	400.5	98.89	61.97	28279	1122	1.129
53	14.95	64.81	64.89	373.1	375.7	93.75	68.47	28279	238	1.812
54	16.11	114.86	114.88	349.5	351.9	85.29	73.52	28279	143	2.060
55	16.91	527.52	527.74	330.9	340.7	87.52	77.94	28279	30	2.722
56	17.85	3236.48	3237.03	313.4	327.5	86.69	82.04	28279	5	3.510

Table (2e) - Bridge fatigue lives
L = 27.5 m, U = 180 T/hr., dia = 32 mm

Table (3) - Bridge fatigue lives for loading frequency, U = 360 T/hr.
Bar dia = 32 mm

section number	section modulus F_L KN.M/(N/mm²)	fatigue life in years		centroidal and outer bar simulated stresses (N/mm²)		outer bar stress range (N/mm²)	fatigue limit (N/mm²)	total number of cycles and effective cycles, per week		Log(life)$_m$
		(life)$_m$	(life)$_n$	f_{ss}	f_{sse}	S_{re}	S_e	N_c	N_{ec}	
12	3.71	1.17	1.18	374.3	382.2	152.94	85.83	92338	11669	0.068
13	4.18	3.20	3.21	332.5	344.7	136.84	92.89	92338	4439	0.505
14	4.56	9.78	9.81	310.5	340.1	144.41	96.92	92338	1510	0.990
15	4.86	31.47	31.53	293.7	320.1	134.92	100.38	92338	484	1.498
16	5.45	330.44	330.66	264.3	292.6	122.30	105.30	92338	48	2.519
*17	5.84	15701.6	15701.6	250.0	275.2	113.51	108.14	92338	1	4.196

Table (3a) - Bridge fatigue lives
L = 15.0 m, U = 360 T/hr., dia = 32 mm

*deleted point

section number	section modulus F_L KN.M/(N/mm²)	fatigue life in years		centroidal and outer bar simulated stresses (N/mm²)		outer bar stress range (N/mm²)	fatigue limit (N/mm²)	total number of cycles and effective cycles, per week		Log(life)_m
		$(\text{life})_m$	$(\text{life})_n$	f_{ss}	f_{sse}	S_{re}	S_e	N_c	N_{ec}	
21	5.04	1.386	1.390	381.1	386.2	139.70	80.16	53581	10362	0.142
22	5.43	2.82	2.83	347.3	352.0	126.25	87.02	53581	5105	0.450
23	6.00	9.55	9.57	316.4	340.5	131.12	92.40	53581	1566	0.980
24	6.42	32.55	32.59	299.7	323.4	124.13	95.73	53581	475	1.513
25	6.94	221.28	221.44	275.8	301.1	116.12	100.45	53581	72	2.345
26	7.43	2690.95	2691.11	261.9	284.6	108.13	103.26	5381	6	3.430

Table (3b) - Bridge fatigue lives
L = 17.5 m, U = 360 T/hr., dia = 32 mm

section number	section modulus F_L KN.M/(N/mm²)	fatigue life in years		centroidal and outer bar simulated stresses (N/mm²)		outer bar stress range (N/mm²)	fatigue limit (N/mm²)	total number of cycles and effective cycles, per week		Log(life)_m
		$(\text{life})_m$	$(\text{life})_n$	f_{ss}	f_{sse}	S_{re}	S_e	N_c	N_{ec}	
31	6.66	1.64	1.64	388.5	392.5	133.47	76.03	54018	9147	0.215
32	7.36	5.18	5.19	352.3	355.4	118.88	83.46	54018	2875	0.714
33	7.89	16.65	16.68	325.8	340.7	120.55	88.87	54018	916	1.221
34	8.55	84.56	84.64	301.7	322.0	115.56	93.39	54018	185	1.927
35	9.26	839.12	839.54	280.6	302.2	107.67	97.32	54018	19	2.924
36	9.81	4184.38	4184.43	263.0	285.6	102.49	101.08	54018	4	3.622

Table (3c) - Bridge fatigue lives
L = 20.0 m, U = 360 T/hr., dia = 32 mm

section number	section modulus F_L KN.M/(N/mm²)	fatigue life in years		centroidal and outer bar simulated stresses (N/mm²)		outer bar stress range (N/mm²)	fatigue limit (N/mm²)	total number of cycles and effective cycles, per week		Log(life)_m
		$(\text{life})_m$	$(\text{life})_n$	f_{ss}	f_{sse}	S_{re}	S_e	N_c	N_{ec}	
42	11.73	11.32	11.34	380.8	384.0	105.40	69.56	53611	1336	1.054
43	12.53	13.91	13.92	355.4	358.4	96.75	75.17	53611	1145	1.143
44	13.23	54.01	54.05	333.6	341.6	95.28	80.22	53611	290	1.732
45	13.93	294.47	294.63	314.0	330.7	98.35	84.84	53611	54	2.469
46	14.70	2686.89	2687.20	296.2	313.7	93.70	88.90	53611	6	3.429

Table (3d) - Bridge fatigue lives
L = 25.0 m, U = 360 T/hr., dia = 32 mm

section number	section modulus F_L KN.M/(N/mm²)	fatigue life in years		centroidal and outer bar simulated stresses (N/mm²)		outer bar stress range (N/mm²)	fatigue limit (N/mm²)	total number of cycles and effective cycles, per week		Log(life)$_m$
		(life)$_m$	(life)$_n$	f_{ss}	f_{sse}	S_{re}	S_e	N_c	N_{ec}	
52	14.30	6.94	6.96	397.4	400.5	98.89	61.97	53636	2174	0.841
53	14.95	32.64	32.67	373.1	375.7	93.75	68.47	53636	473	1.514
54	16.11	56.17	56.18	349.5	351.9	85.29	73.52	53636	293	1.750
55	16.91	270.08	270.17	330.9	340.7	87.52	77.94	53636	59	2.431
56	17.85	2310.33	2310.63	313.4	327.5	86.69	82.04	53636	7	3.364

Table (3e) - Bridge fatigue lives
L = 27.5 m, U = 360 T/hr., dia = 32 mm

Table (4) - Bridge fatigue lives for loading frequency, U = 90 T/hr.
Bar dia = 25 mm

section number	section modulus F_L KN.M/(N/mm²)	fatigue life in years		centroidal and outer bar simulated stresses (N/mm²)		outer bar stress range (N/mm²)	fatigue limit (N/mm²)	total number of cycles and effective cycles, per week		$Log(life)_m$
		$(life)_m$	$(life)_n$	f_{ss}	f_{sse}	S_{re}	S_e	N_c	N_{ec}	
127	3.80	4.61	4.63	354.1	362.1	137.11	87.22	25227	2976	0.664
128	4.22	12.33	12.39	328.7	343.6	131.38	91.47	25227	1164	1.091
129	4.51	25.74	25.84	307.3	340.3	139.15	95.10	25227	568	1.411
130	4.82	78.98	79.18	290.1	320.5	130.94	98.80	25227	190	1.898
131	5.14	210.39	210.71	272.5	304.9	124.35	101.84	25227	73	2.323
132	5.44	605.37	605.94	257.1	290.9	118.93	104.71	25227	26	2.782
133	5.85	4163.92	4163.98	243.2	273.2	109.50	107.45	25227	4	3.620

Table (4a) - Bridge fatigue lives
L = 15.0 m, U = 90 T/hr., dia = 25 mm

section number	section modulus F_L KN.M/(N/mm²)	fatigue life in years		centroidal and outer bar simulated stresses (N/mm²)		outer bar stress range (N/mm²)	fatigue limit (N/mm²)	total number of cycles and effective cycles, per week		$Log(life)_m$
		$(life)_m$	$(life)_n$	f_{ss}	f_{sse}	S_{re}	S_e	N_c	N_{ec}	
211	5.19	5.32	5.33	365.9	373.1	131.01	81.57	14583	2704	0.726
212	5.45	8.41	8.43	345.8	352.1	122.49	85.73	14583	1704	0.925
213	5.80	16.71	16.76	326.2	343.6	124.21	89.13	14583	877	1.223
214	6.24	49.04	49.16	308.8	339.0	130.12	92.56	14583	308	1.691
215	6.55	111.74	111.94	293.3	325.2	125.25	95.47	14583	137	2.048
216	6.84	267.75	268.12	279.3	312.6	121.05	98.27	14583	58	2.428
217	7.35	1598.96	1599.86	265.2	294.7	111.92	101.14	14583	10	3.204
218	7.72	8082.95	8083.11	252.7	283.2	107.39	103.49	14583	2	3.908

Table (4b) - Bridge fatigue lives
L = 17.5 m, U = 90 T/hr., dia = 25 mm

section number	section modulus F_L KN.M/(N/mm²)	fatigue life in years		centroidal and outer bar simulated stresses (N/mm²)		outer bar stress range (N/mm²)	fatigue limit (N/mm²)	total number of cycles and effective cycles, per week		Log(life)_m
		$(\text{life})_m$	$(\text{life})_n$	f_{ss}	f_{sse}	S_{re}	S_e	N_c	N_{ec}	
311	6.81	5.70	5.71	384.7	390.8	127.37	74.55	14610	2728	0.756
312	7.20	9.84	9.86	363.2	368.5	118.56	79.00	14610	1522	0.993
313	7.44	15.01	15.04	346.5	351.4	113.27	82.93	14610	995	1.176
314	7.84	35.63	35.70	329.3	342.6	114.87	86.36	14610	423	1.552
315	8.23	79.19	79.35	314.0	340.2	121.36	89.30	14610	193	1.899
316	8.53	162.53	162.79	300.8	329.2	118.96	92.10	14610	95	2.211
317	8.90	409.18	409.68	288.3	317.9	114.89	94.48	14610	38	2.612
318	9.29	1205.07	1206.08	276.5	306.9	110.65	96.75	14610	13	3.081
319	9.72	3186.92	3188.02	265.9	297.2	106.62	98.60	14610	5	3.503

Table (4c) - Bridge fatigue lives
L = 20.0 m, U = 90 T/hr., dia = 25 mm

section number	section modulus F_L KN.M/(N/mm²)	fatigue life in years		centroidal and outer bar simulated stresses (N/mm²)		outer bar stress range (N/mm²)	fatigue limit (N/mm²)	total number of cycles and effective cycles, per week		$Log(life)_m$
		$(life)_m$	$(life)_n$	f_{ss}	f_{sse}	S_{re}	S_e	N_c	N_{ec}	
411	11.15	20.38	20.44	395.8	400.4	109.87	65.64	14584	730	1.309
412	11.65	54.09	54.20	378.5	382.8	104.06	69.53	14584	281	1.733
413	12.22	53.23	53.26	362.0	366.0	97.96	73.09	14584	305	1.726
414	12.66	63.21	63.23	346.8	350.3	93.51	76.79	14584	249	1.801
415	13.29	171.58	171.71	333.2	342.0	93.72	79.56	14584	91	2.234
416	13.70	434.89	435.31	320.7	339.4	100.37	82.66	14584	36	2.638
417	14.13	1124.80	1125.56	309.7	329.4	97.70	85.11	14584	14	3.051
418	14.70	3183.80	3184.67	299.5	319.9	94.49	87.12	14584	5	3.503
419	15.22	8206.29	8206.41	289.0	310.1	91.80	89.46	14584	2	3.914

Table (4d) - Bridge fatigue lives
L = 25.0 m, U = 90 T/hr., dia = 25 mm

section number	section modulus F_L KN.M/(N/mm²)	fatigue life in years		centroidal and outer bar simulated stresses (N/mm²)		outer bar stress range (N/mm²)	fatigue limit (N/mm²)	total number of cycles and effective cycles, per week		$Log(life)_m$
		$(life)_m$	$(life)_n$	f_{ss}	f_{sse}	S_{re}	S_e	N_c	N_{ec}	
512	14.53	51.19	51.28	388.6	392.7	94.98	63.26	14597	299	1.709
513	14.70	128.77	128.95	375.3	379.2	93.22	67.15	14597	119	2.110
514	15.36	432.98	433.40	360.4	363.9	88.23	70.52	14597	36	2.636
515	16.10	219.56	219.59	347.0	350.1	83.12	73.39	14597	75	2.342
516	16.84	469.81	469.91	334.3	341.9	83.36	76.20	14597	34	2.672
517	17.24	1131.76	1132.39	323.7	340.1	89.90	78.93	14597	14	3.054
518	17.80	3197.26	3198.01	313.6	331.1	87.89	81.21	14597	5	3.505
519	18.20	8143.54	8143.65	304.1	322.2	86.34	83.62	14597	2	3.911

Table (4e) - Bridge fatigue lives
L = 27.5 m, U = 90 T/hr., dia = 25 mm

Table (5) - Bridge fatigue lives for loading frequency, U = 180 T/hr.
Bar dia = 25 mm

section number	section modulus F_L KN.M/(N/mm²)	fatigue life in years		centroidal and outer bar simulated stresses (N/mm²)		outer bar stress range (N/mm²)	fatigue limit (N/mm²)	total number of cycles and effective cycles, per week		Log(life)_m
		$(\text{life})_m$	$(\text{life})_n$	f_{ss}	f_{sse}	S_{re}	S_e	N_c	N_{ec}	
127	3.80	2.39	2.40	354.1	362.1	137.11	87.22	48778	5731	0.378
128	4.22	6.38	6.40	328.7	343.6	131.38	91.47	48778	2242	0.805
129	4.51	13.04	13.09	307.3	340.3	139.15	95.10	48778	1119	1.115
130	4.82	38.47	38.56	290.1	320.5	130.94	98.80	48778	393	1.585
131	5.14	111.24	111.39	272.5	304.9	124.35	101.84	48778	139	2.046
132	5.44	337.80	338.07	257.1	290.9	118.93	104.71	48778	47	2.529
133	5.85	2783.25	2783.28	243.2	273.2	109.50	107.45	48778	6	3.445

Table (5a) - Bridge fatigue lives
L = 15.0 m, U = 180 T/hr., dia = 25 mm

section number	section modulus F_L KN.M/(N/mm²)	fatigue life in years		centroidal and outer bar simulated stresses (N/mm²)		outer bar stress range (N/mm²)	fatigue limit (N/mm²)	total number of cycles and effective cycles, per week		$Log(life)_m$
		$(life)_m$	$(life)_n$	f_{ss}	f_{sse}	S_{re}	S_e	N_c	N_{ec}	
211	5.19	2.75	2.76	365.9	373.1	131.01	81.57	28258	5223	0.439
212	5.45	4.27	4.28	345.8	352.1	122.49	85.73	28258	3359	0.630
213	5.80	8.52	8.55	326.2	343.6	124.21	89.13	28258	1717	0.930
214	6.24	24.29	24.34	308.8	339.0	130.12	92.56	28258	624	1.385
215	6.55	57.24	57.33	293.3	325.2	125.25	95.47	28258	269	1.758
216	6.84	142.44	142.61	279.3	312.6	121.05	98.27	28258	110	2.154
217	7.35	1003.44	1003.97	265.2	294.7	111.92	101.14	28258	16	3.001
218	7.72	5400.13	5400.22	252.7	283.2	107.39	103.49	28258	3	3.732

Table (5b) - Bridge fatigue lives
L = 17.5 m, U = 180 T/hr., dia = 25 mm

section number	section modulus F_L KN.M/(N/mm²)	fatigue life in years		centroidal and outer bar simulated stresses (N/mm²)		outer bar stress range (N/mm²)	fatigue limit (N/mm²)	total number of cycles and effective cycles, per week		Log(life)_m
		$(\text{life})_m$	$(\text{life})_n$	f_{ss}	f_{sse}	S_{re}	S_e	N_c	N_{ec}	
311	6.81	2.94	2.94	384.7	390.8	127.37	74.55	28360	5295	0.468
312	7.20	4.98	4.98	363.2	368.5	118.56	79.00	28360	3014	0.697
313	7.44	7.78	7.79	346.5	351.4	113.27	82.93	28360	1915	0.891
314	7.84	17.87	17.90	329.3	342.6	114.87	86.36	28360	845	1.252
315	8.23	38.92	38.98	314.0	340.2	121.36	89.30	28360	395	1.590
316	8.53	84.44	84.56	300.8	329.2	118.96	92.10	28360	184	1.927
317	8.90	220.87	221.12	288.3	317.9	114.89	94.48	28360	71	2.344
318	9.29	747.91	748.47	276.5	306.9	110.65	96.75	28360	21	2.874
319	9.72	2005.42	2006.02	265.9	297.2	106.62	98.60	28360	8	3.302

Table (5c) - Bridge fatigue lives
L = 20.0 m, U = 180 T/hr., dia = 25 mm

section number	section modulus F_L KN.M/(N/mm²)	fatigue life in years		centroidal and outer bar simulated stresses (N/mm²)		outer bar stress range (N/mm²)	fatigue limit (N/mm²)	total number of cycles and effective cycles, per week		Log(life)_m
		$(\text{life})_m$	$(\text{life})_n$	f_{ss}	f_{sse}	S_{re}	S_e	N_c	N_{ec}	
411	11.15	10.53	10.56	395.8	400.4	109.87	65.64	28275	1411	1.022
412	11.65	27.47	27.52	378.5	382.8	104.06	69.53	28275	554	1.439
413	12.22	27.01	27.03	362.0	366.0	97.96	73.09	28275	602	1.432
414	12.66	31.79	31.80	346.8	350.3	93.51	76.79	28275	495	1.502
415	13.29	86.23	86.29	333.2	342.0	93.72	79.56	28275	182	1.936
416	13.70	238.72	238.93	320.7	339.4	100.37	82.66	28275	66	2.378
417	14.13	659.99	660.40	309.7	329.4	97.70	85.11	28275	24	2.820
418	14.70	2003.42	2004.06	299.5	319.9	94.49	87.12	28275	8	3.302
419	15.22	5480.84	5480.90	289.0	310.1	91.80	89.46	28275	3	3.739

Table (5d) - Bridge fatigue lives
L = 25.0 m, U = 180 T/hr., dia = 25 mm

section number	section modulus F_L KN.M/(N/mm²)	fatigue life in years		centroidal and outer bar simulated stresses (N/mm²)		outer bar stress range (N/mm²)	fatigue limit (N/mm²)	total number of cycles and effective cycles, per week		Log(life)_m
		$(\text{life})_m$	$(\text{life})_n$	f_{ss}	f_{sse}	S_{re}	S_e	N_c	N_{ec}	
512	14.53	25.92	25.96	388.6	392.7	94.98	63.26	28279	591	1.414
513	14.70	64.47	64.55	375.3	379.2	93.22	67.15	28279	239	1.809
514	15.36	237.66	237.87	360.4	363.9	88.23	70.52	28279	66	2.376
515	16.10	114.53	114.54	347.0	350.1	83.12	73.39	28279	144	2.059
516	16.84	258.49	258.55	334.3	341.9	83.36	76.20	28279	62	2.412
517	17.24	720.45	720.81	323.7	340.1	89.90	78.93	28279	22	2.858
518	17.80	2009.64	2010.17	313.6	331.1	87.89	81.21	28279	8	3.303
519	18.20	5438.34	5438.40	304.1	322.2	86.34	83.62	28279	3	3.735

Table (5e) - Bridge fatigue lives
L = 27.5 m, U = 180 T/hr., dia = 25 mm

Table (6) - Bridge fatigue lives for loading frequency, U = 360 T/hr.
Bar dia = 25 mm

section number	section modulus F_L KN.M/(N/mm²)	fatigue life in years		centroidal and outer bar simulated stresses (N/mm²)		outer bar stress range (N/mm²)	fatigue limit (N/mm²)	total number of cycles and effective cycles, per week		Log(life)$_m$
		(life)$_m$	(life)$_n$	f_{ss}	f_{sse}	S_{re}	S_e	N_c	N_{ec}	
117	3.80	1.25	1.26	363.0	372.0	146.19	87.22	92338	10900	0.097
118	4.22	3.30	3.32	336.7	345.1	132.79	91.47	92338	4323	0.519
119	4.51	6.68	6.70	314.8	341.8	140.50	95.10	92338	2187	0.825
120	4.82	19.75	19.79	297.2	328.4	138.09	98.80	92338	764	1.296
121	5.14	55.36	55.44	279.0	312.2	131.13	101.84	92338	279	1.743
122	5.50	345.85	346.06	263.7	292.9	121.59	104.94	92338	46	2.539
123	5.85	1657.24	1657.64	248.7	279.4	115.48	107.45	92338	10	3.219

Table (6a) - Bridge fatigue lives
L = 15.0 m, U = 360 T/hr., dia = 25 mm

section number	section modulus F_L KN.M/(N/mm²)	fatigue life in years		centroidal and outer bar simulated stresses (N/mm²)		outer bar stress range (N/mm²)	fatigue limit (N/mm²)	total number of cycles and effective cycles, per week		$Log(life)_m$
		$(life)_m$	$(life)_n$	f_{ss}	f_{sse}	S_{re}	S_e	N_c	N_{ec}	
211	5.19	1.45	1.45	365.9	373.1	131.01	81.57	53581	9924	0.161
212	5.45	2.23	2.24	345.8	352.1	122.49	85.73	53581	6413	0.348
213	5.80	4.41	4.42	326.2	343.6	124.21	89.13	53581	3316	0.644
214	6.24	12.80	12.83	308.8	339.0	130.12	92.56	53581	1180	1.107
215	6.55	28.96	29.00	293.3	325.2	125.25	95.47	53581	531	1.462
216	6.84	71.54	71.62	279.3	312.6	121.05	98.27	53581	219	1.855
217	7.35	619.19	619.52	265.2	294.7	111.92	101.14	53581	26	2.792
218	7.72	2731.50	2731.66	252.7	283.2	107.39	103.49	53581	6	3.436

Table (6b) - Bridge fatigue lives
L = 17.5 m, U = 360 T/hr., dia = 25 mm

section number	section modulus F_L KN.M/(N/mm²)	fatigue life in years		centroidal and outer bar simulated stresses (N/mm²)		outer bar stress range (N/mm²)	fatigue limit (N/mm²)	total number of cycles and effective cycles, per week		$Log(life)_m$
		$(life)_m$	$(life)_n$	f_{ss}	f_{sse}	S_{re}	S_e	N_c	N_{ec}	
311	6.81	1.55	1.55	384.7	390.8	127.37	74.55	54018	10059	0.190
312	7.20	2.62	2.62	363.2	368.5	118.56	79.00	54018	5730	0.418
313	7.44	4.07	4.07	346.5	351.4	113.27	82.93	54018	3659	0.610
314	7.84	9.31	9.33	329.3	342.6	114.87	86.36	54018	1620	0.969
315	8.23	20.28	20.31	314.0	340.2	121.36	89.30	54018	756	1.307
316	8.53	41.63	41.68	300.8	329.2	118.96	92.10	54018	374	1.619
317	8.90	109.51	109.61	288.3	317.9	114.89	94.48	54018	144	2.039
318	9.29	387.93	388.19	276.5	306.9	110.65	96.75	54018	41	2.589
319	9.72	1457.45	1457.98	265.9	297.2	106.62	98.60	54018	11	3.164

Table (6c) - Bridge fatigue lives
L = 20.0 m, U = 360 T/hr., dia = 25 mm

section number	section modulus F_L KN.M/(N/mm²)	fatigue life in years		centroidal and outer bar simulated stresses (N/mm²)		outer bar stress range (N/mm²)	fatigue limit (N/mm²)	total number of cycles and effective cycles, per week		Log(life)_m
		$(\text{life})_m$	$(\text{life})_n$	f_{ss}	f_{sse}	S_{re}	S_e	N_c	N_{ec}	
411	11.15	5.46	5.47	395.8	400.4	109.87	65.64	53611	2724	0.737
412	11.65	14.38	14.40	378.5	382.8	104.06	69.53	53611	1057	1.158
413	12.22	14.09	14.10	362.0	366.0	97.96	73.09	53611	1154	1.149
414	12.66	16.56	16.56	346.8	350.3	93.51	76.79	53611	950	1.219
415	13.29	43.70	43.73	333.2	342.0	93.72	79.56	53611	359	1.640
416	13.70	124.43	124.52	320.7	339.4	100.37	82.66	53611	127	2.095
417	14.13	355.06	355.25	309.7	329.4	97.70	85.11	53611	45	2.550
418	14.70	1455.75	1456.18	299.5	319.9	94.49	87.12	53611	11	3.163
419	15.22	4117.64	4117.69	289.0	310.1	91.80	89.46	53611	4	3.615

Table (6d) - Bridge fatigue lives
L = 25.0 m, U = 360 T/hr., dia = 25 mm

section number	section modulus F_L KN.M/(N/mm²)	fatigue life in years		centroidal and outer bar simulated stresses (N/mm²)		outer bar stress range (N/mm²)	fatigue limit (N/mm²)	total number of cycles and effective cycles, per week		Log(life)$_m$
		(life)$_m$	(life)$_n$	f_{ss}	f_{sse}	S_{re}	S_e	N_c	N_{ec}	
512	14.53	13.58	13.60	388.6	392.7	94.98	63.26	53636	1127	1.133
513	14.70	32.53	32.57	375.3	379.2	93.22	67.15	53636	474	1.512
514	15.36	123.88	123.97	360.4	363.9	88.23	70.52	53636	127	2.093
515	16.10	56.17	56.17	347.0	350.1	83.12	73.39	53636	294	1.750
516	16.84	132.51	132.54	334.3	341.9	83.36	76.20	53636	121	2.122
517	17.24	389.90	390.07	323.7	340.1	89.90	78.93	53636	41	2.591
518	17.80	1461.25	1461.63	313.6	331.1	87.89	81.21	53636	11	3.165
519	18.20	4085.30	4085.34	304.1	322.2	86.34	83.62	53636	4	3.611

Table (6e) - Bridge fatigue lives
L = 27.5 m, U = 360 T/hr., dia = 25 mm

REFERENCES

1- British Standard, "Steel, concrete and composite bridges". BS5400, Code of practice for fatigue, part 10, 1980. pp 2-40.

2- British Standard, "Specifications for steel girder bridges". BS153, 1972.

3- A. Buch, "The damage sum in fatigue of structure components". Engineering Fracture Mechanics, Vol. 10, No. 2, 1978. pp 233-247.

4- G. Nordby, "Fatigue of concrete, a review of research". ACI Journal, Vol. 55, No. 12, August 1958. pp 191-219.

5- E. Krempl, "The influence of state of stress on low cycle fatigue of structural materials, a literature survey and interpretive report". ASTM STP 549, 1974. p46.

6- D. Raske and J. Morrow, "Mechanics of materials in low cycle fatigue testing". ASTM STP 465, 1969. pp 1-26.

7- L. Fryba, "Railway bridges subjected to traffic loads and their design for fatigue". Rail International, October 1980. pp 573-598.

8- M. Miner, "Cumulative damage in fatigue". Journal of Applied Mechanics, Vol. 12-3, Trans. ASME, Vol. 67, 1945. pp A-159-164.

9- K. Inoue and K. Nakagawa, "Energy criterion for low cycle fatigue on the basis of distributed element model". Journal of the Society of Materials and Science, Japan, Vol. 24, No. 266, November 1975. pp 1038-1043 (in Japanese).

10- S. Manson, J. Freche and C. Ensign, "Application of a double linear damage rule to cumulative fatigue". ASTM STP 415, Fatigue Crack Propagation, 1967. pp 384-412.

11- T. Bui-Quoc and A. Biron, "Order effect of strain applications in low-cycle cumulative fatigue at high temperatures". Transactions of the International Conference on Structural Mechanics in Reactor Technology, San Francisco, 1977, Volume L, L 912. pp 1-10.

12- D. Henry, "A theory of fatigue damage accumulation in steel". Transactions of the ASME, Vol. 77, August 1955. pp 913-918.

13- R. Gatts, "Application of a cumulative damage concept to fatigue". Journal of Basic Engineering, Transactions of the ASME, Series D, Vol. 83, December 1961. pp 529-540.

14- J. Hanson, "Design for fatigue". Handbook of Structural Concrete, Edited by Kong, Evans, Cohen and Roll, Chapter 16, Published by Pitman, 1983. p 35.

15- J. Murdock, "A critical review of research on fatigue of plain concrete". Engineering Experiment Station, University of Illinois, Urbana, Bulletin No. 475, 1965. p 25.

16- K. Gylltoft, K. Cederwall and L. Elfgren, "Fatigue strength of reinforced concrete structures". Nordisk Betong, No. 6, 1979. pp 27-32.

17- J. Murdock and C. Kesler, "Effect of range of stress on fatigue strength of plain concrete beams". ACI Journal, Vol. 55, No. 12, August 1958. pp 221-231.

18- J. McCall, "Probability of fatigue failure of plain concrete". ACI Journal, Vol. 55, No. 12, August 1958. pp 233-244.

19- J. Hanson, K. Burton and E. Hognestad, "Fatigue tests of reinforcing bars - effect of deformation pattern". Journal of the PCA Research and Development Laboratories, Vol. 10, No. 3, September 1968. pp 2-13.

20- J. Hanson, M. Somes and T. Helgason, "Investigation of design factors affecting fatigue strength of reinforcing bars - test program". Fatigue of Concrete, Abeles Symposium, ACI Publications, SP - 41, 1974. pp 71-105.

21- T. Helgason, J. Hanson, N. Somes, W. Gene Corley and E. Hognestad, "Fatigue strength of high-yield reinforcing bars". National Co-operative Highway Research Program, report No. 164, Transportation Research Board, Washington, D.C., 1976.

22- K. Waagaard, "Design recommendations for offshore concrete structures". Proc. Int. Ass. Bridge Struct., Eng. Colloq., Lausanne 1982, IABSE Rep. Vol. 37. pp 59-67.

23- British Standard, "Steel, concrete and composite bridges". BS5400, part 4, 1984. pp 8-16.

24- S. Cheng, "Low cycle fatigue in reinforced concrete beams". B.Sc. Dissertation, Civil Engineering Department, Southampton University, May 1986. p 70.

25- K. Stoodley, "Basic Statistical Techniques". Bradford University Press, 1974.

26- W. Hines and D. Montgomery, "Probability and Statistics". The Ronald Press Co., 1972.

27- S. Kuo, "Numerical Methods and Computers". Addison-Wesley, 1965.

28- J. Hammersley and D. Handscomb, "Monte Carlo Methods". Methuen and Co., 1964.

29- T. Newman and P. Odell. "The Generation of Random Variates". Griffin, 1971.

30- G. Mihram, "Simulation". Academic Press, 1972.

31- T. Naylor, J. Balinitfy, D. Burdick and K. Chu, "Computer Simulation Techniques". John Wiley and Sons, 1966.

32- B. Jansson, "Random Number Generators". Victor Pettersons Bokindustri Aktiebolag, 1966.

33- K. Tocher, "The Art of Simulation". The English Universities Press, 1963.

34- Nag Fortran Library Manual, "Random number generators". Vol. 6, G05.

35- C. Heins, "Field measurements and load spectra of highway bridges". Vol. 1, Proceedings of the National Structural Engineering Conference - Methods of Structural Analysis, ASCE, Madison, Wisconsin, August 1976. pp 133-152.

36- E. Charret and J. Webber, "The control of heavy vehicle loading on bridges". Australian Road Research Board Proceedings, Vol. 8, Session 31, 1976. pp 33-43.

37- C. Garson, G. Goble and F. Moses, "Traffic loading and its analytical and measured description". Speciality Conference, Safety and Reliability of Metal Structures, 1972. pp 27-53.

38- D. Harman and A. Davenport, "The formulation of vehicular loading for the design of highway bridges in Ontario". Ontario Joint Transportation and Communications Research Program, Project L-4, December 1976. p 79.

39- D. Harman and A. Davenport, "A statistical approach to traffic loading on highway bridges". Canadian Journal of Civil Engineering, Vol. 6, No. 4, December 1979. pp 494-513.

40- R. Garson and F. Moses, "Reliability design for fatigue under random loading". Speciality Conference, Safety and Reliability of Metal Structures, 1972. pp 399-426.

41- ICL 2900 Series Technical Publications, "Fortran Language", 1976.

42- Y. Fujino and M. Ito, "Probabilistic analysis of traffic live loading on highway bridges". Proceedings of the 3rd International Conference, Applications of Statistics and Probability in Soil and Structural Engineering, Sydney, January 1979. pp 539 - 550.

43- H. Neave, "Elementary Statistics Tables". G. Allen and Unwin, 1981.

44- C. Galambos, "International road federation in-depth study on fatigue fracture and stress corrosion problems of highway bridges". International Road Federation Research and Development, December 1972. pp 332-365.

45- The Committee on Loads and Forces on Bridges of the Committee on Bridges of the Structural Division, ASCE, "Recommended design loads for bridges". Journal of the Structural Division, Vol. 107, No. 7, July 1981. pp 1161 - 1213.

46- C. Reynolds and J. Steedman, "Reinforced concrete designer's handbook". Cement and Concrete Association, 1981.

47- F. Kong and R. Evans, "Reinforced and Prestressed Concrete". Nelson and Sons, 1980.

48- British Standards Institution, "The structural use of concrete". CP110 : Part 1 : 1972.

49- P. Hughes, "Limit State Theory for Reinforced Concrete Design". Pitman, 1976.

50- P. Watson and R. Rebbeck, "Modern methods of fatigue assessment". Railway Engineering Journal, Vol. 4, No. 6, November 1975. pp 10-23.

51- P. Watson and B. Dabell, "Cycle counting and fatigue damage". Journal of the Society of Environmental Engineers, September 1976. pp 3-8.

52- T. Endo, K. Mitsunaga, K. Takahashi, K. Kobayashi and M. Matsuishi, "Damage evaluation of metals for random or varying loading". Vol. 1, Proceedings of the Symposium on Mechanical Behaviour of Materials, Kyoto, August 1974. pp 371-380.

53- R. Stark and R. Nicholls, "Mathematical Foundations for Design". McGraw - Hill, 1972.

BIBILIOGRAPHY

1- M. Moroney, "Facts from Figures". Penguin Books, 1957.

2- J. Benjamin and C. Cornell, "Probability, Statistics and Decision for Civil Engineers". McGraw-Hill, 1970.

3- C. Chatfield, "Statistics for Technology". Chapman and Hall, 1978.

4- J. Bogdanoff and F. Kozin, "Probabilistic Models of Cumulative Damage". J. Wiley, 1985.

5- D. Blockley and E. Ellison, "A new technique for estimating systems uncertainty in design". Proc. I. Mech. E., Vol. 193, 1979. pp 159-168.

6- D. Blockley, "The Nature of Structural Design and Safety". Ellis Harwood, 1980.

7- A. Freudenthal, "Safety and the probability of structural failure". ASCE. Trans. Vol. 121, paper 2843, 1956. pp 1337-1375.

8- A. Pugsley, "The engineering climatology of structural accidents". Proc. Int. Conf. on Structural Safety and Reliability, Ed. by A. Freudenthal, 1969. pp 335-340.

9- A. Kraker, J. Tichler and A. Vrouwenvelder, "Safety, reliability and service life of structures". Heron, Vol. 27, No. 1, 1982. p 87.

10- T. Brondum-Nielsen, "Stress analysis of concrete sections under service load". ACI. Journal, Vol. 76, No. 2, Feb. 1979. pp 195-211.

11- S. Mirza, M. Hatzinikolas and J. MacGregor, "Statistical description of strength of concrete". ASCE. J. Struct. Div., Vol. 105, No. ST6 14628, June 1979. pp 1021-1037.

12- J. Costello and K. Chu, "Failure probabilities of reinforced concrete beams". ASCE. J. Struct. Div., Vol. 95, No. ST10 6848, Oct. 1969. pp 2281-2304.

13- R. Park and T. Paulay, "Reinforced Concrete Structures". J. Wiley, 1975.

14- P. Csagoly and R. Dorton, "Proposed Ontario bridge design load". RR 186, Research and Development Division, Ministry of Transportation and Communications, Ontario, Nov. 1973. p 32.

15- C. Michael Walton, C. Yu, P. Ng and S. Tobias, "An assessment of recent state truck size and weight studies". Research Report 241-4, Texas Univ., Austin, Texas State Department of Highways and Public Trans., Research Study 3-18-78-241, July 1982. p 164.

16- R. Wen, "Dynamic response of beams traversed by two-axle loads". ASCE. J. Eng. Mech. Div., Vol. 86, No. EM5 2624, Oct. 1960. pp 91-111.

17- J. Fenwick, "Bridge live loads for limit state design". Austr. Road Res. Board Proceedings, Vol. 8, Session 14, 1976. pp 32-36.

18- F. Moses, "Probabilistic approaches to bridge design loads". Transportation Research Record, No. 711, 1979. pp 14-23.

19- J. Buffington, D. Schafer and W. Adkins, "Procedures for estimating the total load experience of a highway as contributed by cargo vehicles". Texas Transportation Institute, Texas Highway Department, Research report 131-2F, Sept. 1970.

20- L. Fryba, "Estimation of fatigue life of railway bridges under traffic loads". J. Sound and Vibration, Vol. 70, No. 4, June 1980. pp 527-541.

21- J. Fisher and I. Viest, "Fatigue life of bridge beams subjected to controlled truck traffic". Congress Int. Assoc. Bridge and Struct. Eng., 7th, 1964. pp 497-510.

22- C. Schilling and K. Klippstein, "Fatigue of steel beams by simulated bridge traffic". ASCE. J. Struct. Div., Vol. 103, No. ST8 3123, Aug. 1977. pp 1561-1575.

23- B. Gerwick, "High-amplitude low-cycle fatigue in concrete sea structures". J. Prestressed Conc. Inst., Vol. 26. No. 5, 1981. pp 82-96.

24- H. Cornelissen, "Fatigue failure of concrete in tension". Heron, Vol. 29, No. 4, 1984. p 68.

25- T. Stelson and J. Cernica, "Fatigue properties of concrete beams". J. ACI. Title No. 55-15, Aug. 1958. pp 255-259.

26- T. Chang and C. Kesler, "Fatigue behaviour of reinforced concrete beams". J. ACI, Title No. 55-14, Aug. 1958. pp 245-254.

27- G. Kulkarni and S. Ng, "Behaviour of limited prestressed beams under repeated loads". Can. J. Civ. Eng., Vol. 6, 1979. pp 544-556.

28- R. Rowe, "An appreciation of the work carried out on fatigue in prestressed concrete structures". Cem. and Conc. Assoc., Magazine of Conc. Res., March 1957. pp 3-8.

29- S. Manson, A. Nachtigall and J. Freche, "A proposed new relation for cumulative fatigue damage in bending". ASTM. Proc., Vol. 61, 1961. pp 679-703.

30- S. Manson, A. Nachtigall, C. Ensign and J. Freche, "Further investigation of a relation for cumulative fatigue damage in bending". ASME. J. of Eng. for Industry, Vol. 87, 1965. pp 25-35.

31- S. Subramanyan, "A proposed relation for the estimation of reduction in fatigue limit". J. Inst. Eng. (India), Mech. Eng. Div., Vol. 59, pt. 6, May 1979. pp 282-286.

32- J. Spindel and E. Haibach, "The method of maximum likelihood applied to the statistical analysis of fatigue data". Int. J. Fatigue, Vol. 1, No. 2, April 1979. pp 81-88.

33- J. Schijve, "Aspects of aeronautical fatigue". AGARD Lect. Ser. No. 62, Fatigue life predic. for Aircr. struct. and mat., May 1973. p 23.

34- V. Matolcsy Matyas, "General fatigue problems of stochastically loaded (vehicle) structures". Material Pruf., Vol. 18, No. 4, April 1976. pp 115-122.

35- F. Cicci and P. Csagoly, "Assessment of the fatigue life of a steel girder bridge". RR 192, Ministry of Transp. and Communications, Ontario, Sept. 1974. p 29.

36- P. Wirsching and J. Kempert, "Design codes that fight fatigue". Machine Design, Vol. 48, No. 21, Sept. 1976. pp 108-113.

37- W. Kirkby, P. Forsyth and R. Maxwell, "Design against fatigue - current trends". Collect. of Tech. pap. - AIAA/R Aes/CASI/AAAF. Atl. Aeronaut. Conf., Williamsburg, Va., March 1979. pp 27-39.

38- I. Le May, "Symposium summary and an assessment of research progress in fatigue mechanisms". ASTM STP.675, Fatigue Mechanisms, Ed. by J. Fong, Symp. Kansas City, Mo., May 1978. pp 873-888.

39- J. Fong, "Direct observations - the essential ingredients for discovering fundamental mechanisms of fatigue". ASTM STP 675, Fatigue Mechanisms, Ed. by J. Fong, Symp. Kansas City, Mo., May 1978. pp 287-291.

40- J. Yao and M. Shinozuka, "Probabilistic structural design for repeated loads". Safety and Reliability of Metal Structures, Speciality Conf., 1972. pp 371-397.

41- A. Ang, "Probabilistic bases of safety, performance and design". Safety and Reliability of Metal Structures, Speciality Conf., 1972. pp 321-345.

42- P. Wirsching and J. Yao, "A probabilistic design approach using the Palmgren-Miner hypothesis". Proc. Nat. Struct. Eng. Conf., Methods of Struct. Analysis, ASCE, Vol. 2, Aug. 1976. pp 324-339.

43- S. Nishijima, "Property of scatter in fatigue test results of several metallic materials". Proc. Symp. on Mechanical Behaviour of Materials., Kyoto, Aug. 1974. pp 417-426.

44- J. Drapier, "Survey of activities in the field of low cycle high temperature fatigue - critical report". AGARD Rep. No. 618, 1974. p 144.

45- C. Garnier, G. Kowalczuk and R. Roche, "Low cycle fatigue of steels for nuclear pressure vessels in hot water". Int. Conf. on Struct. Mech. in React. Technol., 4th, Vol. L, Inelastic Analy. of Metal Struct., San Francisco, Aug. 1977. L 8/8 - p 9.

46- D. Sidey and L. Coffin, Jr., "Low-cycle fatigue damage mechanisms at high temperature". ASTM STP 675, Fatigue Mechanisms , Ed.by J. Fong, Symp. Kansas City, Mo., May 1978. pp 528-568.

47- J. Runkle and R. Pelloux, "Micromechanisms of low-cycle fatigue in nickel-based superalloys at elevated temperatures". ASTM STP 675, Fatigue Mechanisms, Ed. by J. Fong, Symp.Kansas City, Mo., May 1978. pp 501-527.

48- D. Broek and B. Leis, "Fatigue crack initiation and growth analysis for structures". Society of Automotive Engineers, prepr. No. 790511, 1979. p 12.

49- S. Rolfe, "Designing to prevent brittle fractures in bridges". Safety and Reliability of Metal Structures, Speciality Conference, 1972. pp 175 - 216.

50- A. Pickett and S. Grigory, "Prediction of the low cycle fatigue life of pressure vessels". ASME J. of Basic Eng., Vol. 89, Dec. 1967. pp 858-870.

51- W. Heath, L. Nicholls and W. Kirkby, "Practical applications of fracture mechanics techniques to aircraft structural problems". AGARD Conf. Proc. No. 221, London, Sept. 1976. p 22.

52- P. Paris and F. Erdogan, "A critical analysis of crack propagation laws". ASME J. of Basic Eng., Vol. 85, Dec. 1963. pp 528-534.

53- R. Forman and V. Kearney and R. Engle, "Numerical analysis of crack propagation in cyclic-loaded structures". ASME J. of Basic Eng., Sept. 1967. pp 459-464.

54- H. Wood, "The use of fracture mechanics principles in the design and analysis of damage tolerant aircraft structures". AGARD Lect. Ser. No. 62, Lecture 4, May 1973, p 13.

55- H. Wood, "A summary of crack growth prediction techniques". AGARD Lect. Ser. No. 62, Lecture 8, May 1973. p 31.

56- B. Dabell and S. Hill, "The use of computers in fatigue design and development". Proc. of Int. Conf., Appl. of Comput. in Fatigue, Warwick Univ., Coventry, Apr. 1978. p 33.

57- R. Fischer and U. Wendt, "Handling of fatigue data in computer analysis". Proc. of Int. Conf., Appl. of Computer in Fatigue, Warwick Univ., Coventry, Apr. 1978. p 24.

58- A. Conle and T. Topper, "Evaluation of small cycle omission criteria for shortening of fatigue service histories". Proc. of Int. Conf. , Appl. of Comput. in Fatigue, Warwick Univ., Coventry, Apr. 1978. p 17.

59- D. Styles and I. Baker, "Microcomputer control of fatigue crack-growth experiments". Proc. of Int. Conf., Appl. of Comput. in Fatigue, Warwick Univ., Coventry, Apr. 1978. p 13.

60- J. Page, J. Dennis and H. Howells, "Analysis of measured traffic induced stresses in bridges". Proc. of Int. Conf., Appl. of Comput. in Fatigue, Warwick Univ., Coventry, Apr. 1978. p 17.

61- J. Schijve, "The analysis of random load time histories with relation to fatigue tests and life calculations". Fatigue of Aircraft Structures, Ed. by Barrois and Ripley, Pergamon Press, 1963.

62- D. Webber, "Working stresses related to fatigue in military bridges". ICE Conference on Stresses in Service, London, 1966.

APPENDICES

A. Derivation of Inoue-Nakagawa's Equation

B. The Rainflow Computer Program

C. The Least Squares Method and Its Computer Program

D. The Safe Curve Computer Program

E. The Effect of an Increased Value of The Section Modulus on The Fatigue Life

F. Computer Program for The Fatigue Life Prediction

G. Computer Program for The Design of Beam Sections

APPENDIX A

A. Derivation of Inoue-Nakagawa's Equation

If we assume that the hysteresis loop of an element subjected to fully reversed straining (zero mean strain), is as shown in Figure (A.1), then the strain energy accumulated in a cycle, ΔW_i is

$$\Delta W_i = 4(E-H)\ (e_a-e_i)\ e_i$$

where e_a is the maximum applied strain, e_i is the yield strain, E and H are the slopes of the elastic and plastic parts of the idealized stress-strain curve of the material.

Also, if we assume that the form of the hysteresis loop is constant during the life, then the total strain energy of an element is:

$$W_i = n\ \Delta W_i = 4n\ (E-H)\ (e_a-e_i)\ e_i \qquad \ldots.(A.1)$$

The yield strain value e_{im} which maximises W_i can be obtained from

$$\frac{dW_i}{de_i} = 0 \qquad \text{which leads to } e_{im} = \tfrac{1}{2}\ e_a$$

Then the maximum value of W_i is:

$$W_m = n\ (E-H)\ e_a^2$$

Fatigue failure is assumed to occur when the accumulated strain energy, at an element where hysteresis energy is maximum W_m, reaches a certain value W_{mc}, then:

$$W_{mc} = N(E-H)\ e_a^2 \qquad \text{at failure}$$

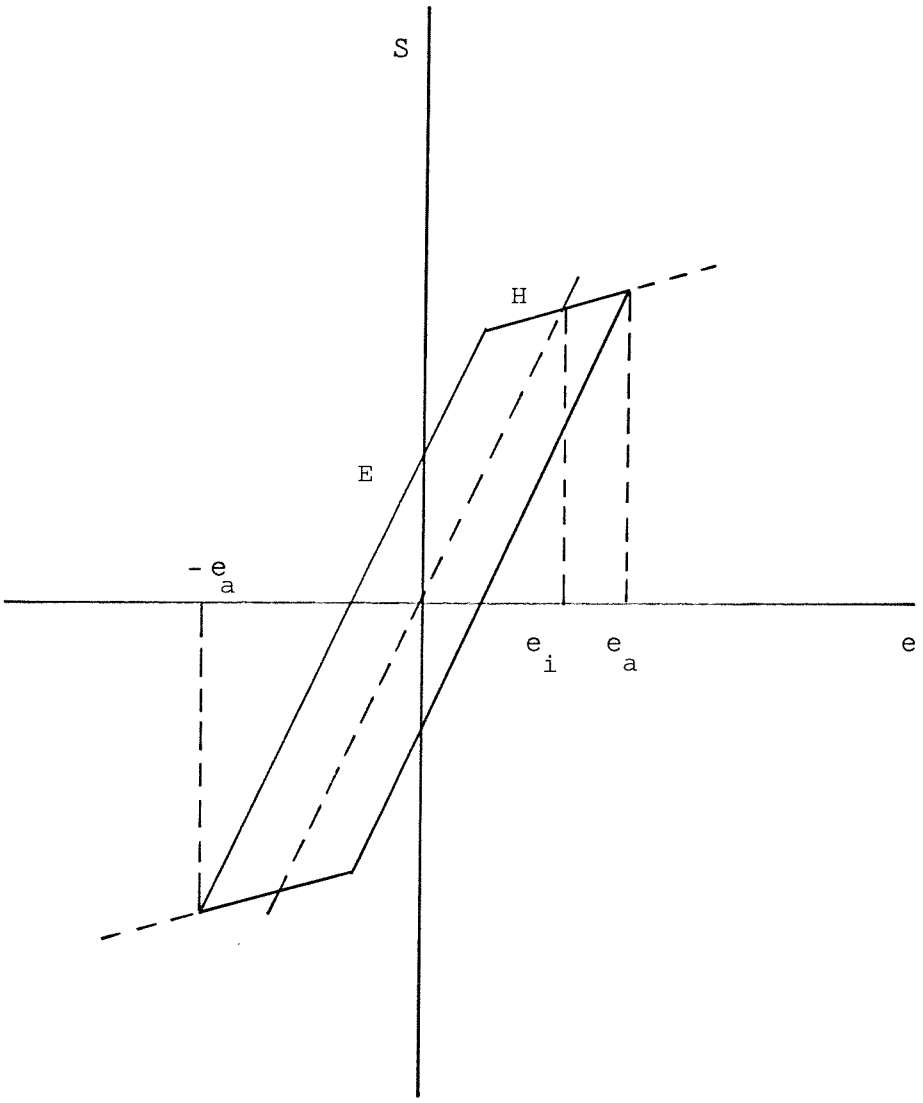

Figure (A.1)

Stress-strain hysteresis loop of an element with yield strain e_i

Inoue and Nakagawa have demonstrated that, it has been verified experimentally that W_{mc} is almost constant with respect to the variation in the imposed strain amplitude.

Then, at failure:

$$Ne_a^2 = \frac{W_{mc}}{E-H} = C \qquad \ldots. \text{ (A.2)}$$

where C is a material constant.

If an element with yield strain (e_i) is subjected to a variable strain amplitude test; e_1 for n_1 cycles, e_2 for n_2 , ...,e_n for n_n , then from Equation (A.1), the total strain energy is:

$W = 4\ (E-H)\ [n_1\ (e_1-e_i)e_i + n_2\ (e_2-e_i)e_i + \text{---} + n_n\ (e_n-e_i)e_i]$. Whence

$$\frac{dW}{de_i} = 4(E-H)\ [n_1\ (e_1 - 2e_i) + n_2\ (e_2 - 2e_i) + \text{---} + n_n\ (e_n - 2e_i)]$$

The value of the yield strain which gives maximum W is:

$$e_{im} = \frac{n_1\ e_1 + n_2\ e_2 + \text{-----} + n_n\ e_n}{2(n_1 + n_2 + \text{-----} + n_n)}$$

and the corresponding maximum value of W is:

$$W_m = \frac{(E-H)\ (n_1\ e_1 + n_2\ e_2 + \text{-----} + n_n\ e_n)^2}{n_1 + n_2 + \text{-----} + n_n}$$

As assumed above, failure occurs when W_m reaches the critical value W_{mc} , then at failure:

$$\frac{W_{mc}}{E-H} = \frac{(n_1\ e_1 + n_2\ e_2 + \text{------} + n_n\ e_n)^2}{n_1 + n_2 + \text{-----} + n_n} = C \qquad \ldots. \text{ (A.3)}$$

From Equation (A.2), the following relations can be estabished:

$$N_1 e_1^2 = C \quad \text{or} \quad e_1 = \sqrt{\frac{C}{N_1}}$$

$$N_2 e_2^2 = C \quad \text{or} \quad e_2 = \sqrt{\frac{C}{N_2}}$$

$$N_n e_n^2 = C \quad \text{or} \quad e_n = \sqrt{\frac{C}{N_n}}$$

Substituting e_1 , e_2 , -----, e_n in Equation (A.3) gives :

$$\frac{\left(\frac{n_1}{\sqrt{N_1}} + \frac{n_2}{\sqrt{N_2}} + \text{-----} + \frac{n_n}{\sqrt{N_n}}\right)^2}{n_1 + n_2 + \text{-----} + n_n} = 1$$

or $$\frac{n_1}{\sqrt{N_{SC}N_1}} + \frac{n_2}{\sqrt{N_{SC}N_2}} + \text{-----} + \frac{n_n}{\sqrt{N_{SC}N_n}} = 1$$

where $$N_{SC} = n_1 + n_2 + \text{-----} + n_n$$

Thus, the damage sum at failure is:

$$\sum \frac{n_i}{\sqrt{N_{SC}N_i}} = 1$$

Reference:

K. Inoue and K. Nakagawa, "Energy criteria for low cycle fatigue on the basis of distributed element model". Journal of the Society of Materials and Science, Japan, Vol. 24, No. 266, November 1975. pp 1038 - 1043 (in Japanese).

APPENDIX B

B. The Rainflow Computer Program

```
      PROGRAM RAIN FLOW
C
C  REAL  ST(200)
C
C  ST: THE ACTUAL STRESS VALUE WHICH CORRESPONDS TO A TURNING POINT
C      IN THE STRESS SPECTRUM.
C
C  INTEGER  IES,K,NC,IS(80)
C
C  IES: THE SERIAL NUMBER OF THE LAST POINT IN THE STRESS SPECTRUM.
C
C  K: THE TOTAL NUMBER OF THE POINTS STORED BECAUSE OF THE PRESENCE
C     OF DECREASE-DECREASE PATTERNS.
C
C  NC: THE NUMBER OF THE COUNTED CYCLES.
C
C  IS: THE SERIAL NUMBER OF THE POINTS STORED BECAUSE OF THE PRESENCE
C      OF DECREASE-DECREASE PATTERNS.
C
      DIMENSION ST(200),IS(80)
C
      READ*,IES
      READ(5,*) (ST(I),I=1,IES)
C
      K=0
      NC=0
C
      I1=1
      I2=2
      I3=3
      I4=4
C
 1003 DST1=ST(I2)-ST(I1)
 2003 DST2=ST(I3)-ST(I2)
 3003 DST3=ST(I4)-ST(I3)
C
      D1=ABS(DST1)
      D2=ABS(DST2)
      D3=ABS(DST3)
C
      IF(D3.LE.D2) GO TO 4003
      IF(D2.LE.D1) GO TO 203
      GO TO 303
C
 4003 IF(D2.GT.D1) GO TO 403
C
C     DECREASE-DECREASE PATTERN
C
      K=K+1
      IS(K)=I1
C
C  THE FOLLOWING IF STATEMENT IS REQUIRED TO DEAL WITH END POINTS
C
      IF(I4.EQ.IES) GO TO 1250
```

```
C
      I1=I2
      I2=I3
      I3=I4
      I4=I4+1
C
      DST1=DST2
      DST2=DST3
      GO TO 3003
C
 1250 IG=I2
      DO 1300 J=1,K
      STR=ST(IG)-ST(IS(K-J+1))
C
C  NEGATIVE VALUE OF STR REPRESENTS UNLOADING WHILE POSITIVE
C  REPRESENTS LOADING.
C
      WRITE(6,1715) IS(K-J+1),IG,STR
 1300 IG=IS(K-J+1)
C
      GO TO 1600
C
C  THE ABOVE DO STATEMENT COUNTS ALL RANGES AND CYCLES FROM I2
C  BACKWARDS. RANGES I2-I3 AND I3-I4 WILL BE DEALT WITH BY LINE
C  LABEL (1600).
C
C     DECREASE-INCREASE PATTERN
C
 203  IC=I2
      IR=MOD(IC,2)
      IF(IR.EQ.0) IC=I3
C
C  IN THIS PROGRAM THE COUNTED CYCLE SEQUENCE IS CONSIDERED TO BE
C  CONTROLLED BY ITS TROUGH POINT WHOSE INDEX IC IS GIVEN AS AN
C  ODD NUMBER.
C
      NC=NC+1
      ICM=(IC+1)/2
      STRC=D2
      WRITE(6,1720) ICM,I2,I3,STRC
 1720 FORMAT('STRC(',I6,')',' FROM ',I6,' TO ',I6,' = ',F6.2)
C
      IF(K.GT.0) GO TO 1450
C
      IF(I4.EQ.IES) GO TO 1400
C
      I2=I4
      I3=I4+1
      I4=I4+2
C
      IF(I4.GT.IES) GO TO 1800
C
      GO TO 1003
C
 1450 IF(K.GT.1) GO TO 1500
```

```
C
      IF(I4.EQ.IES) GO TO 1350
C
      I2=I1
      I1=IS(1)
      I3=I4
      I4=I4+1
C
      K=0
C
      GO TO 1003
C
 1350 STR=ST(I1)-ST(IS(1))
      WRITE(6,1715) IS(1),I1,STR
C
 1400 STR=ST(I4)-ST(I1)
      WRITE(6,1715) I1,I4,STR
C
      GO TO 5000
C
 1500 I3=I1
      I2=IS(K)
      I1=IS(K-1)
C
      K=K-2
      GO TO 1003
C
C     INCREASE-INCREASE PATTERN
C
 303  STR=DST1
      WRITE(6,1715) I1,I2,STR
C
      STR=DST2
      WRITE(6,1715) I2,I3,STR
C
      IF(I4.EQ.IES) GO TO 1550
C
      I1=I3
      I2=I4
      I3=I4+1
      I4=I4+2
C
      IF(I4.GT.IES) GO TO 1800
C
      DST1=DST3
      GO TO 2003
C
C     INCREASE-DECREASE PATTERN
C
 403  STR=DST1
      WRITE(6,1715) I1,I2,STR
C
      IF(I4.EQ.IES) GO TO 1600
C
      I1=I2
```

```
      I2=I3
      I3=I4
      I4=I4+1
C
      DST1=DST2
      DST2=DST3
C
      GO TO 3003
C
C  THE FOLLOWING SECTION DEALS WITH POINTS NEAR THE END POINT OF
C  THE SPECTRUM
C
 1800 STR=ST(I2)-ST(I1)
      WRITE(6,1715) I1,I2,STR
C
      STR=ST(I3)-ST(I2)
      WRITE(6,1715) I2,I3,STR
C
      GO TO 5000
C
 1600 STR=DST2
      WRITE(6,1715) I2,I3,STR
C
 1550 STR=DST3
      WRITE(6,1715) I3,I4,STR
 1715 FORMAT('STR',I6,'   TO   ',I6,'   =   ',F8.2)
C
 5000 WRITE(6,1750) NC
 1750 FORMAT('END OF  COUNTING ,   NO. OF CYCLES = ' , I6)
      STOP
      END
```

APPENDIX C

C. Least Squares Method and Its Computer Program

If we have n linear equations connecting a set of m unknowns, say X_1 , X_2 .... , X_m , $n > m$:

$$\sum_{j=1}^{m} a_{ij} X_j = b_i \qquad i = 1, 2, \ldots, n$$

Since the number of equations n exceeds the number of unknowns m, the system does not yield an exact solution, i.e. there is no set of values for X_1 , X_2 , ..., X_m for which each equation is satisfied.

if we consider the residuals:

$$r_i = \sum_{j=1}^{m} a_{ij} X_j - b_i \neq 0 \qquad i = 1, 2, \ldots, n$$

The method of least squares is simply a process for finding the values of X_1 , X_2 , ..., X_m which will make:

$$E = \sum_{i=1}^{n} r_i^2$$

as small as possible. To minimize E, we must equate to zero each of its first partial derivatives :

$$\frac{\partial E}{\partial X_1} , \frac{\partial E}{\partial X_2} , \text{----} , \frac{\partial E}{\partial X_m}$$

Thus, we have obtained a system of m linear equations in the m unknowns X_1 , X_2 , ...,X_m , whose solution is a routine matter.

If we have to fit a pth degree polynomial to a certain data:

$$a_0 + a_1X + a_2X^2 + ... + a_pX^p$$

The above equation is still linear, in that it is linear in the unknown parameters a_j. Thus the a_j may be calculated by the aforementioned technique.

References:

1 - C. Wylie, "Advanced Engineering Mathematics". McGraw-Hill 1966.

2 - W. Hines and D. Montgomery, "Probability and Statistics". Ronald, 1972.

C.1 G02CJF Subroutine

G02CJF subroutine of the NAG Library, has been used in this study to find the least squares second degree polynominal for the Section modulus F_L - Log (life) data. This subroutine performs the fitting for one or more dependent variables separately on the same set of independent variables. The data consists of values of q dependent variables (Y_1 , Y_2 , ..., Y_q) and m independent variables (X_1 , X_2 , ...,X_m), each being observed n times. For each Y_q , G02CJF fits linear model:

$$Y_q = a_{1q} X_1 + a_{2q} X_2 + ... + a_{mq} X_m$$

The 'a' parameters are estimated from the data to minimize the sum of squares of the residuals.

There is no explicit provision in the routine for a constant term in the equation(s). However, the addition of a dummy variable whose value is always (1.0) will produce a corresponding coefficient 'a' equal to the constant term.

In our case, to fit Log(life) = $a_0 + a_1 F_L + a_2 F_L^2$, we take:

$q = 1$

$Y =$ Log(life)

$X_j = (F_L)^{j-1}$ $\qquad j = 1, 2, 3$

The listing of the program used in this study, to find the least squares curve, is given here.

Reference

NAG Fortran Library manual, "Correlation and regression analysis". G02.

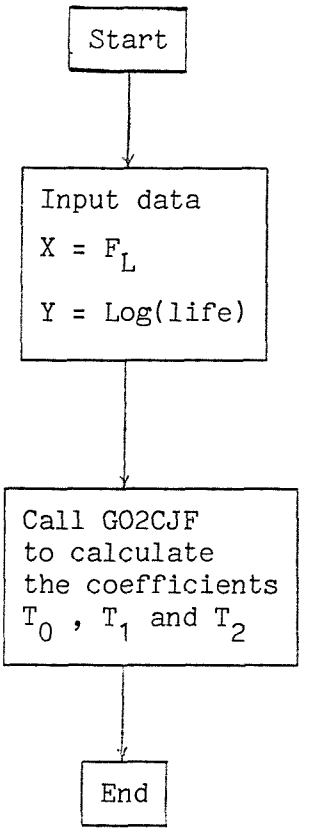

Figure (C.1)

Flow chart of the program which calculates the coefficients for the 2nd degree least squares polynomial

C.2 Computer Program

```
C  PROGRAM LEAST SQUARES CURVE
C
C  THIS PROGRAM FITS A LEAST SQUARES POLYNOMIAL TO A CERTAIN
C  X-Y DATA:
C
C  Y=A+C1*X+C2*X**2+.......+CNN*X**NN
C
C  IN THIS STUDY:
C
C  X=FL
C  Y=ALOG10(LIFE)
C
      REAL X(300,10),Y(300,1),THETA(10,1),SIGSQ(1),C(300,10),
     * WK1(10,4),WK2(300),YE(300),R(300),XD(300),YD(300)
C  IX=300
C  M=10
C  IY=300
C  IR=1
C  IT=10
C  IC=300
C  N=300
C
C  FOR INSTRUCTIONS OF USE AND DEFINITIONS OF THE AFOREMENTIONED
C  TERMS REFER TO NAG LIBRARY MANUAL, SUBROUTINE G02CJF.
C
      INTEGER IPIV(10)
      READ(5,*) N
C
C  N:  NUMBER OF OBSERVATIONS.
C
      READ(5,*)(XD(I),YD(I),I=1,N)
 1000 READ(5,*) NN
C
C  NN: THE LARGEST POWER OF X.
C
      M=NN+1
      IF(NN.EQ.0) STOP
C
      DO 10 J=1,N
      DO 10 JJ=1,M
      X(J,JJ)=XD(J)**(JJ-1)
   10 CONTINUE
C
      DO 20 J=1,N
      Y(J,1)=YD(J)
   20 CONTINUE
C
      WRITE(6,998)(Y(I,1),X(I,1),X(I,2),I=1,N)
  998 FORMAT('  DATA VALUES'/' Y         X1       X2'/300(1X,F5.3,
     * 2(3X,F6.3)/))
C
      IFAIL=0
C
      CALL G02CJF(X,300,Y,300,N,M,1,THETA,10,SIGSQ,C,300,IPIV,
```

```
C
     * WK1,WK2,IFAIL)
C
      DO 30 J=1,M
      WRITE(6,997) J,THETA(J,1)
 997  FORMAT('  THETA',I2,'  = ',F10.4)
  30  CONTINUE
C
      WRITE(6,97) SIGSQ(1)
  97  FORMAT('  VARIANCE OF RESIDUALS= ',F10.4)
      SS=0.0
      J=1
  75  S=0.0
C
      DO 50 JJ=1,M
      A=THETA(JJ,1)
      S=S+A*X(J,JJ)
  50  CONTINUE
C
      YE(J)=S
      R(J)=S-YD(J)
      SS=SS+R(J)*R(J)
      J=J+1
      IF(J.GT.N) GO TO 70
      GO TO 75
C
  70  WRITE(6,91)
  91  FORMAT(//'          YD              YE              R  ')
      WRITE(6,92) (YD(J),YE(J),R(J),J=1,N)
  92  FORMAT(3F15.3)
      WRITE(6,89) SS,IFAIL
  89  FORMAT('  SUM OF R*R= ', F9.6,'   IFAIL =   ',I3)
C
      GO TO 1000
C
      END
```

APPENDIX D

D. The Safe Curve Computer Program

D.1 E04MBF Subroutine

E04MBF subroutine of the NAG Library, has been used in this study to find the safe second degree polynomial curve for the Section modulus F_L - Log (life) data.

This subroutine solves linear programming problems or finds a feasible point for such problems. E04MBF solves problems of the form:

minimize $\quad E = a_1 X_1 + a_2 X_2 + \ldots + a_m X_m$

subject to the bounds $\quad l \leq X_j \leq u \qquad j = 1, 2, \ldots, m$

and the general constraints:

$$l \leq b_{1i} X_1 + b_{2i} X_2 + \ldots + b_{mi} X_m \leq u \qquad i = 1, 2, \ldots, k$$

There are m variables and k general linear constraints. k may be zero in which case the problem is subject only to bounds on the variables. Upper and lower bounds are specified for all the variables and constraints. This form allows full generality in specifying other types of constraints. For example the ith constraint may be specified as equality by setting, $l_i = u_i$. If certain bounds are not present, the associated elements of l or u can be set to special values that will be treated as $(-\infty)$ or $(+\infty)$. An initial estimate of the solution must be supplied by the user.

In this study, we have to fit a safe second degree polynomial curve $(\text{Log(life)} = a_0 + a_1 F_L + a_2 F_L^2)$ through n points. Therefore E is given by :

$$E = -na_0 - a_1 \sum_{1}^{n} F_{Li} - a_2 \sum_{1}^{n} F_{Li}^2$$

$$X_j = a_j - 1 \qquad j = 1, 2, 3$$

The bounds and the initial solution are estimated from the relevant least squares curve coefficients, while constraints are given by:

$$a_0 + a_1 F_{Li} + a_2 F_{Li}^2 \leq Y_i \qquad i = 1, 2, \ldots, n$$

where Y = Log(life).

The listing of the program used in this study, to find the safe curve, is given here.

Reference:

NAG Fortran Library Manual, "Minimizing or maximizing a function". E04.

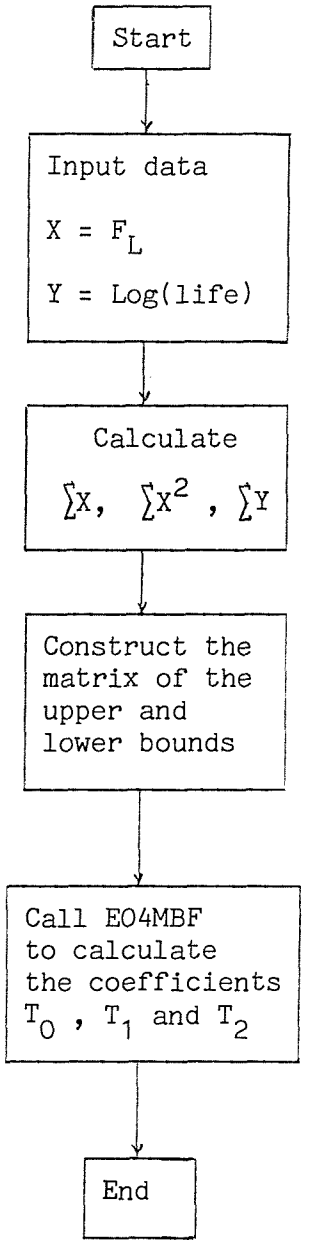

Figure (D.1)

Flow chart of the program which calculates the coefficients for the 2nd degree safe curve polynomial

D.2 Computer Program

```
C  PROGRAM SAFE CURVE
C
C  THIS PROGRAM FITS A SAFE CURVE SECOND DEGREE POLYNOMIAL,
C  SECTION 6.3.1, TO A CERTAIN X-Y DATA :
C
C  Y=T+T1*X+T2*X*X
C
C  IN THIS STUDY :
C
C  X=XD=FL
C  Y=ALOG10(LIFE)
C
      REAL OBJLP
      INTEGER I,IFAIL,ITMAX,J,LIWORK,LWORK,MSGLVL,N,NCLIN,
     * NCTOTL,NROWA
      LOGICAL LINOBJ
      REAL A(12,3),BL(15),BU(15),CLAMDA(15),CVEC(3),
     * WORK(200),X(3),Y(15),YE(15),XD(15)
      INTEGER ISTATE(15),IWORK(50)
      DATA NROWA /12/ , LIWORK /50/ , LWORK /200/
C
C  FOR INSTRUCTIONS OF USE AND DEFINITIONS OF THE AFOREMENTIONED
C  TERMS REFER TO NAG LIBRARY MANUAL, SUBROUTINE E04MBF.
C
      CALL X04ABF(1,6)
      N=3
C
C  THE FOLLOWING SIX LINES SPECIFY THE UPPER AND LOWER BOUNDS FOR
C  T,T1 AND T2
C
      TL=-10.0
      TU=100.0
      T1L=-25.0
      T1U=5.0
      T2L=-5.0
      T2U=5.0
C
      READ(5,*) NP
C
C  NP:  NUMBER OF OBSERVATIONS.
C
      NCLIN=NP
      READ(5,*)(XD(I),Y(I),I=1,NP)
      READ(5,*)(X(J),J=1,N)
      NCTOTL=N+NCLIN
      ITMAX=50
      MSGLVL=1
      LINOBJ=.TRUE.
C
      SX=0.0
      SXX=0.0
      SY=0.0
C
      DO 10 J=1,NP
```

```
      SX=SX+XD(J)
      SXX=SXX+XD(J)*XD(J)
      SY=SY+Y(J)
   10 CONTINUE
C
      CVEC(1)=-1.0*NP
      CVEC(2)=-1.0*SX
      CVEC(3)=-1.0*SXX
C
      DO 20 I=1,NCLIN
      DO 20 J=1,N
      A(I,J)=XD(I)**(J-1)
   20 CONTINUE
C
      BL(1)=TL
      BL(2)=T1L
      BL(3)=T2L
      BU(1)=TU
      BU(2)=T1U
      BU(3)=T2U
C
      DO 30 J=4,NCTOTL
      BL(J)=0.0
      BU(J)=Y(J-N)
   30 CONTINUE
C
      IFAIL=1
C
      CALL E04MBF(ITMAX,MSGLVL,N,NCLIN,NCTOTL,NROWA,A,BL,
C
     * BU,CVEC,LINOBJ,X,ISTATE,OBJLP,CLAMDA,IWORK,LIWORK,
     * WORK,LWORK,IFAIL)
C
      SP=OBJLP
      RESS=SP+SY
C
      TR=X(1)
      TR1=X(2)
      TR2=X(3)
C
      WRITE(6,111) RESS
  111 FORMAT('  RESS=  ',F9.6)
      WRITE(6,222) TR,TR1,TR2
  222 FORMAT('  TR= ',F9.6,' , TR1= ',F9.6,' , TR2= ',F9.6)
C
      SRS=0.0
      DO 40 I=1,NP
      YE(I)=TR+TR1*XD(I)+TR2*XD(I)*XD(I)
      SRS=SRS+(YE(I)-Y(I))**2
      WRITE(6,333) I,XD(I),Y(I),YE(I)
  333 FORMAT(' NP=',I3,' , X= ',F9.3,' , Y= ',F9.3,' , YE= ',F10.5)
   40 CONTINUE
C
      WRITE(6,444) SRS
  444 FORMAT('  SRS=  ', F9.6)
```

```
C
C  THE FOLLOWING SECTION CACULATES THE SECTION MODULUS VALUE WHICH
C  CORRESPONDS TO A DESIGN FATIGUE LIFE OF (100) YEARS.
C
      BLF=100.0
      YL=ALOG10(BLF)
      AP=TR2
      BP=TR1
      CP=TR-YL
      DP=SQRT(BP*BP-4.0*AP*CP)
      FL1=0.5*(-BP+DP)/AP
      FL2=0.5*(-BP-DP)/AP
      WRITE(6,555) BLF,FL1,FL2
  555 FORMAT('  BLF= ',F6.1,' , FL1= ',F9.3,' , FL2= ',F9.3)
      STOP
      END
```

APPENDIX E

E. The Effect of an Increased Value of The Section Modulus on The Fatigue Life

The following calculations have been made to breakdown the variation in the fatigue lives, resulting from an increase in the section modulus value (F_L), to its two components. The first component is caused by the change in F_L itself, while the second and the most important component is caused by excluding more stress ranges, because they become less than the endurance limit. The calculations given below is for section (111) which, for sections reinforced with 32 mm bars, has the maximum deviation in the fatigue life (Sec. 6.6) ;

let:

F_{L1} = the minimum of Z_L and Z_{LH} .

F_{L2} = the maximum of Z_L and Z_{LH} .

$(life)_1$, $(life)_2$ = fatigue lives in years.

D_1, D_2 = the damage sums in one week.

S_{re1}, S_{re2} = the maximum stress ranges in the outer bar, in N/mm^2.

S_e = the endurance limit in N/mm^2.

N_{ec1} , N_{ec2} = the numbers of the effective stress cycles in one week (with value > S_e)

$(life)_1$, D_1 , S_{re1} and N_{ec1} correspond to F_{L1} , while $(life)_2$, D_2 , S_{re2} and N_{ec2} correspond to F_{L2} .

Now, for section (111) :

$D_1/D_2 = (life)_2/(life)_1 = 1.331$

$F_{L2}/F_{L1} = 1.0359$

$\Delta N_{ec} = N_{ec1} - N_{ec2} = 289$

Since S_e = 92.893 N/mm^2, then by increasing F_L from F_{L1} to F_{L2} , all stress ranges, below S_{ro} = 92.893 x F_{L2}/F_{L1} = 92.893 x 1.0359 = 96.228 and above S_e = 92.893, would be excluded from the damage sum. An average value for these lost stress ranges is; S_{ra} = 0.5 (S_e + S_{ro}) = 94.561 N/mm^2 , with a corresponding N = 857126 (N is the required number of cycles to failure, given by ; logN = 6.9077 - 0.002 f_{sde} - 0.00591 S_{re}).

Whence the difference in the damage sum is approximated by :

$$D = \Delta N_{ec}/N = \frac{289}{857126} = 0.0337 \text{ percent}$$

and

$$D/D_2 \simeq 28 \text{ percent}$$

This means that a difference of 3.59 percent in F_L value gives a 33 percent difference in the damage sum and life values. Out of this figure, about 28 percent difference results from the cycles excluded because they become lower than the endurance limit, while about only 5 percent is due to the change in the stress range values.

Similar calculations have been made for the remaining sections which are reinforced with 32 mm bars. All results are given in Table (E.1).

sec. no.	F_{L1}	F_{L2}	S_{re1}	S_{re2}	S_e	N_{ec1}	N_{ec2}	D_1 (%)	D_2 (%)	$(life)_1$ (yrs.)	$(life)_2$ (yrs.)	F_{L2}/F_{L1}	$\frac{(life)_2}{(life)_1}$	S_{ra}	N	D/D_2 (%)
110	3.71	3.86	143.83	137.36	85.83	3198	2696	0.447	0.372	4.289	5.155	1.0404	1.2020	87.57	854262	15.80
111	4.18	4.33	135.40	134.49	92.89	1191	902	0.160	0.120	11.98	15.94	1.0359	1.3310	94.56	857126	28.10
112	4.56	4.66	137.43	134.50	96.92	391	313	0.051	0.040	37.82	47.47	1.0219	1.2550	97.98	865442	22.53
113	4.86	4.96	127.93	125.36	100.38	122	94	0.015	0.012	124.1	161.8	1.0206	1.3038	101.42	866813	26.92
114	5.45	5.58	115.97	113.28	105.30	14	11	0.0017	0.0013	1125.0	1459.0	1.0239	1.2970	106.56	865626	26.69

Table (E.1) - The effect of the variation in the section modulus (F_L) on the damage sum and the fatigue life

- For definitions of the terms, see pages (342 ,343)
  Stresses are given in N/mm^2
  Section moduli are given in $KN.M/(N/mm^2)$

APPENDIX F

F. Computer Program for The Fatigue Life Prediction

```
      PROGRAM LIFE
C
C  THIS PROGRAM SIMULATES THE MOMENT AND STRESS SPECTRA
C  FOR A SINGLE LANE SIMPLY SUPPORTED BRIDGE UNDER TRUCK
C  LOADING. ALSO IT PERFORMS CYCLE COUNTING BY THE PATTERN
C  CALSSIFICATION PROCEDURE (RAIN FLOW METHOD) AND CALCULATES
C  THE FATIGUE LIFE OF THE BRIDGE. BEFORE RUNNING THIS PROGRAM,
C  THE BRIDGE HAS TO BE DESIGNED TO SUSTAIN THE MAXIMUM LIVE
C  LOAD MOMENT, INCLUDING IMPACT, WHICH CAN BE OBTAINED BY
C  RUNNING A PROGRAM SIMILAR TO THE FIRST PART OF THIS PROGRAM,
C  WITH THE MODIFICATION THAT IT STORES THE ABSOLUTE MAXIMUM
C  MOMENT AT ANY STAGE (SECTIONS 5.3 AND 3.6).
C
C  REAL  AT,BL,BLM,BLN,BM1,BM2,BMS(2K),D(M,K2),DAT(I),DM,DN,
C        DY,FL,FMIN,FMINE,FN,P(M,K2),RC(I),RT(I),RW1(J),RW2(J),
C        SE0,SF,SP,SS(2K),ST,STC(K),STCX,T,TMIN,TOT,U,W(I),
C        WL(K2),WM,WP,WS,WW,X(K2).
C
C  INTEGER
C        IDD,IDI,IES,IID,III,IL1,IL2,IS(K1),KL,KS,MAX,MM,N,
C        NCC,ND,NI,NR,NRC,NS.
C
C  REAL QUANTITIES:
C
C  AT: THE TOTAL ARRIVAL TIME OF TRUCK I.
C  BL: THE BRIDGE SPAN IN METRES.
C  BLM,BLN: THE FATIGUE LIVES IN YEARS BASED ON PALMGREN-MINER'S
C           THEORY AND INOUE-NAKAGAWA'S THEORY RESPECTIVELY.
C  BM1: THE LOCAL MAXIMUM OR MINIMUM MOMENT OBTAINED SO FAR.
C  BM2: THE TOTAL INSTANTANEOUS MOMENT PRODUCED BY THE TRUCKS
C       PRESENT ON THE BRIDGE WHOLLY OR PARTLY.
C  BMS(2K): THE VALUE OF THE TURNING POINT IN THE MOMENT SPECTRUM
C           WHICH REPRESENTS THE TOTAL LIVE LOAD MOMENT, EXCLUDING
C           IMPACT, WHICH IS TO BE SHARED BETWEEN THE BRIDGE
C           TWO BEAMS.
C  D(M,K2): THE SPACING OF ANY AXLE TO THE FRONT ONE, FOR ANY
C           TRUCK K2 WHICH EXISTS WHOLLY OR PARTLY ON THE BRIDGE.
C           M=1, REPRESENTS THE REAR AXLE AND M=5, REPRESENTS
C           THE FRONT AXLE.
C  DAT(I): THE ARRIVAL TIME OF TRUCK I.
C  DM,DN: THE DAMAGE SUMS IN ONE WEEK BASED ON PALMGREN-MINER'S
C         THEORY AND INOUE-NAKAGAWA'S THEORY RESPECTIVELY.
C  DY: IMPACT FACTOR + 1.0
C  FL: THE SECTION MODULUS IN KN.M/(N/MM*MM) BASED ON THE LIVE
C      LOAD MOMENT (SECTION 4.7.1).
C  FMIN,FMINE: THE CENTROIDAL DEAD LOAD STRESS AND THE DEAD LOAD
C              STRESS IN THE OUTER BAR IN N/(MM*MM).
C  FN: THE NUMBER OF CYCLES TO FAILURE CORRESPONDING TO THE
C      STRESS RANGE STC(K).
C  P(M,K2): THE AXLE FRACTION OF WEIGHT FOR ANY TRUCK K2 WHICH
C           EXISTS WHOLLY OR PARTLY ON THE BRIDGE.
C  RC(I),RT(I): THE RANDOM NUMBERS REQUIRED TO SIMULATE THE
C               TYPE AND ARRIVAL TIME OF TRUCK I RESPECTIVELY.
C  RW1(J),RW2(J): THE RANDOM NUMBERS REQUIRED TO SIMULATE THE
```

```
C                  GROSS WEIGHT OF TRUCK I BY THE REJECTION
C                  METHOD (SECTION 3.4.2).
C  SE0: THE FATIGUE ENDURANCE LIMIT.
C  SF: THE RATIO BETWEEN THE OUTER BAR STRAIN AND THE
C      CENTROIDAL STRAIN (SECTION 4.7.1).
C  SP: THE TRUCK SPEED IN METRES PER SECOND EQUIVALENT TO 50 KM/HR.
C  SS(2K): THE ACTUAL STRESS VALUE, WHICH CORRESPONDS TO
C          A TURNING POINT IN THE STRESS SPECTRUM, IN N/(MM*MM).
C  ST: THE TOTAL SIMULATION TIME IN SECONDS, EQUIVALENT TO
C      ONE WEEK IN THIS STUDY.
C  STC(K): THE STRESS RANGE VALUE OF A COUNTED CYCLE.
C  STCX: THE MAXIMUM STRESS RANGE VALUE.
C  T: THE INSTANTANEOUS TOTAL TIME USED FOR THE TRUCK
C     MODEL SIMULATION.
C  TMIN: THE MINIMUM ARRIVAL TIME OF A TRUCK.
C  TOT: THE INSTANTANEOUS TOTAL TIME USED FOR THE MOMENT
C       SPECTRUM SIMULATION.
C  U: THE RATE OF TRUCK LOADING IN TRUCKS PER SECOND.
C  W(I): THE GROSS WEIGHT OF TRUCK I, IN KN.
C  WL(K2): THE GROSS WEIGHT OF TRUCK K2 WHICH EXISTS ON THE
C          BRIDGE WHOLLY OR PARTLY.
C  WM,WP,WS,WW: THE AVERAGE VALUE, THE UPPER BOUND VALUE,
C               THE STANDARD DEVIATION AND THE LOWER BOUND VALUE
C               OF THE GROSS WEIGHT (SECTION 3.5.1).
C  X(K2): THE LOCATION OF THE FRONT AXLE OF TRUCK K2, WHICH
C         EXISTS WHOLLY OR PARTLY ON THE BRIDGE, WITH RESPECT
C         TO THE DOWNSTREAM SUPPORT.
C
C  INTEGERS:
C
C  IDD,IDI: THE NUMBER OF PATTERNS CLASSIFIED AS
C           DECREASE-DECREASE PATTERNS (DD) AND
C           DECREASE-INCREASE PATTERNS (DI) RESPECTIVELY.
C  IES: THE SERIAL NUMBER OF THE LAST POINT IN THE MOMENT OR
C       STRESS SPECTRUM.
C  IID,III: THE NUMBER OF PATTERNS CALSSIFIED AS
C           INCREASE-DECREASE PATTERNS (ID) AND
C           INCREASE-INCREASE PATTERNS (II) RESPECTIVELY.
C  IL1,IL2: THE SERIAL NUMBERS OF THE TURNING POINTS OF
C           A COMPLETE CYCLE.
C  IS(K1): THE SERIAL NUMBER OF THE POINTS STORED BECAUSE OF
C          THE PRESENCE OF DECREASE-DECREASE PATTERNS.
C  KL: THE TOTAL NUMBER OF THE RANDOM NUMBERS RW1 AND RW2.
C  KS: THE TOTAL NUMBER OF THE RANDOM NUMBERS RC AND RT.
C      KS=INT(ST*U)
C      KL=NK*KS
C      KL SHOULD BE APPRECIABLY LARGER THAN KS. THIS IS
C      BECAUSE OF THE NATURE OF THE REJECTION METHOD. FROM
C      SEVERAL TRIALS IT SEEMS THAT, NK=3, IS ADEQUATE
C      FOR THIS STUDY.
C  MAX: A PARAMETER TO DEFINE THE NATURE OF THE LAST TURNING POINT.
C       MAX=1, MEANS THAT IT IS A MAXIMUM. MAX=0, MEANS THAT IT IS
C       A MINIMUM.
C  MM: THE SERIAL NUMBER OF A PAIR CONSISTING OF ONE MINIMUM
C      AND THE NEXT MAXIMUM POINT.
```

```
C  N: THE LOCAL SERIAL NUMBER OF THE TRUCKS WHICH ARE ON THE
C     BRIDGE WHOLLY OR PARTLY. N=1, REPRESENTS THE NEAREST
C     TRUCK TO THE DOWNSTREAM SUPPORT.
C  NCC: THE NUMBER OF COUNTED CYCLES EXTRACTED FROM FULL CYCLES.
C  ND: A PARAMETER TO INDICATE WHETHER A NEW TRUCK HAS ENTERED
C      THE BRIDGE. ND=1, MEANS THAT THERE IS A NEW TRUCK ON
C      THE BRIDGE. ND=0, MEANS UNCHANGED SITUATION.
C  NI: THE TOTAL NUMBER OF EFFECTIVE CYCLES.
C  NR: THE NUMBER OF COUNTED RANGES (HALF CYCLES).
C  NRC: THE NUMBER OF COUNTED CYCLES EXTRACTED FROM TWO EQUAL
C       HALF CYCLES.
C  NS: THE NUMBER OF SECTIONS WHICH HAVE TO BE ANALYZED.
C
      COMMON DAT(54000),W(54000)
      COMMON RC(54000),RT(54000),RW1(148000),RW2(148000)
      COMMON STC(97000),SS(194000),IS(1000),BMS(194000)
      DIMENSION WL(15),X(15),D(5,15),P(5,15)
C
      ST=604800.0
      READ(5,*) BL,NS,U
      DT=0.0015*BL
C
C  DT: THE TIME INCREMENT IN SECONDS.
C      THIS VALUE OF DT IS EQUIVALENT TO THE TIME REQUIRED FOR AN
C      AXLE TO MOVE A DISTANCE OF SPAN/48 WITH A SPEED OF 50 KM/HR.
C
      KS=INT(ST*U)
      KL=3*KS
      DY=1.0+50.0/(125.0+3.281*BL)
C
C  G05CBF GENERATES RANDOM NUMBERS, WITH REPEATABLE SEQUENCE, BY THE
C  MULTIPLICATIVE CONGRUENTIAL METHOD (SECTION 3.3)
C
      CALL G05CBF(795)
      DO 10 I=1,KS
      Y=G05CAF(Y)
 10   RC(I)=Y
C
      CALL G05CBF(226)
      DO 20 I=1,KS
      Y=G05CAF(Y)
 20   RT(I)=Y
C
      CALL G05CBF(371)
      DO 30 I=1,KL
      Y=G05CAF(Y)
 30   RW1(I)=Y
C
      CALL G05CBF(225)
      DO 40 I=1,KL
      Y=G05CAF(Y)
 40   RW2(I)=Y
C
      WRITE(6,43)
      WRITE(6,41) KS,KL,U
```

```
 41   FORMAT(' KS=  ',I8,'   KL=  ',I8,'   U=  ',F6.3)
 43   FORMAT(33H END OF RANDOM NUMBERS GENERATION)
      WRITE(6,431)
C
      L=0
      K=0
C
C  L IS THE SERIAL NUMBER OF RW1 AND RW2.
C  K IS THE SERIAL NUMBER OF RC AND RT.
C
      DAT(1)=0.00
      TOT=0.00
 45   K=K+1
C
      IF(RC(K).GT.0.79) GO TO 80
      IF(RC(K).GT.0.73) GO TO 70
      IF(RC(K).GT.0.66) GO TO 60
      IF(RC(K).GT.0.41) GO TO 49
C
C  TRUCK TYPE 3S2
      TMIN=1.436
      WP=533.760
      WW=88.960
      WM=231.296
      WS=71.168
      GO TO 90
C
C  TRUCK TYPE 2S2
 49   TMIN=1.392
      WP=444.800
      WW=44.480
      WM=182.368
      WS=57.824
      GO TO 90
C
C  TRUCK TYPE 2S1
 60   TMIN=1.371
      WP=400.320
      WW=44.480
      WM=160.128
      WS=53.376
      GO TO 90
C
C  TRUCK TYPE 3D
 70   TMIN=0.899
      WP=355.840
      WW=44.480
      WM=155.680
      WS=48.928
      GO TO 90
C
C  TRUCK TYPE 2D
 80   TMIN=0.855
      WP=222.400
      WW=22.240
```

```
      WM=62.272
      WS=26.688
C
C  THE FOLLOWING FIVE LINES GENERATE TRUCK WEIGHTS BY THE
C  REJECTION METHOD
C
 90   L=L+1
      WT=WW+(WP-WW)*RW1(L)
      FW=EXP(-0.5*((WT-WM)/WS)**2)
      IF(RW2(L).GT.FW) GO TO 90
      W(K)=WT
C
C  THE FOLLOWING STATEMENT IS REQUIRED TO AVOID INFINITE VALUES
C  FOR THE ARRIVAL TIME
C
      IF(RT(K).EQ.0.00) RT(K)=1.2E-77
C
C  THE FOLLOWING LINE GENERATES TRUCK ARRIVAL TIMES BY THE INVERSE
C  TRANSFORMATION METHOD (SECTION 3.4.1)
C
      DAT(K+1)=TMIN-ALOG(RT(K))/U
C
      TOT=TOT+DAT(K)
      SP=13.889
C
C  THE FOLLOWING ELEVEN LINES ARE REQUIRED TO ENSURE THAT THERE
C  IS NO TRUCK ON THE BRIDGE AT THE END OF THE SIMULATION
C
      IF(TOT-(ST-(BL+12.649)/SP)) 45,92,93
 92   KF=K
      DATK=DAT(KF)
      DAT(KF+1)=ST-TOT
      DAT(KF+2)=DAT(KF+1)
      GO TO 91
 93   KF=K-1
      DATK=DAT(KF+1)
      DAT(KF+1)=ABS(ST-TOT)+DATK
      DAT(KF+2)=DAT(KF+1)
 91   LF=L
C
      WRITE(6,98) K,KF,LF
 98   FORMAT(' K= ',1I7,'   KF=  ',1I7,'   LF=  ',1I7)
      WRITE(6,96) TOT,DATK,DAT(KF+1)
 96   FORMAT(' TOT= ',F14.3,' DATK= ',F7.3,'  DATKFP1=',F7.3)
      WRITE(6,97)
 97   FORMAT(' END OF TRAFFIC SIMULATION')
      WRITE(6,431)
C
      K=1
C
C  K: THE GENERAL SERIAL NUMBER OF THE TRUCKS.
C
      MM=1
      AT=DAT(1)
C
```

```
C  THE FRONT AXLE OF THE FIRST TRUCK IS PLACED ON THE BRIDGE
C  DOWNSTREAM SUPPORT.
C
150    T=AT
       I=2*MM-1
C
C  I IS THE SERIAL NUMBER OF THE MINIMUM POINT AND THE NEXT
C  MAXIMUM POINT.
C
       BMS(I)=0.000
       BM1=0.000
       MAX=0
       ND=1
       N=1
C
       X(1)=0.000
       AT=AT+DAT(K+1)
C
200    T=T+DT
       IF(T.GT.ST)GO TO 199
       IF(AT.GE.T) GO TO 1000
C
C  THE FOLLOWING TWO DO STATEMENTS RENUMBER EACH TRUCK PARAMETERS.
C  THIS IS REQUIRED WHEN A NEW TRUCK ENTERS THE BRIDGE BECAUSE THE
C  RECENT TRUCK ALWAYS HAS N=1
C
       DO 50 J=1,N
       WL(N+2-J)=WL(N+1-J)
50     X(N+2-J)=X(N+1-J)
       X(1)=(T-AT-DT)*SP
C
       DO 125 J=1,N
       DO 125 M=1,5
       D(M,N+2-J)=D(M,N+1-J)
125    P(M,N+2-J)=P(M,N+1-J)
C
       K=K+1
       ND=ND+1
       N=N+1
       AT=AT+DAT(K+1)
1000   IF(ND.EQ.0) GO TO 1200
C
C  THE FOLLOWING SECTION DEFINES THE PARAMETERS FOR THE RECENT TRUCK
C  FOR WHICH N=1
C
       D(5,1)=0.000
       WL(1)=W(K)
C
       IF(RC(K).LE.0.41) GO TO 52
       IF(RC(K).LE.0.66) GO TO 42
       IF(RC(K).LE.0.73) GO TO 32
       IF(RC(K).LE.0.79) GO TO 22
C
       D(1,1)=4.572
       D(2,1)=0.000
```

```
      D(3,1)=0.000
      D(4,1)=0.000
      P(1,1)=0.750
      P(2,1)=0.250
      P(3,1)=0.000
      P(4,1)=0.000
      P(5,1)=0.000
      GO TO 1200
C
22    D(1,1)=5.182
      D(2,1)=3.962
      D(3,1)=0.000
      D(4,1)=0.000
      P(1,1)=0.375
      P(2,1)=0.375
      P(3,1)=0.250
      P(4,1)=0.000
      P(5,1)=0.000
      GO TO 1200
C
32    D(1,1)=11.735
      D(2,1)=3.505
      D(3,1)=0.000
      D(4,1)=0.000
      P(1,1)=0.400
      P(2,1)=0.400
      P(3,1)=0.200
      P(4,1)=0.000
      P(5,1)=0.000
      GO TO 1200
C
42    D(1,1)=12.040
      D(2,1)=10.820
      D(3,1)=3.505
      D(4,1)=0.000
      P(1,1)=0.250
      P(2,1)=0.250
      P(3,1)=0.400
      P(4,1)=0.100
      P(5,1)=0.000
      GO TO 1200
C
52    D(1,1)=12.649
      D(2,1)=11.430
      D(3,1)=4.724
      D(4,1)=3.505
      P(1,1)=0.200
      P(2,1)=0.200
      P(3,1)=0.200
      P(4,1)=0.200
      P(5,1)=0.200
C
1200  DO 300 J=1,N
300   X(J)=X(J)+SP*DT
C
```

```
C  THE FOLLOWING IF STATEMENT CHECKS WHETHER THE TRUCK NEAREST TO
C  THE UPSTREAM SUPPORT IS STILL ON THE BRIDGE WHOLLY OR PARTLY
C
      IF((X(N)-D(1,N)).LT.BL)GO TO 400
C
      N=N-1
      IF(N.GT.0)GO TO 400
      K=K+1
C
C  THE FOLLOWING IF STATEMENT IS INTRODUCED TO DEAL WITH LARGE
C  VALUES OF DT. IF THE NEXT POINT IS A MAXIMUM, THEN IT ENSURES THAT
C  IT WILL BE STORED, EVEN IF THE BRIDGE IS SUDDENLY UNLOADED
C
      IF(MAX.EQ.0) GO TO 875
C
      GO TO 150
C
400   BM2=0.000
      IF(N-2)550,600,650
C
C  THE FOLLOWING DO STATEMENTS CALCULATE THE MID SPAN MOMENT,
C  FOR ANY CONCENTRATED LOAD P LOCATED AT A DISTANCE 'A'
C  FROM THE SUPPORT OF A SIMPLY SUPPORTED BEAM WHOSE SPAN
C  IS L, USING THE GENERAL FORMULA:
C
C  M=0.5*P*AMIN1(A,(L-A))
C
C  ALSO THEY DEAL WITH THE TRUCKS WHICH EXIST PARTLY ON THE BRIDGE
C
650   DO 500 J=2,N-1
      DO 500 M=1,5
      Z0=X(J)-D(M,J)
500   BM2=BM2+0.5*P(M,J)*WL(J)*AMIN1(Z0,(BL-Z0))
C
600   DO 700 M=1,5
      Z1=X(N)-D(M,N)
      Z2=BL-Z1
      Z3=AMIN1(Z1,AMAX1(Z2,0.0))
700   BM2=BM2+0.50*P(M,N)*WL(N)*Z3
C
550   DO 800 M=1,5
      Z1=X(1)-D(M,1)
      Z2=BL-Z1
      Z3=AMIN1(AMAX1(Z1,0.0),AMAX1(Z2,0.0))
800   BM2=BM2+0.50*P(M,1)*WL(1)*Z3
C
      ND=0
C
C  THE FOLLOWING LINES CHECK WHETHER THE CALCULATED MOMENT IS
C  A MAXIMUM OR MINIMUM
C
      IF(MAX.EQ.1) GO TO 590
      IF((BM1-BM2).LE.0.1) GO TO 580
 875  I=2*MM
      BMS(I)=BM1
```

```
      MM=MM+1
C
      IF(N.EQ.0) GO TO 150
C
      MAX=1
      BM1=BM2
      GO TO 200
C
 580  BM1=BM2
      GO TO 200
C
 590  IF((BM2-BM1).GT.0.1) GO TO 595
      BM1=BM2
      GO TO 200
C
 595  I=2*MM-1
      BMS(I)=BM1
      MAX=0
      BM1=BM2
      GO TO 200
C
 199  WRITE(6,802) ST,T,AT
      WRITE(6,805) BL,DT,DY
      MMF=MM
      IES=2*MMF-1
      WRITE(6,803) MMF,IES
C
C  THE FOLLOWING DO STATEMENT SIMULATES THE STRESS SPECTRUM,
C  PERFORMS THE CYCLE COUNTING AND ESTIMATES THE FATIGUE LIFE
C  FOR EACH BRIDGE SECTION
C
      DO 2345 II=1,NS
      READ(5,*) FL,SF,FMIN,FMINE
      DYFL=0.5*DY/FL
      FOF=FMINE/FMIN
      SF=AMAX1(SF,FOF)
      WRITE(6,1333) FL,SF,FMIN,FMINE
      WRITE(6,431)
C
C  THE FOLLOWING DO STATEMENT CONVERTS THE MOMENT SPECTRUM INTO
C  OUTER BAR STRESS SPECTRUM (SECTION 5.1)
C
      DO 1234 I=1,IES
      SS(I)=DYFL*BMS(I)
      IF(SS(I).LE.0.0001) GO TO 1234
      FSS=SS(I)+FMIN
      ESE=SF*(5.0E-06*FSS+23.5294E-06*AMAX1((FSS-340.0),0.0))
      FSE=200000.0*ESE-164948.45*AMAX1((ESE-0.0017),0.0)
      SSE=FSE-FMINE
      SS(I)=SSE
 1234 CONTINUE
C
 805  FORMAT(' BL=  ',F12.3,'  DT= ',F9.6,'   DY= ',F9.3)
 802  FORMAT('  ST=',F10.3,'  T=',F10.3,'  AT=',F10.3)
      WRITE(6,1111) SS(IES),SS(1)
```

```
 1111 FORMAT('   SSF= ',F9.3,' , SS1= ',1F9.3)
 803  FORMAT('END OF MOMENT SIMULATION','MMF=',1I7,'IES= ',1I6)
      WRITE(6,431)
C
C  CYCLE COUNTING IS PERFORMED BY THE PATTERN CLASSIFICATION
C  PROCEDURE (SECTION 5.2.2.3)
C
      STCX=0.00
C
      K=0
      KX=0
C
C  K IS THE SERIAL NUMBER OF THE POINTS STORED BECAUSE OF THE
C  PRESENCE OF DECREASE-DECREASE PATTERNS.
C  KX IS THE MAXIMUM VALUE OF K.
C
      NCC=0
      NRC=0
      NR=0
C
      IDD=0
      IDI=0
      III=0
      IID=0
C
      I1=1
      I2=2
      I3=3
      I4=4
C
 1003 DST1=SS(I2)-SS(I1)
 2003 DST2=SS(I3)-SS(I2)
 3003 DST3=SS(I4)-SS(I3)
C
      D1=ABS(DST1)
      D2=ABS(DST2)
      D3=ABS(DST3)
C
      IF(D3.LE.D2) GO TO 4003
      IF(D2.LE.D1) GO TO 203
      GO TO 303
C
 4003 IF(D2.GT.D1) GO TO 403
C
C     DECREASE-DECREASE PATTERN
C
      IDD=IDD+1
      K=K+1
      IF(K.GT.KX) KX=K
      IS(K)=I1
C
C  THE FOLLOWING IF STATEMENT IS REQUIRED TO DEAL WITH END POINTS
C
      IF(I4.EQ.IES) GO TO 1250
C
```

```
      I1=I2
      I2=I3
      I3=I4
      I4=I4+1
C
      DST1=DST2
      DST2=DST3
      GO TO 3003
C
 1250 IG=I2
      DO 1300 J=1,K
      ISL=IS(K-J+1)
      STR=SS(IG)-SS(ISL)
C
C  NEGATIVE VALUE OF STR REPRESENTS UNLOADING WHILE POSITIVE
C  REPRESENTS LOADING.
C
      NR=NR+1
      IF(MOD(J,2).EQ.0) GO TO 1255
      STRL=STR
      IG=ISL
      GO TO 1300
C
C  THE FOLLOWING IF STATEMENT COMPARES EVERY TWO SUCCESSIVE RANGES
C  TO CHECK WHETHER THEY COULD BE CONSIDERED EQUAL
C
 1255 IF(ABS(STR+STRL).LE.0.1) GO TO 1275
      IG=ISL
      GO TO 1300
C
 1275 IC=IG
C
C  IN THIS PROGRAM THE COUNTED CYCLES SEQUENCE IS CONSIDERED TO BE
C  CONTROLLED BY ITS TROUGH POINT WHOSE INDEX (IC) IS GIVEN AS AN
C  ODD NUMBER.
C
      IR=MOD(IC,2)
      IF(IR.EQ.0) IC=ISL
      ICM=(IC+1)/2
      STC(ICM)=ABS(STR)
      IF(STC(ICM).GT.STCX) STCX=STC(ICM)
      NR=NR-2
      NRC=NRC+1
      IG=ISL
 1300 CONTINUE
C
      GO TO 1600
C
C  THE ABOVE DO STATEMENT COUNTED ALL RANGES AND CYCLES FROM I2
C  BACKWARDS. RANGES I2-I3 AND I3-I4 WILL BE DEALT WITH BY LINE
C  LABEL (1600).
C
C     DECREASE-INCREASE PATTERN
C
 203  IC=I2
```

```
      IDI=IDI+1
      STRL=0.000
      IR=MOD(IC,2)
      IF(IR.EQ.0) IC=I3
      NCC=NCC+1
      ICM=(IC+1)/2
      STC(ICM)=D2
      IF(STC(ICM).GT.STCX) STCX=STC(ICM)
C
      IF(K.GT.0) GO TO 1450
C
      IF(I4.EQ.IES) GO TO 1400
C
      I2=I4
      I3=I4+1
      I4=I4+2
C
      IF(I4.GT.IES) GO TO 1800
C
      GO TO 1003
C
 1450 IF(K.GT.1) GO TO 1500
C
      IF(I4.EQ.IES) GO TO 1350
C
      I2=I1
      I1=IS(1)
      I3=I4
      I4=I4+1
C
      K=0
      GO TO 1003
C
 1350 STR=SS(I1)-SS(IS(1))
      STRL=STR
      NR=NR+1
C
      IL1=IS(1)
      IL2=I1
C
 1400 STR=SS(I4)-SS(I1)
      NR=NR+1
C
      IF(ABS(STR+STRL).LE.0.1) GO TO 1560
C
      GO TO 5000
C
 1500 I3=I1
      I2=IS(K)
      I1=IS(K-1)
C
      K=K-2
      GO TO 1003
C
C  IN THIS STUDY, VALUES OF ALL THE TROUGH POINTS ARE NOT LESS
```

```
C  THAN THE VALUE OF THE STARTING POINT. CONSEQUENTLY NO
C  INCREASE-INCREASE OR INCREASE-DECREASE PATTERNS ARE EXPECTED.
C  HENCE, THE FOLLOWING TWO RELATED SECTIONS OF THE PROGRAM COULD
C  BE DELETED.
C
C     INCREASE-INCREASE PATTERN
C
 303  STR=DST1
      III=III+1
      STRL=0.000
      STR=DST2
      NR=NR+2
C
      IF(I4.EQ.IES) GO TO 1550
C
      I1=I3
      I2=I4
      I3=I4+1
      I4=I4+2
C
      IF(I4.GT.IES) GO TO 1800
C
      DST1=DST3
      GO TO 2003
C
C     INCREASE-DECREASE PATTERN
C
 403  STR=DST1
      IID=IID+1
      NR=NR+1
C
      IF(I4.EQ.IES) GO TO 1600
C
      I1=I2
      I2=I3
      I3=I4
      I4=I4+1
C
      DST1=DST2
      DST2=DST3
C
      GO TO 3003
C
C  THE FOLLOWING SECTION DEALS WITH POINTS NEAR THE END POINT OF
C  THE SPECTRUM
C
 1800 STR=SS(I2)-SS(I1)
      STRL=STR
      NR=NR+1
C
      IL1=I1
      IL2=I2
C
      STR=SS(I3)-SS(I2)
      NR=NR+1
```

```
C
      IF(ABS(STR+STRL).LE.0.1) GO TO 1560
C
      GO TO 5000
C
 1600 STR=DST2
      STRL=STR
      NR=NR+1
C
      IL1=I2
      IL2=I3
C
 1550 STR=DST3
      NR=NR+1
C
      IF(ABS(STR+STRL).LE.0.1) GO TO 1560
C
      GO TO 5000
C
 1560 IC=IL2
      IR=MOD(IC,2)
      IF(IR.EQ.0) IC=IL1
      ICM=(IC+1)/2
      STC(ICM)=ABS(STR)
C
      IF(STC(ICM).GT.STCX) STCX=STC(ICM)
      NR=NR-2
      NRC=NRC+1
 5000 WRITE(6,1750) NR,K
 1750 FORMAT(' END OF CYCLE COUNTING ,   NR = ' , I6,'  K= ',1I6)
      WRITE(6,1751) NRC,NCC,KX
 1751 FORMAT(' NRC=  ',1I7,'  NCC=  ',1I7,'  KX=',1I5  )
      WRITE(6,1752) IDD,IDI,III,IID
 1752 FORMAT(' IDD=',1I6,'  IDI=',1I6,'  III=',1I6,'  IID=',1I6)
C
      NC=NCC+NRC
C
      WRITE(6,431)
 431  FORMAT('==============================================')
 9999 FORMAT('----------------------------------------------')
C
C  THE FOLLOWING SECTION ESTIMATES THE FATIGUE LIFE USING THE
C  PALMGREN-MINER'S THEORY AND INOUE-NAKAGAWA'S THEORY (CHAPTER 5)
C
      NI=0
      SE0=161.5-0.33*FMINE
C
      WRITE(6,5001) STCX,STC(1),SE0
 5001 FORMAT(' STCX= ',F9.3,'  STC(1)= ',F9.3,'  SE0= ',F9.3)
      WRITE(6,431)
C
      DM=0.0
      DN=0.0
C
      PDN=0.0
```

```
      PFN=0.002*FMINE
C
      DO 1399 J=1,NC
C
      IF(STC(J).LE.SE0)GO TO 1399
      NI=NI+1
      AFN=6.9085
C
C  THIS VALUE OF AFN IS FOR 25 MM DIAMETER. FOR 32 MM DIAMETER,
C  AFN=6.9077.
C
      FN=10.00**(AFN-PFN-0.00591*STC(J))
      DM=DM+1.00/FN
      PDN=PDN+1.00/SQRT(FN)
 1399 CONTINUE
C
      SN=NI
      DN=PDN*PDN/SN
      WRITE(6,4444) NI,PDN
 4444 FORMAT('  NI= ', 1I9,' , PDN= ',1F12.6    )
      WRITE(6,9999)
      WRITE(6,5007) DM,DN
 5007 FORMAT( '  DM= ',E12.6,' , DN= ',E12.6)
 1333 FORMAT('  FL=',F6.3,',SF=',F8.6,',FMIN=',F6.2,',FMINE=',F6.2)
 799  FORMAT(' END OF CUMULATIVE DAM CALC,  NS= ',1I7,' , NC=',1I7)
      WRITE(6,431)
      CL=1.9165E-02
      BLM=CL/DM
      BLN=CL/DN
      WRITE(6,4321) BLM,BLN
 4321 FORMAT('  BLM= ',F12.3,' , BLN= ',F12.3,' : IN YEARS')
      WRITE(6,799) II,NC
      WRITE(6,431)
 2345 CONTINUE
      STOP
      END
```

APPENDIX G

G. Computer Program for The Design of Beam Sections

```
      PROGRAM DESIGN
C
C  THIS PROGRAM DESIGNS THE BRIDGE SECTION USING PROCEDURE
C  PROPOSED IN CHAPTER 4. IT CALCULATES THE REQUIRED
C  SECTION DIMENSIONS, CHECKS THE DEFLECTION AND SLENDERNESS
C  REQUIREMENTS, ROUNDS OFF THE DIMENSIONS TO THE
C  NEAREST 50 MM, CALCULATES THE REQUIRED REINFORCEMENT
C  AREA AND CALCULATES THE ACTUAL STRESS IN THE REIFORCEMENT.
C
      DIMENSION SS(20),SN(20)
C
C  SS(I),SN(I): THE STRESS AND STRAIN IN REINFORCEMENT
C               LAYER I.
C
      PRINT*,'SPECIFY BM IN KN.M, BL AND BC IN M,BV IN KN'
      READ(5,*) BM,BL,BC,BV
C
C  BM,BV: THE TOTAL LIVE LOAD MOMENT AND SHEAR TO BE SHARED
C         BETWEEN THE BRIDGE TWO BEAMS.
C  BC,BL: THE BEAM WIDTH AND SPAN.
C
      WRITE(6,10) BM,BL,BC,BV
 10   FORMAT('BM=  ',1F9.3,' BL=  ',1F6.3,'  BC=  ',1F6.3,
     *'   BV=',F9.3)
      WRITE(6,30)
C
      TC=10000.0
      IF(BL.GT.22.0) TC=15000.0
C
C  TC: THE DISCREPANCY IN THE TENSILE FORCE WHICH IS
C      CONSIDERED ACCEPTABLE WHEN CALCULATING ACTUAL
C      STRESS IN THE REINFORCEMENT.
C
      DIS=10.0
      IF(BL.GT.22.0) DIS=12.0
C
C  DIS: THE DIAMETER OF THE SHEAR REINFORCEMENT.
C
      PRINT*,'TC= ',TC,' , DIS=  ',DIS,' MM'
C
      BM=BM*1.0E06
      BL=BL*1.0E03
      BC=BC*1.0E03
C
      BMDS=3.125*BL*BL
C
C  BMDS: THE MOMENT CAUSED BY THE BRIDGE DEAD LOAD OTHER
C        THAN THE BEAM SELF WEIGHT (ASSUMED TO BE 25 KN/M
C        FOR EACH BEAM).
C
      BMU=BMDS+0.5*BM
      READ(5,*) DI
C
C  DI: THE RINFORCEMENT DIAMETER IN MM.
```

```
C
      DO 1000 J=1,20
C
      PRINT*,' SPECIFY FSI IN N/(MM*MM), DPT  IN MM, N '
      READ*, FSI,DPT,N
      WRITE(6,40) FSI,DPT
 40   FORMAT('CALC. DB, FSI= ',1F9.3,', DPT= ',1F9.3)
C
      RD=50.0
C
C  FSI: THE INITIAL DESIGN STRESS IN THE REINFORCEMENT.
C  DPT: OVERALL DEPTH - EFFECTIVE DEPTH.
C  N: NUMBER OF BARS IN ONE LAYER.
C  DB: THE BEAM EFFECTIVE DEPTH.
C  RD: ROUNDING OFF PARAMETER.
C
      NC1=0
      NC2=0
      NC3=0
C
      HP=DPT
 444  FS=FSI
C
      NC3=NC3+1
      HMD=DPT
C
      ES=FS/200000.0+AMAX1((FS-340.0),0.0)/42500.0
C
C  ES,FS: THE CENTROIDAL STRAIN AND STRESS IN THE
C         REINFORCEMENT.
C
      IF(FS.LE.340.0) GO TO 300
C
C  CALCULATION OF THE SECTION DIMENSIONS (SECTION 4.3.2)
C
C  CASE 1 (FS.GT.0.8*FY=340 N/MM*MM)
C
      XOD=122.680/(FS-157.732)
C
C  XOD: THE RATIO OF THE NEUTRAL AXIS DEPTH TO THE
C       EFFECTIVE DEPTH.
C
      IF(XOD.GE.0.50) GO TO 100
C
C  CASE 1A (XOD.LT.0.50)
C
      R=XOD
      CR=21.978*R
      AR=1.0-0.4345*R
C
      GO TO 200
C
C  CASE 1B OR 2A (EC.GE.0.0015)
C
C  EC: THE MAXIMUM CONCRETE STRAIN. (0.0015) REPRESENTS
```

```
C       THE VALUE OF THE INITIAL PLASTIC STRAIN.
C
 100  R=0.5
      EC=ES
C
 150  SK=0.0015/EC
      CR=4.2735*(3.0-SK)
      SL=0.25*(SK*SK-4.0*SK+6.0)/(3.0-SK)
      AR=1.0-0.5*SL
C
      GO TO 200
C
C  CASE 2 (FS.LE.0.8*FY)
C
 300  EC=ES
      R=0.5
      IF (EC.GE.0.0015) GO TO 150
C
C  CASE 2B (EC.LT.0.0015)
C
      FC=5500.0*EC*(6.202-2062.5*EC)
C
C  FC: THE MAXIMUM CONCRETE STRESS.
C
      RP=666.667*EC
      CR=0.1667*FC*(3.0-RP)/(2.0-RP)
      AR=0.125*(20.0-7.0*RP)/(3.0-RP)
C
C  CALCULATION OF THE  BEAM DEPTH
C
 200  A=CR*BC*AR
      B=3.0E-06*BC*BL*BL
      C=BMU+HMD*B
      D=SQRT(B*B+4.0*A*C)
      DBI=0.5*(B+D)/A
C
C  DBI: THE REQUIRED EFFECTIVE DEPTH OF THE BEAM.
C
      DB=INT((DBI+HMD)/RD)*RD+RD-HMD
      RI=R
C
C  CHECK DEFLECTION AND SLENDERNESS REQUIREMENTS
C
      IF((DB+HMD).GE.(0.0588*BL)) GO TO 450
      DB=INT(0.0588*BL/RD)*RD+RD-HMD
 450  BLM1=60.0*BC
C
      BLM2=250.0*BC*BC/DB
      IF(BLM2.GE.BLM1) GO TO 550
      BCI=SQRT(0.004*BL*DB)
C
C  BCI: THE INITIAL REVISED WIDTH.
C
      BC=INT(BCI/RD)*RD+RD
C
```

```
 550  BMD=3.0E-06*BC*BL*BL*(DB+HMD)
      BMT=BMU+BMD
      BMDT=BMD+BMDS
C
C  BMD: THE MOMENT CAUSED BY THE BEAM SELF WEIGHT.
C  BMT: THE TOTAL MOMENT.
C  BMDT: THE TOTAL DEAD LOAD MOMENT.
C
C  CALCULATION OF THE REVISED NEUTRAL AXIS EFFECTIVE
C  DEPTH RATIO ;R (SECTION 4.3.3)
C
C  CASE 1 (EC.GE.0.0015)
C
      RM=0.468*BMT/(BC*DB*DB)
C
      EOS=0.0015/ES
      COF=EOS*(EOS+4.0)
      A=COF+6.0
      B=2.0*A
      C=COF+RM
      D=SQRT(B*B-4.0*A*C)
      R=0.5*(B-D)/A
C
      EC=ES*R/(1.0-R)
      RV=R
      ECV=EC
      IV=1
C
      IF(EC.LT.0.0015) GO TO 430
C
      FSI=FS
      CR=8.547*R*(3.0-0.0015/EC)
C
      GO TO 400
C
C  CASE 2 (EC.LT.0.0015)
C
 430  RM=3.108*RM
C
      DA=1.0/EOS
      A0=-2.0*DA*RM*DA
      A1=(DA-4.0)*RM*DA
      A2=2.0*RM*(DA-1.0)+74.421*DA
      A3=RM+49.614-61.932*DA
      A4=12.375*DA-43.355
      A5=9.281
      X=0.5
C
 650  YT=A0+X*(A1+X*(A2+X*(A3+X*(A4+X*A5))))
      YB=A1+X*(2.0*A2+X*(3.0*A3+X*(4.0*A4+X*5.0*A5)))
      X1=X-YT/YB
      IF(ABS(X-X1).LE.0.0001) GO TO 750
      X=X1
C
      GO TO 650
```

```
C
 750  RP=X
      R=X/(DA+X)
C
      EC=0.0015*RP
      FSI=FS
      RV=R
      ECV=EC
      IV=2
      FC=5500.0*EC*(6.202-2062.5*EC)
      CR=0.3333*R*FC*(3.0-RP)/(2.0-RP)
C
C  CALCULATION OF THE REINFORCEMENT AREA (SECTION 4.3.3)
C
 400  CF=CR*BC*DB
      TF=CF
      ASR=TF/FSI
      NOB=INT(1.27324*ASR/(DI*DI))+1
C
C  NOB: NUMBER OF THE REINFORCING BARS.
C
      ASP=0.7853982*NOB*DI*DI
      RR=100.0*ASP/(BC*DB)
C
C  RR: THE REINFORCEMENT RATIO.
C
      FSA=FSI*ASR/ASP
      HT=DB+HMD
      BMC=BMT
      FS1=FSA
      DP1=HMD
      IC=1
C
C  IC=1,REPRESENTS FULL MOMENT (BMT).
C  IC=2,REPRESENTS HALF MAX L.L. + D.L. MOMENT (BMTH).
C  IC=3,REPRESENTS DEAD LOAD MOMENT ONLY (BMDT).
C
C  CALCULATION OF THE ACTUAL STRESSES DUE TO BMT, BMTH
C  AND BMDT (FSA,FSH AND FMIN (SECTION 4.3.4))
C
C  CASE 1 (EC.GE.0.0015)
C
 920  DBA=HT-DP1
      NC2=NC2+1
      BET=0.117*ASP/(BC*DBA)
      RM=0.468*BMC/(BC*DBA*DBA)
C
 890  ES=FS1/200000.0+AMAX1((FS1-340.0),0.0)/42500.0
      IB=0
      IF(FS1.GT.340.0) IB=1
C
      C1=(300.0-247.423*IB)*BET
      C2=-280.412*BET*IB
      A0=-6.0*C1*C1
      A1=C1*(36.0-4.0*C1+12.0*C2)
```

```
      A2=-9.0*RM+C1*(24.0-C1+8.0*C2)-6.0*C2*(C2+6.0)
      A3=-6.0*RM+6.0*C1-C2*(24.0-2.0*C1+4.0*C2)
      A4=-RM-3.0-C2*(6.0+C2)
      X=0.0015/ES
C
 875  YT=A0+X*(A1+X*(A2+X*(A3+X*A4)))
      YB=A1+X*(2.0*A2+X*(3.0*A3+X*4.0*A4))
      X1=X-YT/YB
      IF(ABS(X1-X).LE.1.0E-04) GO TO 880
      X=X1
      GO TO 875
C
 880  ES=0.0015/X
      R=(C1/X-C2+X)/(3.0+X)
C
      IB1=0
      IF(ES.GT.0.0017) IB1=1
      FS1=200000.0*ES-AMAX1((ES-0.0017),0.0)*164948.45
      IF(IB1.NE.IB) GO TO 890
C
      FS2=FS1
      EC=ES*R/(1.0-R)
      IA=1
      IF(EC.LT.0.0015) GO TO 420
C
      TCR=1.0
      RP=1.0
      IF(IC.EQ.1) RT=R
      GO TO 900
C
C  CASE 2 (EC.LT.0.0015)
C
 420  X=1.0
C
      RM=3.108*RM
 421  A=2.0*RM-X*RM
      B=X*(4.0*RM-X*(2.0*RM+74.421-X*(61.932-X*12.375)))
      C=X*(X*(2.0*RM-X*(RM+49.614-X*(43.355-X*9.281))))
      D=SQRT(B*B-4.0*A*C)
      DA1=0.5*(D-B)/A
      ES=0.0015*DA1
      FS1=200000.0*ES-AMAX1((ES-0.0017),0.0)*164948.45
      R=X/(DA1+X)
      RP=X
      CF=2.75*RP*(3.0-RP)*(6.202-3.094*RP)*R*BC*DBA/(2.0-RP)
      TF=FS1*ASP
      IF(ABS(CF-TF).LE.TC) GO TO 610
      X=X-0.001
      GO TO 421
C
 610  FS2=FS1
      TCR=TF/CF
      EC=0.0015*RP
      IF(IC.EQ.1) RT=R
      IA=2
```

```
C
C  THE FOLLOWING SECTION IS REQUIRED TO CHECK WHETHER
C  THE ASSUMED VALUE OF DPT IS ADEQUATELY NEAR TO ITS
C  ACTUAL VALUE, CACULATED AS THE LOCATION OF THE TOTAL
C  TENSILE FORCE
C
 900  SP=DI+25.0
      CV=30.0+0.5*DI
      IF(BL.GT.22000.0) CV=CV+2.0
C
C  SP: THE VERTICAL SPACING BETWEEN BARS.
C  CV: THE COVER MEASURED TO THE CENTRE OF THE OUTER LAYER.
C
      DP=DP1
      ASB=0.7853982*DI*DI
C
C  ASB: THE REINFORCING BAR AREA.
C
      NOL=(NOB-1)/N+1
C
C  NOL:  NUMBER OF LAYERS.
C
 111  TF=0.0
      TM=0.0
      DBA=HT-DP
      NC1=NC1+1
C
      DO 333 I=1,NOL
C
C  I=1, REPRESENTS THE OUTER BAR
C
      BI=I-1
      SN(I)=(1.0+(DP-CV-BI*SP)/((1.0-R)*DBA))*ES
      SS(I)=200000.0*SN(I)-AMAX1((SN(I)-0.0017),0.0)*164948.45
      NP=N
      IF(I.EQ.NOL) NP=NOB-(NOL-1)*N
      TF=TF+NP*ASB*SS(I)
C
 333  TM=TM+NP*ASB*SS(I)*(CV+BI*SP)
      TMA=ASP*FS2*DP
C
C  TM: THE MOMENT SUMMATION OF THE TENSILE FORCES IN
C      THE VARIOUS LAYERS.
C  TMA: THE TOTAL TENSILE FORCE MOMENT.
C
      IF((ABS(TMA-TM)/TM).LE.0.01) GO TO 222
      DP=DP-0.01
      GO TO 111
C
 222  IF((ABS(DP-DP1)/DP).LE.0.01) GO TO 666
      DP1=DP
      GO TO 920
C
 666  ESE=SN(1)
      FSE=SS(1)
```

```
C
C  ESE,FSE: THE STRAIN AND STRESS IN THE OUTER LAYER.
C
      SF=ESE/ES
      IF(IC.NE.1) GO TO 555
      DPT=DP
      IF((ABS(DPT-HMD)/DPT).GT.0.01) GO TO 444
      PRINT*,' N= ',N,' , NOL= ',NOL,' , SP= ',SP
      PRINT*,' RI= ',RI,' , DBI= ',DBI,' , DB= ',DB
      PRINT*,' RV= ',RV,' , ECV= ',ECV,' , IV= ',IV
      WRITE(6,35)
C
      PRINT*,' ASR= ',ASR,' , ASP= ',ASP,' , CV= ',CV
      PRINT*,' NOB= ',NOB,' , RR= ',RR,' , DI= ',DI
      PRINT*,' BC= ',BC,' , HT= ',HT
      WRITE(6,35)
C
 555  PRINT*,' NC1= ',NC1,' , NC2= ',NC2,' , NC3= ',NC3,'
     *, IA= ',IA
      PRINT*,' TCR= ',TCR,' , RP= ',RP,' , R= ',R
      PRINT*,' ES= ',ES,' , ESE= ',ESE,' , EC= ',EC
C
      GO TO (902,905,910) , IC
C
 902  FSA=FSE
      FSA1=FS2
      SFT=SF
C
C  FSA,FSA1,SFT: THE OUTER BAR STRESS, THE CENTROIDAL STRESS
C                AND THE STRAIN FACTOR, CORRESPONDING TO BMT.
C
      PRINT*,' FSA1= ',FSA1,' , SFT= ',SFT,' , DPT= ',DPT
      WRITE(6,50) FSA
      WRITE(6,35)
C
      BMC=BMT-0.25*BM
      IC=2
      FS1=FSA1*BMC/BMT
      DP1=HP
      NC1=0
      NC2=0
      GO TO 920
C
 905  FSH=FSE
      FSH1=FS2
      SFH=SF
C
C  FSH,FSH1,SFH: THE OUTER BAR STRESS, THE CENTROIDAL STRESS
C                AND THE STRAIN FACTOR, CORRESPONDING TO BMTH.
C
      PRINT*,' FSH1= ',FSH1,' , SFH= ',SFH,' , DPH= ',DP
      PRINT*,'FSH= ',FSH
      WRITE(6,35)
C
      BMC=BMDT
```

```
      IC=3
      FS1=FSA1*BMC/BMT
      DP1=HP
C
      NC1=0
      NC2=0
      GO TO 920
C
 910  FMIN=FSE
      FMIN1=FS2
      SFD=SF
C
C  FMIN,FMIN1,SFD: THE OUTER BAR STRESS, THE CENTROIDAL STRESS
C                  AND THE STRAIN FACTOR, CORRESPONDING TO BMDT.
C
      PRINT*,' FMIN1= ',FMIN1,' , SFD= ',SFD,' , DPD= ',DP
      PRINT*,'FMIN=  ',FMIN,'  N/(MM*MM)'
 50   FORMAT('FSA=  ',1F9.3,'  N/(MM*MM)')
      WRITE(6,35)
C
      PRINT*,'FSI= ',FSI,' , FSA= ',FSA,'  N/(MM*MM)'
      PRINT*,'FSH= ',FSH,' , FMIN= ',FMIN,'  N/(MM*MM)'
      WRITE(6,35)
C
      PRINT*,' FSI= ',FSI,' , FSA1= ',FSA1
      PRINT*,' FSH1= ',FSH1,' FMIN1= ',FMIN1
      WRITE(6,35)
C
      BVT=0.5*BL*(24.0E-06*BC*HT+25.0)+500.0*BV
C
C  BVT: THE TOTAL SHEAR FORCE.
C
      DBT=HT-DPT
      VM=BVT/(BC*DBT)
      PRINT*,'VM= ', VM,'   N/(MM*MM)'
C
C  VM: THE MAXIMUM SHEAR STRESS.
C
      BMT=BMT*1.0E-06
      BMTH=BMT-(0.25*BM)*1.0E-06
      BMDT=BMDT*1.0E-06
      BVT=BVT*1.0E-03
      PRINT*,'DEAD LOAD MOMENT= ',BMDT,' KN.M'
      PRINT*,'INT. MOMENT     = ',BMTH,' KN.M'
      PRINT*,'TOTAL MAX MOMENT= ',BMT,'  KN.M'
      PRINT*,'TOTAL MAX SHEAR= ',BVT,' KN'
      WRITE(6,35)
C
C  THE FOLLOWING SECTION CALCULATES THE SECTION MODULI
C  AND THEIR RELATIVE DIFFERENCES
C
      ZT=BMT/FSA
      ZTH=BMTH/FSH
      ZD=BMDT/FMIN
      ZL=(BMT-BMDT)/(FSA-FMIN)
```

```
      ZLH=(BMTH-BMDT)/(FSH-FMIN)
      PRINT*,'ZT= ',ZT,', ZTH= ',ZTH,', ZD= ',ZD
      PRINT*,'ZL= ',ZL,', ZLH= ',ZLH
      WRITE(6,35)
C
      ZT1=BMT/FSA1
      ZTH1=BMTH/FSH1
      ZD1=BMDT/FMIN1
      ZL1=(BMT-BMDT)/(FSA1-FMIN1)
      ZLH1=(BMTH-BMDT)/(FSH1-FMIN1)
      PRINT*,' ZT1= ',ZT1,' , ZTH1= ',ZTH1,' , ZD1= ',ZD1
      PRINT*,' ZL1= ',ZL1,' , ZLH1= ',ZLH1
      WRITE(6,35)
C
      ZXT1=AMAX1(ZT1,(AMAX1(ZTH1,ZD1)))
      ZNT1=AMIN1(ZT1,(AMIN1(ZTH1,ZD1)))
      DZT1=(ZXT1-ZNT1)/ZNT1
      DZA1=(ABS(ZT1-ZTH1))/(AMIN1(ZT1,ZTH1))
      DZL1=(ABS(ZL1-ZLH1))/(AMIN1(ZL1,ZLH1))
      DCA=2.0-2.0E06*ZT1/(ASP*DBT)
      RA=0.02*FSA1*ASP/(BC*DCA*DBT)
      ALPH=DCA*RA/RT
C
C  ALPH: THE RATIO OF THE AVERAGE CONCRETE COMPRESSIVE
C        STRESS TO THE CONCRETE COMPRESSIVE STRENGTH ;FCU.
C
      ZXT=AMAX1(ZT,AMAX1(ZTH,ZD))
      ZNT=AMIN1(ZT,AMIN1(ZTH,ZD))
      DZT=(ZXT-ZNT)/ZNT
      DZA=(ABS(ZT-ZTH))/(AMIN1(ZT,ZTH))
      DZL=(ABS(ZL-ZLH))/(AMIN1(ZL,ZLH))
      PRINT*,'ALPH=  ',ALPH,' , DZT=  ',DZT
      PRINT*,'DZA =  ',DZA ,' , DZL=  ',DZL
      WRITE(6,35)
C
C  THE FOLLOWING SECTION CALCULATES AND COMPARES THE
C  ACTUAL AND THE SIMULATED STRESS AND STRESS RANGE
C  VALUES
C
      F=AMIN1(ZTH1,(0.5*(ZT1+ZD1)))
      FL=AMIN1(ZL1,ZLH1)
      SF=AMAX1(SFH,(0.5*(SFT+SFD)))
      SXT=AMAX1(SFT,(AMAX1(SFH,SFD)))
      SNT=AMIN1(SFT,(AMIN1(SFH,SFD)))
      DSF=(SXT-SNT)/SNT
      PRINT*,' DSF= ',DSF,' , DZT1= ',DZT1
      PRINT*,' DZA1= ',DZA1,' , DZL1= ',DZL1
      WRITE(6,35)
C
      PRINT*,' FL= ',FL,' , F= ',F,' , SF= ',SF
      PRINT*,' SFT= ',SFT,' , SFH= ',SFH,' , SFD= ',SFD
      WRITE(6,35)
C
      SE0=161.5-0.33*FMIN
      FSR=FSA1-FMIN1
```

```
      STT=BMT/F-FMIN1
      BMP=BM*1.0E-06
      STL=0.5*BMP/FL
      DST=(ABS(STT-STL))/(AMIN1(STT,STL))
      SHT=BMTH/F-FMIN1
      SHL=0.25*BMP/FL
      DSH=(ABS(SHT-SHL))/(AMIN1(SHT,SHL))
      STCX=AMAX1(STT,STL)
      DFRX=(STCX-FSR)/(AMIN1(STCX,FSR))
      STCH=AMAX1(SHT,SHL)
      FSRH=FSH1-FMIN1
      DFRH=(STCH-FSRH)/(AMIN1(STCH,FSRH))
      PRINT*,'FSR=  ',FSR,', STCX= ',STCX
      PRINT*,'DFRX= ',DFRX,' , DST= ',DST
      PRINT*,'STT= ',STT,' , STL= ',STL
      WRITE(6,35)
C
      FSCX=STCX+FMIN1
      ESXE=SF*(FSCX/200000.0+AMAX1((FSCX-340.0),0.0)/42500.0)
      FSXE=200000.0*ESXE-AMAX1((ESXE-0.0017),0.0)*164948.45
      STXE=FSXE-FMIN
      FSRE=FSA-FMIN
      PRINT*,' FSRE= ',FSRE,' , STXE= ',STXE
      DFXE=(STXE-FSRE)/(AMIN1(STXE,FSRE))
      PRINT*,' DFXE= ',DFXE,' , SE0= ',SE0
      WRITE(6,35)
C
      PRINT*,'FSRH=',FSRH,',STCH=',STCH,',DFRH=',DFRH
      PRINT*,'SHT= ',SHT,' , SHL= ',SHL,' , DSH= ',DSH
      WRITE(6,35)
C
      FSCH=STCH+FMIN1
      ESHE=SF*(FSCH/200000.0+AMAX1((FSCH-340.0),0.0)/42500.0)
      FSHE=200000.0*ESHE-AMAX1((ESHE-0.0017),0.0)*164948.45
      STHE=FSHE-FMIN
      FSHE=FSH-FMIN
      DFHE=(STHE-FSHE)/(AMIN1(STHE,FSHE))
      PRINT*,'FSHE=',FSHE,',STHE=',STHE,',DFHE=',DFHE
      PRINT*,' DPT= ',DPT
      WRITE(6,30)
C
 30   FORMAT('==========================================')
 35   FORMAT('------------------------------------------')
C
 1000 CONTINUE
C
      WRITE(6,60)
 60   FORMAT(' END OF THE BRIDGE DESIGN' )
C
      STOP
      END
```